Non-invasive Coronary Imaging With Multislice Computed Tomography Coronary Angiography

Nico R. Mollet

ISBN 90-5335-067-5

Lay-out: A.W. Zwamborn
Cover: A.W. Zwamborn
Backside: 64-slice CT scan of a portrait by Carel Fabritius (1622-1654), probably the most gifted pupil of Rembrandt. He was killed during the great gunpowder explosion in Delft in October 1654 at the age of 32 and most of his paintings were destroyed. If he had lived longer, he could have become as famous as his master. In fact, until recently, most of his paintings were thought to be by Rembrandt. I would like to thank Marcel Dijkshoorn for the acquisition and post-processing of this unique image.
Illustrations: N.R. Mollet

Printed by Ridderprint B.V. Ridderkerk 

NON-INVASIVE CORONARY IMAGING WITH MULTISLICE COMPUTED TOMOGRAPHY CORONARY ANGIOGRAPHY

NIET-INVASIEVE BEELDVORMING VAN DE KRANSSLAGADEREN MET MULTISLICE COMPUTED TOMOGRAPHY ANGIOGRAFIE

PROEFSCHRIFT

ter verkrijging van de graad van doctor aan de
Erasmus Universiteit Rotterdam
op gezag van de
rector magnificus

Prof.dr. S.W.J. Lamberts

en volgens besluit van het College voor Promoties.

De openbare verdediging zal plaatsvinden op
woensdag 12 October 2005 om 11.45 Uur

door

Nico Robert Arnold Mollet
geboren te Delft

PROMOTIECOMMISSIE

Promotoren:	Prof.dr. P.J. de Feyter
	Prof.dr. G.P. Krestin
Co-promotor:	Dr. F. Cademartiri

Overige leden:	Prof.dr. J. Bogaert
	Prof.dr. P.M.T. Pattynama
	Prof.dr. D. Poldermans
	Prof.dr. W.M. Prokop
	Prof.dr. P.W.J.C. Serruys
	Prof.dr. E.E. van der Wall

Financial support by the Netherlands Heart Foundation for the publication of this thesis is gratefully acknowledged.

Financial support by the department of Radiology, Erasmus MC, University Medical Center Rotterdam, for the publication of this thesis is gratefully acknowledged.

For my parents

Part 1: Preface

Part 2: Technical Optimization of Multislice Computed Tomography Coronary Angiography

Part 3: Multislice Computed Tomography Coronary Angiography in the Detection of Obstructive Coronary Artery Disease

Part 4: Pitfalls of Multislice Computed Coronary Angiography in the Detection of Obstructive Coronary Artery Disease

Part 5: Coronary Plaque Imaging With Multislice Computed Tomography Coronary Angiography

Part 7: Clinical Applications of Multislice Computed Tomography Coronary Angiography

Part 8: Summary and Conclusions

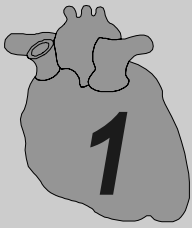

Chapter 1

Introduction

Nico R. Mollet

Atherosclerosis is a systemic, chronic inflammatory disease of the intima layer of the vessel wall affecting both large and medium-sized muscular arteries. The process of atherosclerosis is complex and develops progressively during time, already starting in the 2nd and 3rd decade of life[1]. Symptoms do not occur during the earlier phases of atherosclerosis and remain absent for several decades[2]. Chronic symptoms occur when an atherosclerotic plaque causes a significant obstruction of the coronary arteries, which limits the blood supply to the heart. Patients typically develop chest pain (angina pectoris) during exercise, when the heart needs more oxygen, but symptoms disappear after a short period of rest. Acute clinical manifestations may develop from advanced, high-risk lesions (e.g. plaques with a large necrotic, lipid-rich core and thin fibrous cap), which ruptures causing a thrombotic lesion with complete or partial blockage of the blood supply to the heart followed by myocardial infarction or sudden cardiac death. As in many other industrialized countries, atherosclerosis is the number one cause of mortality in the Netherlands[3].

Conventional coronary angiography is considered to be the gold standard to evaluate the impact of atherosclerosis on the coronary lumen. This is an invasive technique that requires puncture of a peripheral artery, advancement of a catheter towards the heart, and injection of contrast material directly into the coronary arteries. During this procedure, conventional X-ray images are obtained which allows real-time evaluation of high-resolution images of the coronary lumen. The degree of coronary stenoses can be calculated using quantitative contour detection algorithms.

Catheter based tools to determine the hemodynamic significance of obstructive coronary disease (e.g. flow velocity and pressure gradient measurement), or vessel wall morphology (e.g. intra-coronary ultrasound) can be applied during the procedure. However, conventional coronary angiography is an expensive and invasive imaging modality associated with a small, but not negligible, risk of serious procedure-related complications[4]. Moreover, application of more advanced catheter based diagnostic modalities is generally expensive, time-consuming, and only performed in specialized catheterisation laboratories.

These disadvantages prompted the development of imaging modalities allowing non-invasive visualization of the coronary arteries. However, such modalities require several technical prerequisites to achieve this objective. High spatial resolution is needed to evaluate the coronary lumen of small (2-3 mm), but clinically important branches and the -even smaller- coronary vessel wall. High temporal resolution is required to limit motion artifacts related to displacement of the coronary arteries during the contraction of the heart. In addition, the acquired data should be synchronized with the electrocardiogram to identify phases during the cardiac cycle when the heart is relatively less moving. Data acquisition time should be short to avoid motion artifacts related to displacement of the thorax due to respiration during the scan. High contrast resolution is needed to distinguish between different plaque tissue components, allowing identification of different stages of coronary atherosclerosis. Finally, such technique should be robust, fast and patient-friendly to become part of the routine diagnostic armamentarium in the clinical work-up of patients suspected of coronary artery disease.

Several imaging modalities have been developed that allow non-invasive visualization of the coronary arteries: Electron-Beam Computed Tomography, Magnetic Resonance Imaging, and, more recently, Multislice Spiral Computed Tomography[5-7]. Every technique has certain advantages and disadvantages (Table 1), but none of them did mature into a routinely used imaging modality for the purpose of non-invasive coronary angiography yet.

Table 1. Strengths and weaknesses of each of the three non-invasive coronary angiography techniques

Magnetic Resonance Imaging	Electron-Beam Computed Tomography	Multislice Computed Tomography
Equipment widely available	Limited availability	Equipment widely available
No iodinated contrast required	Requires iodinated contrast	Requires iodinated contrast
No radiation required	Requires radiation	Requires radiation
High temporal resolution	High temporal resolution	Limited temporal resolution
Limited (through-plane) spatial resolution	Limited (through-plane) spatial resolution	High spatial resolution
Long data acquisition (30-45 min)	Short data acquisition (40 seconds)	Short data acquisition (10-20 seconds)

This thesis will focus on Multislice Spiral Computed Tomography, the most rapidly developing technique among these different modalities. Computed Tomography (CT) was developed in the early 1970's by G. Hounsfield and A.M. McCormack, who were awarded the Nobel Prize in 1979. However, several technical advances were necessary before non-invasive imaging of the coronary arteries became feasible. The first spiral or helical CT scanners were introduced in 1990, which allowed scanning of extended volumes in a shorter time period. The first Multislice Spiral Computed Tomography (MSCT) scanners were introduced in 1998, which could acquire 4-slices simultaneously during the scan. This was the first generation CT scanners which offered a spatial and temporal resolution which was sufficient to visualize the small and rapidly moving coronary arteries[7-11]. Moreover, the entire heart could be scanned during a single breath hold, thereby avoiding the need for multiple contrast injections to visualize the entire coronary system. From that moment, Multislice CT technology developed rapidly with the introduction of 16-slice and 64-slice MSCT scanners in 2002 and 2004, respectively (Table 2)[12-20]. These newer MSCT scanner generations allow scanning of the entire heart during a single breath hold of less then 20 seconds, which is a manageable breath hold for practically all patients. Moreover, these scanners provide sub-millimetre spatial resolution (up to 0.4 mm in all dimensions), and offer a temporal resolution, which is sufficient to visualize the entire coronary tree including the more rapidly moving parts, in patients with lower heart rates. Patients with higher heart rates (generally above 70 beats/minute) receive oral or intravenous β-blockers when applicable to lower the heart rate thereby reducing the frequency of motion artifacts[21].

MSCT coronary angiography provides morphologic information regarding the presence or absence of coronary artery disease by means of non-invasive evaluation of both the coronary lumen and coronary vessel wall[22-25].

Table 2. Technical features of 4-, 16-, and 64-slice (Siemens) scanners

	4-slice CT	16-slice CT (1st generation)	16-slice CT (2nd generation)	64-slice CT
Rotation time (ms)	500	420	375	330
Slices per rotation	4	16[1]	16	64
Number of detectors	4	16	16	32
Individual detector width (mm)	1.0	0.75	0.75	0.6
Reconstructed slice thickness (mm)	1.25	1.0	1.0	0.75
Acquisition time (s)[2]	≈ 45[3]	≈ 20	≈ 18	≈12
Contrast material needed (ml)[4]	140	100	100	80

Note: features are only applicable for the purpose of CT coronary angiography
[1] First prototypes could only apply the 12 inner detectors for ECG-gated scanning
[2] Values are based on a scan range of 14 cm
[3] Generally a pitch of 0.375 was selected in patients with a pre-scan heart rate <80 beats/minute.
[4] Amount of contrast material needed is also depending on the injection rate (generally 4-5 ml/s)

The technique and potential clinical applications of MSCT coronary angiography are reviewed more detailed in **Part 1** (Chapters 2,3). **Part 2** contains studies related to the technical optimization of this technique, in particular the administration of contrast material and image reconstruction in patients with mild heart rhythm irregularities (Chapters 4-6). The diagnostic performance of 16- and 64-slice MSCT coronary angiography to detect significant coronary stenoses as compared to conventional coronary angiography in selected patients is discussed in **Part 3** (Chapters 7-9). **Part 4** emphasizes on the pitfalls of this technique in the detection of significant stenoses and discusses the influence of coronary calcification and image evaluation protocol on diagnostic performance (Chapters 10,11). The potential of contrast-enhanced MSCT in the in-vivo evaluation of the presence, extent, type, and anatomical distribution of coronary atherosclerosis is discussed in **Part 5** as well as limitations of CT in the classification of different plaque types on the basis of absolute density measurements (Chapters 12-16). **Part 6** is focused on the diagnostic accuracy of 16-slice MSCT coronary angiography to detect in-stent re-stenosis in patients who underwent percutaneous coronary intervention followed by stent implantation of the left main coronary artery or other coronary segments (Chapters 17,18). Finally, potential clinical applications of MSCT coronary angiography are being discussed in **Part 7** (Chapters 19,20).

References

1. Tuzcu EM, Kapadia SR, Tutar E, et al. High prevalence of coronary atherosclerosis in asymptomatic teenagers and young adults: evidence from intravascular ultrasound. Circulation 2001;103(22):2705-10.
2. U.S. Department of Health and Human Services (DHHS). National Center for Health Statistics. Third National Health and Nutrition Examination Survey, 1988–1994, NHANES III data files.
3. Koek H, Van Leest L, Verschuren W, ML. B. Hart- en vaatziekten in Nederland 2004, cijfers over leefstijl- en risicofactoren, ziekte en sterfte. Den Haag: Nederlandse Hartstichting 2004; 2004.
4. Johnson LW, Lozner EC, Johnson S, et al. Coronary arteriography 1984-1987: a report of the Registry of the Society for Cardiac Angiography and Interventions. I. Results and complications. Cathet Cardiovasc Diagn 1989;17(1):5-10.
5. Achenbach S, Moshage W, Ropers D, Nossen J, Daniel WG. Value of electron-beam computed tomography for the noninvasive detection of high-grade coronary-artery stenoses and occlusions. N Engl J Med 1998;339(27):1964-71.
6. Kim WY, Danias PG, Stuber M, et al. Coronary magnetic resonance angiography for the detection of coronary stenoses. N Engl J Med 2001;345(26):1863-9.
7. Nieman K, Oudkerk M, Rensing BJ, et al. Coronary angiography with multi-slice computed tomography. Lancet 2001;357(9256):599-603.
8. Achenbach S, Giesler T, Ropers D, et al. Detection of coronary artery stenoses by contrast-enhanced, retrospectively electrocardiographically-gated, multislice spiral computed tomography. Circulation 2001;103(21):2535-8.
9. Knez A, Becker CR, Leber A, et al. Usefulness of multislice spiral computed tomography angiography for determination of coronary artery stenoses. Am J Cardiol 2001;88(10):1191-4.
10. Vogl TJ, Abolmaali ND, Diebold T, et al. Techniques for the detection of coronary atherosclerosis: multi-detector row CT coronary angiography. Radiology 2002;223(1):212-20.

11. Kopp AF, Schroeder S, Kuettner A, et al. Non-invasive coronary angiography with high resolution multidetector-row computed tomography. Results in 102 patients. Eur Heart J 2002;23(21):1714-25.
12. Flohr TG, Schoepf UJ, Kuettner A, et al. Advances in cardiac imaging with 16-section CT systems. Acad Radiol 2003;10(4):386-401.
13. Nieman K, Cademartiri F, Lemos PA, Raaijmakers R, Pattynama PM, de Feyter PJ. Reliable noninvasive coronary angiography with fast submillimeter multislice spiral computed tomography. Circulation 2002;106(16):2051-4.
14. Ropers D, Baum U, Pohle K, et al. Detection of coronary artery stenoses with thin-slice multi-detector row spiral computed tomography and multiplanar reconstruction. Circulation 2003;107(5):664-6.
15. Mollet NR, Cademartiri F, Nieman K, et al. Multislice Spiral CT Coronary Angiography in Patients With Stable Angina Pectoris. J Am Coll Cardiol 2004;43(12):2265-70.
16. Martuscelli E, Romagnoli A, D'Eliseo A, et al. Accuracy of thin-slice computed tomography in the detection of coronary stenoses. Eur Heart J 2004;25(12):1043-8.
17. Kuettner A, Trabold T, Schroeder S, et al. Noninvasive detection of coronary lesions using 16-detector multislice spiral computed tomography technology: initial clinical results. J Am Coll Cardiol 2004;44(6):1230-7.
18. Hoffmann U, Moselewski F, Cury RC, et al. Predictive value of 16-slice multidetector spiral computed tomography to detect significant obstructive coronary artery disease in patients at high risk for coronary artery disease: patient-versus segment-based analysis. Circulation 2004;110(17):2638-43.
19. Mollet NR, Cademartiri F, Krestin GP, et al. Improved Diagnostic Accuracy With 16-row Multislice CT Coronary Angiography. J Am Coll Cardiol 2005;45(1):128-32.
20. Kuettner A, Beck T, Drosch T, et al. Diagnostic accuracy of noninvasive coronary imaging using 16-detector slice spiral computed tomography with 188ms temporal resolution. J Am Coll Cardiol 2005;45(1):123-7.
21. Nieman K, Rensing BJ, van Geuns RJ, et al. Non-invasive coronary angiography with multislice spiral computed tomography: impact of heart rate. Heart 2002;88(5):470-4.
22. Schroeder S, Kopp AF, Baumbach A, et al. Noninvasive detection and evaluation of atherosclerotic coronary plaques with multislice computed tomography. J Am Coll Cardiol 2001;37(5):1430-5.
23. Achenbach S, Moselewski F, Ropers D, et al. Detection of calcified and noncalcified coronary atherosclerotic plaque by contrast-enhanced, submillimeter multidetector spiral computed tomography: a segment-based comparison with intravascular ultrasound. Circulation 2004;109(1):14-7.
24. Leber AW, Knez A, Becker A, et al. Accuracy of multidetector spiral computed tomography in identifying and differentiating the composition of coronary atherosclerotic plaques: a comparative study with intracoronary ultrasound. J Am Coll Cardiol 2004;43(7):1241-7.
25. Achenbach S, Ropers D, Hoffmann U, et al. Assessment of coronary remodeling in stenotic and nonstenotic coronary atherosclerotic lesions by multidetector spiral computed tomography. J Am Coll Cardiol 2004;43(5):842-7.

Chapter 2

NON-INVASIVE MULTISLICE CT CORONARY IMAGING

Abstract

Multislice spiral computed tomography (MSCT) coronary angiography is a promising non-invasive technique for the detection of coronary stenoses[1–4]. The advent of the technically improved 16 row MSCT scanner, with higher spatial and temporal resolution, has permitted more reliable detection of coronary plaques and significant obstructive coronary lesions[5]. It appears likely that MSCT coronary angiography will mature into a non-invasive diagnostic tool that will become integrated into the management of patients with known or suspected coronary atherosclerosis. This review will focus on the basics of the scanner, the diagnostic performance, and potential future applications.

Nico R Mollet[1,2]
Filippo Cademartiri[2]
Pim J de Feyter[1,2]

Departments of
Cardiology [1] and
Radiology [2],
Erasmus MC, University
Medical Center
Rotterdam,
The Netherlands

Heart 2005;91(3):401-7.

BASICS OF MSCT CORONARY ANGIOGRAPHY

What is computed tomography?

A CT scanner consists of an *x* ray tube and a row of detectors, which rotate around the patient who is positioned in the centre. The tube produces a fan shaped x ray beam, which passes through the patient and hits the detector on the other side (fig 1). The atomic density of a tissue that an x ray beam encounters determines its attenuation with a higher atomic tissue density resulting in a higher attenuation. The various tissues in a cross section can be distinguished because they have differences in atomic density and attenuation. The attenuation of the x ray beam is expressed as an absolute value measured in Hounsfield units (HU). The rotation of the x ray tube allows calculation of the attenuation at every single point of the slice, which is used to produce a cross sectional image of the body.

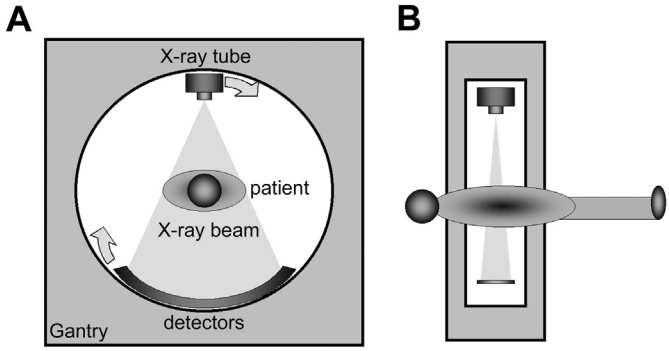

Figure 1. Frontal (A) and side (B) view of a computed tomography (CT) scanner.

The first generation CT scanners used a sequential acquisition pattern, also known as ''step-and-shoot''. These scanners produced an axial image while the table remained motionless and for each other slice the table moved to a different position. This sequence of events was repeated throughout the scan range (fig 2A). Sequential CT scanning was both time consuming and extremely sensitive to respiratory movements and was therefore not suitable for cardiac imaging.

To what do the terms ''spiral CT'' and ''multi-slice spiral CT'' refer?

The total scan time was significantly reduced with the introduction of spiral CT scanners. The scan is performed while the patient is continuously moving at a pre-defined speed through the scanner. The resulting trajectory of the x ray tube rotating around the patient can be plotted as a helix or spiral (fig 2B). These scanners acquire volumetric data and cross sectional images can be reconstructed later for any anatomic region. This configuration significantly reduced the total scan time, but still was not fast enough for cardiac scanning.

Multislice spiral CT (MSCT) is a recent development in spiral CT. MSCT scanners are equipped with multiple and thinner detector rows, and have a faster x ray tube rotation speed. These technical advances have an important impact on image quality and will be discussed in detail.

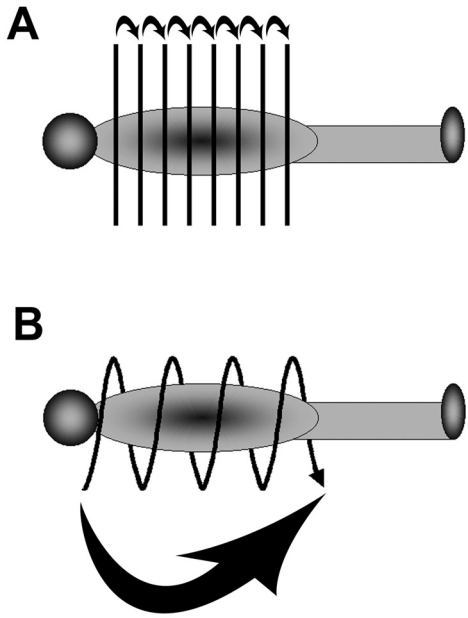

Figure 2. Sequential (A) and spiral (B) CT scanning.

What does the term "retrospective ECG gating" mean?

The contraction of the heart can cause severe motion artefacts on MSCT. To overcome this problem, only data obtained during the diastolic phase of the cardiac cycle (when cardiac motion is reduced) is used for image reconstruction.

The ECG trace of the patient is continuously monitored during the scan procedure, and retrospective ECG gating is used to generate images in the diastolic phase of the cardiac cycle. This retrospective gating technique is based on data acquisition during the whole cardiac cycle. After data acquisition, retrospectively, the optimal reconstruction window is chosen among all available time positions during the diastolic phase to ensure the least cardiac motion artefacts (fig 3). The retrospective gating technique allows flexibility in the position of reconstruction windows to diminish artefacts related to rapid coronary motion and extrasystoles. However, this flexibility is obtained at the cost of a high radiation exposure.

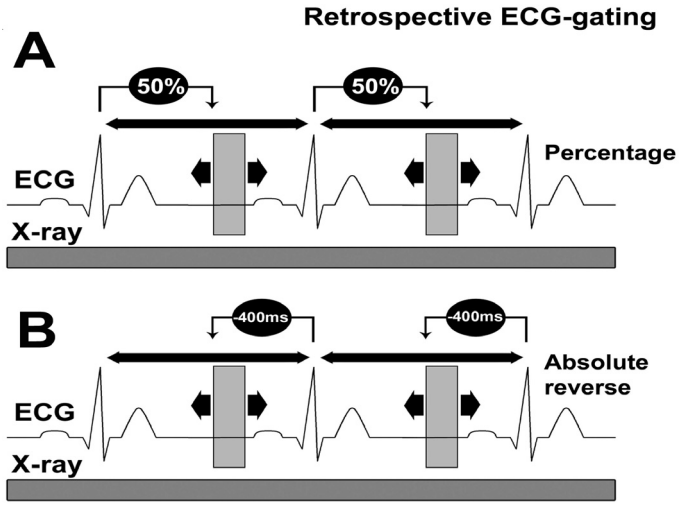

Figure 3. Scanning during the entire cardiac cycle allows retrospective gating. Different reconstruction windows during the diastolic phase can be explored to obtain images with the least motion artefacts. Two methods can be used to adjust reconstruction windows. One method selects different percentages of the cardiac cycle (A). Another method selects different positions based on an absolute time interval before the next R wave (B). No data are currently available to prove the superiority of either method and both methods are commonly used.

What are the technical requirements for MSCT coronary angiography?

Non-invasive visualisation of the coronary arteries is challenging. High temporal and high spatial resolution are both prerequisites to visualise the small, tortuous, and rapidly moving coronary arteries. Moreover, the scan must be performed within a single breath hold to diminish artefacts related to breathing.

The spatial resolution in the x/y axis of current MSCT scanners is 0.4 x 0.4 mm. The spatial resolution in the z axis is determined by the minimum slice thickness, which varies from 0.5–0.75 mm depending on the manufacturer. These features permit reconstruction of high quality images with a sub-millimetre, nearly isotropic (same size in every dimension) voxel size. This high spatial resolution reduces partial volume effects and also allows visualisation of coronary segments down to diameters of 1.5–2 mm.

A high temporal resolution is needed to minimise artefacts related to coronary motion. The temporal resolution is dependent on the rotation speed of the x ray tube and the detector. Usually a reconstruction algorithm is applied which uses data obtained over half the rotation time of the x ray tube. The temporal resolution using this algorithm currently ranges from 188–250 ms, depending on the manufacturer. In clinical practice, a temporal resolution within this range is sufficient for reliable visualisation of the coronary arteries in patients with a heart rate below 70 beats/min.

Current state-of-the-art MSCT scanners are equipped with 16 detector rows. This feature, combined with the increased rotation speed of the x ray, allows scanning of the heart (generally 11–14 cm in the cranio-caudal axis) in a single breath hold of less than 20 seconds, which is a manageable breath hold for practically all patients.

What are the limitations and pitfalls of MSCT coronary angiography?

MSCT coronary angiography is feasible in patients with a stable heart rhythm, able to breath-hold for 20 seconds. The image quality is degraded by artefacts in patients with irregular heart rhythms; atrial fibrillation is a contraindication for MSCT imaging while frequent extra-systoles can severely degrade image quality, although in the case of occasional extra-systoles this can be overcome by sometimes lengthy manual reconstruction of the images. Breathing during the scan can also severely degrade image quality. Other limitations of CT angiography in general are contraindications to x ray exposure (for example, pregnancy) or to the administration of intravenous iodinated contrast material (for example, allergy, renal failure, or hyperthyroidisms).

Well known pitfalls of MSCT coronary angiography include motion artefacts and severe coronary calcification. The temporal resolution of current 16 row MSCT scanners allows reliable evaluation of the coronary arteries at stable heart rates below 70 beats/min. Oral or intravenous β blockers should be administered to patients with higher resting heart rates to reduce the frequency of motion artefacts. The most rapidly moving coronary segment is the mid part of the right coronary artery where motion artefacts are most frequently observed. Adequate image quality at this level is usually a guarantee of good image quality in the rest of the coronary tree.

Large deposits of calcium in the coronary wall also influence image quality. Coronary calcifications are high density structures causing beam hardening and partial volume artefacts.

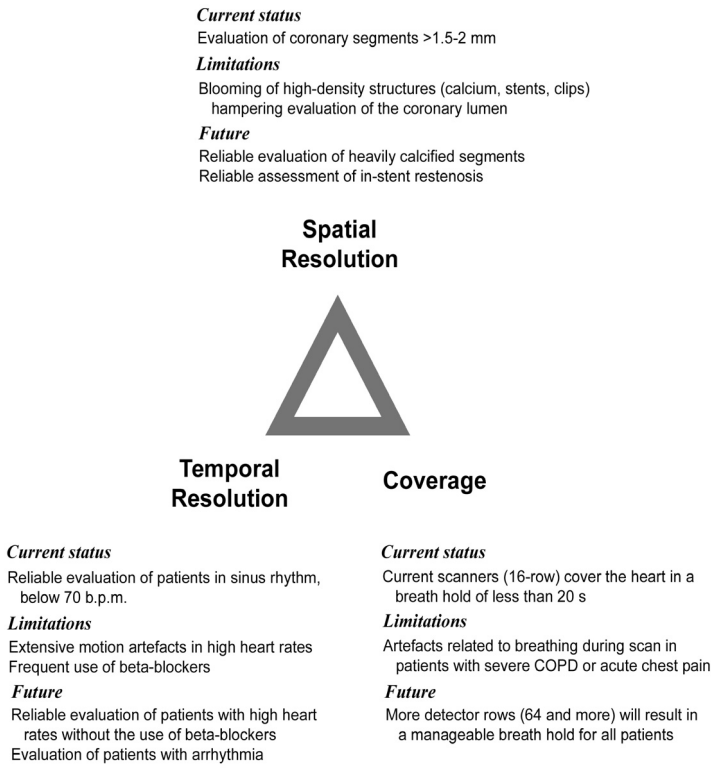

Figure 4. Influence of spatial resolution, temporal resolution, and coverage on the diagnostic performance of MSCT coronary angiography.

These artefacts result in over-projection (blooming) of the calcifications on the coronary lumen hampering assessment of coronary lesions (fig 4). Therefore, assessment of both the presence and severity of coronary lesions is compromised in heavily calcified vessels.

The radiation exposure during MSCT coronary angiography, generally between 7.1–10.9 mSv, remains a source of concern[6–9]. Prospective x ray tube modulation can be applied to reduce radiation exposure. This setting reduces radiation output during systole and decreases the calculated effective radiation exposure by up to 50% at low heart rates. The resultant calculated effective radiation exposure (4.3 mSv) is of the same order of magnitude as that of an invasive diagnostic coronary angiogram (2–6 mSv)[9].

Clinical Applications

Detection of significant obstructive coronary lesions: historical perspectives

The clinical application of MSCT coronary angiography using the previous generation four row MSCT scanners was limited for several reasons. A significant number of vessels were nonassessable because of the relatively low temporal and spatial resolution. Furthermore, the long scan time (~40 s) frequently resulted in breathing artefacts during the latter part of the scan[1–4].

Table 1. Detection of significant (>50%) coronary lesions with MSCT coronary angiography

	n	Excl (%)	Sens (%)	Spec (%)	PPV (%)	NPV (%)	Acc (%)
4 row MSCT							
Nieman *et al*[1]	31	27	81	97	81	97	95
Achenbach *et al*[2]	64	32	85	76	56	94	79
Knez *et al*[3]	44	6	78	98	84	96	94
Vogl *et al*[4]	38	19	75	99	92	98	98
16 row MSCT							
Nieman *et al*[10]	58	0	95	86	80	97	97
Ropers *et al*[11]	77	12	92	93	79	97	93
Mollet *et al*[12]	128	0	92	95	79	98	95

Excl, excluded; Sens, sensitivity; Spec, specificity; PPV, positive predictive value; NPV, negative predictive value; Acc, accuracy.

These limitations resulted in exclusion of up to 32% of the vessels from the analysis because of insufficient image quality (table 1)[2].

Detection of significant obstructive coronary lesions: current status

The sensitivity and specificity for detection of significant (≥50% lumen narrowing) lesions with the current generation of 16 row MSCT scanners, when appropriate measures are taken to ensure an appropriate heart rate (use of β blockers for pre-scan heart rates above 60 beats/min), is around 90% (fig 5)[10–12].

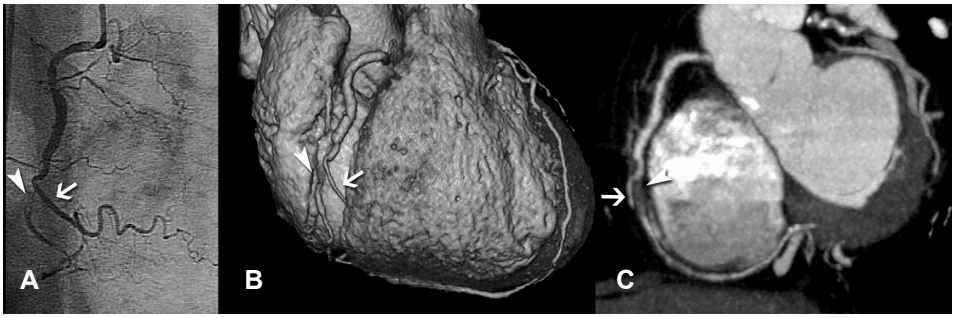

Figure 5. Conventional angiography image (A) showing a subtotal occlusion (arrowhead) of the mid part of the right coronary artery, distal to a right ventricular (RV) branch (arrow). Corresponding CT images using different image post-processing techniques: volume rendered (B), curved multiplanar (C), and maximum intensity projection (D) images showing the subtotal occlusion (arrowhead) and RV branch (arrow). (A full color version of this illustration can be found in the color section (Chapter 21)).

More importantly, the number of non-assessable vessels has been significantly reduced with the 16 row MSCT scanner.

Ropers *et al* excluded only 12% of the vessels and both Nieman *et al* and Mollet *et al* did not exclude any vessels for this reason (table 1). This is an important advance because clinical application of this technique presupposes reliable visualisation of the entire coronary tree.

Coronary plaque imaging

MSCT coronary calcium score: assessment of the calcium burden

Coronary calcium quantification was first reported with electron beam CT (EBCT) scanners. Histological studies have shown that attenuation values >130 HU were closely correlated with the presence of calcified plaque[13]. Agatston proposed a calcium score to classify calcium deposits in the coronary wall. This score used an area threshold of ≥1 mm^2 and a density threshold of >130 HU to identify a calcified lesion and the Agatston score was calculated by multiplying the area of each calcified lesion with the peak density of the plaque[14]. Long term follow up studies have suggested that the Agatston score has incremental prognostic value in the prediction of sudden coronary death or non-fatal myocardial infarction in asymptomatic, high risk patients although this is still somewhat controversial. The presence of calcium is a surrogate for the presence of atherosclerosis and the extent of coronary calcium correlates with the overall atherosclerotic plaque burden. A high calcium score is associated with a higher likelihood of an adverse coronary event, but the presence of calcium in a plaque cannot be considered, at present, as an indicator of plaque vulnerability. Furthermore, a negative calcium score is not a guarantee that the vessel is free from atherosclerotic lesions, including vulnerable plaques, although it renders their presence less likely[15]. Coronary calcium is also a function of age and sex, and the predictive accuracy of calcium scoring is improved when adjusted for these parameters.

Several prospective follow up studies have been published to establish the prognostic value of coronary calcium in intermediate to high risk asymptomatic subjects (table 2)[16–19].

Table 2. Prognostic value of coronary calcium in intermediate and high risk individuals (EBCT studies)

Study	Subject (n)	Mean age (years)	Follow up	Adverse events*	Cut off value†	Relative risk ‡
Detrano *et al*[16]	1196	66	41 (months)	46	44	2.3
Arad *et al*[17]	1173	53	43	39	160	22.2
Raggi *et al*[18]	676	52	32	30	>0	0.12 v 3.0§
Kondos *et al*[19]	5635¶	M:50, F:54	37	58	>0	M:5.8, F:1.8

*Adverse events defined as: death and myocardial infarction.
†Cut off value: threshold based on Agatston score, considered as having an increased risk.
‡Relative risk is calculated against the patients with a lower risk score.
§Annual risk.
¶Follow up rate only 64%.
M, male; F, female.

However, the incremental value, over conventional risk factors, of calcium scoring for screening asymptomatic, high risk patients is currently still somewhat controversial because of conflicting data. Large, randomised, prospective follow up studies are needed to establish the real prognostic value of coronary calcium.

A good correlation between calcium scoring with EBCT and MSCT scanners has been described and currently both techniques are used for calcium scoring[20]. Most studies have been performed using EBCT scanners, but nowadays this will gradually be taken over by MSCT scanners, which are widely available.

MSCT coronary angiography: assessment of the total MSCT plaque burden

Coronary calcium quantification with EBCT correlates with the extent of atherosclerosis, but severely underestimates the total coronary plaque burden[13]. In fact, the amount of calcium detected with EBCT reflects only one fifth of the measured atherosclerotic plaque burden[13]. In individual patients, there is wide variation in the extent and severity of coronary plaques. Sixteen row MSCT coronary angiography not only permits reliable detection of significant obstructive lesions, but also detection and classification of coronary plaques into calcified or non-calcified plaques (fig 6)[21–23]. The total MSCT plaque burden provides additional information about the extent, distribution, and location of coronary atherosclerosis, and might correlate more closely with the total plaque burden found on histology.

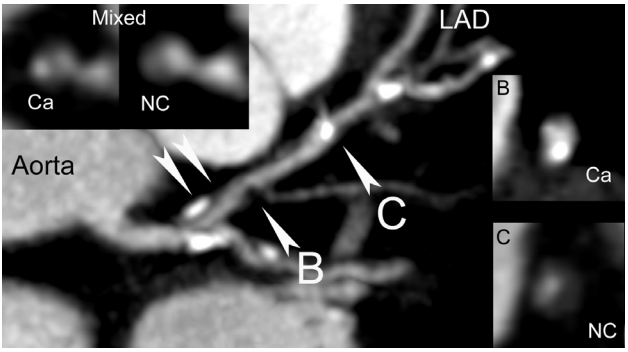

Figure 6. Maximum Intensity Projected (MIP) CT image of the left main and left anterior descending coronary artery showing mixed (inlays), calcified (B), and non-calcified (C) plaques. Ca, calcified; LAD, left anterior descending coronary artery; NC, non-calcified.

It has been suggested that the attenuation, in Hounsfield units, of the components of non-calcified plaques could reliably identify the presence of lipid or of fibrous tissue. This might help to identify potentially vulnerable plaques[23–26]. More extensive studies are needed to establish the full potential of MSCT coronary angiography in plaque detection and characterisation. An important limitation is the absence of dedicated software able to quantify accurately the amount of calcified as well as non-calcified plaques on a contrast enhanced scan.

Left ventricular function with MSCT coronary angiography

Information of left ventricular function (LVF) can be derived from the scan data obtained during MSCT coronary angiography. Reconstruction of datasets during different phases of the cardiac cycle enables calculation of end diastolic and end systolic volumes of the left ventricle, stroke volume, and ejection fraction (fig 7).

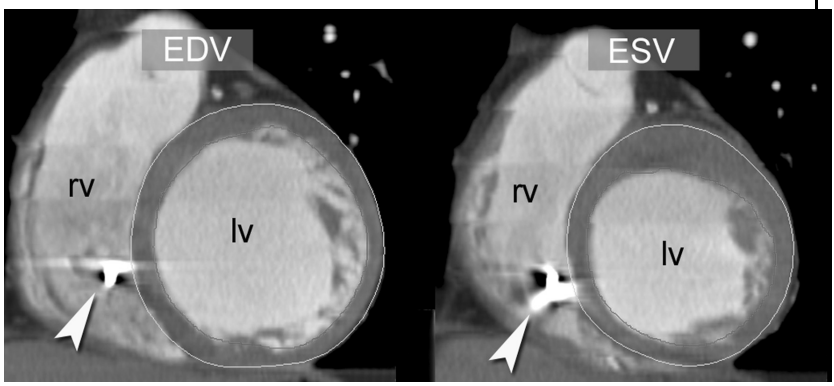

Figure 7. Reconstruction of datasets at end diastole (left) and end systole (right) allow calculation of ejection fraction and volumes. Reconstruction of additional datasets during the cardiac cycle is required for assessment of wall motion abnormalities. This patient has an impaired ejection fraction due to a previous inferoseptal infarction, which is visualised by reduced thickening of the septal myocardium. MSCT angiography is a potential alternative for patients who cannot undergo MRI—for example, patients with pacemakers (in the present case, a pacemaker lead is visualised in the right ventricle; arrowhead). EDV, end diastolic volume; ESV, end systolic volume; lv, left ventricle; rv, right ventricle.

A good correlation between ejection fraction measured with MSCT and either magnetic resonance imaging (MRI) or conventional biplane ventriculography has been demonstrated[27–28]. MSCT is a less suitable technique for the assessment of wall motion abnormalities because of its lower temporal resolution when compared with MRI or echocardiography. However, the primary aim of MSCT is non-invasive evaluation of the coronary arteries and the provision of functional information is a bonus.

Non-invasive multislice CT: key points

- Multislice spiral computed tomography (MSCT) coronary angiography is a non-invasive technique that can visualise both the lumen and the wall of the coronary arteries
- A low dose non-enhanced MSCT scan can be used for calcium scoring
- The latest MSCT scanners allow reliable detection of significant obstructive lesions in native coronary arteries in selected patients
- Improvements in MSCT technology are required for reliable evaluation of less selected patient groups
- The clinical value of MSCT coronary angiography needs to be established in multi-centre studies, evaluating populations with differing prevalence and presentations of coronary atherosclerosis

Other applications of cardiac MSCT

The use of a higher tube current and edge enhancing reconstruction filters allows assessment of stent patency (fig 8). However, beam hardening artefacts related to high density stent materials hamper reliable visualisation of the coronary lumen in stents and do not permit accurate assessment of non-obstructive intima hyperplasia.

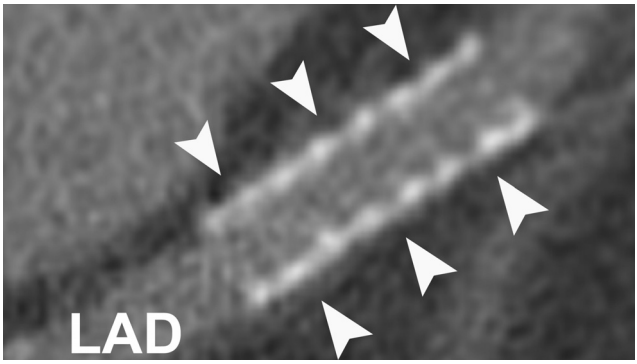

Figure 8. Contrast is well visualised inside the stent allowing assessment of stent patency. This is also shown on the cross sectional image located between the two arrowheads.

MSCT angiography is not restricted to native coronary arteries. It provides morphologic information about coronary veins and cardiac chambers, which can be useful for venous mapping or detection of intracardiac thrombi. This technique can also be used to evaluate venous or arterial bypass grafts (fig 9).

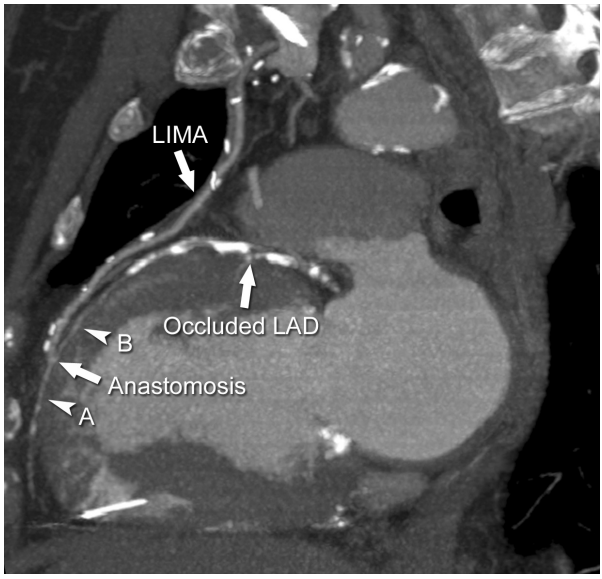

Figure 9. This maximum intensity projection image shows a patent arterial graft (left internal mammary artery, LIMA) inserted on an occluded left anterior descending artery (LAD). The anastomosis is clearly visualised and antegrade filling of the distal part of the LAD (A) as well as retrograde filling of the mid part of the LAD (B) is shown.

Preliminary studies, using four row MSCT scanners, showed a high sensitivity and specificity for the detection of occluded venous grafts (97–100% and 98%, respectively)[29–30]. Diagnostic accuracy for the detection of non-occlusive stenoses in venous grafts and evaluation of arterial grafts was suboptimal; this finding, in conjunction with the fact that a significant percentage of bypass segments (up to 42% of arterial bypasses) were non-assessable limits current clinical application.

Future Role of MSCT Coronary Angiography

Current 16 row MSCT scanners allow non-invasive evaluation of both the lumen and wall of the coronary artery. In the near future, MSCT coronary angiography might become an alternative to diagnostic conventional angiography for the detection of significant obstructive lesions. Further studies are needed to determine the role of MSCT coronary angiography in various patient groups such as asymptomatic high risk individuals, asymptomatic patients with known coronary artery disease, or in the evaluation of coronary obstructions in patients with stable angina or acute coronary syndromes.

References

1 Nieman K, Oudkerk M, Rensing BJ, et al. Coronary angiography with multislice computed tomography. Lancet 2001;357:599–603. c First study comparing the results of four row multislice CT coronary angiography with that of conventional angiography for the detection of significant obstructive stenoses.
2 Achenbach S, Giesler T, Ropers D, et al. Detection of coronary artery stenoses by contrast-enhanced, retrospectively electrocardiographically-gated, multislice spiral computed tomography. Circulation 2001;103:2535–8.
3 Knez A, Becker CR, Leber A, et al. Usefulness of multislice spiral computed tomography angiography for determination of coronary artery stenoses. Am J Cardiol 2001;88:1191–4.
4 Vogl TJ, Abolmaali ND, Diebold T, et al. Techniques for the detection of coronary atherosclerosis: multi-detector row CT coronary angiography. Radiology 2002;223:212–20.
5 Flohr TG, Schoepf UJ, Kuettner A, et al. Advances in cardiac imaging with 16-section CT systems. Acad Radiol 2003;10:386–401.
6 Jakobs TF, Becker CR, Ohnesorge B, et al. Multislice helical CT of the heart with retrospective ECG gating: reduction of radiation exposure by ECG controlled tube current modulation. Eur Radiol 2002;12:1081–6.
7 Hunold P, Vogt FM, Schmermund A, et al. Radiation exposure during cardiac CT: effective doses at multi-detector row CT and electron-beam CT. Radiology 2003;226:145–52.
8 Morin RL, Gerber TC, McCollough CH. Radiation dose in computed tomography of the heart. Circulation 2003;107:917–22.
9 Trabold T, Buchgeister M, Kuttner A, et al. Estimation of radiation exposure in 16-detector row computed tomography of the heart with retrospective ECGgating. Rofo Fortschr Geb Rontgenstr Neuen Bildgeb Verfahr 2003;175:1051–5.
10 Nieman K, Cademartiri F, Lemos PA, et al. Reliable noninvasive coronary angiography with fast submillimeter multislice spiral computed tomography. Circulation 2002;106:2051–4. c First study comparing the results of 16 row multislice CT coronary angiography with that of conventional angiography for the detection of significant obstructive stenoses.
11 Ropers D, Baum U, Pohle K, et al. Detection of coronary artery stenoses with thin-slice multi-detector row spiral computed tomography and multiplanar reconstruction. Circulation 2003;107:664–6.
12 Mollet NR, Cademartiri F, Nieman K, et al. Multislice spiral CT coronary angiography in patients with stable angina pectoris. J Am Coll Cardiol 2004;43:2265–70.
13 Rumberger JA, Simons DB, Fitzpatrick LA, et al. Coronary artery calcium area by electron-beam computed tomography and coronary atherosclerotic plaque area. A histopathologic correlative study. Circulation 1995;92:2157–62.
14 Agatston AS, Janowitz WR, Hildner FJ, et al. Quantification of coronary artery calcium using ultrafast computed tomography. J Am Coll Cardiol 1990;15:827–32.

15 Wexler L, Brundage B, Crouse J, et al. Coronary artery calcification: pathophysiology, epidemiology, imaging methods, and clinical implications. A statement for health professionals from the American Heart Association writing group. Circulation 1996;94:1175–92.
16 Detrano RC, Wong ND, Doherty TM, et al. Coronary calcium does not accurately predict near-term future coronary events in high-risk adults. Circulation 1999;99:2633–8.
17 Arad Y, Spadaro LA, Goodman K, et al. Prediction of coronary events with electron beam computed tomography. J Am Coll Cardiol 2000;36:1253–60.
18 Raggi P, Cooil B, Callister TQ. Use of electron beam tomography data to develop models for prediction of hard coronary events. Am Heart J 2001;141:375–82.
19 Kondos GT, Hoff JA, Sevrukov A, et al. Electron-beam tomography coronary artery calcium and cardiac events: a 37-month follow-up of 5635 initially asymptomatic low- to intermediate-risk adults. Circulation 2003;107:2571–6.
20 Becker CR, Knez A, Jakobs TF, et al. Detection and quantification of coronary artery calcification with electron-beam and conventional CT. Eur Radiol 1999;9:620–4.
21 Schoenhagen P, Tuzcu EM, Stillman AE, et al. Non-invasive assessment of plaque morphology and remodeling in mildly stenotic coronary segments: comparison of 16-slice computed tomography and intravascular ultrasound. Coron Artery Dis 2003;14:459–62.
22 Achenbach S, Moselewski F, Ropers D, et al. Detection of calcified and noncalcified coronary atherosclerotic plaque by contrast-enhanced, submillimeter multidetector spiral computed tomography: a segment-based comparison with intravascular ultrasound. Circulation 2004;109:14–7. c Study comparing the results of 16 row MSCT coronary angiography to detect coronary plaques with that of intracoronary ultrasound.
23 Leber AW, Knez A, Becker A, et al. Accuracy of multidetector spiral computed tomography in identifying and differentiating the composition of coronary atherosclerotic plaques: a comparative study with intracoronary ultrasound. J Am Coll Cardiol 2004;43:1241–7. c Study comparing the results of 16 row MSCT coronary angiography to detect coronary plaques with that of intracoronary ultrasound and correlation with CT density measurements for classification of coronary plaques into soft, fibrous, or calcified plaques.
24 Schroeder S, Kopp AF, Baumbach A, et al. Noninvasive detection and evaluation of atherosclerotic coronary plaques with multislice computed tomography. J Am Coll Cardiol 2001;37:1430–5. c First study demonstrating the potential of MSCT coronary angiography to classify non-calcified plaques into soft or fibrous plaque based on CT density measurements.
25 Becker CR, Nikolaou K, Muders M, et al. Ex vivo coronary atherosclerotic plaque characterization with multi-detector-row CT. Eur Radiol 2003;13:2094–8.
26 Nikolaou K, Becker CR, Muders M, et al. Multidetector-row computed tomography and magnetic resonance imaging of atherosclerotic lesions in human ex vivo coronary arteries. Atherosclerosis 2004;174:243–52.
27 Juergens KU, Grude M, Fallenberg EM, et al. Using ECG-gated multidetector CT to evaluate global left ventricular myocardial function in patients with coronary artery disease. Am J Roentgenol 2002;179:1545–50.
28 Grude M, Juergens KU, Wichter T, et al. Evaluation of global left ventricular myocardial function with electrocardiogram-gated multidetector computed tomography: comparison with magnetic resonance imaging. Invest Radiol 2003;38:653–61.
29 Ropers D, Ulzheimer S, Wenkel E, et al. Investigation of aortocoronary artery bypass grafts by multislice spiral computed tomography with electrocardiographic-gated image reconstruction. Am J Cardiol 2001;88:792–5.
30 Nieman K, Pattynama PM, Rensing BJ, et al. Evaluation of patients after coronary artery bypass surgery: CT angiographic assessment of grafts and coronary arteries. Radiology 2003;229:749–56.

Chapter 3

COMPUTED TOMOGRAPHY CORONARY ANGIOGRAPHY

Introduction

Nico R. Mollet

From the Departments of Radiology and Cardiology, Erasmus MC, University Medical Center Rotterdam, The Netherlands.

Chapter in: **Advances in MDCT Volume 2, Pt. 1: Cardiac Imaging.** Clinical Publishing Ltd (in press).

Multislice computed tomography (CT) coronary angiography is an emerging technique that permits non-invasive detection of coronary stenoses. Various studies exploring the diagnostic performance of CT coronary angiography for detecting significant coronary stenoses have been published. The first studies evaluated the diagnostic performance of this technique using four-slice CT scanners. However, these scanners required a relatively long scan time and provided limited resolution resulting in a significant number of non-evaluable segments (up to 43% of the included segments).[1] In 2002 the results of studies exploring the diagnostic performance of a newer generation 16-slice CT scanner in detecting significant coronary stenoses were published.[2-3] These 16-slice CT scanners had several technical advances when compared to four-slice scanners, e.g. an increased spatial and temporal resolution and shorter scan time, which resulted in an improved diagnostic performance.[2-4] Most importantly, the number of non-evaluable vessels has been significantly reduced. Initially, only the results of a 16-slice CT scanner of a single vendor were available, but recently the results of other vendors showing comparable results have been published.

Direct comparison between the various studies exploring the diagnostic performance of 16-slice CT coronary angiography in detecting significant lesions is very difficult, because different CT scanners and patient inclusion criteria were used. The aim of this chapter is to enhance the interpretation of the results presented in the current literature. In addition, we will discuss the role of coronary calcium on the diagnostic performance of CT coronary angiography, which is the subject of ongoing debate.

Diagnostic performance of computed tomography coronary angiography using first-generation 16-slice scanners

All currently available studies exploring the performance of 16-slice CT coronary angiography administered oral or intravenous β-blockers in patients with high heart rates (generally above 65 beats/min) before scanning in order to lower the heart rate, thereby reducing the frequency of motion artefacts. All of the patients included had a stable heart rhythm, whereas patients with severe arrhythmia (e.g. frequent premature beats or atrial fibrillation) were excluded. A threshold of ≥50% lumen diameter reduction determined by quantitative conventional coronary angiography was used for classifying lesions as significant. We have chosen to discuss the results of three representative studies, which used different CT vendors. Differences in the study methodologies and scanner characteristics are discussed in order to provide a general overview of the performance of first-generation 16-slice CT scanners in detecting significant coronary lesions.

Multislice spiral computed tomography coronary angiography in patients with stable angina pectoris

Mollet NR, Cademartiri F, Nieman K, et al. J Am Coll Cardiol 2004; 43: 2265–70

Background

This was a prospective, single-centre study exploring the diagnostic performance of CT coronary angiography in 128 patients with stable angina pectoris using a 16-slice Siemens scanner with a rotation time of 420 ms and a detector collimation of 0.75 mm. The mean scan time was approximately 18 s. Patients with pre-scan heart rates above 65 beats/min received a single oral dose of 100 mg of metoprolol 1 h before the scan, resulting in a mean heart rate of 58 beats/min during the scan. All available segments without stents of ≥2 mm that were visualized on the conventional angiogram were included. In addition, one patient was excluded from further analysis due to a technical failure during the CT scan. A comparison between CT and invasive coronary angiography was performed on a per-segment, per-vessel and per-patient level.

Interpretation

The diagnostic performance of CT coronary angiography in detecting significant lesions is summarized in Table 1. The image quality was classified as poor in 7% of the coronary segments. The causes of poorly assessable segments were motion artefacts (63%), severe calcifications (30%) and low contrast-to-noise ratios (7%). The mean lumen diameter reductions of missed and overestimated lesions on the CT scan were 61% (false-negative segments) and 40% (false-positive segments), respectively.

Comment

The authors reported a high sensitivity (94%) and specificity (91%) of CT coronary angiography in detecting significantly obstructed coronary arteries in a large patient cohort with a high pre-test likelihood of having significant coronary artery disease (CAD) (predominantly male patients with stable angina pectoris). These results were obtained after inclusion of all available non-stented segments with a lumen diameter of ≥2 mm, irrespective of image quality,

Table 1. Results: Detection of Significant (≥50%) Stenoses With 16-Row Multislice Spiral Computed Tomography Coronary Angiography

Coronary Segment	N	TP	TN	FP	FN	Sensitivity	Specificity	Positive PV	Negative PV
All segments	1,384	216	1,092	58	18	92%(216/234)	95%(1,092/1,150)	70%(216/274)	98%(l,092/1,110)
LM	124	6	118	0	0	100%(6/6)	100%(118/118)	100%(6/6)	100%(118/118)
LAD	473	90	350	27	6	94%(90/96)	93%(350/377)	77%(90/117)	98%(350/356)
Proximal	124	37	74	10	3	93%(37/40)	88%(74/84)	79%(37/47)	96%(350/353)
Middle	111	41	65	5	0	100%(41/41)	93%(65/70)	89%(41/46)	100%(65/65)
Distal	102	5	94	3	0	100%(5/5)	97%(94/97)	63%(5/8)	100%(94/94)
Side branches	136	7	117	9	3	70%(7/10)	93%(317/126)	44%(7/16)	95%(117/120)
CX	395	49	325	12	9	84%(49/58)	96%(325/337)	80%(49/61)	97%(325/334)
Proximal	111	16	90	3	2	89%(16/18)	97%(90/93)	84%(16/19)	98%(90/192)
Middle	102	13	81	4	4	76%(13/17)	95%(81/85)	76%(13/17)	95%(81/85)
Side branches	182	20	154	5	3	87%(20/23)	97%(154/159)	80%(49/61)	98%(154/157)
RCA	392	71	299	19	3	96%(71/74)	94%(299/318)	79%(71/90)	99%(299/302)
Proximal	120	30	81	9	0	100%(30/30)	90%(81/90)	77%(30/39)	100%(30/30)
Middle	103	31	63	8	1	97%(31/32)	89%(63/71)	79%(31/39)	98%(63/64)
Distal	91	8	80	2	1	89%(8/9)	98%(80/82)	80%(8/10)	99%(80/81)
PDA	78	2	75	0	1	67%(2/3)	100%(75/75)	100%(2/2)	99%(75/76)

CX = circumflex coronary artery, FN = false negative, FP = false positive, LAD = left anterior descending coronary artery, LM = left main coronary artery, PDA = posterior descending artery, RCA = right coronary artery, PV = predictive value, TN = true negative, TP = true positive. *Source: Mollet et al. (2004)*

which is an important improvement when compared to previous four-slice CT coronary angiography studies. The vast majority of significant lesions that were incorrectly classified on the CT scan (14 out of 18) were underestimated, which reflects the semi-quantitative nature of the evaluation of coronary lesions with CT. The remaining lesions were not visible on the CT scan due to motion artefacts (two) and severe calcifications (two). It is noteworthy that all patients with significant CAD were correctly identified on the CT scan, whereas only a few patients without significant CAD were overestimated. This observation suggests that 16-slice CT coronary angiography could be of use in the triage of patients with stable angina pectoris who are being considered for revascularization therapy.

Accuracy of thin-slice computed tomography in the detection of coronary stenoses
Martuscelli E, Romagnoli A, D'Eliseo A, et al. Eur Heart J 2004; 25: 1043–8

BACKGROUND

This was a prospective, single-centre study exploring the diagnostic performance of a 16-slice GE scanner with a rotation time of 500 ms and a detector collimation of 0.625 mm in 64 stable patients referred for conventional coronary angiography because of suspected CAD. The mean scan time was 22 s. Patients received 50–100 mg of atenolol orally starting at least 3 days before the CT scan, resulting in a mean heart rate of 59 beats/min during the CT scan. Patients who had previously undergone percutaneous coronary intervention were excluded from the study. Only evaluable segments on the CT scan with a mean lumen diameter of ≥1.5 mm were included in the comparative analysis with conventional coronary angiography. Moreover, three patients who underwent the CT coronary angiography were excluded from further analysis due to various reasons resulting in impaired image quality.

INTERPRETATION

Table 2 shows the evaluability of CT coronary angiography in different coronary vessels. Overall, 16% of the included segments were classified as non-evaluable due to severe calcifications (64%), motion artefacts (25%), poor contrast attenuation (7%) and blending of an artery with an adjacent vein (3%). Table 3 summarizes the diagnostic performance of this scanner in the detection of significant coronary stenoses on a per-segment level, including the mean lumen diameter of the analysed coronary segments.

Table 2. Evaluability by multislice CT of each coronary segment and the entire vessel

Vessel	LM	LAD*	Prox LAD	Mid LAD	Dist LAD	Diag	Cx*	Prox Cx	Dist CX	Marg	RI	RCA*	Prox RCA	Mid RCA	Dist RCA	PDA
Number of angiographic segments > 1,5 mm	61	61	61	60	59	60	61	61	61	61	5	61	61	59	60	60
Number of segments evaluable by MSCT	61	51	60	59	51	41	50	52	50	39	4	52	53	52	52	39
Evaluable by MSCT (%)	100	84	98	98	86	68	82	85	82	64	80	85	87	88	87	65

Cx: circumflex artery; Diag: diagonal branch; LAD: left anterior descending artery; LM: left main; Marg: obtuse marginal branch; MSCT: multislice computed tomography; RCA: right coronary artery; RI: ramus intermedius; PDA: posterior descending artery; Prox: proximal.
*LAD, CX and RCA are used to indicate the entire vessel.
Source: Martuscelli *et al. (2004).*

COMMENT

This study reported a high sensitivity (89%) and a very high specificity (98%) in a population comprising stable patients with variable clinical presentations and a prevalence of 73% of significant CAD (determined by conventional coronary angiography). However, one should bear in mind that these results were obtained after exclusion of 16% of the included coronary segments due to impaired image quality.

Table 3. Accuracy of multislice CT in the detection of significant stenosis in each evaluable coronary segment and the entire vessel

	LAD*	Prox LAD	Mid LAD	Dist LAD	Diag	Cx*	Prox Cx	Dist CX	Marg RI	RCA*	Prox RCA	Mid RCA	Dist RCA	PDA
Mean diameter (mm)**		3,5	2,9	2,2	1,9		2,9	2,6	2,2	2,3		3,1	2,8	2,3	1,8
Number of angiographic stenoses in segments >1.5 mm	32	10	20	3	5	11	1	11	15	2	24	9	11	5	1
True positive	30	10	20	2	3	10	1	10	13	1	21	9	10	3	1
True negative	118	48	36	48	36	85	50	36	24	2	132	44	41	47	38
False positive	3	2	3	0	0	4	1	3	0	0	0	0	0	0	0
False negative	2	0	0	1	2	1	0	1	2	1	3	0	1	2	0
Sensitivity (%)	94	100	100	67	60	91	100	91	87	50	87	100	91	60	100
Specificity (%)	97	96	92	100	100	95	98	92	100	100	100	100	100	100	100
Positive predictive value (%)	91	83	87	100	100	71	50	77	100	100	100	100	100	100	100
Negative predictive value (%)	98	100	100	98	95	99	100	97	92	67	98	100	98	96	100

Cx: circumflex artery; Diag: diagonal branch; LAD: left anterior descending artery; Marg: obtuse marginal branch; MSCT: multislice computed tomography; RCA: right coronary artery; RI: ramus intermedius; PDA: posterior descending artery; Prox: proximal.
*LAD, CX, and RCA are used to indicate the entire vessel.
**Mean diameter is intended as average diameter of the proximal part of the segment (mm).
Source: Martuscelli *et al. (2004).*

This relatively high number of non-evaluable segments could be due to the somewhat lower temporal resolution (250 versus 210 ms in low heart rates) of this scanner when compared to other first-generation 16-slice scanners. On the other hand, this scanner is equipped with a higher through-plane spatial resolution (detector collimation 0.625 versus 0.75 mm), which could be beneficial in the evaluation of smaller or severely calcified vessels. The authors did not provide a per-vessel or per-patient analysis as well as a sensitivity analysis including all available coronary segments, which makes it difficult to interpret these results with regard to the clinical application of this technique.

Non-invasive coronary angiography with multislice computed tomography
Hoffmann MHK, Shi H, Schmitz BL, et al. JAMA 2005; 293: 2471–8

BACKGROUND

This was a prospective, single-centre study investigating the diagnostic performance of CT coronary angiography in a consecutive patient cohort comprising 103 patients suspected of CAD using a Philips scanner with a rotation time of 420 ms and a detector collimation of 0.75 mm. Various CT pitch levels were used resulting in a wide scan time range (16–25 s). A threshold of a lumen diameter of ≥1.5 mm was used for the inclusion of coronary segments in the comparative analysis with conventional coronary angiography. Patients with heart rates above 75 beats/min received intravenous metoprolol up to a maximum dose of 20 mg, resulting in a mean heart rate of 68 beats/min.

INTERPRETATION

Patients with variable clinical presentations were included, resulting in a prevalence of 56% (determined by conventional angiography) of having significant stenoses. This study found a very high sensitivity and specificity of CT coronary angiography in detecting significant coronary lesions in a segment-based (95 and 98%), vessel-based (97 and 96%) and patient-based (97 and 87%) analysis. However, 6.4% of the included segments were classified as non-evaluable and were excluded from the comparative analysis. Most importantly, the segment-based exclusions due to low image quality correlated with 14 and 27% exclusion rates in the vessel- and patient-based levels. Motion artefacts were the major cause in the vast majority of non-assessable segments (68%) and were predominantly located at the mid part of the right coronary artery (the most rapidly moving part of the coronary tree). Motion artefacts were significantly more frequent in patients with higher heart rates (≥70 beats/min) (Table 4). An additional cause of motion artefacts could be the rather long scan time (in some cases 25 s). An example of coronary anatomy as seen with CT is shown in Figure 1.

Table 4. Relationship of heart rate and segment (vessel) assessment by multislice CT

Assessment level	Heart rate									
	<60 beats/min		60–70 beats/min		71–80 beats/min		>80 beats/min		Total	
	n/total	%	n/total	%	n/total	%	n/total	%	n/total	%
Segments	295/302	98	530/549	97	335/374	90*	136/159	85*	1296/1384	93
Vessels	81/88	92	143/159	90	85/109	78*	36/47	77*	345/403	86
Patients	18/22	82	30/41	73	19/28	68	8/12	67	75/103	73

*Statistically significant differences detected versus groups with heart rates ≥70 beats/min ($P < 0.01$ by c^2-test). No significant differences were apparent for the patient groups. *Source: Hoffmann et al. (2005)*

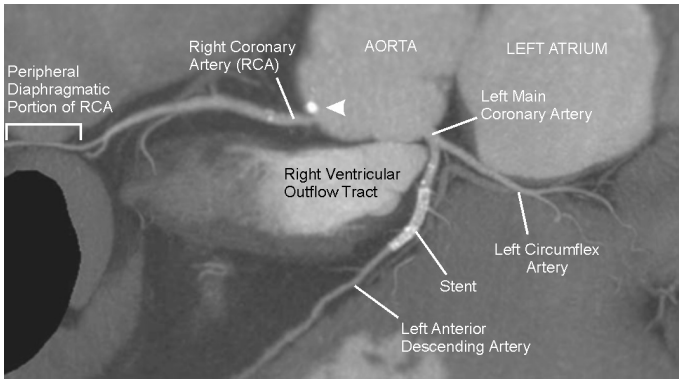

Figure 1. Example of multislice CT: unfolded globe view.
Source: Hoffmann et al. (2005)

Comment

This was a nicely conducted study that provides a thorough analysis of the potential of 16-slice CT coronary angiography. However, it should be noted that the relatively low prevalence of significant CAD (56%) within this study has important implications for the comparison of these results with other studies, which generally included patients with a higher prevalence of significant CAD. These patients had less advanced CAD and a lower calcium burden. However, severe coronary calcifications are a well-known cause of misinterpretation of lesions on a CT scan. A calcium-scoring scan was not performed prior to the angiographic scan, but the overall calcium score of the patient population included would enhance the interpretation of the results presented. In addition, the authors did not provide a sensitivity analysis including all available coronary segments visualized on the conventional angiogram, which would strengthen our understanding of the potential of this technique in routine clinical practice. Despite these remarks, this study convincingly shows the potential of this technique in patients with an intermediate-to-high likelihood of significant CAD.

Section conclusion

Current literature shows a high diagnostic performance of 16-slice CT coronary angiography in detecting significant stenoses when compared to conventional coronary angiography. Promising results from single-centre studies have been published, which were performed by multiple research groups using various scanners of different CT vendors. The sensitivities and specificities for detecting significant lesions are generally high (both around 90%), but vary among different studies. However, the negative predictive value is high (around 99%) in all published studies, suggesting that this technique might be a useful tool for excluding significant coronary lesions in patients suspected of CAD.

Diagnostic performance of computed tomography coronary angiography using second-generation 16-slice scanners

A new generation 16-slice CT scanner (Sensation 16 Straton®, Siemens) was introduced in 2003. These scanners are equipped with a shorter X-ray tube rotation time (375 ms) and offer the ability for scanning with a higher X-ray tube current (up to 700 mAs). These are important scanner characteristics for the purpose of CT coronary angiography, as a shorter rotation time results in a higher temporal resolution and a higher X-ray tube current results in an improved contrast-to-noise ratio. To date, only two studies have been published exploring the diagnostic performance of CT coronary angiography using this advanced 16-slice scanner. Both studies have important methodological differences, which are important to discuss in view of the results provided.

Diagnostic accuracy of non-invasive coronary imaging using 16-detector slice spiral computed tomography with 188 ms temporal resolution
Kuettner A, Beck T, Drosch T, et al. J Am Coll Cardiol 2005; 45: 123–7

Background

This was a prospective, single-centre study exploring the results of a second-generation 16-slice CT scanner in 72 consecutive patients with suspected CAD scheduled for invasive diagnostic coronary angiography. An X-ray tube current of 650 mAs during the angiography scan was applied in all patients. Patients with pre-scan heart rates ≥65 beats/min received an oral dose of 50–100 mg of metoprolol resulting in a mean heart rate of 64 beats/min during the scan. The authors sought to evaluate the entire coronary tree and included all coronary segments as seen on the conventional angiogram, irrespective of lumen diameter, using a 13-model American Heart Association (AHA) classification.

Interpretation

The prevalence of significant CAD in the patient population included was 50%. Almost 7% of the included coronary segments were classified as non-evaluable, but these segments were included in the comparative analysis. The authors found a sensitivity and a specificity of CT coronary angiography for detecting significant coronary stenoses on a per-segment level of 82 and 98%, respectively. The majority of the missed lesions were located in distal segments or side branches. The correct diagnosis of the presence or absence of significant lesions was achieved in 90% of the included patients. However, all significant lesions were found in only 72% of patients.

Comment

This was an important study introducing the concept of evaluation of the entire coronary tree with CT. The authors found a lower diagnostic performance of CT coronary angiography in smaller coronary segments. This observation is not surprising, as the spatial resolution of these CT scanners is significantly lower then that of conventional angiography. No threshold of a minimum lumen diameter was used for including segments in the comparative analysis, but coronary lesions located in segments with a lumen diameter that is beyond the resolution of CT will definitely be missed. However, one should realize that generally only coronary segments with a minimum diameter of at least 1.5 or 2 mm are amenable for coronary intervention. Thus, missed lesions below this threshold might not lead to differences in patient management and could be of less importance in the triage of patients who are being considered for revascularization therapy.

Improved diagnostic accuracy with 16-row multi-slice computed tomography coronary angiography

Mollet NR, Cademartiri F, Krestin GP, et al. J Am Coll Cardiol 2005; 45: 128–32

BACKGROUND

This was a prospective, single-centre study exploring the role of a second-generation CT scanner in a study population comprising patients with atypical chest pain and stable angina pectoris scheduled for conventional coronary angiography on an outpatient basis. The coronary arteries were divided into segments using a commonly used 15-segment AHA classification. Only segments with a mean lumen diameter of ≥2 mm were included. An oral dose of 100 mg of metoprolol was administered in patients with pre-scan heart rates above 70 beats/min, resulting in a heart rate of 57 beats/min during the scan.

INTERPRETATION

The prevalence of patients with significant CAD was 63%. The results of CT coronary angiography for detecting significant lesions on a per-segment, per-vessel and a per-patient level are summarized in Table 5. All available coronary segments ≥2 mm were included for comparison with conventional angiography, irrespective of image quality.

Table 5. Diagnostic performance of MSCT-CA for detection of ≥50% stenoses

	N	Sensitivity	Specificity	Positive PV	Negative PV
Segment-based	610	61/64 (95,86-99)	537/546 (98,96-99)	61/70 (87,76-98)	537/540 (99,98-99)
LM (1)	51	5/5 (100,47-100)	46/46 (100,92-100)	5/5 (100,47-100)	46/46 (100,92-100)
LAD (3-5)	205	24/24 (100,85-100)	175/181 (97,92-98)	24/30 (80,61-96)	175/175 (100,97-100)
CX (3-5)	172	15/17 (88,63-99)	154/155 (99,96-99)	15/16 (94,69-99)	154/156 (99,95-99)
RCA (3-4)	182	17/18 (94,72-99)	162/164 (99,95-99)	17/19 (90,66-99)	162/163 (94,96-99)
Vessel-based	202	51/53 (96,87-99)	143/149 (96,91-98)	51/57 (90,78-97)	143/145 (99,95-99)
LM	51	5/5 (100,47-100)	46/46 (100,92-100)	5/5 (100,47-100)	46/46 (100,92-100)
LAD	51	16/16 (100,79-100)	31/35 (89,73-96)	16/20 (80,56-95)	31/31 (100,88-100)
CX	50	13/14 (93,66-99)	35/36 (97,85-99)	13/14 (93,66-99)	35/36 (97,85-99)
RCA	50	17/18 (94,72-99)	31/32 (97,83-99)	17/18 (94,72-99)	31/32 (97,83-99)
Patient-based	51	31/31 (100,88-100)	17/20 (85,62-96)	31/34 (91,76-97)	17/17 (100,80-100)

PV = Predictive Value. Values are n (%, 95% confidence interval) *Source: Mollet et al. (2005).*

All patients with significant CAD were correctly identified on the CT scan, whereas three out of 20 patients without significant lesions were incorrectly classified as having significant CAD. An example of a patient with a significantly obstructed left anterior descending coronary artery is shown in Figure 2.

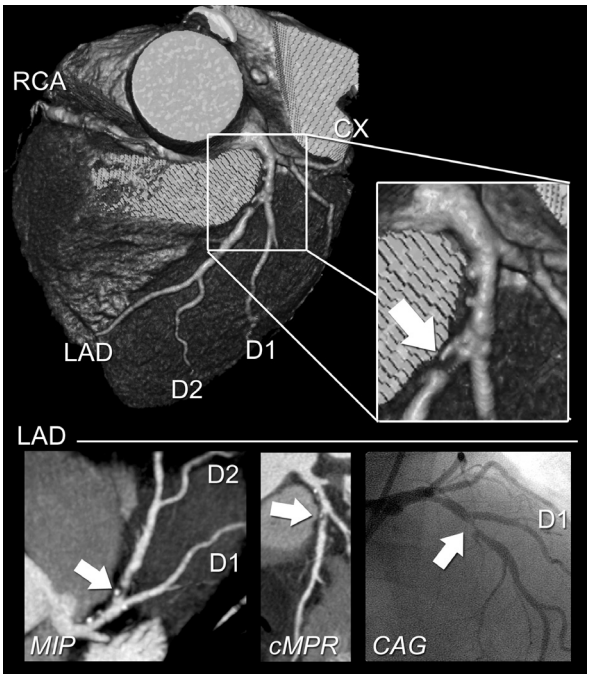

Figure2. Volume-rendered maximum intensity project and curved multiplanar reconstructed CT images demonstrate a significantly obstructed left anterior descending coronary artery (arrow) which was confirmed on conventional angiography. CX, circumflex coronary artery; D, diagonal branch; RCA, right coronary artery.
(A full color version of this illustration can be found in the color section (Chapter 21)).
Source: Mollet et al. (2005).

Comment

This study found a remarkably high sensitivity and specificity of CT coronary angiography in detecting significant lesions. In part, these results can be attributed to the improved scanner characteristics. The authors included all available segments with a minimum lumen diameter of 2 mm, a threshold that was frequently used in previous studies, thereby making it easier to compare the results of older studies then those presented by Kuettner et al. However, one should bear in mind that these results were obtained in a highly selected patient population comprising patients in sinus rhythm, able to breath hold for at least 20 s and who had never undergone coronary intervention or bypass surgery. Thus, the population included did not represent the normal patient population, which is generally older, has more advanced CAD and frequently suffers from atrial fibrillation and severe chronic obstructive pulmonary disease. However, this study showed that this scanner is one step further in the development of CT coronary angiography.

Section conclusion

Few data exploring the potential of CT coronary angiography using a second-generation 16-slice scanner are available. Despite an improved temporal resolution, the use of pre-scan β-blockers in patients with faster heart rates (≥70 beats/min) remains mandatory. An important issue is the fact that a higher X-ray tube current results in a significantly higher radiation exposure when compared to previous scanner generations. However, current available studies show a diagnostic accuracy that is significantly higher when compared to other non-invasive imaging techniques able to visualize the coronary arteries, e.g. electron beam CT and magnetic resonance imaging.

THE ROLE OF CORONARY CALCIUM ON THE DIAGNOSTIC PERFORMANCE OF 16-SLICE COMPUTED TOMOGRAPHY CORONARY ANGIOGRAPHY

High-density material, such as calcified plaques or metal stent struts, causes artefacts that result in several artefacts (blooming, partial volume, and beam hardening artefacts), which may hamper reliable visualization of the adjacent coronary lumen. Severe calcifications were reported as a major cause of missed coronary lesions on CT in the four-slice era.[1] Although these artefacts are reduced due to the improved through-plane spatial resolution offered by 16-slice CT scanners, over-projection of calcified plaques still remains. Several studies in which a non-enhanced calcium-scoring scan was performed prior to the angiographic scan have explored the influence of coronary calcifications on the diagnostic performance of CT coronary angiography. The total calcium burden can be quantified using dedicated software, which is often expressed as the total Agatston score. This scoring method is commonly used and calculates the total amount of calcium based on the number, areas and peak Hounsfield units of the detected calcified lesions. We selected two studies in which the diagnostic performance of CT coronary angiography for detecting significant lesions in patients with low and high calcium scores was assessed.

Non-invasive detection of coronary lesions using 16-detector multislice spiral computed tomography technology: initial clinical results

Kuettner A, Trabold T, Schroeder S, et al. J Am Coll Cardiol 2004; 44: 1230–7

BACKGROUND

This was a prospective, single-centre study in which CT coronary angiography was performed in 60 patients scheduled for conventional coronary angiography using a first-generation 16-slice scanner. The mean calcium score in the study population was an Agatston score of 506 ± 743. Twenty-two per cent of the included patients had a calcium score that was an Agatston score of ≥1.000, a threshold that was arbitrarily chosen to define patients with a high calcium score.

INTERPRETATION

Overall, 52 out of 75 significant stenoses were correctly classified on CT coronary angiography, resulting in a sensitivity and specificity of CT for detecting significant lesions of 72 and 97%, respectively. After the exclusion of patients with high calcium scores, 39 of the 40 remaining stenoses were correctly identified, resulting in a remarkably high sensitivity and specificity of 98% for both (Table 6).

Table 6. Lesion detection stenosis ≥50%

	All Segments	Patients With Ca score < 1,000
Patients (n)	60	46
Segments (n)	780	598
Lesions by CCA (n)	75	40
Correct positive lesions by MSCT(n)	54	39
False positve (n)	21	10
Sensitivity	0.72	0.98
Specificity	0.97	0.98
Positive predictive value	0.72	0.80
Negative predictive value	0.9 7	1.0

CCA = conventional coronary angiography,
MSCT = multislice computed tomography

COMMENT

This study showed that a high diagnostic performance of CT coronary angiography is achieved in patients with low-to-medium calcium scores. However, the observers applied an exclusion-driven rather then a detection-driven scoring algorithm, resulting in a low sensitivity, but an already very high specificity of CT for detecting significant lesions in the overall study population. Using such a scoring approach, severe calcifications are a major contributor of false-negative findings on the CT scan. However, one can argue that patients suspected of CAD may benefit more from an imaging technique with a high sensitivity for detecting significant lesions, as some patients would potentially be treated pharmacologically on the basis of the CT scan while coronary revascularization would have been indicated.

Impact of coronary calcium score on diagnostic accuracy for the detection of significant stenosis with multislice computed tomography coronary angiography

Cademartiri F, Mollet NR, Lemos PA, et al. Am J Cardiol 2005; 95: 1225–7

BACKGROUND

This was a single-centre study in which 120 patients who underwent both calcium scoring and CT coronary angiography retrospectively were enrolled in order to explore the diagnostic performance of a first-generation 16-slice CT scanner in patients with low and high calcium scores. The mean Agatston score for the overall population was 296 ± 578 and a total of 219 significant lesions were present.

Interpretation

The patient population was sorted into two groups and classified as having a low (mean Agatston score 14 ± 16) and high calcium score (mean Agatston score 578 ± 516) ($P < 0.001$). No significant differences were found in the overall sensitivity, specificity and positive and negative predictive values of CT coronary angiography for the detection of significant stenosis when compared to conventional coronary angiography. The sensitivity and specificity was 90 and 97% in patients with low calcium scores and 92 and 91% in patients with high calcium scores.

Comment

The observers applied a detection-driven scoring algorithm resulting in an overall high sensitivity and a somewhat lower specificity for detecting significant coronary lesions. This study showed that symptomatic patients with high calcium scores might still benefit from CT coronary angiography. Moreover, the role of calcium scoring as a gatekeeper for CT coronary angiography may be limited by the fact that patients with a similar calcium score but a different distribution among the coronary tree may have a different impact on the CT findings. However, direct comparison with the study of Kuettner et al. is very difficult, as different thresholds were used for defining patients with low and high calcium scores.

Section conclusion

Several studies have proposed a calcium-scoring scan as a gatekeeper for CT coronary angiography. Indeed, exclusion of significant coronary lesions can be difficult in patients with high calcium scores. In addition, patients with a high calcium score have an increased probability of significant CAD and may benefit less from non-invasive evaluation than patients with a lower probability of having significant lesions. The study of Cademartiri et al. showed that the sensitivity in detecting significant lesions remains high, even in patients with a high calcium score. However, it is known that severe calcifications are a major contributor of false-positive results on a CT scan. This has important implications in screening settings, as asymptomatic patients with only non-significant lesions would incorrectly be sent to conventional coronary angiography, which has a small but potentially life-threatening risk of procedure-related complications.

Conclusion

Promising results have been published using non-invasive 16-slice CT coronary angiography for detecting significant lesions as compared to conventional coronary angiography, which is currently the undisputable gold standard. However, several limitations still remain. Not all patients are suitable for being examined by CT coronary angiography. Patients need to be able to perform a sufficient breath hold manoeuvre and must have a stable heart rhythm. Thus, a persistent irregular heart rhythm such as frequent extra-systoles and atrial fibrillation (a common finding in the elderly patient population) preclude multislice CT coronary angiography. However, manual repositioning of the reconstruction windows can diminish motion artefacts caused by mild arrhythmia (e.g. a single ventricular extra-systole). The use of β-blockers in patients with high heart rates is still mandatory in the 16-slice era, but β-blockers cannot be applied in all patients.

The limited spatial resolution of current multislice CT scanners only allows qualitative assessment of coronary stenoses. Partial voluming and artefacts related to coronary calcifications seriously hamper the development of reliable software that is able to detect and quantify the degree of coronary stenoses. However, such software would make multislice CT coronary angiography a more robust and reproducible technique. The high radiation exposure related to CT coronary angiography is of concern. The radiation exposures of a second-generation 16-slice scanner using a high X-ray tube current were calculated as 11.8 (male) and 16.3 mSv (female), which is approximately three times the radiation exposure during conventional coronary angiography (see Mollet et al. (2005) reviewed above). The radiation exposure can be reduced by technical adjustments such as prospective X-ray tube current modulation. This technique reduces the radiation exposure by nearly 50% in patients with low heart rates, but is sensitive to arrhythmia and limits the possibility of reconstructing data sets during the end-systolic phase.[5] However, end-systolic data sets provide essential information in approximately one-third of patients. The high radiation exposure of CT coronary angiography compels physicians to select patients who might benefit from this technique carefully. It can be expected that the anatomical information of the coronary lumen provided by CT is complementary to the functional information of the myocardium provided by stress tests. Such studies are not yet available, but are needed in order to establish the true role of CT coronary angiography in the non-invasive work-up of patients suspected of having CAD.

Most recently, a new generation of CT scanners has been introduced, which render 64 slices/rotation and offer an unprecedented temporal and spatial resolution when compared to previous scanner generations. These scanners are rapidly being installed throughout the world and will soon become the standard in cardiac CT. Publication of initial studies exploring the potential of 64-slice CT coronary angiography can soon be expected and will most likely be the focus in the next edition of this book.

References

1. Kuettner A, Kopp AF, Schroeder S, Rieger T, Brunn J, Meisner C, Heuschmid M, Trabold T, Burgstahler C, Martensen J, Schoebel W, Selbmann HK, Claussen CD. Diagnostic accuracy of multidetector computed tomography coronary angiography in patients with angiographically proven coronary artery disease. J Am Coll Cardiol 2004; 43(5): 831–9.
2. Nieman K, Cademartiri F, Lemos PA, Raaijmakers R, Pattynama PM, De Feyter PJ. Reliable non-invasive coronary angiography with fast submillimeter multislice spiral computed tomography. Circulation 2002; 106(16): 2051–4.
3. Ropers D, Baum U, Pohle K, Anders K, Ulzheimer S, Ohnesorge B, Schlundt C, Bautz W, Daniel WG, Achenbach S. Detection of coronary artery stenoses with thin-slice multi-detector row spiral computed tomography and multiplanar reconstruction. Circulation 2003; 107(5): 664–6.
4. Hoffmann U, Moselewski F, Cury RC, Ferencik M, Jang IK, Diaz LJ, Abbara S, Brady TJ, Achenbach S. Predictive value of 16-slice multidetector spiral computed tomography to detect significant obstructive coronary artery disease in patients at high risk for coronary artery disease: patient-versus segment-based analysis. Circulation 2004; 110(17): 2638–43.
5. Trabold T, Buchgeister M, Kuttner A, Heuschmid M, Kopp AF, Schroder S, Claussen CD. Estimation of radiation exposure in 16-detector row computed tomography of the heart with retrospective ECG-gating. Rofo 2003; 175(8): 1051–5.

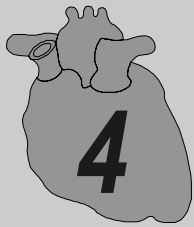

Chapter 4

IV CONTRAST ADMINISTRATION FOR CT CORONARY ANGIOGRAPHY ON MULTIDETECTOR-ROW HELICAL CT: IMPACT OF IODINE CONCENTRATION ON VASCULAR ATTENUATION

Abstract

125 patients undergoing retrospectively ECG-gated 16-MDCT coronary angiography were prospectively randomized into five groups with respect to the IV administration of a 140ml bolus of contrast material (CM) at 4ml/s: group 1 (Iohexol 300mgI/ml), group 2 (Iodixanol 320mgI/ml), group 3 (Iohexol 350mgI/ml), group 4 (Iomeprol 350mgI/ml), group 5 (Iomeprol 400mgI/ml). The attenuation was measured in the descending aorta and in the coronary arteries. A one-way ANOVA test was used to compare groups.

The mean attenuation values in descending aorta were significantly ($p<0.05$) lower in group 1 and higher in group 5 compared to the other 3 groups. The same pattern was observed in the coronary arteries.

CM with higher iodine concentration provides significantly higher attenuation in the descending aorta and in the coronary arteries.

Filippo Cademartiri [1]
Nico R. Mollet [1,2]
Aad van der Lugt [1]
Eugene McFadden [2]
Theo Stijnen [3]
Pim J de Feyter [1,2]
Gabriel P Krestin [1]

From the Departments of Radiology[1], Cardiology[2], and Epidemiology and Biostatistics[3]
Erasmus M C,
University Medical Center
Rotterdam ,
The Netherlands.

Radiology; 2005 (in press)

INTRODUCTION

Current data suggest that significant coronary artery stenosis can be detected with 16-multidetector-row computed tomography (16-MDCT) angiography[1-5]. The increased number of detector rows and faster gantry rotation with 16-MDCT compared to the previous 4-MDCT generation have improved the diagnostic performance of the technique and reduced the time needed to cover the entire heart to ~20s[3]. The type and iodine concentration of contrast material (CM) has assumed increasing importance in CT angiography (CTA) to optimize the diagnostic yield[6] as the attenuation that can be achieved in the vessels greatly affects image quality[7,8]. These considerations are even more important for coronary arteries. Their small caliber, tortuous anatomy, and often extensive vessel wall disease may require a better optimization.

Two main modulable factors affect the attenuation: techniques that optimize synchronization between the arterial passage of CM and CT data acquisition, and the injection parameters for intravenous (IV) administration of CM[6].

For optimal synchronization bolus tracking technique can be effectively applied[9]. For injection parameters, there are several variables that can be manipulated to increase vascular attenuation: the rate of injection, the volume injected and the iodine concentration of CM[6]. Thus, the purpose of our study was to prospectively compare the effect on vascular attenuation at the level of the descending aorta and the coronary arteries of a scan protocol with different concentrations of three different CM.

Materials and Methods

Patients and Contrast Agents

Between March and September 2003, 125 patients (104 male and 21 female; mean age: 59±12 years) scheduled for 16-MDCT coronary angiography were prospectively studied. All patients meeting the inclusion criteria (stable angina pectoris, a stable heart rhythm, and able to hold their breath for 20s) referred from our institution or our referring hospitals, were enrolled. Exclusion criteria were: previous allergic reaction to iodinated CM, renal impairment (serum creatinine >120mmol/L); women of child bearing age who were not taking adequate contraception were also excluded. Our Institutional Review Board approved the study and all patients gave written informed consent.

After enrollment, patients were randomized using a table of random numbers into five groups (n=25 each): group 1 (Iohexol 300mgI/ml), group 2 (Iodixanol 320mgI/ml), group 3 (Iohexol 350mgI/ml), group 4 (Iomeprol 350mgI/ml), group 5 (Iomeprol 400mgI/ml). The molecule of CM was Iohexol (Omnipaque®, Amersham Health, Little Chalfont, UK) for Group 1 and Group 3, Iodixanol (Visipaque®, Amersham Health, Little Chalfont, UK) for Group 2, and Iomeprol (Iomeron® Bracco, Milan, Italy) for Group 4 and 5 (Table I). Iomeron 400 (Bracco, Milan, Italy) is not FDA approved for the use I the United States. The injection volume (140ml) and rate (4ml/s) were constant in all groups. In each patient age, gender, body weight and heart rate during the scan were recorded.

Scan protocol

Studies were performed on a 16-MDCT scanner (Sensation 16, Siemens Medical Solutions, Forchheim, Germany). Prior to the examination the heart rate (HR) was measured.

Patients with a pre-scan HR equal or above 65 bpm, were administered 100 mg of metoprolol orally one hour before the scan.

The CM was injected using a power injector (EnVision, MedRAD, Pittsburgh, PN, USA) through a 18G cannula in an antecubital vein. Contrast material volume and injection rate were respectively 140 ml and 4 ml/s (total injection time of 35s) in all patients. In all groups except group 1 (Iohexol 300mgI/ml), the CM was administered after heating at 37° C. This procedure kept the viscosity of the 5 CM within 7.5 and 11.8 cP.

Table 1. Physical properties of the different contrast materials.

	Group 1	Group 2	Group 3	Group 4	Group 5
Contrast material	Iohexol	Iodixanol	Iohexol	Iomeprol	Iomeprol
Commercial name	Omnipaque®	Visipaque®	Omnipaque®	Iomeron®	Iomeron®
Vendor	Amersham	Amersham	Amersham	Bracco	Bracco
Type	Monomeric	Dimeric	Monomeric	Monomeric	Monomeric
Iodine concentration (mgI/ml)	300	320	350	350	400
Osmolality (mOsm/kg water)	672	290	844	618	726
Absolute viscosity 20° C (cP)	11.8	26.6	20.4	14.5	27.5
Absolute viscosity 37° C (cP)	6.3	11.8	10.4	7.5	12.6
Iodine load (g)*	42	44.8	49	49	56
Iodine rate (g/s)*	1.2	1.28	1.4	1.4	1.6

*Using a protocol with a volume of 140ml administered at 4ml/s.
Abbreviations: cP = centiPascal; g = gram; kg = kilogram; mgI = milligrams of iodine; ml = millilitres; mOsm = milliOsmole; s = seconds.

To synchronize the start of the scan with the arrival of CM a real-time bolus tracking technique was applied[9]. This technique is based on real time monitoring of the main bolus during injection with a series of dynamic low dose monitoring scans (120 kV, 20mAs) at the level of the vessel of interest. The monitoring scan was performed at the level of the ascending aorta. A ROI as large as the aortic root was plotted. The dynamic monitoring scans started 10s after the beginning of injection of intravenous contrast material. The trigger threshold inside the ROI was set at +100HU above the baseline (~140-160HU in absolute value). The delay between each monitoring scan was 1.25s. As soon as the threshold was reached the table moved to the cranial start position while the patient was instructed to take a deep breath and hold it. During this interval (4s which were necessary to give to patient breath-hold instruction safely), the contrast material concentration increased up to the desired level of enhancement.

The main scan parameters were: number of detectors 16, individual detector width 0.75 mm, gantry rotation time 420 ms, kV 120, mAs 400, feed/rotation 3.0 mm, feed/second 8.0, scan direction cranio-caudal. For the purpose of the present study, two datasets were reconstructed, both with retrospective ECG gating with time window starting

at 400 ms before the next R wave on the ECG, FOV 200 mm, and a medium smooth convolution filter (B30f). The first dataset (dataset A) was reconstructed with an effective slice width and a reconstruction interval of 3mm and 3mm, respectively; the second dataset (dataset B) was reconstructed with an effective slice width and a reconstruction interval of 1mm and 0.6mm, respectively. The images were transferred to a stand-alone workstation and evaluated using dedicated analysis software (Leonardo, Siemens Medical Solutions, Forchheim, Germany).

Data collection and analysis

One radiologist with four years of experience in CTA (F.C.), collected all the measurements at the workstation.

Two sets of measurements were performed:

1) the attenuation in the descending aorta, and
2) in the coronary arteries.

In order to generate a time-attenuation curve of the descending aorta during the angiographic scan, the attenuation values in HU were extracted from the dataset A as follows. The DICOM layout of the images allowed reading the exact time (down to hundreds of sec^{-1}) of the data acquisition in each reconstructed slice. At intervals of 1 second, in each slice, a rounded ROI was drawn (90% of the aortic area, always avoiding disease of the aortic wall such as calcifications and plaques), throughout the entire data-set in the descending aorta. The variable individual morphology resulted in different scan times as well as in different length of the ROIs along the z-axis. Time-related contrast measurements available in all patients were included in the study.

The mean value (±SD) at each time point in the descending aorta was calculated by averaging the attenuation values. To display the attenuation during time, time/attenuation curve was generated. The start of the scan was designated as time 0. The mean (±SD) attenuation for all the time points of the time-attenuation curve was calculated.

Dataset B was used to measure the attenuation at the origin of the main coronary artery branches. This dataset has, in fact, a higher spatial resolution in the z-axis allowing to measure structures with a diameter of 3-5mm. A ROI (90% of the coronary vessel area), was plotted on the axial image as large as the vessel lumen on a slice where the lumen was easily identified. Regions where there were calcifications in the coronary wall and non-calcified plaques were carefully avoided. Four vessels were studied: left main coronary artery (LM), left anterior descending coronary artery (LAD), left circumflex (CX), and right coronary artery (RCA). The attenuation value in HU was measured on axial images on the dataset B. The mean (±SD) value per patient was calculated by averaging the attenuation values obtained in the four coronary vessels.

Statistical Analysis

The statistical analysis was performed using SPSS 10.1.0 (SPSS Inc., Chicago IL, USA). To rule out significant differences between the two sample populations, an ANOVA test was applied to the following parameters: age, weight, mean HR during the scan. A $p<0.05$ was considered significant.

Interval attenuation data were expressed as mean±standard deviation, minimum and maximum.

Differences between groups were assessed with a one-way ANOVA test followed by Fischer's LSD procedure to compare all pairs of groups. A $p<0.05$ was considered significant.

Interdependency between measurements

In order to address to problem of inter-dependency of the measurements between different vessels the following analysis was performed[9]. For each coronary vessel, the average attenuation was subtracted in the five groups and the differences obtained were compared using an ANOVA-test. A $p<0.05$ indicated low interdependency, while a $p<0.01$ indicated no interdependency.

RESULTS

Baseline characteristics such as age, gender, weight, and heart rate did not differ significantly among the five groups ($p>0.05$). No relevant differences were observed in the scan delay and scan duration between the five groups (Table II). A single immediate adverse reaction to CM that required treatment was recorded in a patient who received Iomeprol 350mgl/ml. The patient was discharged after 2 hours on oral treatment (anti-histaminic and corticosteroid) and his subsequent course was uneventful.

Table 2. Baseline demographic data and protocol information in the study population.

	Group 1	Group 2	Group 3	Group 4	Group 5
Number of patients		25	25	25	25
Male/Female	22/3	20/5	21/4	21/4	20/5
Mean age (yrs)	63±12	57±11	58±13	60±11	58±11
Weight (kg)	71±8	74± 9	72±7	72±7	74±7
Mean heart rate (bpm)	57±8	60±9	61±9	59±7	59±8
Scan delay (seconds)	21.9±3.7	20.7±2.7	21.4±2.8	22.1±2.2	20.6±3.0
Scan duration (seconds)	16.8±2.1	17.2±1.7	17.6±1.3	17.7±2.0	17.6±2.1

No relevant differences between the groups were found.
Abbreviations: yrs= years; kg= kilogram; bpm= beats per minute.

In the descending aorta (Table III and Figure 1), the mean attenuation in group 1 (277±41HU) and group 5 (386 ±78HU) was significantly lower and higher, respectively, compared to all the remaining groups ($p<0.05$).

In the coronary arteries (Table IV), the mean coronary artery attenuation was significantly lower in group 1 (273±45HU) and significantly higher in group 5 (397±72HU), respectively, compared to the remaining groups ($p<0.05$).

The minimum and maximum attenuation values followed the same pattern of variation as the average attenuation (see Table III and IV).

Table 3. Parameters of the attenuation curve in the study population.

	Descending Aorta				
	Group 1	Group 2	Group 3	Group 4	Group 5
Average (HU)	277±41* (179-394)	333±50 (226-473)	315±54 (222-530)	318±42 (209-511)	386±78* (211-656)

Values significantly different ($p<0.05$) from the other groups are highlighted with *.
Between brackets the minimum and maximum attenuation value.
Abbreviations: HU= Hounsfield Units.

Table 4. Attenuation values in the coronary arteries in the study population.

	Group 1	Group 2	Group 3	Group 4	Group 5
Mean (HU)	273±45* (163-379)	333±51 (225-477)	320±55 (234-505)	322±43 (192-416)	397±72* (268-596)

Values significantly different ($p<0.05$) from the other groups are highlighted with *.
Between brackets the minimum and maximum attenuation value.
Abbreviations: HU= Hounsfield units.

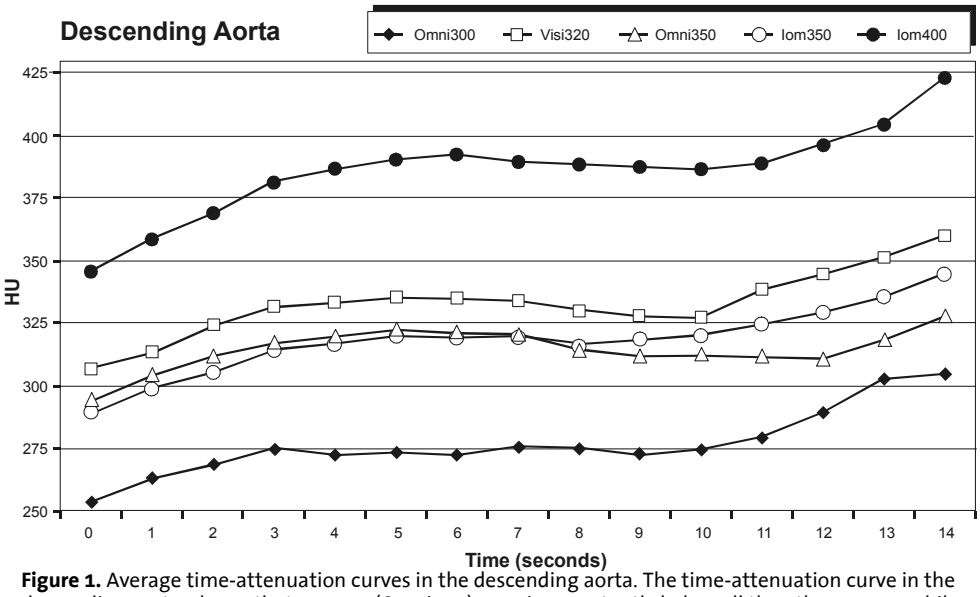

Figure 1. Average time-attenuation curves in the descending aorta. The time-attenuation curve in the descending aorta, shows that group 1 (Omni300) remains constantly below all the other groups while group 5 (Iom400) remains constantly above the all the others. The other groups (Vis320, Omni350, and Iom350) show a comparable attenuation.

Interdependency between measurements

The results of the analysis for interdependency showed high interdependency between LAD and CX, while lower degrees of interdependency were found between all the other combinations of vessels.

DISCUSSION

Imaging of coronary artery suffers from their small size and from stenosis and/or obstruction that reduce the blood flow. A higher iodine concentration in this case allows to depict a vessel which contains a smaller volume of blood[7, 8]. Becker *et al.* considered an attenuation of 250-300HU as optimal for coronary CT angiography[10]. On one hand it is reasonable to expect that a higher attenuation would progressively obscure coronary calcifications, on the other hand there is no available validation data supporting the statement. In fact, we agree with Becker *et al*[10] and we believe that the imaging of coronary calcium and plaques need a rather different approach with CT, than the one required for the assessment of significant stenosis. In the first instance the lumen is less important and therefore a too high attenuation (>300HU) may compromise the assessment of coronary wall. In the second instance, instead, the visualization of the lumen is more important as a higher attenuation may improve the visualization of small coronary vessels.

Only a few studies in animals have examined the impact of different types of CM at different concentrations on image quality during CTA and only one such study was performed in the human coronary circulation. These studies demonstrated that, for a given volume of CM administered at the same rate, higher iodine concentration results in a proportionally higher peak of maximum enhancement without significantly affecting the time to peak of enhancement[11,12].

Recent papers discuss the role of higher iodine concentration for CTA[13-16]. Increasing iodine concentration provide a proportionally higher vascular attenuation[13]. Similarly, an increasing injection rate provides a progressively higher vascular attenuation[13]. The iodine administration rate can be modified more easily by changing the CM injection rate rather than changing the CM iodine concentration. Unfortunately, the injection rates that are feasible in routine clinical practice are up to 4-5 ml/s. Higher injection rates would require larger needles and larger veins, requiring more time to set the IV and a potentially increased risk of CM extra-vasation.

Although iodine concentration is not as effective as injection rate in increasing intra-vascular attenuation, it is always feasible in any condition.

A study from Becker *et al.* compared different iodine concentration (Iomeprol 300 and 400 mgI/ml) and injection rates (2.5 and 3.5 ml/s) while performing 4-MDCT angiography of coronary arteries[10]. The conclusion was that vascular attenuation achieved with 400mgI/ml and 3.5ml/s was significantly higher than the other protocols and that 300mgI/ml and 2.5ml/s provide significantly lower attenuation compared to the other protocols and also insufficient for optimal coronary angiography (range: 148-194HU in the coronary arteries). Based on the results, the authors also conclude that an injection rate of 1gI/s provide the desired iodine load to achieve and maintain the target enhancement.

Our study shows the progressively higher vascular attenuation obtained with higher iodine concentrations[6]. A significant difference was observed between the groups using the two CMs at the extremes of the spectrum of iodine concentration and the remaining groups. Vascular attenuation was not significantly different between monomeric compounds with an iodine concentration of 350mg/ml (iohexol and iomeprol) and the dimeric compound with an iodine concentration of 320 mg/ml (iodixanol). Following the target attenuation applied by Becker *et al.* for optimal coronary angiography all of these three compounds with the protocol applied ranged in the optimal value[10].

A limitation of the study is related to the evaluation of coronary arteries. Ideally the best way to assess the efficacy of a CM protocol would be to measure the length of coronary arteries, and the number of side branches that can be visualized. We preferred to assess quantitatively the origin of the main coronary arteries because the number of patients was too small to account for the many variables that can affect coronary artery visualization regardless of the attenuation of the vessel: the high heart rate, the small vessel size, the variable anatomy, the heavily calcified vessel wall, the presence of stenosis or occluded vessels.

Moreover, the aim of the study was to show the performance of different CM in terms of vascular attenuation and not the effect of vascular attenuation on diagnostic accuracy. In conclusion, the use of CM with higher iodine concentration provides progressively higher vascular attenuation in coronary angiography with 16-MDCT.

References

1. Nieman K, Cademartiri F, Lemos PA, Raaijmakers R, Pattynama PM, de Feyter PJ: Reliable noninvasive coronary angiography with fast submillimeter multislice spiral computed tomography. Circulation 2002; 106:2051-4.
2. Ropers D, Baum U, Pohle K, Anders K, Ulzheimer S, Ohnesorge B, Schlundt C, Bautz W, Daniel WG, Achenbach S: Detection of coronary artery stenoses with thin-slice multi-detector row spiral computed tomography and multiplanar reconstruction. Circulation 2003; 107:664-6.
3. Heuschmid M, Kuttner A, Flohr T, Wildberger JE, Lell M, Kopp AF, Schroder S, Baum U, Schaller S, Hartung A, Ohnesorge B, Claussen CD: [Visualization of coronary arteries in CT as assessed by a new 16 slice technology and reduced gantry rotation time: first experiences]. Rofo 2002; 174:721-4.
4. Flohr T, Stierstorfer K, Bruder H, Simon J, Schaller S: New technical developments in multislice CT - Part 1: Approaching isotropic resolution withsub-millimeter 16-slice scanning. Rofo 2002; 174:839-45.
5. Flohr T, Bruder H, Stierstorfer K, Simon J, Schaller S, Ohnesorge B: New Technical Developments in Multislice CT, Part 2: Sub-Millimeter 16-Slice Scanning and Increased Gantry Rotation Speed for Cardiac Imaging. Rofo 2002; 174:1022-7.
6. Cademartiri F, van der Lugt A, Luccichenti G, Pavone P, Krestin GP: Parameters affecting bolus geometry in CTA: a review. J Comput Assist Tomogr 2002; 26:596-607.
7. Bae KT, Heiken JP, Brink JA: Aortic and hepatic peak enhancement at CT: effect of contrast medium injection rate--pharmacokinetic analysis and experimental porcine model. Radiology 1998; 206:455-64.
8. Fleischmann D, Rubin GD, Bankier AA, Hittmair K: Improved uniformity of aortic enhancement with customized contrast medium injection protocols at CT angiography. Radiology 2000; 214:363-71.

9. Cademartiri F, Nieman K, van der Lugt A, Raaijmakers RH, Mollet N, Pattynama PM, de Feyter PJ, Krestin GP: IV contrast administration for CT coronary angiography on a 16-multidetector-row helical CT scanner: test bolus vs. bolus tracking. Radiology 2004; (in press):XXX-XXX.
10. Becker CR, Hong C, Knez A, Leber A, Bruening R, Schoepf UJ, Reiser MF: Optimal Contrast Application for Cardiac 4-Detector-Row Computed Tomography. Invest Radiol 2003; 38:690-694.
11. Han JK, Kim AY, Lee KY, Seo JB, Kim TK, Choi BI, Lhee CS, Han MC: Factors influencing vascular and hepatic enhancement at CT: experimental study on injection protocol using a canine model. J Comput Assist Tomogr 2000; 24:400-6.
12. Bluemke DA, Fishman EK, Anderson JH: Effect of contrast concentration on abdominal enhancement in the rabbit: spiral computed tomography evaluation. Acad Radiol 1995; 2:226-31.
13. Fleischmann D: Use of high concentration contrast media: principles and rationale-vascular district. Eur J Radiol 2003; 45 Suppl 1:S88-93.
14. Brink JA: Use of high concentration contrast media (HCCM): principles and rationale--body CT. Eur J Radiol 2003; 45 Suppl 1:S53-8.
15. Brink JA: Contrast optimization and scan timing for single and multidetector-row computed tomography. J Comput Assist Tomogr 2003; 27 Suppl 1:S3-8.
16. Merkle EM, Boll DT, Fenchel S: Helical computed tomography of the pancreas: potential impact of higher concentrated contrast agents and multidetector technology. J Comput Assist Tomogr 2003; 27 Suppl 1:S17-22.

Chapter 5

NON-INVASIVE 16-ROW MULTISLICE CT CORONARY ANGIOGRAPHY: USEFULNESS OF SALINE CHASER

Abstract

The aim of this study was to investigate the usefulness of saline chaser in 16-row multislice CT (16- MSCT) coronary angiography. Forty-two patients were divided into two groups for contrast material (CM) administration: group 1 (140 ml at 4 ml/s) and group 2 (100 ml at 4 ml/s followed by 40 ml of saline chaser at 4 ml/s). All patients underwent retrospectively ECG-gated 16-MSCT coronary angiography. The attenuation at the origin coronary vessels was assessed. Three regions of interest (ROIs) were drawn throughout the data set: (a) ascending aorta (ROI 1); (b) descending aorta (ROI 2); and (c) pulmonary artery (ROI 3). The attenuation in the superior vena cava was recorded (ROI 4). The average attenuation and the slope were calculated in each ROI and differences were assessed with a Student's *t* test. The average attenuation in the coronary vessels was not significantly different in the two groups. The average attenuations in ROI 1 were 325 and 327 HU, in ROI 2 were 328 and 329 HU and in ROI 3 were 357 and 320 HU, for groups 1 and 2, respectively ($p>0.05$). The slopes in ROI 1 were -0.2 and 1.1, in ROI 2 were 2.8 and 2.1 ($p>0.05$) and in ROI3 were 3.9 and -9.0 ($p<0.05$), for groups 1 and 2, respectively. The average attenuations in ROI 4 were 927 and 643 HU ($p<0.05$), for groups 1 and 2, respectively. One hundred milliliters of CM with 40 ml of saline chaser provides the same attenuation as 140 ml of CM (35% less) with decreased hyper-attenuation in the superior vena cava.

Filippo Cademartiri [1]
Nico R. Mollet [1,2]
Aad van der Lugt [1]
Koen Nieman [1,2]
Peter MT Pattynama [1]
Pim J de Feyter [1,2]
Gabriel P Krestin [1]

From the Departments of Radiology [1] and Cardiology [2], Erasmus M C, University Medical Center Rotterdam , The Netherlands.

European Radiology, 2004; 14:178–183.

Usefulness of saline chaser in CT coronary angiography

INTRODUCTION

Multislice-CT scanners with 16 rows of detectors (16-row MSCT) and increased spatial and temporal resolution have been introduced.[1-3] The increased number of detector rows and gantry rotation speed reduce the time needed to scan the coronary arteries to <20 s.[3] Early experiences reported improved results in the visualisation of coronary arteries and in the detection of coronary artery disease.[3-6]

The shorter scan time, provided by 16-row MSCT, allows to decrease the volume of contrast material (CM) needed for CT coronary angiography (CTA).[7] Moreover, bolus-tracking technique can be easily applied which allows a better synchronisation of the CTA scan with contrast material passage.[4, 7-12]

The use of a saline solution injected intravenously immediately after the CM main bolus, also known as bolus chaser, has been reported to allow a significant reduction of CM volume with vascular attenuation comparable with the one obtained with larger volumes of CM.[13-15] It is expected that the use of bolus chaser also allows CM volume reduction in MSCT coronary angiography.[16-18]

The aim of this study was the comparison of a "conventional" CM protocol without bolus chaser with a "low-volume" protocol with bolus chaser in non-invasive 16-row MSCT coronary angiography.

MATERIALS AND METHODS

Patient population

In November and December 2002, 42 patients (30 men and 12 women; mean age 59 years, age range 34–79 years), undergoing non-invasive MSCT coronary angiography for suspected coronary artery disease were prospectively enrolled in the study. Exclusion criteria for coronary CTA were irregular heart rates, previous allergic reaction to iodine contrast media, renal insufficiency (serum creatinine >120 mmol/l), pregnancy, respiratory impairment, unstable clinical status, or marked heart failure. The Institutional Review Board approved the study and patients gave informed consent.

After enrollment, patients were randomly divided into two groups with different protocols for intravenous contrast material (Visipaque 320 mg I/ml, Amersham Health, Little Chalfont, UK) administration: group 1 (conventional) 140 ml administered at 4 ml/s and group 2 (low-volume) 100 ml at 4 ml/s followed by 40 ml of saline at 4 ml/s. In each patient, age, body weight and heart rate were recorded.

Multislice-CT scan

Prior to the examination, the patients' heart rate (HR) was measured. Patients with a pre-scan HR ≥65 bpm were given 100 mg of metoprolol per os 1 h before the scan.

The scan parameters for MSCT coronary angiography (Sensation 16, Siemens, Forchheim, Germany) were: number of detectors 12; individual detector width 0.75 mm; gantry rotation time 420 ms; 120 kV; 400–500 mAs; feed/rotation 2.8 mm; and scan direction cranio-caudal. The heart rate during the scan was also recorded. Contrast material administration and synchronisation protocols The iodinated CM was administered intravenously using a prototype of double-head power injector (Stellant, MedRAD, Pittsburgh, Pa.) through an 18-G venflon in the antecubital vein. Two different injection

protocols were applied.

Synchronisation between the passage of CM and data acquisition was achieved with real-time bolus tracking (CARE bolus, Siemens, Forchheim, Germany) using an ROI in the ascending aorta for monitoring a threshold of +100 HU above the baseline attenuation to trigger the scan.

Data collection

Two data sets were reconstructed using retrospective ECG gating with time window starting 400 ms before the next R wave. The first data set was reconstructed for the purpose of coronary artery attenuation assessment with effective slice width 1 mm, reconstruction interval 0.5 mm, field of view (FOV) 160 mm and convolution filter medium smooth. The second data set was reconstructed for the purpose of great thoracic vessel assessment with effective slice width 3 mm, reconstruction interval 3 mm, FOV 200 mm and convolution filter medium smooth.

Coronary artery attenuation

Axial slices in the data set were scrolled to find the best location to measure the attenuation at the origin of the main coronary arteries (Fig. 1): left main coronary artery; left anterior descending; circumflex artery; and right coronary artery (RCA).

The ROI was Fig. 1A–E Assessment of attenuation at the origin of coronary vessels. In A and B two oblique para-axial maximum intensity projection reconstructions show the ascending aorta (Ao), the origin of the right coronary artery (RCA; arrow) and left main coronary artery (LM; arrow). The superior vena cava (SVC) is also shown with very high attenuation. The assessments of attenuation at the origin of the main coronary arteries are performed for RCA (asterisk), for LM (asterisk), for the left anterior descending (LAD; asterisk) and for the circumflex (CX; asterisk) as shown in C, D and E, respectively. RA right atrium, RVOT right ventricle outflow tract drawn as large as possible and calcifications, plaques and stenosis were carefully avoided.

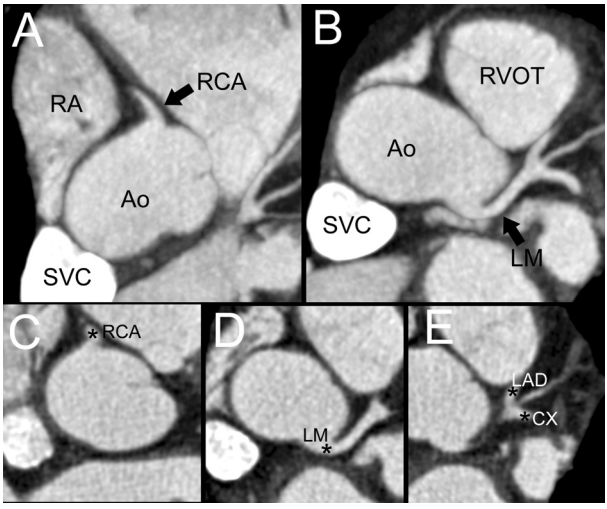

Figure 1A–E. Assessment of attenuation at the origin of coronary vessels. In A and B two oblique para-axial maximum intensity projection reconstructions show the ascending aorta (Ao), the origin of the right coronary artery (RCA; arrow) and left main coronary artery (LM; arrow). The superior vena cava (SVC) is also shown with very high attenuation. The assessments of attenuation at the origin of the main coronary arteries are performed for RCA (asterisk), for LM (asterisk), for the left anterior descending (LAD; asterisk) and for the circumflex (CX; asterisk) as shown in C, D and E, respectively. RA right atrium, RVOT right ventricle outflow tract

Bolus geometry of great vessels

The attenuation in Hounsfield units was measured in three arteries drawing a ROI in consecutive slices (at intervals of ~1 s.) through the data set (Fig. 2): (a) the ascending aorta–left ventricle (ROI 1); (b) the descending aorta (ROI 2); and (c) the pulmonary artery– right ventricle (ROI 3). In addition, the attenuation inside the superior vena cava (ROI 4) at the beginning of the scan (e.g. first slice of the data set) was recorded. Time-related contrast measurements for each vessel, which were available in all patients, were included in the study to maintain homogeneous results.

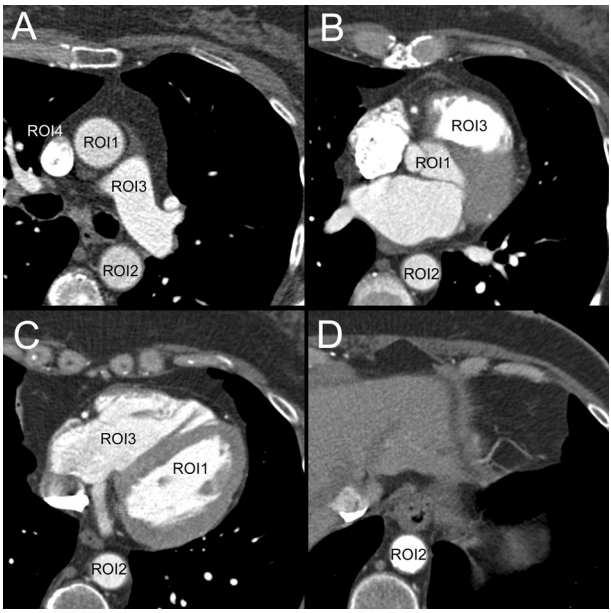

Figure 2A–D. Assessment of bolus geometry through the data set. The assessment of bolus geometry in the great vessels of the thorax have been performed using four regions of interest (ROIs). A, B The first (ROI1) is located in the ascending aorta at the beginning of the scan, whereas C the second part follows the path of the contrast material into the left ventricle. A–D The second ROI (ROI2) is located in the descending aorta all through the data set. A The third ROI (ROI3) is located in the pulmonary artery at the beginning of the scan, and then B follows into the right ventricle outflow tract and C into the right ventricle. The fourth ROI (ROI4) is plotted into the superior vena cava at the beginning of the scan

Data analysis

The attenuation values obtained from the three ROIs in each patient were averaged at each time point to generate the average time/density curves. Bolus geometry was described by two parameters, which represented quantitatively, the amount of CM present in the vessel during the scan (average attenuation) and the pattern of enhancement in the vessel (slope of attenuation). Three additional parameters were considered descriptive of bolus geometry: the attenuation value at the beginning of the scan (time 0), the Fig. 2A–D Assessment of bolus geometry through the data set. The assessment of bolus geometry in the great vessels of the thorax have been performed using four regions of interest (ROIs). A, B The first (ROI1) is located in the ascending aorta at the beginning of the scan, whereas C the second part follows the path of the contrast material into the left ventricle. A–D The second ROI (ROI2) is located in the descending aorta all through the data set. A The third ROI (ROI3) is located in the pulmonary artery at the beginning of the scan, and then B follows into the right ventricle outflow tract and C into the right ventricle. The fourth ROI (ROI4) is plotted into the superior vena cava at the beginning of the scan maximum enhancement value (MEV; the peak of attenuation) and the time to reach the MEV (tMEV).

Significant differences between the two groups were assessed using Student's *t* test. A p value <0.05 was considered significant.

RESULTS

Scans and bolus timing procedures were successfully completed in all patients. No significant adverse reactions to CM were observed. Age, weight, mean heart rate during the scan, mean scan delay and mean scan time were not significantly different in the two groups (Table 1).

Table 1. Patient data

	Group 1	Group 2
No. of patients	21	21
Male/female	16/5	14/7
Mean age (years)	59 (34–74)*	59 (39–79)*
Mean weight (kg)	72 (53–90)*	74 (60–95)*
Mean heart rate (bpm)	60 (48–72)*	60 (49–80)*
Mean scan delay (s)	21.5±1.7	20.9±2.3
Mean scan time (s)	17.9±0.9	18.2±1.6

No significant differences were detected between the two groups (p>0.05)
*Range in parentheses

Coronary artery attenuation

The attenuation at the origin of the four main coronary vessels was higher in group 1, but there was not a significant difference between the two groups (Fig. 3A; Table 2).

Table 2. Coronary vessel attenuation. LM left main, LAD left anterior descending, CX circumflex, RCA right coronary artery

	Group 1	Group 2
LM	324±45	319±46
LAD	318±46	312±42
CX	313±41	304±37
RCA	321±42	319±46

Measurements are in Hounsfield units
The mean density (±SD) at the origin of coronary vessels for group 1 (conventional 140-ml protocol) and group 2 (low-volume protocol with bolus chaser) shows no significant differences (p>0.05)

Ascending aorta-left ventricle The average attenuation and the slope were slightly higher in group 2 but not significantly different (p>0.05; Fig. 3B; Table 3).
The attenuation values at time 0, the MEV and the tMEV were slightly higher in group 2 but not significantly different (p>0.05).

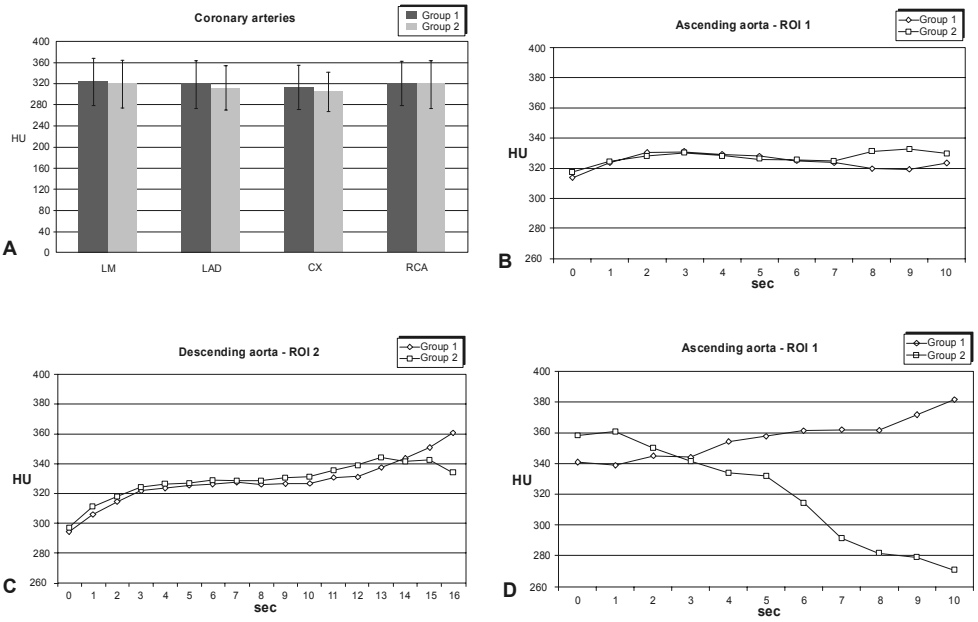

Figure 3A–D. Results of attenuation assessment of coronary arteries and great thoracic vessels. A The results of the attenuation assessment at the level of coronary arteries show slightly lower values for group 2 but not significantly different in all four sample regions. B, C The average time/density curves in the ascending aorta and descending aorta are almost identical for groups 1 and 2. D For the pulmonary artery, instead, group 1 shows more "pooling" of contrast material in the right chambers of the heart

Table 3. Bolus geometry in the great vessels of the thorax. MEV maximum enhancement value, tMEV time to reach the MEV

	Ascending aorta			Descending aorta			Pulmonary artery			Superior vena cava		
	Group 1	Group 2	p value	Group 1	Group 2	p value	Group 1	Group 2	p value	Group 1	Group 2	p value
Average (HU)	325±39	327±48	>0.05	328±49	329±55	>0.05	357±73	320±81	>0.05	927±89	643±170	<0.05
Slope	-0.2	1.1	>0.05	2.8	2.1	>0.05	3.9	-9.0	<0.05	-	-	-
Time 0 (HU)	314±36	318±48	>0.05	295±32	298±44	>0.05	341±62	359±67	>0.05	-	-	-
MEV (HU)	350±40	356±56	>0.05	373±64	374±79	>0.05	422±74	409±88	>0.05	-	-	-
tMEV (s)	4.2±1.7	5.4±3.1	>0.05	14.0±3.0	10.7±4.4	<0.05	6.4±3.5	2.8±3.0	<0.05	-	-	-

The quantitative parameters of bolus geometry for the main vessels of the thorax are displayed for group 1 (conventional 140-ml protocol) and group 2 (low-volume protocol with bolus chaser)

Descending aorta
The average attenuation and the slope were slightly higher in group 2 but not significantly different ($p>0.05$; Fig. 3C; Table 3). The attenuation values at time 0 and the MEV were slightly higher in group 2 but not significantly different ($p>0.05$). The tMEV was significantly higher in group 1 ($p<0.05$).

Pulmonary artery–right ventricle
The average attenuation was higher in group 1 but not significantly different ($p>0.05$; Fig. 3D; Table 3). The slope, instead, was significantly higher in group 1 ($p<0.05$). The attenuation values at time 0 and the MEV were not significantly different between the two groups ($p>0.05$). The tMEV was significantly higher in group 1 ($p<0.05$).

Superior vena cava
The average attenuation was significantly higher in group 1 ($p>0.001$; Table 3).

Discussion
With the new generation of MSCT scanners featuring 16 rows of detectors, the time needed to scan the heart for the purpose of coronary CTA has been reduced to ~20 s;[1-5] yet, no studies have been performed on the optimisation of CM administration in non-invasive coronary imaging with MSCT.

We compared a conventional CM protocol for non-invasive MSCT with a low-volume protocol adding the pushing and washout effects of a bolus chaser. The two protocols showed comparable attenuation values at the level of coronary arteries and similar bolus geometry in the ascending and descending aorta. A significant difference was observed at the level of pulmonary artery where more "pooling" of CM was present for the conventional protocol. This observation is confirmed by the significantly lower attenuation observed in the superior vena cava for the low-volume protocol and supports the conclusion that 100 ml of CM pushed by 40 ml of saline provide optimal coronary artery enhancement with less attenuation in the right cavities of the heart. This result can be beneficial for a better visualisation of the mid-tract (segment 2) of RCA that may suffer from beamhardening artefacts when highly concentrated CM is present in the right atrium and right ventricle. This effect can be a drawback when cardiac masses need to be studied. In this case a conventional CM protocol must be used.

The attenuation at time 0 and the MEV were not significantly different between the two protocols. The tMEV, instead, was significantly longer in the descending aorta (~3.2 s) and significantly shorter in the pulmonary artery (~3.6 s), for the conventional protocol. We have no clear explanation for the differences detected at this level. Previous experiences with bolus chaser support the evidence that the same results, in terms of vascular and parenchymal attenuation, can be achieved using less CM volume (up to 20–40% less) and with a concomitant reduction of the artefacts at the level of superior vena cava.[13-15, 19]

The explanation may be that a saline chaser pushes the injected CM through the veins of the forearm which will give the same result as the injection of a larger contrast volume,

and that the saline chaser prevents the decrease of the contrast material flow in the arm veins which may normally cause an increase in the CM concentration after the end of the contrast injection.[7]

A limitation of this study is that the evaluation of coronary vessels could have been completed by the assessment of the length of coronary artery visualisation and/or the number of side branches visualised. We did not perform this evaluation because of the variable diameter of coronary arteries, heart rate and the degree of vessels with atherosclerotic disease (soft and calcified lesions, vessel stenosis and vessel occlusions). These parameters severely affect the capability of visualisation of the vessel regardless of the performance of the protocol for CM administration (e.g. the attenuation inside the vessel), and the number of patients enrolled in our study was not large enough to account for these variables.

Conclusion

In conclusion, the integration of bolus chaser in the CM administration protocol for non-invasive coronary artery angiography with 16-row MSCT allows to preserve the optimal intra-vascular attenuation, decreasing the volume of CM (35%) and the hyper-attenuating superior vena cava and right heart, with resulting cost savings and decreased risk of CM nephropathy.

References

1. Flohr T, Stierstorfer K, Bruder H, Simon J, Schaller S (2002) New technical developments in multislice CT. Part 1: approaching isotropic resolution with sub-millimeter 16-slice scanning. Rofo Fortschr Geb Rontgenstr Neuen Bildgeb Verfahr 174:839–845
2. Flohr T, Bruder H, Stierstorfer K, Simon J, Schaller S, Ohnesorge B (2002) New technical developments in multislice CT. Part 2: sub-millimeter 16-slice scanning and increased gantry rotation speed for cardiac imaging. Rofo Fortschr Geb Rontgenstr Neuen Bildgeb Verfahr 174:1022–1027
3. Heuschmid M, Kuttner A, Flohr T, Wildberger JE, Lell M, Kopp AF, Schroder S, Baum U, Schaller S, Hartung A, Ohnesorge B, Claussen CD (2002) Visualization of coronary arteries in CT as assessed by a new 16- slice technology and reduced gantry rotation time: first experiences. Rofo Fortschr Geb Rontgenstr Neuen Bildgeb Verfahr 174:721–724 [in German]
4. Nieman K, Cademartiri F, Lemos PA, Raaijmakers R, Pattynama PM, de Feyter PJ (2002) Reliable noninvasive coronary angiography with fast submillimeter multislice spiral computed tomography. Circulation 106:2051–2054
5. Ropers D, Baum U, Pohle K, Anders K, Ulzheimer S, Ohnesorge B, Schlundt C, Bautz W, Daniel WG, Achenbach S (2003) Detection of coronary artery stenoses with thin-slice multi-detector row spiral computed tomography and multiplanar reconstruction. Circulation 107:664–666
6. Cademartiri F, Nieman K, Raaymakers RH, de Feyter PJ, Flohr T, Alfieri O, Krestin GP (2003) Non-invasive demonstration of coronary artery anomaly performed using 16-slice multidetector spiral computed tomography. Ital Heart J 4:56–59
7. Cademartiri F, van der Lugt A, Luccichenti G, Pavone P, Krestin GP (2002) Parameters affecting bolus geometry in CTA: a review. J Comput Assist Tomogr 26:598–607
8. Kopka L, Rodenwaldt J, Fischer U, Mueller DW, Oestmann JW, Grabbe E (1996)

Dual-phase helical CT of the liver: effects of bolus tracking and different volumes of contrast material. Radiology 201:321–326

9. Kirchner J, Kickuth R, Laufer U, Noack M, Liermann D (2000) Optimized enhancement in helical CT: experiences with a real-time bolus tracking system in 628 patients. Clin Radiol 55:368–373
10. Mehnert F, Pereira PL, Trubenbach J, Kopp AF, Claussen CD (2001) Automatic bolus tracking in monophasic spiral CT of the liver: liver-tolesion conspicuity. Eur Radiol 11:580–584
11. Mehnert F, Pereira PL, Trubenbach J, Kopp AF, Claussen CD (2001) Biphasic spiral CT of the liver: Automatic bolus tracking or time delay? Eur Radiol 11:427–431
12. Sandstede JJ, Tschammler A, Beer M, Vogelsang C, Wittenberg G, Hahn D (2001) Optimization of automatic bolus tracking for timing of the arterial phase of helical liver CT. Eur Radiol 11:1396–1400
13. Haage P, Schmitz-Rode T, Hubner D, Piroth W, Gunther RW (2000) Reduction of contrast material dose and artifacts by a saline flush using a double-power injector in helical CT of the thorax. Am J Roentgenol 174:1049–1053
14. Hopper KD, Mosher TJ, Kasales CJ, TenHave TR, Tully DA, Weaver JS (1997) Thoracic spiral CT: delivery of contrast material pushed with injectable saline solution in a power injector. Radiology 205:269–271
15. Bader TR, Prokesch RW, Grabenwoger F (2000) Timing of the hepatic arterial phase during contrast-enhanced computed tomography of the liver: assessment of normal values in 25 volunteers. Invest Radiol 35:486–492
16. Garcia P, Genin G, Bret PM, Bonaldi VM, Reinhold C, Atri M (1999) Hepatic CT enhancement: effect of the rate and volume of contrast medium injection in an animal model. Abdom Imaging 24:597–603
17. Han JK, Kim AY, Lee KY, Seo JB, Kim TK, Choi BI, Lhee CS, Han MC (2000) Factors influencing vascular and hepatic enhancement at CT: experimental study on injection protocol using a canine model. J Comput Assist Tomogr 24:400–406
18. Yamashita Y, Komohara Y, Takahashi M, Uchida M, Hayabuchi N, Shimizu T, Narabayashi I (2000) Abdominal helical CT: evaluation of optimal doses of intravenous contrast material—a prospective randomized study. Radiology 216:718–723
19. Dorio PJ, Lee FT Jr, Henseler KP, Pilot M, Pozniak MA, Winter TC III, Shock SA (2003) Using a saline chaser to decrease contrast media in abdominal CT. Am J Roentgenol 180:929–934

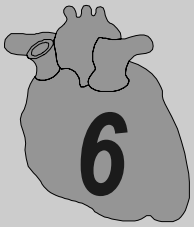

Chapter 6

Reduction of Motion Artefacts from Mild Heart Rhythm Irregularities with ECG-editing Using Multidetector-row Computed Tomography Coronary Angiography

Abstract

Objective.
to reduce the artefacts determined by mild heart rhythm irregularities with ECG-editing using multidetector-row CT coronary angiography (MDCT-CA).

Material and Methods.
38 patients (33 male; mean age 59±11 yrs) who underwent MDCT-CA and conventional coronary angiography (CA) were enrolled in the study. The inclusion criterion was the presence of mild heart rhythm irregularities (premature beats, atrial fibrillation, mis-triggering, low heart rate <40bpm) during the scan. All patients underwent MDCT-CA protocol with the following parameters: collimation 16x0.75mm, rotation time 375ms, feed/rotation 3.0mm, kV 120, eff. mAs 500-600. Images were reconstructed in two settings: 1) before ECG-editing; 2) after ECG-editing. The two series of datasets were scored for image quality (Poor; Sufficient; Good) and for the presence of significant stenoses (≥50% lumen reduction) in coronary segments ≥2mm diameter.

Results.
Image quality was poor in 22% (91) and 4% (15), sufficient in 21% (88) and 26 (107), and good in 57% (237) and 71% (295) before and after ECG-editing, respectively. Ninety-one (22%) and 14 (3%) segments were excluded from the analysis before and after ECG-editing. After inclusion of all diseased segments the sensitivity, specificity, negative and positive predictive value for the detection of significant stenoses before and after ECG-editing were 72% (41/65) and 91% (78/85), 97% (251/260) and 96% (305/317), 87% (62/71) and 87% (81/93), 91% (251/275) and 98% (305/313), respectively.

Conclusion.
ECG-editing reduces the artefacts due to mild heart rate irregularities, thus increasing the number of assessable segments and diagnostic accuracy in a selected population of patients.

Filippo Cademartiri [1]
Nico R. Mollet [1,2]
Eugene P. McFadden [2]
Thomas G. Flohr [3]
Bernd Ohnesorge [3]
Pim J. de Feyter [1,2]
Gabriel P. Krestin [1]

Departments of Radiology [1] and Cardiology [2], Erasmus MC, University Medical Center Rotterdam, The Netherlands
Department of Computed Tomography [3],
Siemens Medical Solutions, Forchheim, Germany

American Journal of Roentgenology (in press).

Chapter 6
ECG-editing in 16-MDCT coronary angiography

Introduction

Multidetector-row computed tomography (MDCT) scanners with sixteen rows of detectors, and increased spatial and temporal resolution have been recently introduced.[1] The increased number of detector rows and gantry rotation speed reduce the time needed to scan the coronary arteries to less than 20s.[1] Early experiences reported improved results in the visualisation of coronary arteries and in the detection of significant coronary artery disease (≥50% lumen reduction) in selected population of patients.[2, 3]

One limitation of MDCT coronary angiography (MDCT-CA) is that high and/or irregular heart rates prevent an adequate visualisation and assessment of coronary vessels, and for this reason are usually excluded from analysis or from scanning.[4] This is because at high heart rates the motion speed of coronary vessels is increased and the temporal window suited for imaging (e.g. mid- and late-diastole) is shortened. In case of irregular heart rates, such as premature beats and atrial fibrillation, the temporal variability of the diastolic phase is increased between contiguous heart cycles. This creates motion artefacts due to the inaccurate location of temporal windows and/or to the lack of data. This prevents the application of homogenous settings for image reconstructions.

In our experience, it is possible to correct and compensate for part or all of the artefacts produced by mild heart rhythm irregularities by means of ECG editing.

The aim of this study was to compare image quality and diagnostic accuracy in a population of patients with mild heart rhythm irregularities, using two different image reconstruction protocols for MDCT-CA.

Material and Methods

Patient population

Between April 2003 and February 2004, 42 patients (34 male; mean age: 59±11yrs) with stable angina and scheduled for coronary angiography (CA) were prospectively enrolled in the study.

Inclusion criteria for the scan were: heart rate (spontaneous or β-blocker induced) <70bpm, the ability to hold the breath for 20s. Inclusion criteria for the study were (see Appendix I): presence of premature beats (PB), atrial fibrillation (AF) with low ventricular response, mis-triggering (MT) of the R wave (e.g. widening of QRS complex, bundle branch block), and low heart rate (LHR; e.g. below 40bpm). This group of criteria is defined as mild heart rhythm irregularities (MHRI).

Exclusion criteria were: high heart rate (>70bpm) previous allergic reaction to iodine contrast media, renal insufficiency (serum creatinine >120mmol/L), pregnancy, respiratory impairment, unstable clinical status, marked heart failure, previous bypass surgery or percutaneous coronary interventions.

Patients meeting the inclusion criteria underwent also non-invasive MDCT-CA.

The Institutional Review Board approved the study and patients gave informed consent.

Multidetector-row ct scan

On arrival, the heart rate (HR) of the patients was measured. Patients with a pre-scan HR ≥ 65bpm, were given 100mg of metoprolol orally and the scan was performed one hour later.

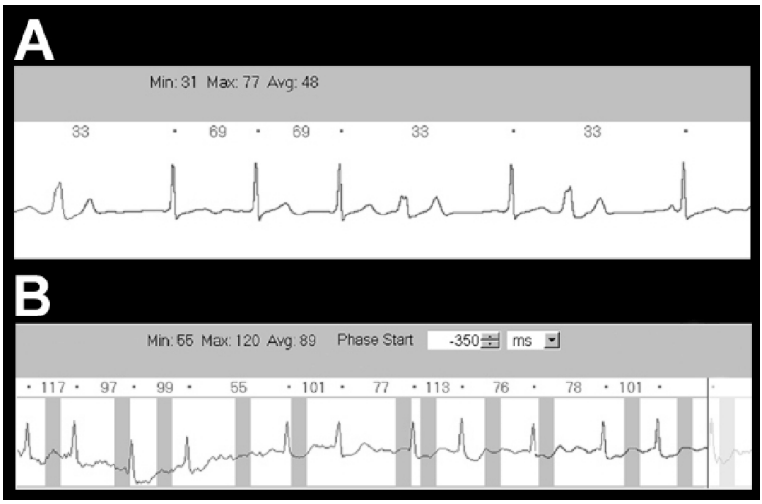

Figure 1. Example of ECG of excluded patients.
Two examples of patients excluded from the study while they were on the scanner table just before starting the procedure. In A an example of premature beat originating from the conduction system in a background heart rate too high to rely on the post extra-systolic pause. In B an example of a high and irregular heart rate due to atrial flutter. The ventricular response to the flutter wave is irregular.

Patients meeting the inclusion criteria were positioned on the CT table and connected to the ECG trace. The variation of HR were observed for 5 minutes and then tested during apnoea (20s). If at rest and during apnoea the variation of HR were compatible with the definition of MHRI the patient underwent the scanning procedure (Figure 1).

In all patients, a bolus (100ml at 4ml/s) of iodinated contrast material (Iomeprol 400 mgI/ml, Iomeron®, Bracco) followed by a saline chaser (40ml at 4ml/s) was administered using a double-head power injector (Stellant®, MedRAD) through an 18G cannula, in an antecubital vein.

The scan parameters for MDCT coronary angiography (Sensation 16®, Siemens) were: number of detectors 16, individual detector width 0.75mm, gantry rotation time 375ms, effective temporal resolution 188ms, kV 120, eff. mAs 500-600, feed/rotation 3.0mm, scan direction cranio-caudal.

Synchronisation between the passage of contrast material and data acquisition was achieved with real time bolus tracking (CARE bolus®, Siemens) using a region of interest in the ascending aorta for monitoring a threshold of +100HU above the baseline attenuation to trigger the scan. The heart rate and ECG track were recorded during the scan.

Image reconstruction

Two datasets were reconstructed using retrospective ECG gating technique. The first dataset (standard reconstruction protocol - STD) was reconstructed without any ECG editing using temporal windows starting at -350ms, -400ms, and -450ms, prior to the next R wave. Two experienced operators in consensus (F.C. and N.R.M.) selected the dataset with least motion artefacts.

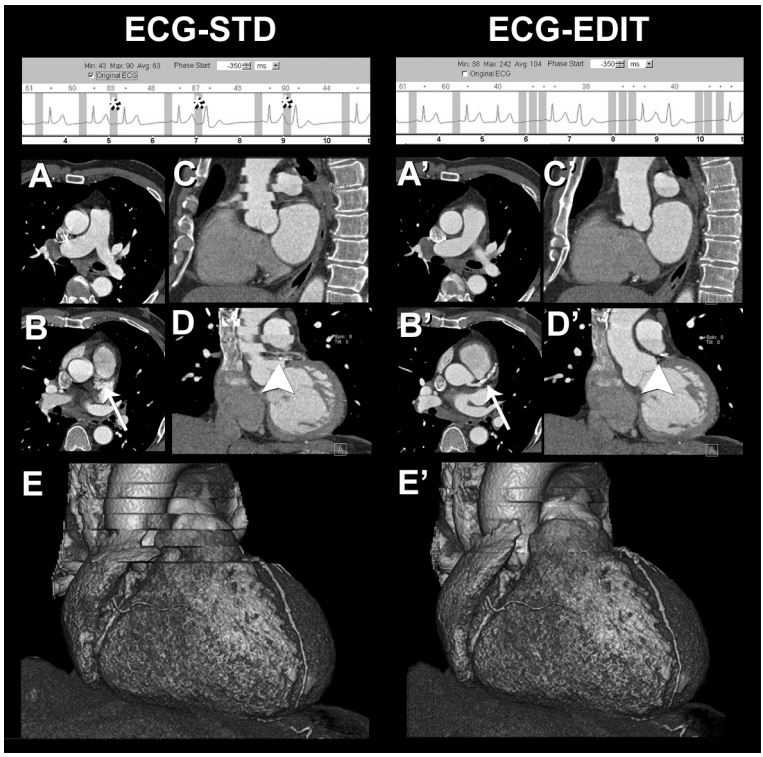

Figure 2. Correction of artefacts from premature beats.
Example of dataset with premature beats before (left panel) and after (right panel) ECG editing. The ECG of the left panel shows three premature beats (asterisks) in a background heart rate of ~45bpm. The dataset resulting from a reconstruction performed without any editing shows motion artefacts at the level of the pulmonary artery (A) and at the origin of the left coronary artery (B - arrow). Sagittal and coronal reconstructions (C and D) show the impact of these three premature beats on the ascending aorta and on the origin of the left coronary artery (D - arrowhead). In E a frontal view of the dataset with three-dimensional volume rendering shows the misalignment of the stacks of images in the cranial part of the dataset. After ECG-editing, the artefacts are ruled out and coronary vessels are assessable (A'-E'). A significant stenosis of proximal left anterior descending was missed because of the artefacts (B' - arrow; D' - arrowhead). (A full color version of this illustration can be found in the color section (chapter 21)).

The second dataset (ECG-editing reconstruction protocol - EDIT) was reconstructed in consensus by two experienced operators using ECG editing available at the MDCT scanner evaluated in correspondence of anomalies of the ECG signal due to: premature beats (PB - Figure 2), atrial fibrillation (AF), mis-triggering (MT - Figure 3), and heart rate below 40bpm (LHR - Figure 4). The ECG-editing procedure varied depending on the type of artefact (see Appendix I). Both datasets were reconstructed with the following parameters: effective slice width 1mm, reconstruction interval 0.5mm, FOV 160mm, convolution filter medium smooth (B30f).

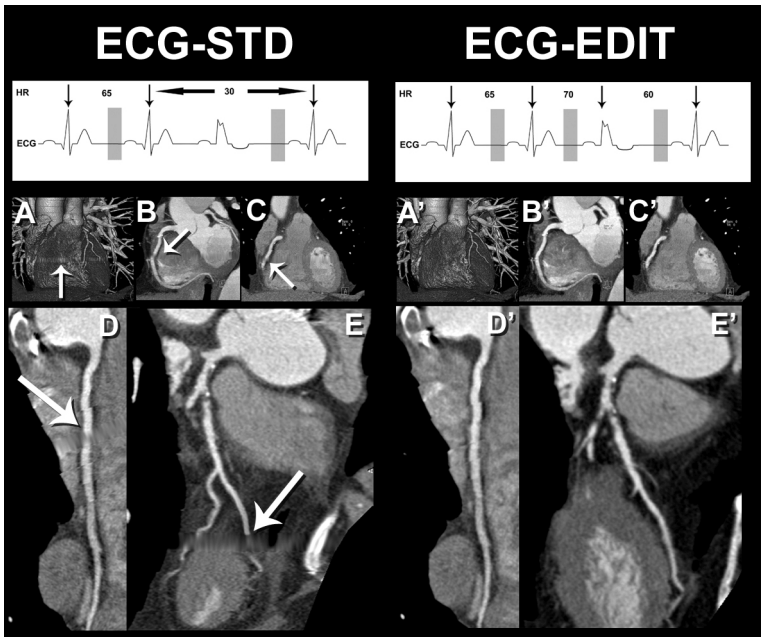

Figure 3. Correction of artefacts from mis-triggering.
Example of dataset with mis-triggering before (left panel) and after (right panel) ECG editing. The ECG on the left panel shows an anomaly of the conduction for one heart beat that result in a missing synchronisation point and very long RR interval. The appearance of this event is showed by the arrow in three-dimensional volume rendering (A), a dedicated double oblique MIP for the right coronary artery (B), a coronal MIP (C), and two curved reconstructions: one for the right coronary artery (D), and one for the left main-left anterior descending (E). The data are missing because the RR interval is too large, and two coronary segments have to be considered not assessable. After ECG editing by means of inserting the synchronisation point in the correct position (ECG in the right panel), all the images are recovered (A'-E'). (A full color version of this illustration can be found in the color section (chapter 21)).

Image analysis

Two experienced observers, blinded to the results of the conventional coronary angiography, assessed in consensus the dataset for image quality (concerning artefacts due to MHRI) and presence of significant stenoses (≥50% lumen reduction). The evaluation of the data was performed 3 months after the reconstruction and selection of the datasets. The evaluation was performed following the classification for coronary segments from the American Heart Association.[5] Image quality was graded as: Poor (artefact present; vessel not visualized); Sufficient (artefact present; vessel visualized); Good (artefact absent; vessel well visualized). Significant stenoses were scored as: absent (<50%) or present (≥50%).

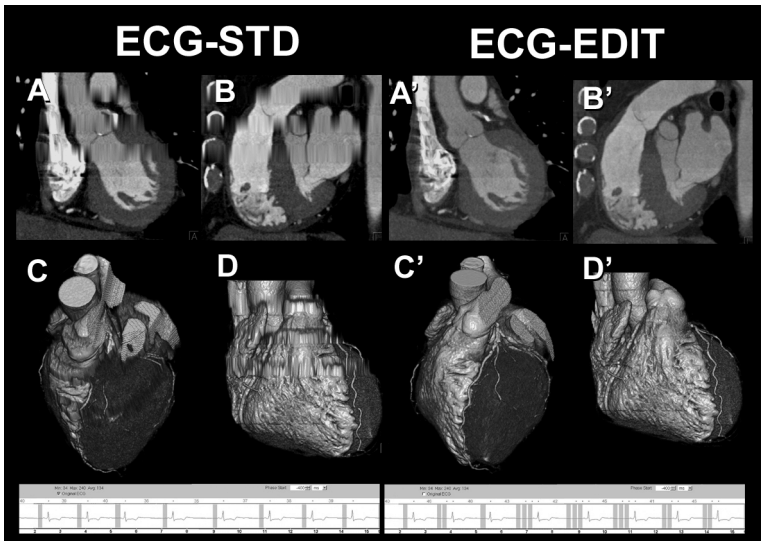

Figure 4. Correction of artefacts from low heart rate.
Example of dataset with low heart rate before (left panel) and after (right panel) ECG editing. The ECG on the left panel shows a very low heart rate almost always below 40bpm. This determines data gaps that appear in coronal (A), sagittal (B), and three-dimensional reconstructions (C and D), as blurring of stacks of images. After ECG editing by means of inserting additional synchronisation points (ECG in the right panel), all the images are recovered (A'-D'). (A full color version of this illustration can be found in the color section (chapter 21)).

Conventional coronary angiography

Conventional coronary angiography (CA) was performed within 2 weeks of MDCT-CA using a standard technique. One experienced observer (P.A.L.), unaware of the results of MDCT-CA, determined the diameter of all coronary branches and evaluated the presence of significant stenoses using quantitative coronary angiography (QCA - CAAS®, Pie Medical Imaging). Lesions with an average diameter stenosis of ≥50% in two orthogonal views were considered as significant obstructions.

Data analysis

The result of QCA performed in two orthogonal projections was used as the reference standard to classify stenoses as significant. The reading of the MDCT-CA was used to calculate sensitivity, specificity, positive, and negative predictive value with 95% confidence intervals.

Results

No significant adverse reactions to contrast material were recorded. Of the 42 patients enrolled in the study, 4 (10%) did not undergo MDCT-CA because the HR variations observed while the patient was on the CT table were not compatible with inclusion criteria regarding MHRI.

Therefore, 38 patients (33 male; mean age 59±11 yrs; Table I) were suitable for MDCT-CA scan, image reconstruction and data analysis. After exclusion of segments with a diameter

Table 1. Patients data.

	Population
Number of patients	38
Male/Female	33/5
Mean age (yrs)	59±11
Mean heart rate (bpm)	54±9

Abbreviations: yrs = years; bpm = beat per minute; sec= seconds.

<2mm, 416 segments remained available for analysis, 88 (21%) of which with a significant stenosis. Of the 38 patients with MHRI, 21 were classified as PB, 4 as AF, 6 as MT, and 7 as LHR.

Image quality (Table II)

Image quality was poor in 22% (91) and 4% (15), sufficient in 21% (88) and 26 (107), and good in 57% (237) and 71% (295) of the segments before and after editing, respectively . Fourteen (3%) segments that were scored as poor were re-scored as sufficient after ECG-editing. Within this fraction of segments there were 3 significant stenoses. Fifty-eight (14%) segments that were scored as poor were re-scored as good after ECG-editing. Within this fraction of segments there were 12 significant stenoses.

Table 2. Image quality of ECG-STD protocol vs. ECG-EDIT protocol.

			Image quality (%)					
			Poor		Sufficient		Good	
AHA	Segment	n.	ECG-STD	ECG-EDIT	ECG-STD	ECG-EDIT	ECG-STD	ECG-EDIT
1	RCA prox.	38	15 (40)	5 (13)	4 (11)	7 (18)	19 (50)	26 (68)
2	RCA mid.	32	7 (22)	1 (3)	4 (13)	4 (13)	21 (66)	27 (84)
3	RCA distal	23	3 (13)	0 (0)	4 (17)	6 (26)	16 (70)	17 (74)
4	PDA	14	2 (14)	0 (0)	10 (71)	10 (71)	2 (14)	4 (29)
5	LM	38	10 (26)	1 (3)	4 (11)	4 (11)	24 (63)	33 (87)
6	LAD prox.	38	15 (40)	3 (8)	4 (11)	9 (24)	19 (50)	26 (68)
7	LAD mid.	35	12 (34)	2 (6)	7 (20)	8 (23)	16 (46)	25 (71)
8	LAD distal	32	5 (16)	0 (0)	9 (28)	10 (31)	18 (56)	22 (69)
9	1st diag.	28	4 (14)	0 (0)	8 (29)	10 (36)	16 (57)	18 (64)
10	2nd diag.	16	1 (6)	1 (6)	8 (50)	8 (50)	7 (44)	7 (44)
11	CX prox.	37	6 (16)	1 (3)	6 (16)	7 (19)	25 (68)	29 (78)
12	1st marg.	33	7 (21)	0 (0)	4 (12)	6 (18)	22 (67)	27 (82)
13	CX mid.	30	3 (10)	0 (0)	6 (20)	8 (27)	21 (70)	22 (73)
14	2nd marg.	15	1 (7)	0 (0)	3 (20)	3 (20)	11 (73)	12 (80)
15	PL	7	0 (0)	0 (0)	7 (100)	7 (100)	0 (0)	0 (0)
All		416	91 (22)	14 (3)	88 (21)	107 (26)	237 (57)	295 (71)

Abbreviations: ECG-STD= standard ECG protocol; ECG-EDIT= ECG-editing protocol; n.= number; AHA= American Heart Association segmental classification; RCA= right coronary artery; LAD= left anterior descending; LM= left main; CX= circumflex; PL= postero-lateral branch.

Table 3. Diagnostic accuracy of ECG-STD protocol vs. ECG-EDIT protocol

AHA	Segment	n.	SDS (%)	Protocol	NA (%)	SDS in NA (%)	Sensitivity (95% CI)
1	RCA prox.	38	7 (18)	ECG-STD	15 (40)	2 (28)	100 (54-100)
				ECG-EDIT	5 (13)	1 (14)	100 (59-100)
2	RCA mid.	32	17 (53)	ECG-STD	7 (22)	4 (24)	100 (75-100)
				ECG-EDIT	1 (3)	0 (0)	100 (80-100)
3	RCA distal	23	6 (26)	ECG-STD	3 (13)	2 (33)	100 (39-100)
				ECG-EDIT	0 (0)	0 (0)	100 (54-100)
4	PDA	14	2 (14)	ECG-STD	2 (14)	0 (0)	50 (1-87)
				ECG-EDIT	0 (0)	0 (0)	50 (1-87)
5	LM	38	0 (0)	ECG-STD	10 (26)	0 (0)	NA
				ECG-EDIT	1 (3)	0 (0)	NA
6	LAD prox.	38	15 (40)	ECG-STD	15 (40)	6 (40)	77.77 (39-98)
				ECG-EDIT	3 (8)	1 (7)	85.71 (57-98)
7	LAD mid.	35	14 (40)	ECG-STD	12 (34)	5 (36)	100 (63-100)
				ECG-EDIT	2 (6)	2 (14)	100 (73-100)
8	LAD distal	32	3 (9)	ECG-STD	5 (16)	0 (0)	100 (29-100)
				ECG-EDIT	0 (0)	0 (0)	100 (29-100)
9	1st diag.	28	1 (4)	ECG-STD	4 (14)	0 (0)	100 (2-100)
				ECG-EDIT	0 (0)	0 (0)	100 (2-100)
10	2nd diag.	16	0 (0)	ECG-STD	1 (6)	0 (0)	NA
				ECG-EDIT	1 (6)	0 (0)	NA
11	CX prox.	37	7 (19)	ECG-STD	6 (16)	0 (0)	100 (47-100)
				ECG-EDIT	1 (3)	0 (0)	85.71 (42-96)
12	1st marg.	33	10 (30)	ECG-STD	7 (21)	2 (20)	100 (63-100)
				ECG-EDIT	0 (0)	0 (0)	100 (69-100)
13	CX mid.	30	5 (17)	ECG-STD	3 (10)	0 (0)	100 (47-100)
				ECG-EDIT	0 (0)	0 (0)	100 (47-100)
14	2nd marg.	15	0 (0)	ECG-STD	1 (20)	0 (0)	NA
				ECG-EDIT	0 (0)	0 (0)	NA
15	PL	7	1 (14)	ECG-STD	0 (0)	0 (0)	100 (2-100)
				ECG-EDIT	0 (0)	0 (0)	100 (2-100)
All	Assessable	416	88 (21)	ECG-STD	91 (22)	21 (24)	95.38 (87-98)
				ECG-EDIT	14 (3)	4 (5)	95.29 (88-98)
	Assessable[1]			ECG-STD	70 (17)	0 (0)	72.09 (61-88)
				ECG-EDIT	10 (2)	0 (0)	91.01 (83-97)

Abbreviations: ECG-STD= standard ECG protocol; ECG-EDIT= ECG editing protocol; n.= number; AHA= American Heart Association segmental classification; SDS = significantly diseased segments (>50% lumen reduction at Quantitative Coronary Angiography); RCA= right coronary artery; LAD= left anterior descending; LM= left main; CX= circumflex; PL= postero-lateral branch; NA= not assessable; CI= confidence intervals.
1Calculation performed including the significantly diseased segments as false negatives.

Specificity (95% CI)	PPV (95% CI)	NPV (95% CI)	Accuracy (95% CI)
88.23 (63-98)	75 (34-97)	100 (78-100)	91.3 (80-100)
92.3 (74-99)	77.77 (39-98)	100 (85-100)	93.9 (86-100)
83.33 (51-97)	86.66 (59-98)	100 (69-100)	92 (81-100)
85.71 (57-98)	89.47 (66-98)	100 (73-100)	93.55 (85-100)
93.75 (69-99)	80 (28-99)	100 (78-100)	95 (85-100)
94.11 (71-99)	85.71 (42-99)	100 (79-100)	95.65 (87-100)
100 (69-100)	100 (2-100)	90.9 (58-99)	91.67(76-100)
100 (73-100)	100 (2-100)	92.3 (63-99)	92.86 (79-100)
100 (87-100)	NA	100 (87-100)	100 (100-100)
100 (90-100)	NA	100 (90-100)	100 (100-100)
92.85 (66-99)	87.5 (47-99)	86.66 (59-98)	86.96 (73-100)
90.47 (69-98)	85.71 (57-98)	90.47 (69-98)	88.57 (78-99)
100 (78-100)	100 (63-100)	100 (78-100)	100 (100-100)
100 (83-100)	100 (73-100)	100 (83-100)	100 (100-100)
95.83 (78-99)	75 (19-99)	100 (85-100)	96.3 (89-100)
96.55 (82-99)	75 (19-99)	100 (87-100)	96.88 (91-100)
95.65 (78-99)	50 (1-99)	100 (84-100)	95.83 (88-100)
92.59 (75-99)	33.33 (0-95)	100 (86-100)	92.86 (83-100)
100 (78-100)	NA	100 (78-100)	100 (100-100)
100 (78-100)	NA	100 (78-100)	100 (100-100)
100 (86-100)	100 (47-100)	100 (86-100)	100 (100-100)
100 (88-100)	100 (54-100)	96.66 (82-99)	97.22 (92-100)
100 (81-100)	100 (63-100)	100 (81-100)	100 (100-100)
95.65 (78-99)	90.9 (58-99)	100 (84-100)	96.97 (91-100)
95.45 (77-99)	83.33 (35-99)	100 (83-100)	96.3 (89-100)
96 (79-99)	83.33 (35-99)	100 (85-100)	96.67 (90-100)
100 (76-100)	NA	100 (76-100)	100 (100-100)
100 (78-100)	NA	100 (78-100)	100 (100-100)
100 (54-100)	100 (2-100)	100 (54-100)	100 (100-100)
100 (54-100)	100 (2-100)	100 (54-100)	100 (100-100)
96.53 (93-98)	87.32 (77-97)	98.81 (96-99)	96.31 (94-98)
96.21 (93-98)	87.09 (78-94)	98.7 (96-99)	96.02 (94-98)
96.53 (93-98)	87.32 (77-97)	91.27 (87-94)	90.46 (87-94)
96.21 (93-98)	87.09 (78-94)	97.44 (95-98)	95.07 (93-97)

Diagnostic accuracy (Table III)

The segments available for comparison were 325 (78%) and 402 (97%) for STD and EDIT protocol, respectively. The rate of excluded segments was 22% (91) for STD protocol and 3% (14) for EDIT protocol. Twenty-one (24%) significant lesions were excluded from analysis with STD protocol and 4 (5%) with EDIT protocol because located in not assessable segments.

Sensitivity, specificity, negative predictive value and positive predictive value for the detection of significant stenoses for STD and EDIT protocols were 95% (62/65) and 95% (81/85), 97% (251/260) and 96% (305/317), 87% (62/71) and 87% (81/93), 99% (251/254) and 98% (305/309), respectively. Considering significant stenoses in excluded segments as false negatives the value of sensitivity, specificity, negative and positive predictive were 72% (41/65) and 91% (78/85), 97% (251/260) and 96% (305/317), 87% (62/71) and 87% (81/93), 91% (251/275) and 98% (305/313), respectively.

Discussion

With the new generation of MDCT scanners featuring 16 rows of detectors the time needed to scan the heart for the purpose of coronary CTA has been reduced to ~20s.[1-3] Preliminary encouraging results have been published regarding the detection of significant stenoses with 16-row MDCT-CA in selected population of patients.[2, 3] High and irregular hear rates are known as limitations of this technique.[1] To date, they are used as exclusion criteria for the studies and aggressively treated with oral β-blockers.[2, 3] Yet, for milder hear rate irregularities there remains room for interaction with the raw data and the ECG trace.

The main drawback of high heart rates is the increased speed of coronary arteries and the reduced duration of the diastole.[6] With a temporal resolution of ~200ms this results in a limited possibility to adapt the position of the temporal window within the cardiac cycle.

This limitation is less compromising at lower heart rates and, due to the longer diastolic phase, ECG editing is more flexible. In fact, mild heart rhythm irregularities, as described above and in Appendix I, can be ruled out after careful ECG editing, providing both an increased image quality and diagnostic accuracy.

In our study we compared the reconstruction capabilities of a 16- row MDCT scanner in the presence of mild heart rhythm irregularities before and after ECG editing.

The improvement in image quality is demonstrated by the steep reduction of segments scored as poor (-77 segments; from 22% to 3%) and by concomitant increased number of segments scored as good (+58 segments; from 57% to 71%) after ECG editing. This improvement in image quality has also an impact on diagnostic accuracy in the selected population of patients with stable angina enrolled in this study. In fact, the sensitivity and the negative predictive value for the detection of significant stenoses after inclusion of all diseased segments in the analysis were 72% vs. 91%, and 91% vs. 97% before and after ECG-editing, respectively. Specificity and positive predictive value did not differ. The difference has to be attributed to the number of significantly diseased segments that were excluded from the analysis.

The effect of mild heart rhythm irregularities on image quality can be quantified and is not affected by the presence of significant stenoses. Their impact on diagnostic accuracy, instead, is fairly dependent on the number of significant stenoses that are present in the population. The relative impact of ECG-editing on diagnostic accuracy will depend on the number and distribution of lesions throughout the coronary tree. A population with a lower probability of disease (e.g. younger, or with less evident symptoms) would probably show a smaller variation in sensitivity than the one demonstrated in our study.

Our results suggest that from the technical point of view, heart rhythm irregularities are

not an absolute limitation for proper image quality. In fact, our results exploit the flexibility of retrospective reconstruction to the limit. Other techniques already applied to non-invasive coronary artery imaging (electron-beam CT or magnetic resonance) are based on prospective ECG triggering. Even though with higher temporal resolution when compared to MDCT, for these techniques it would be impossible to compensate for the mild heart rhythm irregularities as described in our study. Prospective ECG triggering allows to acquire only one segment of the cardiac cycle without any possibility of retrospective modification.

The motion speed of the coronary vessels, especially if compared with effective temporal resolution of MDCT, remains a limitation. To compensate this limitation, slow HR and/or shorter rotation time are required.

Limitations

The patients with heart rates above 70bpm were not enrolled in this study to prevent image degradation from other sources than the ones subjects of our study.

Only mild heart rhythm irregularities could be included in the evaluation due the still limited effective temporal resolution.

The scan of patients with mild heart rhythm irregularities does not allow to use X-ray reduction software such as ECG-pulsing.[7] This is because the algorithm for dose reduction works with a prospective triggering based on the R wave. In presence of heart rate abnormalities the location of the low dose period will be variable and can fall within the diastole.

In addition, the presence of heart rhythm irregularities, with the exclusion of low heart rates, do not allow the application of multi-segmental reconstruction algorithms.[8, 9] This is because the variable diastolic filling of the heart prevents a proper interpolation between the data originating from neighbouring heart cycles.

Conclusions

Editing of the ECG in 16-row MDCT-CA reduces the negative impact of mild heart rhythm irregularities on image quality, which results in a significant increase of assessable segments and in diagnostic accuracy in a selected population of patients with stable angina. Improvements in scanner technology (e.g. faster rotation time) and software capabilities (e.g. automatic recognition and editing of heart rhythm irregularities), could allow to scan routinely patients with mild arrhythmias with a good diagnostic accuracy.

References

1. Flohr TG, Schoepf UJ, Kuettner A, Halliburton S, Bruder H, Suess C, Schmidt B, Hofmann L, Yucel EK, Schaller S, Ohnesorge BM: Advances in cardiac imaging with 16-section CT systems. Acad Radiol 2003; 10:386-401.
2. Nieman K, Cademartiri F, Lemos PA, Raaijmakers R, Pattynama PM, de Feyter PJ: Reliable noninvasive coronary angiography with fast submillimeter multislice spiral computed tomography. Circulation 2002; 106:2051-4.

3. Ropers D, Baum U, Pohle K, Anders K, Ulzheimer S, Ohnesorge B, Schlundt C, Bautz W, Daniel WG, Achenbach S: Detection of coronary artery stenoses with thin-slice multi-detector row spiral computed tomography and multiplanar reconstruction. Circulation 2003; 107:664-6.
4. Nieman K, Rensing BJ, van Geuns RJ, Vos J, Pattynama PM, Krestin GP, Serruys PW, de Feyter PJ: Non-invasive coronary angiography with multislice spiral computed tomography: impact of heart rate. Heart 2002; 88:470-4.
5. Austen WG, Edwards JE, Frye RL, Gensini GG, Gott VL, Griffith LS, McGoon DC, Murphy ML, Roe BB: A reporting system on patients evaluated for coronary artery disease. Report of the Ad Hoc Committee for Grading of Coronary Artery Disease, Council on Cardiovascular Surgery, American Heart Association. Circulation 1975; 51:5-40.
6. Achenbach S, Ropers D, Holle J, Muschiol G, Daniel WG, Moshage W: In-plane coronary arterial motion velocity: measurement with electron-beam CT. Radiology 2000; 216:457-63.
7. Jakobs TF, Becker CR, Ohnesorge B, Flohr T, Suess C, Schoepf UJ, Reiser MF: Multislice helical CT of the heart with retrospective ECG gating: reduction of radiation exposure by ECG-controlled tube current modulation. Eur Radiol 2002; 12:1081-6.
8. Dewey M, Laule M, Krug L, Schnapauff D, Rogalla P, Rutsch W, Hamm B, Lembcke A: Multisegment and halfscan reconstruction of 16-slice computed tomography for detection of coronary artery stenoses. Invest Radiol 2004; 39:223-9.
9. Halliburton SS, Stillman AE, Flohr T, Ohnesorge B, Obuchowski N, Lieber M, Karim W, Kuzmiak SA, Kasper JM, White RD: Do segmented reconstruction algorithms for cardiac multi-slice computed tomography improve image quality? Herz 2003; 28:20-31.

REDUCTION OF MOTION ARTEFACTS FROM MILD HEART RHYTHM IRREGULARITIES WITH ECG-EDITING USING MULTIDETECTOR-ROW COMPUTED TOMOGRAPHY CORONARY ANGIOGRAPHY

APPENDIX I.

MILD HEART RHYTHM IRREGULARITIES: DEFINITION AND MANAGEMENT

Following we describe the "Mild Heart Rhythm Irregularities" that we used as inclusion criteria for the study on Multidetector-row computed tomography coronary angiography (MDCT-CA). High heart rate (HR) above 70 beat-per-minute (bpm), was considered as an exclusion criteria.[10]

Electrocardiogram basics for MDCT-CA (Figure I)

As a baseline information we remind that a heart cycle is constituted by a systole and a diastole. The systole involves the contraction of the atria followed by the contraction of the ventricles. The synchronized contraction is driven by a conduction system starting in the right atrium from the sino-atrial node (SA-node). The impulse then propagates to the atrio-ventricular node (AV-node) through the walls of the atria. At the AV-node the impulse is lead into a conduction system through the septum and ventricular walls. This phenomenon is represented by the electrocardiogram (ECG) track that shows the typical sequence of waves (Figure IA): P-wave (atrial contraction), the QRS-complex (ventricular contraction), T-wave (repolarization of the ventricles). Normally the P-R interval is <0.2s, the QRS complex is <0.12s, and the Q-T interval is ~0.42s. Therefore, a complete systolic contraction with repolarization wave will last ~0.55s. This means that for a heart rate of 60bpm systole and diastole will represent roughly 50% of the cardiac cycle (Figure IB). The diastolic period will be about 0.45s. In this interval it is usually placed the temporal windows of ~200ms for retrospectively ECG-gated reconstruction with MDCT-CA (Figure IA). The most favourable location is usually the mid- to end-diastolic phase just prior to the P-wave.

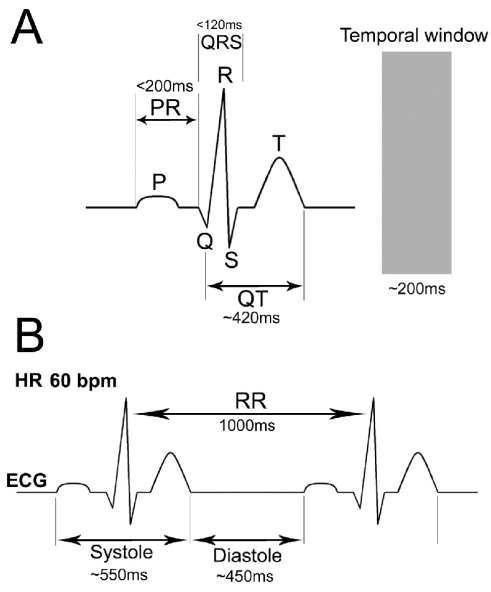

Figure I.

Scan basics for MDCT-CA (Figure II)

Currently the standard technique for cardiac MDCT scanning is based on retrospective ECG gating. This means that data have to be sampled at a slow table-feed with overlapping acquisition in the z-direction throughout the cardiac cycle in order to be retrospectively synchronized. Depending on the patients heart rate and the width of the detector, a maximum table feed per second should not be exceeded. Cardiac examinations with the same CT-system at different rotation times will therefore require different pitch values to keep the table feed per second constant.

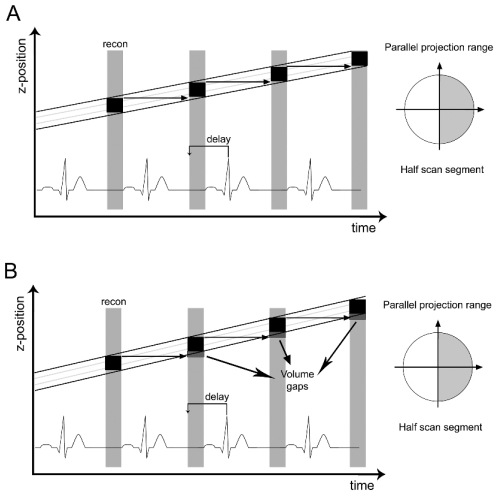

Figure II.

With 16 rows of 0.75mm width and a rotation time of 375ms, the minimum HR that can be accepted without data loss is ~40 bpm for a pitch of 0.25 (Figure IIA).

Below this threshold the software cannot find enough data between two contiguous temporal windows, and the gaps will be closed by interpolation at the expenses of a loss of spatial resolution (Figure IIB). The low pitch (e.g.: oversampling of the data) allows the scanner to cover the same z-axis position for ~1500ms with adjacent detector slices. When the RR interval, and therefore the distance between two contiguous temporal windows is >1500ms, a data gap is created and interpolation is performed to fill with information from the stack of images before and after the gap.

Definition and management of Mild heart rhythm irregularities

1. Premature beats (PB)

Definition

A PB is a premature (compared to the previous RR interval) excitation of an area of the myocardium. This area can be located in the conduction system or in the myocardium. A PB usually results in a shorter diastolic time followed by a longer diastole. The duration of the 2 RR intervals involved in the extra-systole is usually the same as 2 RR intervals at the HR that was preceding the PB.

In MDCT-CA, even an irregularity of the heart in which, a normal heart beat happens earlier than expected based on the previous heart rate can be configured as a PB. A typical example of this is a low average heart rate around 45bpm with one or more isolated heart beats (from the SA-node) at 65bpm. For the study were included all patients with single

isolated PB and a maximum number of 5 PB during the scan. Patients with bi-gemini or tri-gemini PB were excluded.

Management (Figure III)

When a PB is present in the ECG the conventional protocol for image reconstruction locates the temporal window too early in the diastolic phase when compared with previous and next heart beats (Figure IIIA – b). In this case, while all other beats are reconstructed in a late diastolic phase, the PB determines an early diastolic reconstruction. This cannot be effective for two reasons: the first is that there may be too much motion in that phase and the second that it is not the same phase as for the other beats.

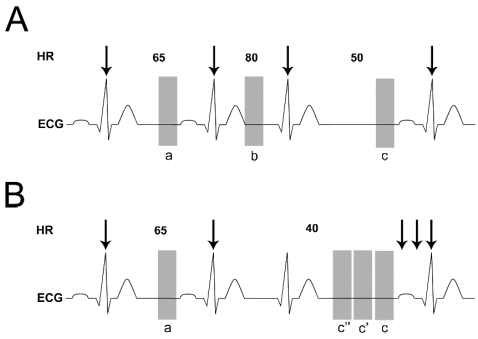

Figure III.

Therefore, we rule out the PB (Figure IIIB). To do that we delete temporal window applied to the PB and we fill the next diastolic interval with one or more temporal windows (Figure IIIB - 0 c′ and c′′). The threshold RR interval of 40bpm that avoids data gaps determines the number of additional temporal windows.

2. Atrial fibrillation (AF)

Definition

With AF we define an irregular and anarchic contraction of myocardial walls of the atria with hemodynamic effect. The AV-node picks up an impulse once in a while depending on its receptivity. Therefore, AV conduction is irregular. For the purpose of the study we included only patient with AF and low AV response. In these cases average HR was irregular but below 70bpm.

Management (Figure IV)

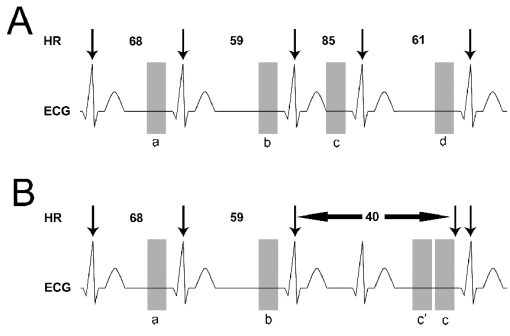

Figure IV.

The problem created in MDCT-CA by AF with low ventricular response is due the irregularity of the RR interval between contiguous heart beats.

If variability remains within an acceptable range no additional editing needs to be done. When the HR in the isolated RR interval exceeds 70bpm (Figure IVA - c) that heart beat should be eliminated. If the next RR interval shows a high HR, usually the newly created RR interval is above the 40bpm threshold. When instead the next RR

shows a low HR, it will necessary to insert additional temporal windows (Figure IVB - c'), as described for PB.

3. MIS-TRIGGERING (MT)

Definition

With MS we define an event characterized by a regular or only slightly irregular HR with missed or inaccurate detection of R wave. This can happen when the ECG signal is low (e.g. small R waves, or when the waves are not usually shaped (e.g. bundle branch block, enlargement of QRS-complex). In these cases a sharp R-wave is difficult to obtain and the software can set the synchronisation point in the wrong position or miss it completely.

Management (Figure V)

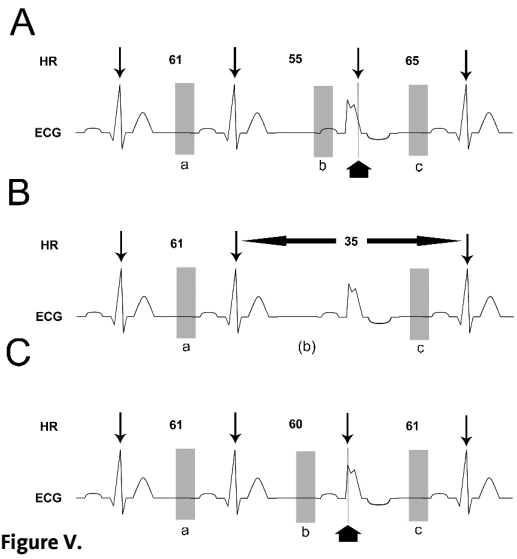

Figure V.

The result of MT in MDCT-CA is inaccurate location of the temporal window or missing data. In the first case, the synchronisation point (thin arrows) is not on top of the R wave (Figure V a - thick arrow) and therefore the temporal window (Figure V a - b) is located later than it should, on top of the P wave. In the second case, the whole synchronisation complex is missing (Figure V b) and the RR interval is overstretched. To solve the problem it is sufficient to relocate manually the synchronisation point or insert one in the correct position (Figure V b - thick arrow).

4. LOW HEART RATE (LHR)

Definition

A low HR for an MDCT-CA study is below 40 bpm. To solve this problem scanners currently adopt a dedicated "low heart rate" protocol, which is based on a lower pitch (e.g. ~0.20-0.15). With this protocols the HR threshold that allows to reconstruct images is lower (e.g. ~32-24bpm). Unfortunately there are a few drawbacks of this technique. The first is that a lower pitch means a longer scan time and corresponding increase in radiation exposure. The second is that usually the patient who would need this protocol present with a HR lower than average but not in the range observed during the scan. A typical example is the patient presenting with a HR of 50bpm that only during apnoea drops to 40bpm or below. A further problem is that for many of these patients with low HR we had only few cardiac cycles below a HR 40bpm. This means that for the majority of patients with low HR using a dedicated "low heart rate" protocol would determine an

unnecessary increase of radiation dose and a longer apnoea, while all the information for a proper reconstruction are available using the standard protocol.

Management (Figure VI)

Scanning patients with isolated, clustered or diffused LHR in MDCT-CA determines data gaps (see above). These gaps are present with RR intervals below 40bpm (Figure VIA - a and b). To fill the gaps the operator needs to insert additional temporal windows in order to bring the HR of the RR above 40bpm (Figure VIB - a', b' and b'').

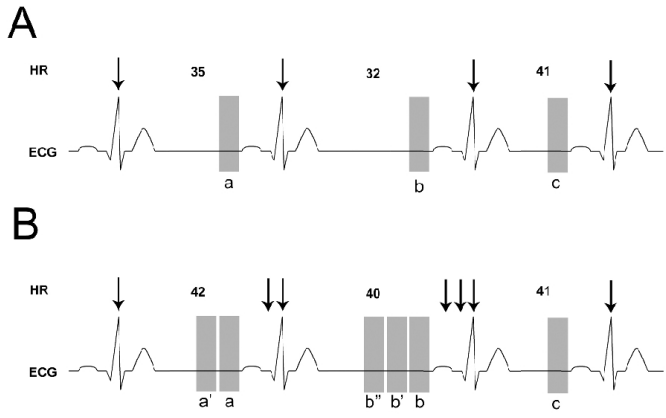

Figure VI.

Chapter 7

MULTISLICE SPIRAL COMPUTED TOMOGRAPHY CORONARY ANGIOGRAPHY IN PATIENTS WITH STABLE ANGINA PECTORIS

Nico R. Mollet [1,2]
Filippo Cademartiri [2]
Koen Nieman [1]
Francesco Saia [1]
Pedro A. Lemos [1]
Eugene P. McFadden [1]
Peter M. T. Pattynama [2]
Patrick W. Serruys [1]
Gabriel P. Krestin [2]
Pim J. de Feyter [1,2]

From the Departments of Cardiology [1] and Radiology [2] Erasmus MC, University Medical Center Rotterdam, The Netherlands

Journal of the American College of Cardiology, 2004; 43 (12): 2265-2270

Abstract

Objectives.
This study was designed to prospectively evaluate the diagnostic performance of multislice spiral computed tomography (msct) coronary angiography for the detection of significant lesions in all segments of the coronary tree potentially suitable for revascularization.
Background.
Non-invasive msct coronary angiography is a promising coronary imaging technique.
Methods.
Sixteen-row msct coronary angiography was performed in 128 patients (89% men, mean age 58.9 11.7 years) in sinus rhythm with stable angina pectoris scheduled for conventional coronary angiography. Sixty percent (77 of 128) of patients received pre-scan oral β-blockers, resulting in a mean heart rate of 57.7 7.7 beats/min. The diagnostic performance of msct for detection of significant lesions (50% diameter reduction) was compared with that of quantitative coronary angiography (qca).
Results.
The sensitivity of msct for detection of significant lesions was 92% (216 of 234, 95% confidence interval [ci]: 88 to 95). Specificity was 95% (1,092 of 1,150, 95% ci: 93 to 96), positive predictive value 79% (216 of 274, 95% ci: 73 to 88), and negative predictive value 98% (1,092 of 1,110, 95% ci: 97 to 99). Two 50% lesions were missed because of motion artifacts and two because of severe coronary calcifications. The rest (78%, 14 of 18) were detected but incorrectly classified as 50% obstructions. All patients with and 86% (18 of 21) of patients without significant lesions on qca were correctly classified by msct. All patients with significant left main disease or total occlusions were correctly identified on msct.
Conclusions.
Sixteen-row msct coronary angiography permits reliable detection of significant obstructive coronary artery disease in patients with stable angina in sinus rhythm.

MSCT Coronary Angiography in Stable Angina

Multislice spiral computed tomography (MSCT) coronary angiography is a promising non-invasive technique for the detection of obstructive epicardial coronary artery disease (CAD), and 16-row MSCT scanners have the potential to further improve its diagnostic performance.[1] Complete visualization of all clinically important coronary segments is a prerequisite for MSCT coronary angiography to become an accepted clinical tool for the assessment of patients with suspected CAD. Previous studies performed in relatively small numbers of patients showed high sensitivity and specificity for the detection of significant obstructive lesions.[2,3] However, in one study, a significant number of coronary segments were excluded because of poor image quality, and neither report presented a comprehensive lesion-by-lesion comparative analysis.

We prospectively evaluated the diagnostic accuracy of MSCT coronary angiography for the detection of significant lesions in coronary segments potentially amenable to revascularization (≥2 mm in diameter).

Methods

Study population.

During a period of six months, we studied 128 patients (113 men, 15 women, mean age 58.9±11.7 years) with stable angina pectoris scheduled for conventional coronary angiography. Only patients in sinus rhythm able to perform a 20-s breath-hold were included. Exclusion criteria were contraindications to iodinated contrast (e.g., known allergy, serum creatinine >120 mmol/l, and thyroid disorders), patients with previous bypass surgery, and patients presenting with an acute coronary syndrome. No patients of the previously reported studies were included in the present study.

The institutional review board of our institution approved the study and all patients gave written, informed consent.

Patient preparation

A single oral dose of 100 mg metoprolol (Selokeen, AstraZeneca Pharma-ceutics, London, United Kingdom) was administered 1 h before the scan if the heart rate was ≥65 beats/min.

Scan protocol and image reconstruction

All scans were performed using a 16-row MSCT scanner (Sensation 16, Siemens, Germany). Scan parameters were: detector collimation 16 x 0.75 mm, tube rotation time 420 ms, table feed 3 mm/rotation, tube voltage 120 kV, and tube current 400 to 450 mAs. Prospectively triggered X-ray tube current modulation was applied in patients with a heart rate below 60 beats/min and in the absence of any rhythm disturbances during a monitoring period of approximately 1 min. This feature reduces the radiation output of the X-tube during the less important systolic phase, thereby decreasing the total radiation dose by 40% to 50% in patients with low heart rates.[4,5] A bolus of 100 ml of contrast (Visipaque 320, Amersham Health, United Kingdom) was injected intravenously at a flow rate of 4 ml/s. An automated bolus tracking system was used to synchronize the arrival of the contrast material with initiation of the scan. All data were acquired during a single breath-hold of approximately 20 s, and images were reconstructed using retrospective ECG gating. To obtain motion-free images, standard reconstruction windows were selected during the mid-to-end diastolic phase (350, 400, and 450 ms before the next R-wave).

Additional image reconstruction windows were explored when deemed necessary. The reconstruction algorithm uses data obtained in half gantry rotation time, resulting in a temporal resolution of up to 210 ms. In case of a heart rate of >70 beats/min, a bi-segmental reconstruction algorithm is applied that uses data obtained from two consecutive heartbeats, reducing the effective reconstruction interval per heart cycle down to 105 ms, depending on the heart rate.[1]

Quantitative coronary angiography (QCA)

The mean (SD) interval between the MSCT scan and conventional coronary angiography was 19.1±10.4 days. The coronary arteries were divided into segments according to the American Heart Association classification.[6] A single observer, unaware of the MSCT results, classified all coronary segments as <2 and ≥2 mm in diameter using a QCA algorithm (CAAS, Pie Medical, Maastricht, Netherlands). Only segments classified as ≥2 mm were considered for comparison with MSCT. The severity of coronary stenoses was quantified in two orthogonal views, and a stenosis was classified as significant if the mean lumen diameter reduction was ≥50%.

MSCT image evaluation

Two observers blind to the results of conventional coronary angiography independently evaluated all of the MSCT scans. Thin-slab maximum intensity projections with a slice thickness of 2 to 6 mm, depending on the presence of adjacent structures or coronary calcifications, were used to screen for coronary stenoses. Multiplanar reconstructions were used to obtain more detailed information.

All main branches as well as large (2 mm in lumen diameter) side branches of the coronary tree were evaluated for the presence of significant ≥50% diameter reduction) obstructive stenoses. Segments with stents were excluded from analysis because beam-hardening artifacts and partial volume effects hamper reliable visualization of the coronary lumen. Image quality of all segments was classified as good, adequate, or poor. Good image quality was classified as the absence of any image-degrading artifacts related to motion, noise, or calcification. In the presence of image-degrading artifacts, image quality was classified as adequate or poor. Adequate image quality allowed the assessment of significant lesions with moderate confidence, whereas poor image quality allowed the assessment of significant lesions with only a low confidence.

The presence of calcium in the coronary wall was systematically assessed. Each segment was classified as non-calcified, moderately calcified (small isolated eccentric high-density lesions in the coronary wall), or heavily calcified (high-density lesions extending longitudinally along the coronary wall, causing beam hardening and partial volume artifacts). Disagreements were resolved by consensus.

Statistical analysis

The diagnostic performance of MSCT coronary angiography for the detection of significant obstructive lesions, with QCA as the standard of reference, is presented as sensitivity, specificity, and negative and positive predictive value. These diagnostic parameters are expressed with a 95% confidence interval calculated with binomial expansion. On a lesion-by-lesion analysis, inter- and intra-observer variability for the detection of significant lesions was calculated and expressed as kappa values. The most proximal significant stenosis was considered as the predominant lesion in the vessel-based analysis.

RESULTS

Sixty percent (77 of 128) of the patients received a β-blocker before the MSCT scan and 42 of these patients were already receiving beta-blockers. The mean (±SD) heart rate was 57.7±7.7 during the scan procedure. The total scan time was 18.2±1.4 s. One scan could not be evaluated because of technical failure. Prospectively triggered X-tube modulation was applied in 64% (81/127) of the remaining patients.

Conventional coronary angiography revealed no significant stenoses in 17% (21 of 127), one-vessel disease in 35% (44 of 127), two-vessel disease in 35% (44 of 127), and three-vessel disease in 14% (18 of 127) of patients. Six patients had significant left main stenosis.

Lesion-by-lesion analysis: overall performance of MSCT

A total of 1,384 non-stented segments with a diameter 2 mm were analyzed for the detection of significant obstructive coronary stenoses (37 segments with stents were excluded). Per patient, we included 10.9±1.9 segments for analysis. Image quality was classified as good in 75% (1,049 of 1,384) of segments, adequate in 18% (243 of 1,384) of segments, and poor in 7% (92 of 1,384) of segments. Causes of poorly assessable segments were motion artifacts (63%, 58 of 92), severe calcification (30%, 28 of 92), and low contrast-to-noise ratio (7%, 6 of 92). Motion artifacts were most frequently located in the midright coronary artery. Inter- and intra-observer variability for the detection of significant lesions had kappa values of 0.71 and 0.79, respectively.

The sensitivity was 92% (216 of 234, 95% confidence interval [CI]: 88 to 95), the specificity was 95% (1,092 of 1,150, 95% CI: 93 to 96), the positive predictive value was 79% (216 of 274, 95% CI: 73 to 88), and the negative predictive value was 98% (1,092 of 1,110, 95% CI: 97 to 99) (Table 1) for the detection of significantly obstructed lesions.

Nineteen percent (268 of 1,384) of all segments were classified as heavily calcified, 31% (430 of 1,384) as moderately calcified, and 50% (686 of 1,384) as non-calcified. The diagnostic performance of MSCT coronary angiography for detection of significant obstructive lesions in non-calcified, moderately calcified, and heavily calcified segments is tabulated in Table 2.

Lesion-by-lesion analysis: false-negative results on MSCT

Eighteen significantly obstructed segments with a mean diameter reduction of 61.1±7.5% (range 51% to 72% using QCA) were missed on the MSCT scan. The majority of the missed lesions were located in the circumflex coronary artery or in smaller side branches (13 of 18, 72%). Two lesions were missed because of severe calcifications and two because of motion artifacts; the severity of the stenosis was underestimated in the remaining 14 lesions.

Lesion-by-lesion analysis: false-positive results on MSCT

Fifty-eight segments were incorrectly classified as significantly obstructed because of overestimation of the severity of the lesion. Fifteen non-calcified and 17 moderately calcified lesions (mean diameter reduction 41.2±5.1%, range 30% to 48%) were overestimated. Twenty-six heavily calcified lesions were overestimated; in the majority of these lesions conventional angiography revealed only minor wall irregularities. Overestimation of heavily calcified lesions was likely related to beam-hardening artifacts and partial volume effects resulting in blooming of the coronary calcifications.

Table 1. Results: Detection of Significant (≥50%) Stenoses With 16-Row Multislice Spiral Computed Tomography Coronary Angiography

Coronary Segment	N	TP	TN	FP	FN	Sensitivity	Specificity	Positive PV	Negative PV
All segments	1,384	216	1,092	58	18	92%(216/234)	95%(1,092/1,150)	70%(216/274)	98%(l,092/1,110)
LM	124	6	118	0	0	100%(6/6)	100%(118/118)	100%(6/6)	100%(118/118)
LAD	473	90	350	27	6	94%(90/96)	93%(350/377)	77%(90/117)	98%(350/356)
Proximal	124	37	74	10	3	93%(37/40)	88%(74/84)	79%(37/47)	96%(350/353)
Middle	111	41	65	5	0	100%(41/41)	93%(65/70)	89%(41/46)	100%(65/65)
Distal	102	5	94	3	0	100%(5/5)	97%(94/97)	63%(5/8)	100%(94/94)
Side branches	136	7	117	9	3	70%(7/10)	93%(317/126)	44%(7/16)	9S%(117/120)
CX	395	49	325	12	9	84%(49/58)	96%(325/337)	80%(49/61)	97%(325/334)
Proximal	111	16	90	3	2	89%(16/18)	97%(90/93)	84%(16/19)	98%(90/192)
Middle	102	13	81	4	4	76%(13/17)	95%(81/85)	76%(13/17)	95%(81/85)
Side branches	182	20	154	5	3	87%(20/23)	97%(154/159)	80%(49/61)	98%(154/157)
RCA	392	71	299	19	3	96%(71/74)	94%(299/318)	79%(71/90)	99%(299/302)
Proximal	120	30	81	9	0	100%(30/30)	90%(81/90)	77%(30/39)	100%(30/30)
Middle	103	31	63	8	1	97%(31/32)	89%(63/71)	79%(31/39)	98%(63/64)
Distal	91	8	80	2	1	89%(8/9)	98%(80/82)	80%(8/10)	99%(80/81)
PDA	78	2	75	0	1	67%(2/3)	100%(75/75)	100%(2/2)	99%(75/76)

CX = circumflex coronary artery, FN = false negative, FP = false positive, LAD = left anterior descending coronary artery, LM = left main coronary artery, PDA = posterior descending artery, RCA = right coronary artery, PV = predictive value, TN = true negative, TP = true positive.

Source: Mollet et al. (2004)

Table 2. Diagnostic Performance of Multislice Spiral Computed Tomography Coronary Angiography for the Detection of Significant Obstructive Lesions

Segments	N	TP	TN	FP	FN	Sensitivity	Specificity	Positive PV	Negative PV
Non-calcified	686	60	602	15	9	87% (76–97)	98% (96–98)	80% (69–91)	90% (97–99)
Moderately calcified	430	64	342	17	7	90% (80–97)	95% (92–97)	79% (68–90)	98% (95–99)
Heavily calcified	268	92	148	26	2	98% (92–94)	85% (78–90)	78% (69–86)	99% (95–99)
Overall	1,384	216	1,092	58	18	92% (88–95)	95% (93–96)	79% (73–88)	98% (97–99)

Non-calcified = complete absence of coronary calcification; moderately calcified = Small isolated eccentric calcified deposits; Heavily calcified = Large deposits of calcium expanding longitudinally along the coronary wall, causing partial volume effects and beam-hardening artifacts. Abbreviations as in Table 1.

Vessel-based analysis

The sensitivity for classification of vessels with or without CAD was 94% (177 of 188, 95% CI: 89 to 95); specificity was 91% (298 of 329, 95% CI: 86 to 93), positive predictive value

was 85% (177 of 208, 95% CI: 79 to 91), and negative predictive value was 96% (298 of 309, 95% CI: 93 to 98). All significantly obstructed left main coronary arteries (n=6) and total occlusions (n=60) were correctly identified on the MSCT scan.

Patient-based analysis

Multislice spiral computed tomography coronary angiography correctly identified 18 of 21 (86%) patients without significant stenoses on angiography. No patient with single-vessel disease (n=44) on angiography was incorrectly classified as having no significant coronary disease on MSCT; however, 15 patients were classified as having multivessel disease. Fifty-five patients with multivessel disease (n=62) on angiography were correctly classified on MSCT; the remaining seven patients were classified as having single-vessel disease.

Overall, all patients with a significant stenosis in one or more vessels were correctly classified as patients with CAD. Sensitivity for classification of patients with or without CAD was 100% (106 of 106, 95% CI: 96 to 100), specificity was 86% (18 of 21, 95% CI: 63 to 96), positive predictive value was 97% (106 of 109, 95% CI: 92 to 98), and negative predictive value was 100% (18 of 18, 95% CI: 81 to 100).

Discussion

Complete visualization of all clinically important coronary segments is a prerequisite for MSCT coronary angiography to become an accepted clinical tool for the assessment of patients with suspected CAD. Previous studies in relatively small cohorts showed high sensitivity and specificity for the detection of significant obstructive lesions (2,3). The major finding of the present study, which compared MSCT with QCA, is that 16-row MSCT is a robust tool for assessing the presence of significantly obstructed coronary artery in the clinically important part of the coronary tree (Figs. 1 and 2).

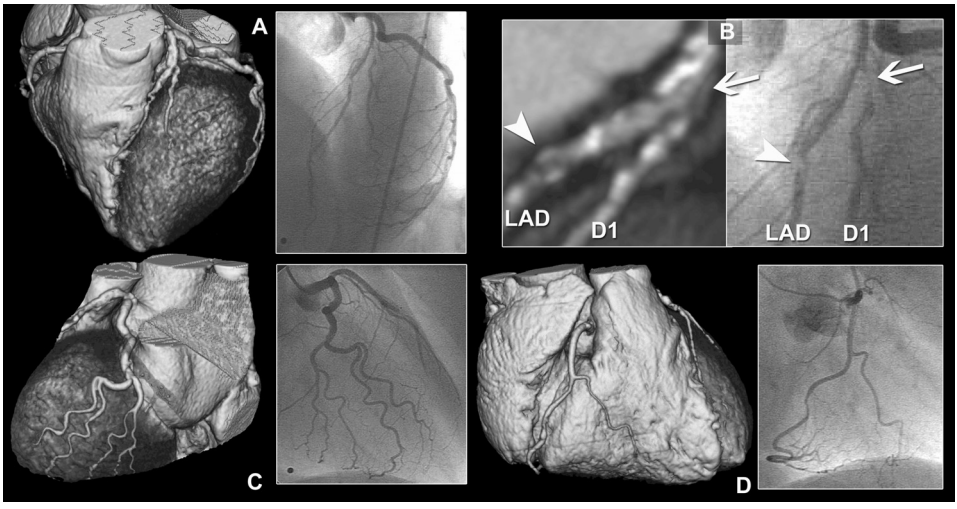

Figure 1. Volume-rendered multislice spiral computed tomography images (left) and corresponding conventional angiography images (right) of the left anterior descending (LAD) (A), circumflex (C), and right coronary artery (D) in a 69-year-old woman with stable angina and a positive bicycle test. Significant lesions were found in the proximal part of the LAD coronary artery (arrowhead) and first diagonal (D1) (arrow), which are demonstrated on the inlay (B).(A full color version of this illustration can be found in the color section (chapter 21)).

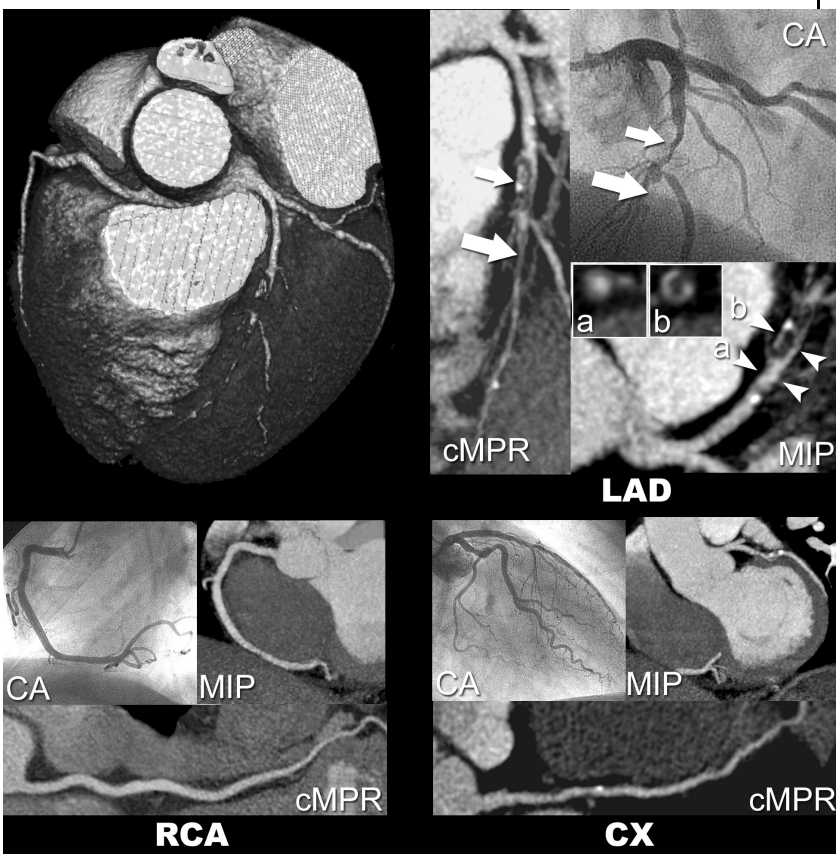

Figure 2. Colored image volume rendered multislice spiral computed tomography (MSCT) image providing an overview of the anatomy of the main coronary arteries. Black and white images MSCT (curved multiplanar reconstructions [cMPR] and maximum intensity projections [MIP]) and conventional coronary angiography (CA) images of the four main coronary arteries (left main/left anterior descending [LAD], circumflex coronary artery [CX], right coronary artery [RCA]) of a single patient. The small arrows highlight a high-grade stenosis and the large arrows an occlusion located at the midpart of the LAD. The arrowheads indicate cross-sectional images proximal (inlay a) and within the occlusion (inlay b). Inlay b shows calcified (displayed as white) and non-calcified (displayed as black) plaque tissue components. (A full color version of this illustration can be found in the color section (chapter 21)).

All MSCT segments corresponding to angiographic segments with a diameter above 2 mm on QCA were analyzed, without any prespecified exclusion criteria based on the quality of the MSCT images. This resulted in 10.9 1.9 available segments per patient. For the segment based analysis, both the overall sensitivity and specificity were found to be above 90% (92% and 94%, respectively). Image quality was classified as poor in 7% of the segments. However, these segments were included in the comparative analysis with QCA.

The current-generation 16-slice scanners have a higher spatial and temporal resolution when compared with previous scanners, resulting in an improvement in the diagnostic accuracy of MSCT angiography.[7–10] One-half of the segments contained calcified deposits in the coronary wall.

Calcifications are high-density structures causing beam-hardening artifacts and partial volume effects on computed tomography. These artifacts have an important impact on the evaluation of calcified lesions. Only two lesions in the present study were missed because of severe calcifications, but 26 heavily calcified lesions were overestimated. The majority of these lesions appeared as wall irregularities on conventional angiography.

Another 32 overestimated lesions with a mean diameter reduction of 40% on QCA (range between 30% and 48%) were non-calcified or moderately calcified. This probably reflects the semiquantitative nature of the evaluation of coronary lesions with MSCT.

One-third of the missed 50% lesions were located in the circumflex and a further one-third in smaller side branches. The circumflex coronary artery is more difficult to evaluate, probably because of its tortuous course
and overlapping structures, whereas the relatively high number of missed lesions in smaller side branches suggest a lower diagnostic performance of MSCT angiography in branches toward the threshold of 2 mm.

All patients with at least one significant obstruction on QCA were correctly classified as having CAD with MSCT. This suggests that the current generation of scanners may be a suitable tool to triage patients with stable angina who are being considered for revascularization. Further studies are needed to determine the role of this technique in the clinical workup of patients with other presentations of coronary disease or who are being evaluated to exclude significant disease.

Study limitations

Only patients with stable angina were included in this study. Whether a broader group of patients might benefit from this technique (excluding patients with severe arrhythmia) must be explored, but there are no reasons to believe that results would differ in patients with acute coronary syndromes.

In our study we noted that the sensitivity of detection for non-calcified obstructive lesions tended to be lower. This is caused by the fact that these lesions have a relatively low tissue contrast and may be missed, especially in small vessel segments. This may be problematic in younger patients with a lower likelihood of lesion calcification. Dedicated automatic software that is able to detect and calculate the degree of coronary stenoses would improve diagnostic accuracy.

The high radiation exposure during MSCT coronary angiography, which is reported between 6.7 and 13.0 mSv,[5,11,12] remains a matter of concern. Further fine-tuning of the prospective X-ray tube current modulation and development of new features lowering radiation exposure is highly desirable.

Conclusions

Multislice spiral computed tomography coronary angiography permits reliable detection of CAD in a population of patients in sinus rhythm with stable angina.

REFERENCES

1. Flohr TG, Schoepf UJ, Kuettner A, et al. Advances in cardiac imaging with 16-section CT systems. Acad Radiol 2003;10:386–401.
2. Nieman K, Cademartiri F, Lemos PA, Raaijmakers R, Pattynama PM, de Feyter PJ. Reliable non-invasive coronary angiography with fast submillimeter multislice spiral computed tomography. Circulation 2002;106:2051–4.
3. Ropers D, Baum U, Pohle K, et al. Detection of coronary artery stenoses with thin-slice multi-detector row spiral computed tomography and multiplanar reconstruction. Circulation 2003;107:664–6.
4. Jakobs TF, Becker CR, Ohnesorge B, et al. Multislice helical CT of the heart with retrospective ECG gating: reduction of radiation exposure by ECG-controlled tube current modulation. Eur Radiol 2002;12:1081–6.
5. Trabold T, Buchgeister M, Kuttner A, et al. Estimation of radiation exposure in 16-detector row computed tomography of the heart with retrospective ECG-gating. Rofo Fortschr Geb Rontgenstr Neuen Bildgeb Verfahr 2003;175:1051–5.
6. Austen WG, Edwards JE, Frye RL, et al. A reporting system on patients evaluated for coronary artery disease. Report of the Ad Hoc Committee for Grading of Coronary Artery Disease, Council on Cardiovascular Surgery, American Heart Association. Circulation 1975;51:5–40.
7. Nieman K, Oudkerk M, Rensing BJ, et al. Coronary angiography with multi-slice computed tomography. Lancet 2001;357:599–603.
8. Achenbach S, Giesler T, Ropers D, et al. Detection of coronary artery stenoses by contrast-enhanced, retrospectively electrocardiographicallygated, multislice spiral computed tomography. Circulation 2001;103: 2535–8.
9. Knez A, Becker CR, Leber A, et al. Usefulness of multislice spiral computed tomography angiography for determination of coronary artery stenoses. Am J Cardiol 2001;88:1191–4.
10. Vogl TJ, Abolmaali ND, Diebold T, et al. Techniques for the detection of coronary atherosclerosis: multi-detector row CT coronary angiography. Radiology 2002;223:212–20.
11. Morin RL, Gerber TC, McCollough CH. Radiation dose in computed tomography of the heart. Circulation 2003;107:917–22.
12. Hunold P, Vogt FM, Schmermund A, et al. Radiation exposure during cardiac CT: effective doses at multi-detector row CT and electron-beam CT. Radiology 2003;226:145–52.

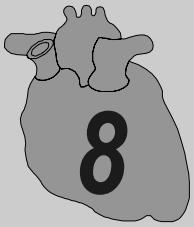

Chapter 8

IMPROVED DIAGNOSTIC ACCURACY WITH 16-ROW MULTISLICE CT CORONARY ANGIOGRAPHY TOMOGRAPHY

Abstract

Nico R. Mollet [1,2]
Filippo Cademartiri [2]
Gabriel P. Krestin [2]
Eugène P. Mc Fadden [1]
Chourmouzios A. Arampatzis [1]
Patrick W. Serruys, MD [1]
Pim.J. de Feyter [1,2]

Departments of Cardiology [1] and Radiology [2]
Erasmus MC,
University Medical Center,
Rotterdam,
The Netherlands

Journal of the American College of Cardiology,
2005; 45 (1):128–32

OBJECTIVES.
To compare the diagnostic value of Multislice Computed Tomography (MSCT) coronary angiography to detect significant stenoses (50% lumen diameter reduction) with that of invasive coronary angiography.
Background:
The latest 16-row MSCT scanner has a faster rotation time (375 ms) and permits scanning with a higher X-ray tube current (500-600 mAs) during MSCT coronary angiography when compared to previous scanners.

METHODS.
We studied 51 patients (37 men, mean age 58.9±10.0 years) with stable angina or atypical chest pain. Patients with pre-scan heart rates ≥70 beats/minute received oral β-blockade. The heart was scanned after intravenous injection of 100 ml contrast (iodine content: 400 mg/ml). Mean scan-time was 18.9±1.0 seconds. The MSCT-scans were analysed by 2 observers unaware of the results of invasive angiography and all available ≥2mm coronary branches were included.

RESULTS.
Invasive coronary angiography demonstrated normal arteries in 16% (8/51), non-significant disease in 21% (11/51), single-vessel disease in 37% (19/51), and multi-vessel disease in 26% (13/51) of patients. There were 64 significant lesions. Sensitivity, specificity, positive and negative predictive value for detection of significant lesions on a segment-based analysis were 95% (61/64, 95% CI 86-99), 98% (537/546, 95% CI 96-99), 87% (61/70, 95% CI 76-98), and 99% (537/540, 95% CI 98-99) respectively. All patients with angiographically normal coronary arteries or significant lesions were correctly identified. Three of 11 patients with <50% lesions were incorrectly classified as having single vessel disease.

CONCLUSIONS.
16-row MSCT coronary angiography reliably detects significant coronary stenoses in patients with atypical chest pain or stable angina pectoris.

INTRODUCTION

Ongoing significant advances in MSCT technology in recent years prompted us to re-evaluate the clinical potential of non-invasive coronary angiography (CA).[1-9] The latest generation 16-row MSCT-scanners have a faster X-ray tube rotation speed that provides higher temporal resolution. In addition, a higher X-ray tube current during MSCT-CA can be selected, which increases the contrast-to-noise ratio and improves image quality.

We now report the current diagnostic performance of MSCT coronary angiography to detect significant coronary stenoses in stable patients referred for conventional angiography on an outpatient basis.

METHODS

Study Population

During a period of 7 months, we studied 51 patients (37 male, mean age 58.9±10.0) with atypical chest pain or stable angina scheduled for conventional-CA to determine the presence and extent of coronary artery disease. Only patients in sinus rhythm, who had never undergone angioplasty or bypass surgery and were able to breath-hold for 20 seconds, were included. Patients presenting with an acute coronary syndrome or in whom administration of intravenous iodinated contrast material was contraindicated (e.g. known allergy, impaired renal function, or thyroid disorders) were excluded. Our institutional review board approved the study protocol and all patients gave written informed consent.

Patient Preparation

Patients with a heart rate above 70 beats/minute received, unless contraindicated, a single oral dose of 100mg metoprolol one hour before the scan.

Scan protocol and Image Reconstruction

All patients were scanned on a 16-row MSCT scanner (Sensation 16 Straton®, Siemens, Forchheim, Germany). Scan parameters: 16 x 0.75 mm detector collimation, rotation time 375 ms, table feed 3.0 mm/rotation, tube voltage 120 kV, effective mAs: 500-600, CTDIvol 51,0 mGy, no X-ray tube modulation. The estimated radiation exposure using this scan protocol is 11.8-16.3 mSv (Male-Female). A bolus of 100 ml contrast material with an iodine content of 400 mg/ml (iomeprol, Iomeron® 400, Bracco, Milan, Italy) was injected through an arm vein (rate: 4 ml/s). A bolus-tracking technique was used to synchronize the arrival of contrast in the coronary arteries with the initiation of the scan. Data was acquired during a single breath-hold of 18.9±1.0 s.

ECG-gated images were standard reconstructed during mid-to-end diastole to obtain optimal image quality. Additional reconstruction windows (e.g. early diastole) were explored when deemed necessary. Generally, best image quality was obtained when the reconstruction windows were positioned -350 ms before the next R-wave, or at 60% of the R-R interval. The reconstruction algorithm uses data of a single heartbeat, obtained during half a rotation time, resulting in a temporal resolution of up to 188 ms.

Quantitative Coronary Angiography (QCA)

All scans were performed within 2 weeks prior to the conventional diagnostic angiogram. A single observer, unaware of the MSCT results, identified coronary segments according to the AHA classification,[10] and classified them as <2 and ≥2mm using a quantitative coronary angiography algorithm (CAAS, Pie Medical, The Netherlands). All available ≥2mm

segments were included for comparison with MSCT-CA. Segments were classified as normal (smooth parallel or tapering borders), as having non-significant disease (luminal irregularities or <50% stenosis), or as having significant stenoses. Stenoses were evaluated in two orthogonal views, and classified as significant if the mean lumen diameter reduction was ≥50%.

MSCT Image Evaluation

All scans were analysed independently by a cardiologist and a radiologist, unaware of the results of conventional-CA. All main coronary arteries and large (≥2 mm) side branches were evaluated. Maximum intensity projections were used to identify coronary lesions and multi-planar reconstructions to classify lesions as significant or non-significant. Disagreement between observers was resolved by consensus.

Statistical Analysis

The diagnostic performance of MSCT-CA for detection of significant lesions in ≥2 mm coronary arteries with QCA as the standard of reference is presented as sensitivity, specificity, positive and negative predictive value with the corresponding 95% confidence intervals. Comparison between MSCT and QCA was performed on 3 levels: segment-by-segment, vessel-by-vessel (no or any disease per vessel), and patient-by-patient (no or any disease per patient). Coronary segments were scored irrespective of the score in other segments or vessels within the same patient, therefore independence between the analyses was assumed. The most proximal coronary lesion determined the diagnostic performance in the vessel-based analysis in coronary branches with >1 significant lesions.

RESULTS

Conventional-CA revealed normal coronary arteries in 16% (8/51), non-significant disease in 21% (11/51), and significant coronary artery disease in 63% (32/51) of patients. Nineteen patients had single- and 13 patients multi-vessel disease; Five patients had significant left main disease. The mean number of included segments per patient was 12.0±1.9. All proximal and mid coronary segments were included in the analysis. Mean heart rate during scanning was 57.1±1.0 (range 43 to 80) beats/minute. A β-blocker was administered before the scan in 25 of the 51 patients; most (80%) were already receiving long-term β-blockade. Inter- and intra-observer variability for detection of significant lesions had κ-values of 0.73 and 0.80.

Diagnostic Performance of MSCT Coronary Angiography

The diagnostic performance of MSCT-CA for detection of significant lesions is detailed in Table 1. Two significant (52% and 57% lumen diameter reduction) lesions on QCA, located in the proximal and mid circumflex coronary artery (CX), were incorrectly classified as non-significant on MSCT. A single significant (67% lumen diameter reduction) lesion in the distal right coronary artery (RCA) was not visualised on the MSCT scan due to motion artifacts. No significant lesions were missed in the left main (LM) or left anterior descending (LAD) coronary arteries. Nine non-significant lesions on QCA were incorrectly classified as ≥50% lesions on MSCT. On conventional-CA 4 of these were non-significant lesions (mean lumen reduction 40%, range 38-42%), and the other 5 were lumen irregularities. The majority (n=7) of these lesions were calcified.

Table 1. Diagnostic performance of MSCT-CA for detection of ≥50% stenoses

	N	Sensitivity	Specificity	Positive PV	Negative PV
Segment-based	610	61/64 (95,86-99)	537/546 (98,96-99)	61/70 (87,76-98)	537/540 (99,98-99)
LM (1)	51	5/5 (100,47-100)	46/46 (100,92-100)	5/5 (100,47-100)	46/46 (100,92-100)
LAD (3-5)	205	24/24 (100,85-100)	175/181 (97,92-98)	24/30 (80,61-96)	175/175 (100,97-100)
CX (3-5)	172	15/17 (88,63-99)	154/155 (99,96-99)	15/16 (94,69-99)	154/156 (99,95-99)
RCA (3-4)	182	17/18 (94,72-99)	162/164 (99,95-99)	17/19 (90,66-99)	162/163 (94,96-99)
Vessel-based	202	51/53 (96,87-99)	143/149 (96,91-98)	51/57 (90,78-97)	143/145 (99,95-99)
LM	51	5/5 (100,47-100)	46/46 (100,92-100)	5/5 (100,47-100)	46/46 (100,92-100)
LAD	51	16/16 (100,79-100)	31/35 (89,73-96)	16/20 (80,56-95)	31/31 (100,88-100)
CX	50	13/14 (93,66-99)	35/36 (97,85-99)	13/14 (93,66-99)	35/36 (97,85-99)
RCA	50	17/18 (94,72-99)	31/32 (97,83-99)	17/18 (94,72-99)	31/32 (97,83-99)
Patient-based	51	31/31 (100,88-100)	17/20 (85,62-96)	31/34 (91,76-97)	17/17 (100,80-100)

PV = Predictive Value. Values are n (%, 95% confidence interval)

On a vessel-based analysis, two significantly obstructed vessels were missed on MSCT: one RCA and one CX. Six vessels without ≥50% lesions were incorrectly classified as significantly obstructed.

All patients with normal coronary angiograms were classified as having neither significant nor non-significant stenosis on MSCT. All patients with significant coronary artery disease were correctly identified on MSCT as having at least single-vessel disease, whereas 3 patients without ≥50% lesions were classified as single-vessel disease. Two examples comparing the results of MSCT-CA with conventional-CA are shown in Figures 1-2.

DISCUSSION

Conventional-CA is currently the standard technique for evaluation of patients with suspected coronary atherosclerosis. It is used both to exclude coronary atherosclerosis as a cause of symptoms and to evaluate the extent and severity of atherosclerosis with a view to referral for revascularization. Previous reports demonstrated that earlier generations of MSCT scanners showed promise for the non-invasive detection of coronary artery stenoses.[1-9] Those scanners acquire fewer slices simultaneously[1-8] (4, 8, or 12 vs. 16 slices) and are equipped with a lower X-ray tube rotation speed[1-9] (500 or 420 ms vs. 375 ms) compared to the latest generation 16-row MSCT scanners. An additional advantage of the new MSCT scanner is the ability to scan with a higher X-ray tube output, which increases the contrast-to-noise ratio and therefore image quality. These technical developments result in a markedly improved diagnostic performance when compared to the results reported with previous scanner generations.

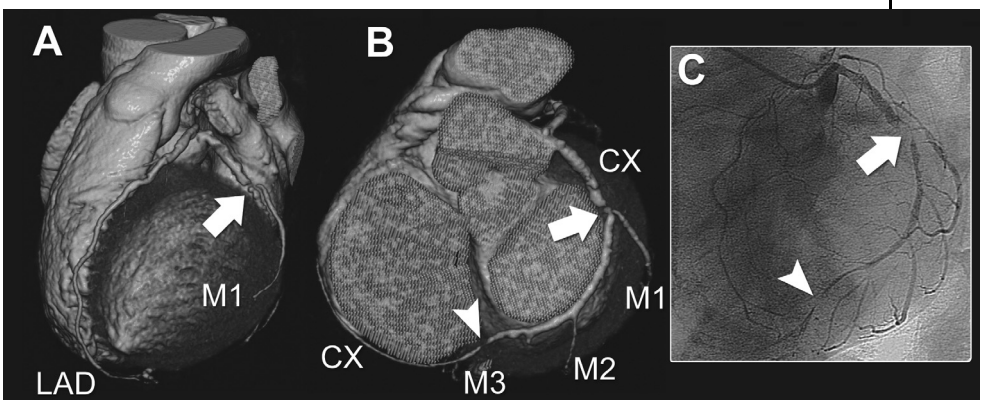

Figure 1a. Volume rendered CT images (A, B) reveal the presence of 2 significant stenoses (arrow, arrowhead) located at the circumflex coronary artery (CX), which was confirmed on the conventional angiogram (C). LAD: left anterior descending coronary artery, M: marginal branch. (A full color version of this illustration can be found in the color section (Chapter 21)).

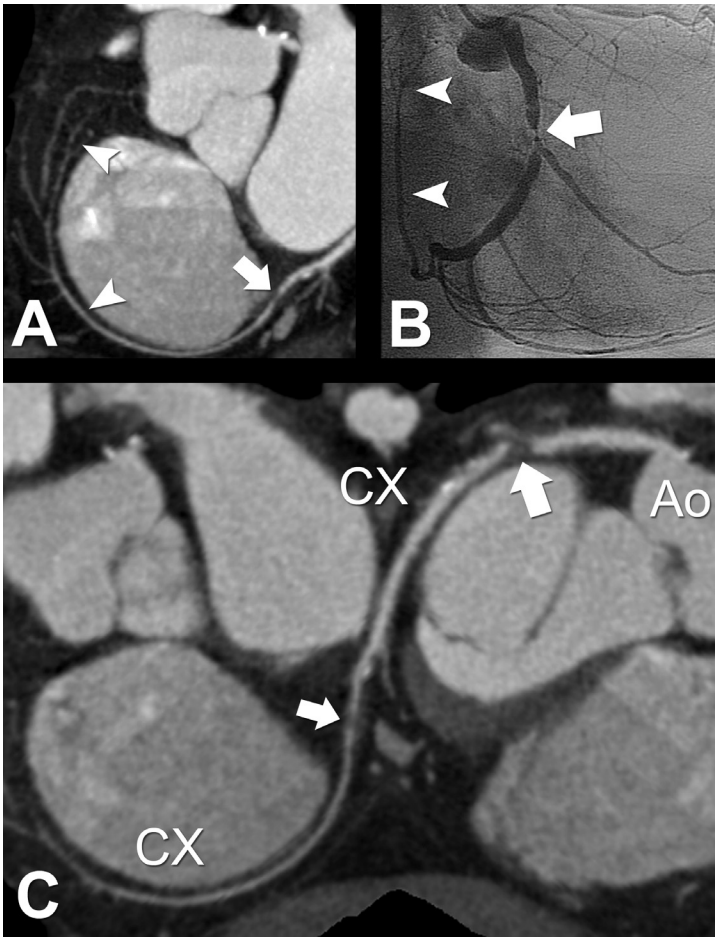

Figure 1b. Maximum intensity projected (A) and curved multiplanar reconstructed (C) CT images showing the trajectory of the circumflex coronary artery (CX), which ends almost at the right coronary sinus. The arrows indicate the stenoses. These findings were confirmed on the conventional angiogram (B).
Ao: Aorta.

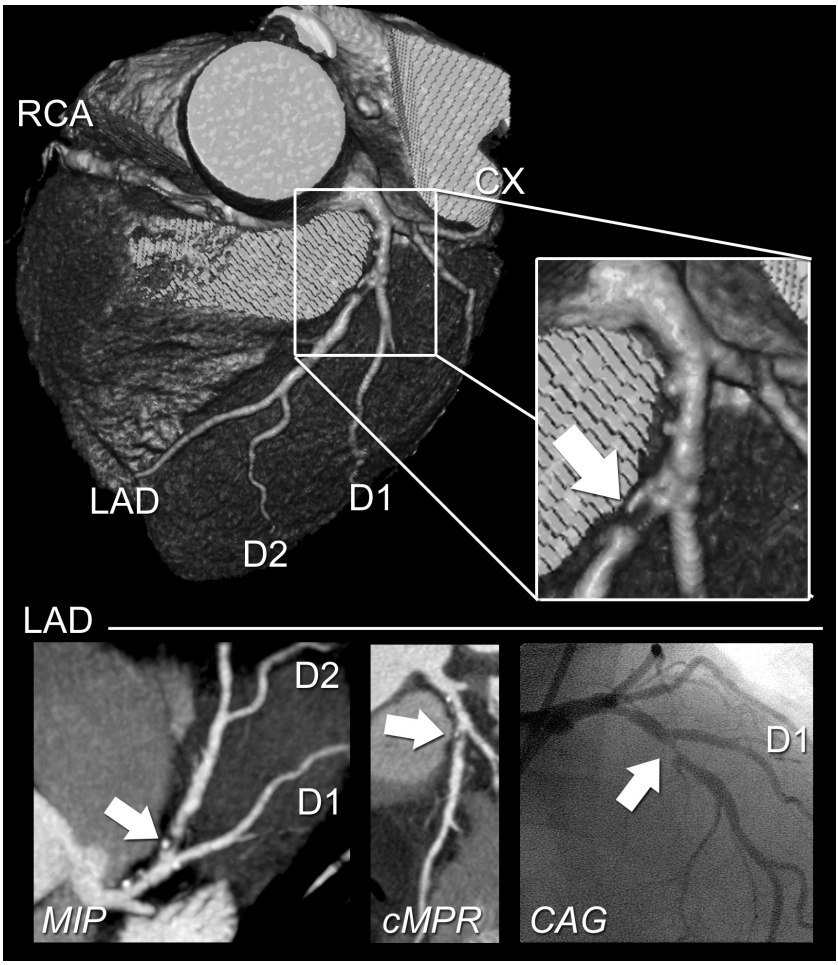

Figure 2. Volume rendered (coloured images), maximum intensity projected (MIP), and curved multiplanar reconstructed (cMPR) CT images demonstrate a significant stenosis (arrow) of the left anterior descending coronary artery (LAD), which was confirmed on the conventional angiogram (CAG).
CX: circumflex coronary artery, D: diagonal branch, RCA: right coronary artery. (A full color version of this illustration can be found in the color section (Chapter 21)).

Our study found that non-invasive CA can detect significant stenoses with a sensitivity of 95%, a specificity of 98% and positive and negative predictive values of 87% and 99% respectively, when compared to conventional-CA. Furthermore, all patients with normal coronary arteries on conventional-CA were classified as having neither significant nor non-significant stenosis on MSCT. These results were obtained in patients with atypical chest pain or stable angina pectoris who had varying degrees of coronary artery disease ranging from no detectable significant obstructive disease to 1, 2, 3 vessel disease or left main disease.

MSCT-CA will not equal either the resolution or real-time imaging capabilities of conventional-CA in the foreseeable future; however, its non-invasive nature renders the

technique more patient-friendly and reduces the risk of iatrogenic injury. This technique may open new avenues for research and contribute to the development of novel management algorithms in selected patients. Potential applications include the evaluation of asymptomatic individuals at high risk of atherosclerosis or assessment of disease progression in patients with known coronary artery disease.

Limitations

We did not investigate patients with an acute coronary syndrome, because of safety and logistic issues associated with the examination of these patients in a setting outside the coronary care unit. However, we do expect that the diagnostic performance of MSCT would be similar in these patients.

The limited spatial resolution of current MSCT scanners only allows qualitative, therefore user-dependent, assessment of coronary stenoses. Development of reliable software able to detect and quantify the degree of coronary stenoses would make MSCT-CA a more robust and reproducible technique.

The estimated radiation dose during MSCT-CA using this scan protocol (11.8-16.3 mSv [Male-Female]) is higher when compared to previously reported doses using older scanner generations (6.7-13.0 mSv)[11,12] or conventional-CA (3-5 mSv). Radiation exposure should be reduced by technical adjustments such as prospective X-ray tube current modulation, which limits the radiation exposure with nearly 50% in patients with low heart rates.[11] However, we did not apply this feature because it limits reconstruction of images during the early-diastolic phase, which can be of importance for evaluation of the RCA.

Persistent irregular heart rhythm such as atrial fibrillation and frequent extra-systoles precludes MSCT-CA. However, in some cases, motion artifacts due to an occasional extra-systole can be corrected by ECG-editing. Severe coronary calcification obscures the coronary lumen and can lead to overestimation of the severity of lesions due to blooming artifacts. In fact, the vast majority of false-positive lesions were calcified (7/9). Improvements in spatial resolution and dedicated post-processing algorithms may diminish the problem.

Motion artifacts associated with higher heart rates may be resolved by faster X-ray tube rotation time or sophisticated reconstruction algorithms that use data obtained from multiple, consecutive heartbeats.

Conclusion

MSCT-CA is a reliable technique to non-invasively detect coronary stenoses in patients with stable angina and atypical chest pain. More studies are needed in other patient groups with different prevalences of disease to show that these initial favourable results are reproducible on a wider scale.

References

1. Nieman K, Oudkerk M, Rensing BJ, et al. Coronary angiography with multi-slice computed tomography. Lancet. 2001;357:599-603.
2. Achenbach S, Giesler T, Ropers D, et al. Detection of coronary artery stenoses by contrast-enhanced, retrospectively electrocardiographically-gated, multislice spiral computed tomography. Circulation. 2001;103:2535-8.

3. Knez A, Becker CR, Leber A, et al. Usefulness of multislice spiral computed tomography angiography for determination of coronary artery stenoses. Am J Cardiol. 2001;88:1191-4.
4. Vogl TJ, Abolmaali ND, Diebold T, et al. Techniques for the detection of coronary atherosclerosis: multi-detector row CT coronary angiography. Radiology. 2002;223:212-20.
5. Kopp AF, Schroeder S, Kuettner A, et al. Non-invasive coronary angiography with high resolution multidetector-row computed tomography. Results in 102 patients. Eur Heart J. 2002;23:1714-25.
6. Nieman K, Cademartiri F, Lemos PA, et al. Reliable noninvasive coronary angiography with fast submillimeter multislice spiral computed tomography. Circulation. 2002;106:2051-4.
7. Ropers D, Baum U, Pohle K, et al. Detection of coronary artery stenoses with thin-slice multi-detector row spiral computed tomography and multiplanar reconstruction. Circulation. 2003;107:664-6.
8. Kuettner A, Kopp AF, Schroeder S, et al. Diagnostic accuracy of multidetector computed tomography coronary angiography in patients with angiographically proven coronary artery disease. J Am Coll Cardiol. 2004;43:831-9.
9. Mollet NR, Cademartiri F, Nieman K, et al. Multislice Spiral CT Coronary Angiography in Patients With Stable Angina Pectoris. J Am Coll Cardiol. 2004;43:2265-70.
10. Austen WG, Edwards JE, Frye RL, et al. A reporting system on patients evaluated for coronary artery disease. Report of the Ad Hoc Committee for Grading of Coronary Artery Disease, Council on Cardiovascular Surgery, American Heart Association. Circulation. 1975;51:5-40.
11. Trabold T, Buchgeister M, Kuttner A, et al. Estimation of Radiation Exposure in 16-Detector Row Computed Tomography of the Heart with Retrospective ECG-gating. Rofo Fortschr Geb Rontgenstr Neuen Bildgeb Verfahr. 2003;175:1051-5.
12. Hunold P, Vogt FM, Schmermund A, et al. Radiation exposure during cardiac CT: effective doses at multi-detector row CT and electron-beam CT. Radiology. 2003;226:145-52.

Chapter 9

High-resolution Spiral CT Coronary Angiography in Patients Referred for Diagnostic Conventional Coronary Angiography

Abstract

Background.
The diagnostic performance of the latest 64-slice Computed Tomography (CT) scanner, with an increased temporal (165 ms) and spatial (0.4 mm^3) resolution, to detect significant stenoses in the clinically relevant coronary tree is unknown.

Methods and Results.
We studied 52 patients (34 men, mean age 59.6±12.1 years) with atypical chest pain, stable or unstable angina pectoris, or non-ST-segment elevation myocardial infarction scheduled for diagnostic conventional coronary angiography. All patients had stable sinus rhythm. Patients with initial heart rates ≥70 beats/minute received β-blockers. The heart was scanned after intravenous injection of 100 ml contrast material. Mean scan-time was 13.3±0.9 seconds. The CT-scans were analysed by 2 observers unaware of the results of invasive coronary angiography, which was used as the standard of reference. Lesions with ≥50 percentage lumenal narrowing were considered as significant stenoses.

Invasive coronary angiography demonstrated absence of significant disease in 25% (13/52), single-vessel disease in 31% (16/52), and multi-vessel disease in 45% (23/52) of patients. One unsuccessful CT-scan was classified as inconclusive. Ninety-four significant stenoses were present in the remaining 51 patients. Sensitivity, specificity, positive and negative predictive value of CT for the detection of significant stenoses on a segment-by-segment analysis were 99% (93/94, 95% CI: 94-99), 95% (601/631, 95% CI: 93-96), 76% (93/123, 95% CI: 67-89), and 99% (601/602, 95% CI: 99-100) respectively.

Conclusions.
Non-invasive 64-slice CT coronary angiography accurately detects coronary stenoses in patients in sinus rhythm and presenting with atypical chest pain, stable or unstable angina, or non-ST-segment elevation myocardial infarction.

Nico R. Mollet [1,2]
Filippo Cademartiri [1,2]
Carlos A.G. van Mieghem [1,2]
Giuseppe Runza [2]
Eugène P. Mc Fadden [1]
Timo Baks [1,2]
Patrick W. Serruys [1]
Gabriel P. Krestin [2]
Pim J. de Feyter [1,2]

From the Departments of Cardiology [1] and Radiology [2]
Erasmus MC,
University Medical Center,
Rotterdam, The Netherlands

Circulation
(in press)

INTRODUCTION

Spiral Computed Tomography (CT) coronary angiography has rapidly emerged thanks to technical improvements as a sensitive diagnostic modality.[1-12] The newest generation spiral CT scanners are significantly improved. It features 64 slices, thinner detectors, and the X-ray tube permits higher X-ray output and faster tube rotation. This results in high quality, nearly motion-free, isotropic image quality. Data is acquired during a single breath hold of approximately 13 seconds. We report the diagnostic performance of 64-slice CT coronary angiography in 52 patients with atypical chest pain, stable or unstable angina, or non-ST-segment elevation myocardial infarction referred for diagnostic invasive coronary angiography to assess the extent and severity of coronary stenoses in the clinically relevant coronary tree.

METHODS

Study Population

We studied during a period of 6 weeks 70 consecutive patients scheduled for diagnostic conventional coronary angiography who fulfilled the following criteria: sinus heart rhythm, able to breath hold for 15 seconds, and no previous percutaneous coronary intervention or coronary bypass surgery. Eighteen patients were excluded due to logistic inability to perform a CT-scan before the conventional angiogram (9), presence of arrhythmia (4), impaired renal function (serum creatinine >120 mmol/L) (4), and known contrast allergy (1). Thus, the study population comprised 52 patients (34 male, mean age 59.6±12.1 years). Our institutional review board approved the study protocol and all patients gave informed consent.

Patient Preparation

Patients with heart rates above 70 beats/minute received, unless they had known overt heart failure or electrocardiographic AV-conduction abnormalities, a single oral dose of 100 mg metoprolol 45 minutes before the scan. Patients with heart rates above 80 beats/minute received in addition a single oral dose of 1 mg lorazepam.

Scan protocol and Image Reconstruction

All patients were scanned using a 64-slice CT scanner (Sensation 64, Siemens, Forchheim, Germany), equipped with a new feature in multislice CT technology, so called Z-axis flying focus technology[13]. The central 32 detector rows acquire 0.6 mm slices and the flying focus spot switches back and forth between 2 Z-positions between each reading. Two slices per detector row are acquired, which results in a higher oversampling rate in the Z-axis, thereby reducing artifacts related to the spiral acquisition and improving spatial resolution down to 0.4 mm^3 [13]. Angiographic scan parameters: number of slices/rotation 32 x 2, individual detector width 0.6 mm, rotation time 330 ms, table feed 3.8 mm/rotation, tube voltage 120 kV, tube current 900 mAs, no prospective X-ray tube modulation. Calcium scoring parameters (similar unless indicated): tube current 150 mAs, prospective X-ray tube modulation. The radiation exposure for CT coronary angiography using this scan-protocol was calculated as 15.2-21.4 (male/female) mSv using dedicated software (WinDose®, Institute of Medical Physics, Erlangen, Germany). The radiation exposure of calcium scoring using a comparable scan-protocol (including prospective X-ray tube modulation) on a 16-slice scanner was calculated as 1.3-1.7 (male/female) mSv[15].

A bolus of 100 ml contrast material (iomeprol, Iomeron® 400, Bracco, Milan, Italy) was injected through an arm vein with a flow rate of 5 ml/s. A bolus-tracking technique was used to synchronize the arrival of contrast in the coronary arteries with the initiation of the scan.

Images were reconstructed using ECG-gating to obtain optimal, motion free image quality. Datasets were reconstructed immediately after the scan following a stepwise pattern. Initially, a single dataset was reconstructed during the mid-to-end diastolic phase (350 ms before the next R-wave). Image quality was assessed on a per-segment level. In case of insufficient image quality of one or more coronary segments, additional datasets were reconstructed (300 ms, 400 ms, and 450 ms before the next R-wave). In case of persistent artifacts related to coronary motion, a second reconstruction approach was carried out, including reconstruction of datasets both during the mid-to-end diastolic phase (between 60% and 70% of the R-R interval) and the end-systolic phase (between 25% and 35% of the R-R interval). If necessary, multiple datasets of a single patient were used separately in order to obtain optimal image quality of all available coronary segments. The reconstruction algorithm uses data from a single heartbeat, obtained during half X-ray tube rotation, resulting in a temporal resolution of 165 ms.

Quantitative Coronary Angiography (QCA)

All scans were performed within 2 weeks of the conventional diagnostic angiogram. A single observer, unaware of the MSCT results, identified coronary segments using a 17-segment modified AHA classification[14] (right coronary artery: 1, proximal; 2, mid; 3, distal; 4a, posterior descending; 4b postero-lateral; left main coronary artery: 5; left anterior descending coronary artery: 6, proximal; 7, mid; 8, distal; 9, 1st diagonal; 10, 2nd diagonal; circumflex coronary artery: 11, proximal; 12, 1st marginal; 13, mid; 14, 2nd marginal; 15, distal; 16, intermediate branch). All segments, irrespective of size, were included for comparison with CT coronary angiography. Segments were classified as normal (smooth parallel or tapering borders), as having non-significant disease (lumenal irregularities or $<50\%$ stenosis), or as having significant stenoses. Stenoses were evaluated in two orthogonal views, and classified as significant if the mean lumen diameter reduction was $\geq 50\%$ using a validated quantitative coronary angiography algorithm (CAAS®, Pie Medical, Maastricht, The Netherlands).

CT Image Evaluation

All scans were analysed independently by a radiologist and a cardiologist, unaware of the results of conventional coronary angiography, using an offline workstation (Leonardo®, Siemens, Forcheim, Germany). Total calcium scores of all patients were calculated using dedicated software and expressed as Agatston scores. The Agatston score is a commonly used scoring method that calculates the total amount of calcium based on the number, areas, and peak Hounsfield units of the detected calcified lesions.[16]

All available coronary segments were visually scored for the presence of significant stenosis. Maximum intensity projections were used to identify coronary lesions and (curved) multi-planar reconstructions to classify lesions as significant or non-significant. Disagreement between observers was resolved by consensus.

Image quality was evaluated on a per segment basis and classified as good (defined as absence of any image-degrading artifacts related to motion, calcification, or noise),

adequate (presence of image-degrading artifacts, but evaluation possible with moderate confidence), or poor (presence of image-degrading artifacts and evaluation only possible with low confidence).

Statistical Analysis

The diagnostic performance of CT coronary angiography for detection of significant lesions in coronary arteries with QCA as the standard of reference is presented as sensitivity, specificity, positive and negative predictive value, positive and negative likelihood ratio, and diagnostic odds ratio with the corresponding exact 95% confidence intervals. Comparison between CT coronary angiography and QCA was performed on 3 levels: segment-by-segment, vessel-by-vessel (no or any disease per vessel), and patient-by-patient (no or any disease per patient). We performed an additional sensitivity-analysis after random selection of a single segment per patient to explore the effect of nesting, whereas repeated assessments (segment-by-segment and vessel-by-vessel) within the same patient were made, which are not independent observations. Intra- and inter-observer variability for the detection of significant coronary stenosis was determined.

RESULTS

Patient characteristics are shown in Table 1. Seventy-three percent (38/52) of the patients received a β-blocker and, in addition, 31% (16/52) received lorazepam. The mean heart rate in these patients dropped within 45 minutes from 68.2±10.2 to 57.8±6.8 beats/minute. The mean scan time was 13.3±0.6 seconds. One unsuccessful CT-scan was classified as inconclusive due to the development of ventricular bigeminy during the angiography scan.

Table 1. Patient characteristics (n=52)

	N	(%)
Symptoms		
Atypical chest pain	6	(12)
Stable angina pectoris	32	(63)
Unstable angina pectoris	3	(6)
Non-ST-elevation myocardial infarction	11	(22)
Risk factors		
Hypertension	17	(33)
Hypercholesterolemia	36	(71)
Diabetes Mellitus	7	(14)
Smoking	15	(29)
Family history of ACS	13	(26)
Obese (BMI ≥30)	14	(28)
Calcium score (median-interquartile range) [1]	231	,15-736
Conventional angiography		
Absence of coronary artery disease	7	(13)
Non-significant disease	6	(12)
Single-vessel disease	16	(31)
Multi-vessel disease	23	(45)

[1] Agatston-score

A single dataset for the assessment of significant stenoses was used in 69%, 2 datasets in 27%, and 3 datasets in 4% of patients in order to obtain optimal image quality of on a per-segment level. Datasets reconstructed during the end-systolic phase were used in 27% (14/51) of patients. Image quality was classified as good in 90%, moderate in 7%, and poor in 3% of coronary segments. Reasons for poor image quality were motion artifacts (60%, 12/20), severe calcifications (20%, 4/20), or low contrast-to-noise ratio (20%, 4/20).

Diagnostic performance of 64-slice CT coronary angiography: Segment-by-segment analysis

A total of 725 segments were included for comparison with quantitative coronary angiography. Potentially, 17 segments per patient can be present for analysis. However, 142 segments were not visualized on the conventional angiogram due to 1) variations in coronary anatomy (absence of an intermediate branch or hypoplastic, non-dominant coronary arteries in which not all segments could be identified; 102 segments), and 2) presence of a proximal occlusion and poorly filled distal segments by collaterals (40 segments).

Table 2. Diagnostic performance and predictive value of 64-slice CT coronary angiography for the detection of ≥50% stenoses on QCA.

	N	Sensitivity		Specificity		PPV		NPV		+LR	-LR
Segment-based analysis											
All segments	725	99%	(94-98%)	95%	(93-96%)	76%	(67-89%)	100%	(99-100%)	20.81	0.01
Proximal segments	204	100%	(89-100%)	97%	(93-98%)	83%	(67-97%)	100%	(97-100%)	29.00	0.00
Mid segments	142	97%	(83-99%)	94%	(88-97%)	81%	(63-96%)	99%	(94-99%)	15.47	0.04
Distal segments	121	100%	(68-100%)	97%	(92-99%)	73%	(39-98%)	100%	(96-100%)	37.67	0.00
Side branches	258	100%	(87-100%)	94%	(90-96%)	65%	(48-85%)	100%	(98-100%)	16.57	0.00
LM	51	100%	(21-100%)	100%	(93-100%)	100%	(92-100%)	100%	(2-100%)		0.00
LAD	230	97%	(85-100%)	92%	(88-95%)	69%	(53-86%)	99%	(96-99%)	12.68	0.03
CX	235	100%	(88-100%)	97%	(94-99%)	83%	(66-97%)	100%	(98-100%)	34.33	0.00
RCA	209	100%	(89-100%)	95%	(91-97%)	77%	(60-95%)	100%	(97-100%)	19.89	0.00
Patient-based analysis											
All segments	51	100%	(91-100%)	92%	(67-99%)	97%	(86-99%)	100%	(73-100%)	13.00	0.00

For segment-based analysis, analysis of 725 segments visualized on the conventional angiogram and classified according to a 17-segment modified AHA classification was performed. Segments are further classified on the basis of their location within the coronary tree (proximal, mid, or distal segments of the main coronary artery arteries, or side-branches) and their location within a single vessel (LM, LAD, CX, or RCA). For patient-based analysis, analysis of 51 patients was performed.
+LR: positive likelihood ratio. -LR: negative likelihood ratio, CX: circumflex coronary artery,
LAD: left anterior descending coronary artery, LM: left main coronary artery, N: number of segments,
NPV: negative predictive value, PPV: positive predictive value, RCA: right coronary artery, QCA: quantitative coronary angiography.
Values in parenthesis represent upper and lower bound for 95% confidence interval.

Inter- and intra-observer variability for detection of significant lesions had κ-values of 0.73 and 0.79, respectively. The diagnostic performance of CT coronary angiography for the detection of significant lesions on a segment-based analysis is detailed in Table 2.

One significant stenosis (lumen diameter reduction: 52%) located at the mid part of the left anterior descending coronary artery (LAD) was detected with CT, but the severity of the stenosis was underestimated and classified as non-significant. Thirty non-significant lesions were detected with CT, but the severity of these stenoses was overestimated which resulted in incorrect classification as significant stenoses on the CT-scan. Conventional angiography revealed only wall irregularities in 8, and non-significant stenoses in the remaining 22 lesions (mean lumen reduction: 34.7±7.9%, range: 23-49%). The vast majority (83%, 25/30) of these segments were calcified. The presence of coronary calcium induced overestimation of the severity of these lesions on the CT-scan (Table 3). Agreement between CT coronary angiography and QCA on a per-segment level was very good (κ-value: 0.83).

Table 3. Influence of coronary calcification on diagnostic accuracy of 64-slice CT coronary angiography on a segment-based analysis.

Calcium Score	N	Mean (± SD) Agatston Score	TP	TN	FP	FN	Sensitivity	Specificity	Positive PV	Negative PV
0-10	12	0 ± 0	8	171	2	0	100% (63-100%)	99% (95-99%)	80% (44-98%)	100% (97-100%)
11-400	21	174 ± 122	36	240	13	0	100% (90-100%)	95% (91-97%)	73% (58-88%)	100% (98-100%)
401-1000	12	718 ± 166	31	129	10	1	97% (83-98%)	93% (87-96%)	76% (59-89%)	99% (95-99%)
>1000	6	1731 ± 621	18	61	5	0	100% (81-100%)	92% (83-97%)	78% (56-96%)	100% (94-100%

N: number of patients, TP: true positive, TN: true negative, FP: false positive, FN: false negative, PV: predictive value, SD: standard deviation.
Values in parenthesis represent upper and lower bound for 95% confidence interval.

After random selection of a single segment per patient, the sensitivity for the detection of significantly diseased vessels was 100% (13/13, 95% CI: 75-100), specificity was 95% (36/38, 95% CI: 82-99), positive predictive value was 87% (13/15, 95% CI: 59-99), and negative predictive value was 100% (36/36, 95% CI: 90-100).

Diagnostic performance of 64-slice CT coronary angiography: Vessel-by-vessel analysis

The diagnostic performance of CT coronary angiography for the detection of significant lesions on a vessel-based analysis is detailed in Table 2. One significantly diseased LAD was incorrectly classified as non-significantly diseased on the CT-scan. Sensitivity for the detection of significantly diseased left anterior descending coronary arteries was 96% and 100% in all other main coronary arteries. Agreement between CT coronary angiography and QCA on a per-vessel level was very good (κ-value: 0.85).

Diagnostic performance of 64-slice CT coronary angiography: Patient-by-patient analysis

The diagnostic performance of CT coronary angiography for the detection of significant lesions on a patient-based analysis is detailed in Table 2. Twelve patients with either an angiographically normal coronary angiogram (7) or with non-significant disease (5) were correctly identified with CT.

However, 1 patient with only wall irregularities on the conventional angiogram was incorrectly classified as having single-vessel disease on the CT-scan. All 38 patients with significant coronary artery disease on conventional angiography were correctly identified on the CT-scan (Figure 1,2). However, in 7 patients with single-vessel disease also another lesion was detected and the severity was overestimated which resulted in incorrect classification as having multi-vessel disease on CT coronary angiography. Agreement between CT coronary angiography and QCA on a per-patient (no or any disease) level was very good (κ-value: 0.95), whereas agreement between both techniques to classify patients as having no, single-, or multi-vessel disease was good (κ-value: 0.72).

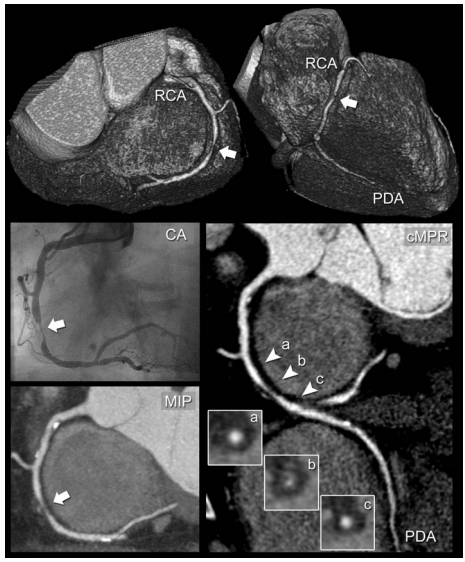

Figure 1a. CT coronary angiogram and corresponding conventional angiogram of the right coronary artery (RCA) in a patient presenting with stable angina pectoris and a calcium (Agatston-) score of 79. The arrow indicates a significant lesion located at the mid RCA. Cross-sectional CT images show a large non-calcific plaque (b) and a normal coronary lumen proximal and distal of the lesion (a, c). Note: Volume rendered images (colored images) provide an excellent anatomical overview of the coronary arteries, but should not be used to score the presence and degree of coronary stenoses. CA, conventional angiogram; cMPR, curved multiplanar reconstruction; MIP, maximum intensity projection; PDA, posterior descending coronary artery. (A full color version of this illustration can be found in the color section (Chapter 21)).

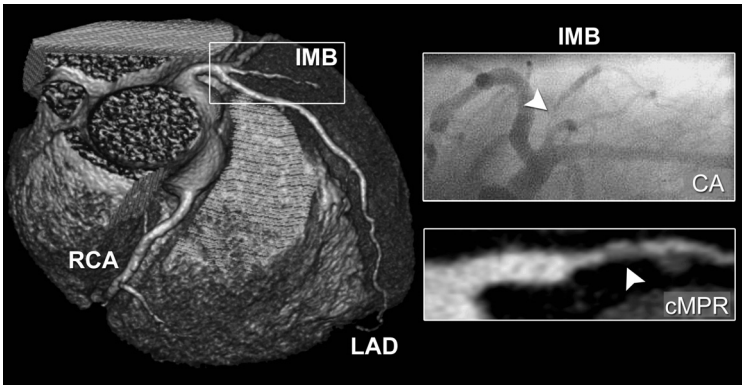

Figure 1b. Volume rendered CT image (colored image) providing an overview of the coronary anatomy and showing a small (lumen diameter 1.5 mm) intermediate branch (IMB). A detailed curved multiplanar reconstructed (cMPR) CT image reveals the presence of a significant stenosis (indicated by the arrowhead) located at the proximal IMB, which was confirmed on the conventional angiogram (CA). The patient was correctly classified as having 2-vessel disease on the CT-scan.
LAD, left anterior descending coronary artery; RCA, right coronary artery. (A full color version of this illustration can be found in the color section (Chapter 21)).

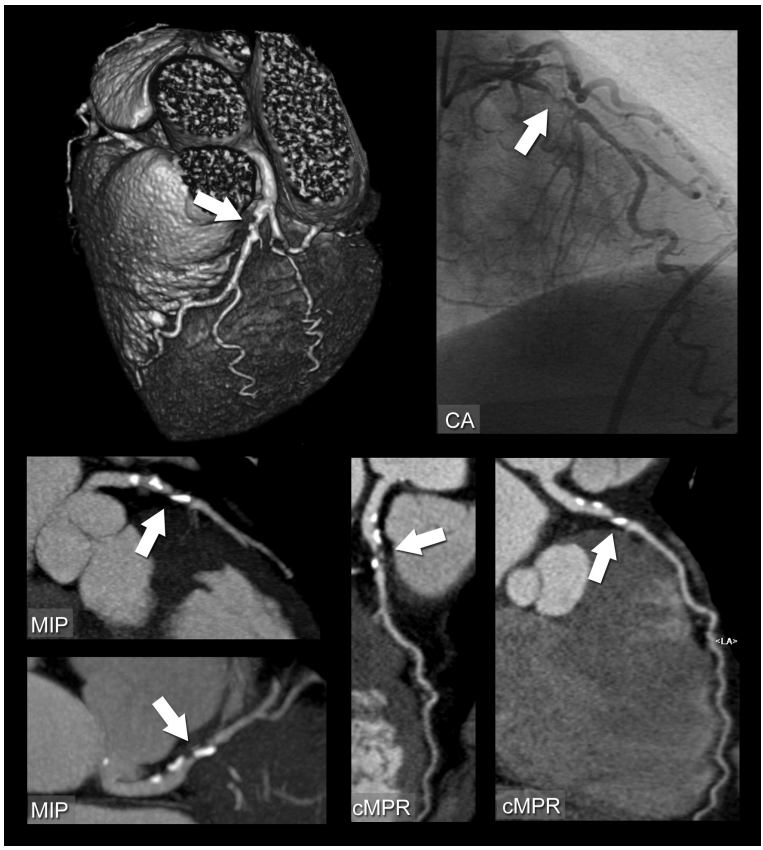

Figure 2. Volume rendered CT image (colored image) providing an overview of the coronary anatomy and suggesting a significant stenosis of the proximal left anterior descending coronary artery (indicated by the arrow). More detailed analysis using different CT post-processing techniques (maximum intensity projections [MIP] and curved multiplanar reconstructions [cMPR]) confirms the presence of a significant stenosis, which corresponds with the conventional angiogram (CA). (A full color version of this illustration can be found in the color section (Chapter 21)).

Discussion

Recent reports demonstrated that earlier generation MSCT scanners showed promise for non-invasive detection of coronary stenoses[1-12]. The reported diagnostic values were high but one should bear in mind that the calculated sensitivity and specificity were based on analysable coronary segments rather than on those of all examined coronary segments. In fact, the most recent reports of 16-slice CT coronary angiography excluded 6% to 17% of the available coronary segments and only a few included all available segments. In addition, only the larger parts of the coronary tree were examined while
smaller parts with a diameter of less than 1.5 mm or 2 mm were excluded from analysis. The newest Multislice CT scanner offers a shorter scan-time and a higher temporal and spatial resolution. Multislice CT coronary angiography of the clinically relevant coronary segments, as have been designated by the AHA classification, is now possible.

We found that significant coronary stenoses were detected using the latest 64-slice CT scanner with a sensitivity of 99% and a specificity of 95% when compared to conventional invasive diagnostic coronary angiography. All but one patients with angiographically normal coronary angiograms were correctly identified rendering the CT-technique highly reliable to identify patients who have no significant coronary obstruction. Furthermore, all patients with significant coronary artery disease were correctly diagnosed and only a single coronary lesion was missed on the CT-scan. We found a good agreement between CT coronary angiography and QCA in the classification of patients with no, single-, or multi-vessel disease. This observation shows that CT coronary angiography may add important information to stress testing in the diagnostic work-up of symptomatic patients, whereas stress tests are limited in the further classification of patients with significant coronary artery disease into single- or multi-vessel disease. Our results were obtained in patients with a wide spectrum of clinical settings including atypical chest pain, stable or unstable angina, or non-ST-segment elevation who had varying degrees of coronary artery disease ranging from normal coronary angiograms to obstructive disease of 1, 2 or 3 vessels. We did not include patients with ST-segment elevation myocardial infarction, whereas these patients should undergo immediate percutaneous intervention without any delay, and the role of CT in these patients is highly questionable. In our study the specificity was somewhat lower due to the fact that we tended to overestimate the severity of a lesion on the CT-scan, resulting in a number of false positive outcomes, rather than to underestimate the lesion severity and thereby "missing" lesions, which may have serious consequences in a symptomatic patient population.

Limitations

The estimated radiation dose during CT coronary angiography (15.2-21.4 mSv [male/female]) is a cause of concern and higher than the radiation dose associated with conventional coronary angiography. The radiation exposure can be reduced by technical adjustments such as prospective X-ray tube current modulation. This technique reduces the radiation exposure by nearly 50% in patients with low heart rates[15], but is sensitive to arrhythmia and limits the possibility to reconstruct datasets during the end-systolic phase. This proved useful in 27% of our patients. Persistent irregular heart rhythm such as atrial fibrillation and frequent extra-systoles preclude multislice coronary angiography. Motion artifacts caused by mild arrhythmia (e.g. a single ventricular extra-systole) can be diminished by manual repositioning the reconstruction windows. Severe coronary calcification obscures the coronary lumen and can lead to overestimation of the severity of lesions due to blooming artifacts resulting in a lower specificity in patients with high calcium scores. The presence of coronary calcifications also severely limits the applicability of quantitative CT coronary angiography algorithms. In fact, no validated software is currently available able to detect and quantify coronary stenoses.

When evaluating the diagnostic performance of CT coronary angiography on 3 levels (segment-by-segment, vessel-by-vessel, and patient-by-patient), repeated assessments within the same patient were made. However, we performed a sensitivity-analysis after random selection of a single segment per patient and found values that are in line with the values obtained after clustering all available segments. This finding suggests that nesting of analyses did not have an important impact on the diagnostic performance of CT to detect

significant stenoses in present study.

Patients with initial heart rates above 70 beats/minute received pre-scan medication resulting in a mean heart rate of 57 beats/minute. Future improvements in temporal resolution should diminish motion artifacts related to high heart rates, which could make the administration of pre-scan β-blockers unnecessary.

CONCLUSIONS

Our results show that non-invasive 64-slice CT coronary angiography is a reliable technique to detect coronary stenoses in patients with sinus rhythm presenting with atypical chest pain, stable or unstable angina pectoris, or non-ST-segment elevation myocardial infarction and suggest that this non-invasive technique can now be considered as an alternative to invasive diagnostic coronary angiography in selected patients.

REFERENCES

1. Nieman K, Oudkerk M, Rensing BJ, van Ooijen P, Munne A, van Geuns RJ, de Feyter PJ. Coronary angiography with multi-slice computed tomography. Lancet. 2001;357:599-603.
2. Achenbach S, Giesler T, Ropers D, Ulzheimer S, Derlien H, Schulte C, Wenkel E, Moshage W, Bautz W, Daniel WG, Kalender WA, Baum U. Detection of coronary artery stenoses by contrast-enhanced, retrospectively electrocardiographically-gated, multislice spiral computed tomography. Circulation. 2001;103:2535-8.
3. Knez A, Becker CR, Leber A, Ohnesorge B, Becker A, White C, Haberl R, Reiser MF, Steinbeck G. Usefulness of multislice spiral computed tomography angiography for determination of coronary artery stenoses. Am J Cardiol. 2001;88:1191-4.
4. Vogl TJ, Abolmaali ND, Diebold T, Engelmann K, Ay M, Dogan S, Wimmer-Greinecker G, Moritz A, Herzog C. Techniques for the detection of coronary atherosclerosis: multi-detector row CT coronary angiography. Radiology. 2002;223:212-20.
5. Kopp AF, Schroeder S, Kuettner A, Baumbach A, Georg C, Kuzo R, Heuschmid M, Ohnesorge B, Karsch KR, Claussen CD. Non-invasive coronary angiography with high resolution multidetector-row computed tomography. Results in 102 patients. Eur Heart J. 2002;23:1714-25.
6. Nieman K, Cademartiri F, Lemos PA, Raaijmakers R, Pattynama PM, de Feyter PJ. Reliable noninvasive coronary angiography with fast submillimeter multislice spiral computed tomography. Circulation. 2002;106:2051-4.
7. Ropers D, Baum U, Pohle K, Anders K, Ulzheimer S, Ohnesorge B, Schlundt C, Bautz W, Daniel WG, Achenbach S. Detection of coronary artery stenoses with thin-slice multi-detector row spiral computed tomography and multiplanar reconstruction. Circulation. 2003;107:664-6.
8. Kuettner A, Trabold T, Schroeder S, Feyer A, Beck T, Brueckner A, Heuschmid M, Burgstahler C, Kopp AF, Claussen CD. Noninvasive detection of coronary lesions using 16-detector multislice spiral computed tomography technology: initial clinical results. J Am Coll Cardiol. 2004;44:1230-7.
9. Mollet NR, Cademartiri F, Nieman K, Saia F, Lemos PA, McFadden EP, Pattynama PMT, Serruys PW, Krestin GP, De Feyter PJ. Multislice Spiral CT Coronary Angiography in Patients With Stable Angina Pectoris. J Am Coll Cardiol. 2004;43:2265-70.
10. Martuscelli E, Romagnoli A, D'Eliseo A, Razzini C, Tomassini M, Sperandio M, Simonetti G, Romeo F. Accuracy of thin-slice computed tomography in the detection of coronary stenoses. Eur Heart J. 2004;25:1043-8.

11. Kuettner A, Kopp AF, Schroeder S, Rieger T, Brunn J, Meisner C, Heuschmid M, Trabold T, Burgstahler C, Martensen J, Schoebel W, Selbmann HK, Claussen CD. Diagnostic accuracy of multidetector computed tomography coronary angiography in patients with angiographically proven coronary artery disease. J Am Coll Cardiol. 2004;43:831-9.
12. Mollet NR, Cademartiri F, Krestin GP, McFadden EP, Arampatzis CA, Serruys PW, De Feyter PJ. Improved Diagnostic Accuracy With 16-row Multislice CT Coronary Angiography. J Am Coll Cardiol. 2005;45:128-32.
13. Flohr T, Bruder H, Stierstorfer K, Schaller S. Evaluation of approaches to reduce spiral artifacts in multi-slice spiral CT. 89th Scientific Assembly of the Radiological Society of North America (abstract). 2004.
14. Austen WG, Edwards JE, Frye RL, Gensini GG, Gott VL, Griffith LS, McGoon DC, Murphy ML, Roe BB. A reporting system on patients evaluated for coronary artery disease. Report of the Ad Hoc Committee for Grading of Coronary Artery Disease, Council on Cardiovascular Surgery, American Heart Association. Circulation. 1975;51:5-40.
15. Trabold T, Buchgeister M, Kuttner A, Heuschmid M, Kopp AF, Schroder S, Claussen CD. Estimation of Radiation Exposure in 16-Detector Row Computed Tomography of the Heart with Retrospective ECG-gating. Rofo Fortschr Geb Rontgenstr Neuen Bildgeb Verfahr. 2003;175:1051-5.
16. Agatston AS, Janowitz WR, Hildner FJ, Zusmer NR, Viamonte M, Jr., Detrano R. Quantification of coronary artery calcium using ultrafast computed tomography. J Am Coll Cardiol. 1990;15:827-32.

Interlude 1

Right Coronary Artery Arising From The Left Circumflex Demonstrated With Multislice Computed Tomography

Abstract

A 38-year-old man was referred to our institution for suspected coronary artery disease. Because of his young age and rather atypical symptoms, we decided to perform multislice computed tomography coronary angiography before other invasive studies. The scan was performed with a 16-row multislice computed tomography scanner (Sensation 16; Siemens) after intravenous administration of iodinated contrast material. It revealed absence of the right coronary artery and a split origin of the left coronary artery (Figure 1). The left circumflex artery lay in the posterior atrioventricular groove ending near the ascending aorta on the opposite side of its own origin (Figure 1). The findings have been confirmed by coronary angiography (Figure 2).

Filippo Cademartiri [1]
Nico R. Mollet [1,2]
Koen Nieman [1,2]
Tamas Szili-Torok [2]
Pim J. de Feyter [1,2]

From the Departments of Radiology [1] and Cardiology [2] Erasmus MC, University Medical Center Rotterdam, The Netherlands.

Circulation,
2004;109:185-186.

RCA arising from LCX demonstrated by MSCT

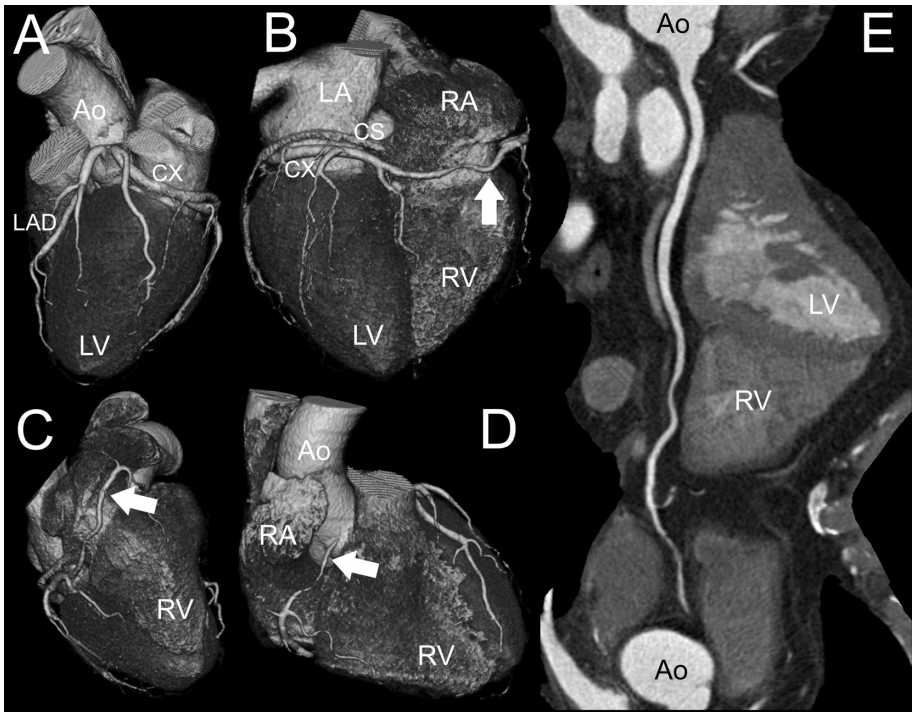

Figure 1. Multislice computed tomography coronary angiography. A 3D volume rendering is applied to the dataset in **A through D**, whereas a curved planar reconstruction is performed along the lumen of the left circumflex in E. The multislice computed tomography scan shows a split origin of the left coronary artery (**A**; Movie I). Therefore, this anomaly cannot be identified as a "single" coronary artery. The left circumflex runs first in the left atrioventricular groove (**A**), crosses the crux (**B**, arrow), and then goes further in the right atrioventricular groove **C**, arrow), ending 1 cm before the wall of the ascending aorta (**D**, arrow) on the opposite side of its own origin (**E**; Movie I). No ostium of the right coronary artery in the region of the right Valsalva sinus was detected (**D and E**; Movie I). Ao indicates ascending aorta; CS, coronary sinus; CX, circumflex; LAD, left anterior descending; LA, left atrium; LV, left ventricle; RA, right atrium; and RV, right ventricle. (A full color version of this illustration can be found in the color section (chapter 21)).

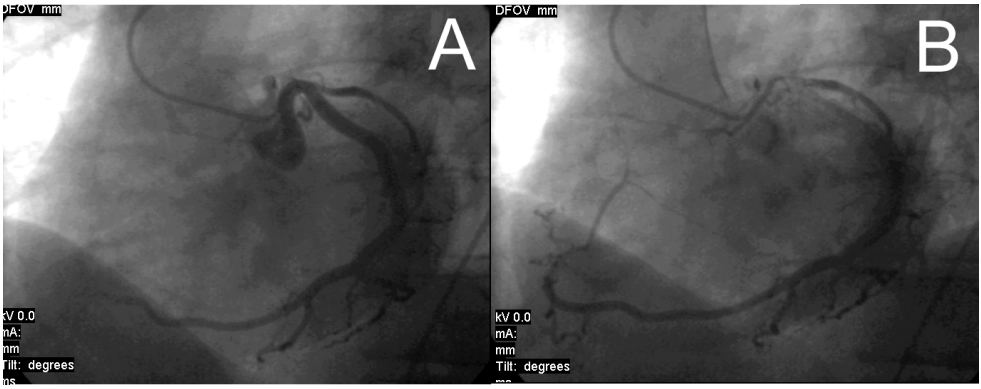

Figure 2. Selective conventional x-ray angiography of the left circumflex coronary artery.

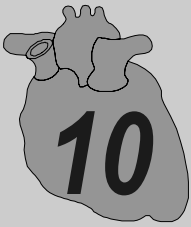

Chapter 10

Impact of Coronary Calcium Score on Diagnostic Accuracy for the Detection of Significant Coronary Stenosis with Multislice Computed Tomography Angiography

Abstract

One hundred twenty patients in sinus rhythm with suspected coronary artery disease who underwent multislice computed tomography of the heart and conventional coronary angiography were retrospectively selected. The population was divided into 2 groups depending on their calcium score (CS) (e.g., low CS and high CS). The diagnostic accuracy of multislice computed tomographic scans for detecting significant lesions (≥50% lumen reduction) in both groups was compared with quantitative coronary angiography. The sensitivity and specificity of multislice computed tomography were 90% and 92%, and 97% and 91% for low and high CS groups, respectively.

Filippo Cademartiri [1,2]
Nico R. Mollet [1,2]
Pedro A. Lemos [3]
Franceso Saia [3]
Giuseppe Runza [3]
Massimo Midiri [3]
Gabriel P. Krestin [1]
Pim J. de Feyter [1,2]

From the Departments of Radiology [1] and Cardiology [2], Erasmus Medical Center, Rotterdam, The Netherlands and Department of Radiology [3], University of Palermo, Palermo, Italy.

American Journal of Cardiology
2005;95:1225–1227

Impact of calcium on diagnostic accuracy

Significant coronary artery stenosis can be reliably detected with multislice computed tomography (MSCT) coronary angiography (CA)[1–3]. However, the capability of evaluating coronary artery stenoses with MSCT can be potentially impaired by several factors, including coronary artery calcifications [4]. It has been suggested that the detection of a high calcium score (CS) before MSCT-CA could be used as a gatekeeper for deferring the procedure[4]. This study compares the diagnostic accuracy of 16-row MSCT-CA for diagnosing significant coronary artery stenosis in 2 groups divided according to CSs (low or high).

We retrospectively included in the study 120 patients (105 men and 15 women; mean age 59±11 years) with suspected coronary artery disease who underwent both conventional CA and MSCT of the coronary arteries (CS evaluation followed by MSCTCA). The mean interval between MSCT-CA and CA was 17.5±9.5 days. All patients had a regular heart rate with sinus rhythm and the ability to breath-hold for 20 seconds. Patients with previous coronary surgery were not included in the present report. A single oral dose of 100 mg of metoprolol was administered 1 hour before the scan if the heart rate was ≥65 beats/min.

A CS scan was performed with the following parameters: collimation 16 x 1.5 mm, gantry rotation time 420 ms, feed/rotation 6.0 mm, effective slice width 3 mm, increment 1.5 mm, kV 120, and effective 150 mA.

The MSCT-CA scan (Sensation 16, Siemens, Germany) was performed after the intravenous administration of 100 ml of iodinated contrast material (iodixanol 320 mg iodine/ml at 4 ml/s; Amersham Health, Little Chalfont, United Kingdom) with the following parameters: collimation 16 x 0.75 mm, gantry rotation time 420 ms, feed/rotation 3.0 mm, effective slice width 1 mm, increment 0.5 mm, 120 kV, and 400 to 500 mA. The temporal windows were set at −350, −400, and −450 ms before the next R wave for electrocardiographic-gated retrospective reconstruction. The data set with least residual motion was selected for evaluation. The estimated radiation dose for the protocol was about 8 mSv in men and 13 mSv in women[5].

For the evaluation, coronary arteries were divided into segments according to the American Heart Association classification[6]. A single observer, unaware of the multislice computed tomographic results, classified all coronary segments as <2 or ≥2 mm in diameter using a quantitative coronary angiographic algorithm (CAAS II, Pie Medical, Maastricht, The Netherlands). Only segments with a reference diameter of ≥2 mm were considered for comparison with MSCT. The severity of coronary stenoses was quantified in 2 orthogonal views, and a stenosis was classified as significant if the mean lumen diameter reduction was ≥50%.

Coronary CS was assessed with a dedicated software application (CaScore, Siemens, Germany). The overall Agatston score was recorded in each patient. Two observers, blinded to the results of conventional CA, independently evaluated all MSCT-CAs using the postprocessing techniques frequently used (e.g., multiplanar reconstructions and maximum intensity projections). All branches (>2 mm in lumen diameter) of the coronary tree were evaluated for the presence of significant (≥50% diameter reduction) obstructive stenoses. Segments with stents were excluded from analysis.

Disagreements were resolved by consensus. The study cohort was divided into 2 groups according to the median Agatston score (value 55) of the entire population (60 patients in the low CS group and 60 patients in the high CS group).

Interval data are expressed as mean ±SD. Diagnostic accuracy is expressed in percentages with 95% confidence intervals. The differences in demographics were tested with an unpaired *t* test. The differences in diagnostic accuracy were tested with Cramer's V test. A p value <0.05 was considered significant.

There were no significant differences between the 2 groups regarding age, gender, body weight, and mean heart rate during the scan (Table 1). The mean Agatston score for the overall population was 296 ± 578. After sorting the population in the 2 study groups, the resulting mean Agatston score was 14 ± 16 and 578 ± 716 ($p <0.0001$) for low and high CS groups, respectively.

TABLE 1. Patient Data

Variable	Low CS (n = 60)	High CS (n = 60)
Mean age (yrs)	57 ± 10	58 ± 11
Men/women	55/5	55/5
Mean heart rate (beats/min)	57 ± 7	58 ± 7
Mean CS (Agatston)*	14 ± 16	578 ± 716
Mean weight (kg)	70 ± 6	72 ± 8

*$p < 0.0001$

In all, 1,310 coronary segments ≥2 mm were analyzed (mean, 10.9 segments/patient): 667 (51%) in the low CS group and 643 (49%) in the high CS group (Table 2). Significant coronary lesions were detected by conventional angiography in 219 segments (86 [39%] in the low CS group and 133 [61%] in the high CS group; $p <0.01$). The overall sensitivity, specificity, and positive and negative predictive values for detecting any significant stenosis by MSCT-CA were 90%, 97%, 80%, and 98% for the low CS group and 92%, 91%, 72%, and 98% for the high CS group, respectively ($p >0.05$). The difference in the diagnostic accuracy of MSCT-CA between the 2 study groups was not significant, even when segments were compared separately ($p >0.05$).

It has been reported that coronary calcium impairs the capability of evaluating coronary arteries with MSCT-CA[4]. However, in our series, the CS has not significantly impaired the overall diagnostic accuracy of MSCT-CA for detecting luminal stenosis. Nevertheless, a slight tendency toward a decreased positive predictive value was noted in patients with highly calcified vessels, with no change in the negative predictive value of the test. Our findings are in line with the notion that MSCT-CA may slightly overestimate the presence of significant coronary stenosis in patients with a high CS. However, the present results do not suggest that coronary calcification should be used as an indication for deferring MSCT-CA.

TABLE 2. Diagnostic Accuracy of Low Calcium Score (L) Group Versus High Calcium Score (H) Group

		No.		SDS		Sensitivity		Specificity	
AHA	Segments	L	H	L	H	L	H	L	H
1	Right proximal	57	58	15	14	100 (78-100)	100 (76-100)	98 (87-99)	98 (87-99)
2	Right middle	49	51	12	20	100 (73–100)	95 (75–96)	97 (85–99)	81 (62–92)
3	Right distal	43	44	1	7	100 (2–100)	86 (42–99)	100 (91–100)	92 (78–98)
4	PDA	40	34	0	3	NA	67 (9–91)	98 (86–99)	100 (88–100)
5	Left main	58	59	2	3	100 (15–100)	100 (29–100)	100 (93–100)	100 (93–100)
6	LAD proximal	57	60	17	21	82 (56–98)	100 (83–100)	93 (79–98)	85 (69–94)
7	LAD middle	50	55	11	24	91 (58–99)	100 (85–100)	97 (86–99)	77 (58–90)
8	LAD distal	51	47	3	2	33 (0–95)	100 (15–100)	96 (85–99)	96 (84–99)
9	1st diagonal	41	38	2	6	50 (1–99)	50 (11–91)	95 (82–99)	75 (56–88)
10	2nd diagonal	31	18	1	0	100 (2–100)	NA	100 (88–100)	89 (65–98)
11	LC proximal	51	54	6	12	100 (54–100)	83 (51–96)	93 (81–98)	88 (74–96)
12	1st marginal	48	51	4	12	75 (19–99)	92 (61–99)	93 (81–98)	97 (86–99)
13	LC middle	48	47	9	6	89 (51–97)	83 (35–97)	100 (90–100)	88 (73–95)
14	2nd marginal	33	22	2	3	100 (15–100)	67 (9–99)	94 (78–99)	95 (73–99)
15	PLB	10	5	1	0	100 (2–100)	NA	100 (66–100)	100 (47–100)
All		667	643	86	133	90 (81–97)	92 (85–93)	97 (94–98)	91 (87–93)

Values of diagnostic accuracy are expressed as percentages (95% confidence intervals). AHA = American Heart Association segmental classification; LAD = left anterior descending; LC = left circumflex artery; NA = not assessable; No. = absolute number of segments; NPV = negative predictive value; PDA = posterior descending artery; PLB = posterolateral branch; PPV = positive predictive value; SDS = absolute number of significantly diseased segments (≥50% lumen reduction at quantitative CA).

One limitation of the present study is that the population was selected retrospectively. Nevertheless, the scan protocol was homogeneous across the study population, and the 2 groups that were derived from it were also homogeneous.

We have shown that diagnostic accuracy is not significantly impaired by the presence of a high coronary CS, which should not be used as a routine indication for deferring MSCT-CA examinations.

PPV		NPV		Cramer V Test	p Value
L	H	L	H		
94 (69–99)	93 (68–99)	100 (91–100)	100 (91–100)	0.101	0.886
92 (63–99)	76 (54–93)	100 (90–100)	96 (80–99)	0.187	0.808
100 (2–100)	67 (29–97)	100 (91–100)	97 (85–99)	0.093	0.968
0 (0–99)	100 (15–100)	100 (90–100)	97 (83–99)	0.086	0.936
100 (15–100)	100 (29–100)	100 (93–100)	100 (93–100)	0.045	0.734
82 (56–98)	78 (57–94)	93 (79–98)	100 (89–100)	0.228	0.432
91 (58–99)	77 (58–92)	97 (86–99)	100 (85–100)	0.186	0.793
33 (0–95)	50 (6–96)	96 (85–99)	100 (91–100)	0.338	0.178
33 (0–95)	27 (6–67)	97 (86–99)	89 (70–97)	0.270	0.746
100 (2–100)	0 (0–93)	100 (88–100)	100 (79–100)	—	—
67 (29–97)	67 (38–93)	100 (91–100)	95 (82–99)	0.236	0.528
50 (11–96)	92 (61–99)	98 (87–99)	97 (86–99)	0.145	0.980
100 (63–100)	50 (18–91)	98 (86–99)	97 (85–99)	0.201	0.674
50 (6–96)	67 (9–99)	100 (88–100)	95 (73–99)	0.174	0.948
100 (2–100)	NA	100 (66–100)	100 (47–100)	—	—
80 (70–91)	72 (64–84)	98 (97–99)	98 (95–98)	0.068	0.632

References

1. Nieman K, Cademartiri F, Lemos PA, Raaijmakers R, Pattynama PM, de Feyter PJ. Reliable noninvasive coronary angiography with fast submillimeter multislice spiral computed tomography. Circulation 2002;106:2051–2054.
2. Ropers D, Baum U, Pohle K, Anders K, Ulzheimer S, Ohnesorge B, Schlundt C, Bautz W, Daniel WG, Achenbach S. Detection of coronary artery stenoses with thin-slice multi-detector row spiral computed tomography and multiplanar reconstruction. Circulation 2003;107:664–666.
3. Mollet NR, Cademartiri F, Nieman K, Saia F, Lemos PA, McFadden EP, Pattynama PM, Serruys PW, Krestin GP, de Feyter PJ. Multislice spiral computed tomography coronary angiography in patients with stable angina pectoris. J Am Coll Cardiol 2004;43:2265–2270.
4. Kuettner A, Kopp AF, Schroeder S, Rieger T, Brunn J, Meisner C, Heuschmid M, Trabold T, Burgstahler C, Martensen J, et al. Diagnostic accuracy of multidetector computed tomography coronary angiography in patients with angiographically proven coronary artery disease. J Am Coll Cardiol 2004;43:831– 839.
5. Hunold P, Vogt FM, Schmermund A, Debatin JF, Kerkhoff G, Budde T, Erbel R, Ewen K, Barkhausen J. Radiation exposure during cardiac CT: effective doses at multi-detector row CT and electron-beam CT. Radiology 2003;226:145–152.
6. Austen WG, Edwards JE, Frye RL, Gensini GG, Gott VL, Griffith LS, McGoon DC, Murphy ML, Roe BB. A reporting system on patients evaluated for coronary artery disease. Report of the Ad Hoc Committee for Grading of Coronary Artery Disease, Council on Cardiovascular Surgery, American Heart Association. Circulation 1975;51:5– 40.

Chapter 11

Standard Versus User-Interactive Assessment of Significant Coronary Stenoses with Multislice Computed Tomography Coronary Angiography

Abstract

Forty-four patients in sinus rhythm with suspected coronary artery disease underwent 16-row multislice computed tomography coronary angiography and conventional coronary angiography. Two protocols for image analysis were applied to the multislice computed tomographic images: standard projections versus interactive postprocessing. The diagnostic accuracy of both methods for the detection of significant lesions (≥50% lumen reduction) was compared with quantitative coronary angiography. Sensitivity and specificity were 58% and 96% and 96% and 97%, for standard projections and interactive postprocessing protocol, respectively.

Filippo Cademartiri [1]
Nico R. Mollet [1,2]
Pedro A. Lemos [2]
Eugene P. McFadden [2]
Riccardo Marano [1]
Timo Baks [1,2]
Theo Stijnen [3]
Pim J. de Feyter [1,2]
Gabriel P. Krestin [1]

From the Departments of Radiology [1], Cardiology [2], and Epidemiology and Biostatistics [3], Erasmus MC, University Medical Center Rotterdam, The Netherlands.

American Journal of Cardiology
2004;94:1590–1593.

Standard versus user-interactive assessment

Sixteen-row multislice computed tomographic (MSCT) coronary angiography (CA) has shown good results in the detection of coronary artery stenoses[1,2]. To implement MSCT-CA in a clinical setting, several aspects of the technique need to be addressed. In many settings in routine radiologic practice, a technician prepares the images, which are subsequently interpreted by a radiologist. Coronary imaging may require a more interactive and "case by case" approach due to the tortuous anatomy and the small size of the vessels. This study compares the diagnostic accuracy, in a selected population of patients undergoing 16-row MSCT-CA, of 2 different protocols for image visualization: a standard projection technique and an interactive postprocessing technique.

Between April and August 2003, 44 patients (38 men; mean age 59 ± 8 years) who underwent conventional CA for suspected coronary artery disease, were retrospectively enrolled in the study. Inclusion criteria for MSCT-CA were regular heart rhythm and heart rate (HR) (spontaneous or β-blocker induced) >65 beats/min, and the ability to hold breath for 20 seconds. Exclusion criteria were: previous allergic reaction to iodine contrast media, renal insufficiency (serum creatinine >120 mmol/L), potential pregnancy, unstable clinical status, marked heart failure, previous bypass surgery or percutaneous coronary intervention, and datasets of nondiagnostic image quality. The institutional review board approved the study and patients gave written informed consent.

On arrival, the HR of the patients was measured. Patients with a prescan HR ≥65 beats/min were given 100 mg of metoprolol orally and the scan was performed 1 hour later. In all patients, a bolus (100 ml at 4 ml/s) of iodinated contrast material (Iodixanol 320 mgI/ml, Amersham Health, Little Chalfont, United Kingdom) was administered using a power injector (EnVisionCT, MedRAD, Pittsburgh, Pennsylvania) through an 18-gauge cannula, in an antecubital vein. Synchronization between the passage of contrast material and data acquisition was achieved using a realtime bolus tracking technique. The scan parameters for MSCT-CA (Sensation 16, Siemens) were: number of detectors 16, patient detector width 0.75 mm, gantry rotation time 420 ms, temporal resolution 210 ms, 120 kV, 500 mA, and feed/rotation 3.0 mm.

Three axial datasets were retrospectively reconstructed at -350, -400, and -450 ms before the next R wave with the following parameters: effective slice width 1 mm, image increment of reconstruction 0.5 mm, field of view 150 to 180 mm, and medium convolution filter (B30f). The dataset with the least motion artifacts was selected for further analysis. This dataset was transferred to a stand-alone workstation and evaluated using dedicated analysis software (Leonardo, Siemens).

Two protocols for image analysis were applied: standard projection (Figure 1) and interactive postprocessing (Figure 2). An experienced radiographer prepared 5 datasets in different projections for the standard protocol. These datasets consisted of the source axial dataset (1 mm thick and 0.5 mm overlapping), a para-axial maximum intensity projection parallel to the path of the left anterior descending artery (3 mm thick and 1.5 mm overlapping), a parasagittal multiplanar reformat parallel to the interventricular groove to visualize the left anterior descending artery (1 mm thick and 0.5 mm overlapping), a paracoronal multiplanar reformat parallel to the atrioventricular groove to visualize the right coronary and the left circumflex arteries (1 mm thick and 0.5 mm overlapping), and a paracoronal maximum intensity projection parallel to the atrioventricular groove to visualize the right coronary and the left circumflex arteries (3 mm thick and 1.5 mm overlapping).

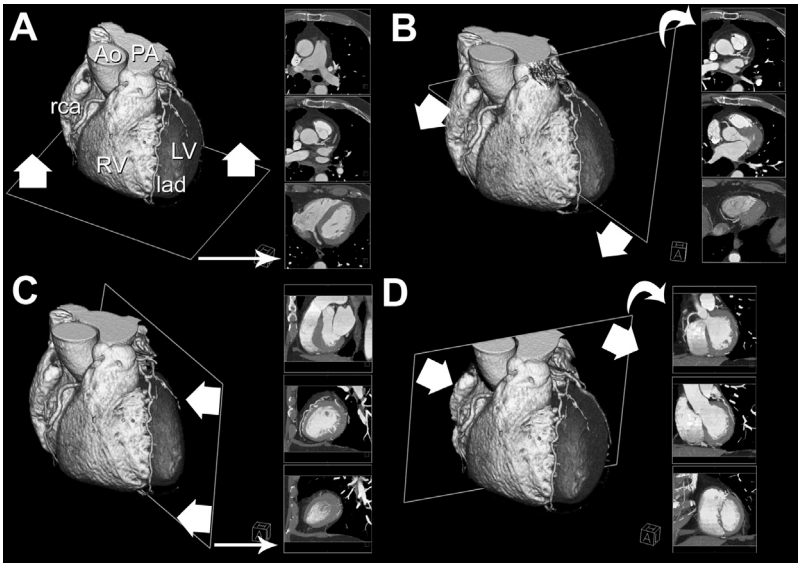

Figure 1. Imaging modalities and planes applied for the standard projections protocol. (**A**) The axial plane is displayed and sample images are shown in the right column from the bottom (caudal end) to the top (cranial end) of the dataset. (**B**) A paraaxial plane parallel to the course of left anterior descending is shown and in the right column sample images show the appearance of the origin of the left coronary artery, the right coronary artery, and the posterior descending artery, from top to bottom. (**C**) The plane is running parallel to the interventricular groove to display the left anterior descending artery and in the right column sequential images are shown. (**D**) The plane is parallel to the atrioventricular groove for the visualization of the right coronary artery and for the left circumflex artery, which are displayed in the right column. In (**A**) to (**D**), thick arrows indicate the direction of scrolling of the plane. Ao ascending aorta; lad left anterior descending; LV left ventricle; PA pulmonary artery; RV right ventricle; rca right coronary artery. (A full color version of this illustration can be found in the color section (chapter 21)).

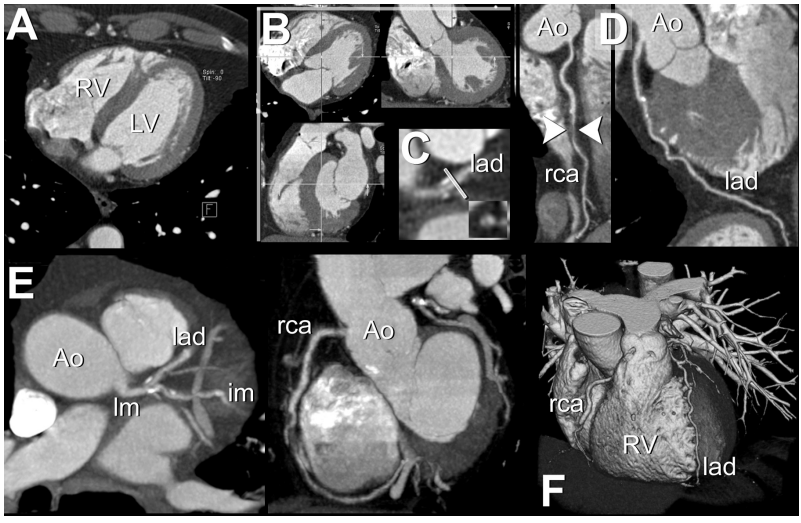

Figure 2. Imaging modalities applied for the interactive postprocessing protocol. Axial slices (**A**) and multiplanar reconstructions (**B**) are the basic tools for image assessment. Then, a multiplanar reconstruction focused on the stenosis (**C**; proximal stenosis of the left anterior descending artery) integrated with dedicated curved reconstructions along the lumen (**D**; stenosis in the midright coronary artery; arrowheads) are performed. In parallel, maximum intensity projections (**E**) and 3-dimensional volume rendering (**F**) are performed to improve panoramic perception. im intermediate branch; lm left main; other abbreviations as in Figure 1. (A full color version of this illustration can be found in the color section (chapter 21)).

Table 1. Diagnostic Accuracy of Standard Protocol Versus Interactive Protocol

				Specificity (95% CI)		Specificity (95% CI)	
AHA	Coronary segment	n	SDS (%)	S	I	S	I
1	Right proximal	44	12	83 (52 - 98)	100 (74 - 100)	88 (71 - 97)	94 (79 - 99)
2	Right middle	33	16	56 (30 - 80)	100 (79 - 100)	100 (81 - 100)	88 (64 - 99)
3	Right distal	26	5	80 (28 - 100)	100 (48 - 100)	100 (84 - 100)	95 (76 - 100)
4	Posterior descending	16	2	50 (1 - 99)	50 (1 - 99)	100 (77 - 100)	100 (77 - 100)
5	Left main	44	0	NA	NA	98 (88 - 100)	100 (92 - 100)
6	LAD proximal	44	14	43 (20 - 71)	86 (57 - 98)	93 (78 - 99)	93 (78 - 99)
7	LAD middle	41	15	53 (27 - 79)	100 (78 - 100)	100 (87 - 100)	100 (87 - 100)
8	LAD distal	38	2	100 (16 - 100)	100 (16 - 100)	100 (90 - 100)	97 (86 - 100)
9	1st diagonal	34	2	50 (1 - 99)	100 (16 - 100)	91 (75 - 98)	94 (79 - 99)
10	2nd diagonal	36	0	NA	NA	50 (33 - 68)	100 (82 - 100)
11	LC-proximal	43	8	88 (47 - 100)	88 (47 - 100)	97 (85 - 100)	97 (85 - 100)
12	1st marginal	37	10	20 (3 - 56)	100 (69 - 100)	96 (81 - 100)	96 (81 - 100)
13	LC middle	33	6	50 (12 - 88)	100 (48 - 100)	96 (81 - 100)	96 (81 - 100)
14	2nd marginal	18	0	NA	NA	89 (65 - 99)	100 (81 - 100)
15	Posterolateral	10	1	100 (3 - 100)	100 (3 - 100)	100 (66 - 100)	100 (66 - 100)
All		478	92	58 (47 - 68)	96 (89 - 99)	96 (94 - 98)	97 (94 - 98)

AHA = American Heart Association segmental classification; CI =confidence intervals; I = interactive protocol;
LAD = left anterior descending; LCx = circumflex; NA = not assessable; S = standard protocol;
SDS = significantly diseased segments (≥50% lumen reduction at quantitative coronary angiography).

The time required to prepare the images was recorded. No image preparation was required for the interactive postprocessing protocol. In the standard protocol the observer was allowed to scroll through the images of the 5 datasets. In the interactive protocol, the observer used all the tools on the workstation: axial images, multiplanar reformats, slab multiplanar maximum intensity projections, curved planar reformats, and 3-dimensional volume rendering.

Two independent observers (1 radiologist and 1 cardiologist), unaware of the results of CA, reviewed all images at the workstation. They were asked to visually identify the presence of significant stenoses (≥50% lumen reduction) on a "per segment" analysis using the American Heart Association classification of coronary segments[3]. Disagreements were resolved in by consensus. The time required to score was recorded.

Conventional CA was performed within 2 weeks of MSCT-CA using a standard technique. One experienced observer, unaware of the results of MSCT-CA, determined the diameter of all coronary branches and evaluated the presence of significant stenoses using quantitative CA (CAAS, Pie Medical Imaging, Maastricht, The Netherlands).

PPV (95% CI)		NPV (95% CI)		Accuracy (95% CI)		
S	I	S	I	S	I	Kappa
71 (42 - 92)	86 (57 - 98)	93 (78 - 99)	100 (88 - 100)	86 (73 - 95)	96 (85 - 99)	0.69
100 (66 - 100)	89 (65 - 99)	71 (49 - 87)	100 (78 - 100)	79 (61 - 91)	94 (80 - 99)	0.48
100 (40 - 100)	83 (36 - 100)	96 (77 - 100)	100 (83 - 100)	96 (80 - 100)	96 (80 - 100)	0.78
100 (3 - 100)	100 (3 - 100)	93 (68 - 100)	93 (68 - 100)	84 (70 - 100)	94 (10 - 100)	1.0
0 (0 - 98)	NA	100 (91 - 100)	100 (92 - 100)	98 (88 - 100)	100 (92 - 100)	NA
75 (35 - 97)	86 (57 - 98)	78 (61 - 90)	93 (78 - 99)	77 (62 - 89)	91 (78 - 98)	0.41
100 (63 - 100)	100 (78 - 100)	79 (61 - 91)	100 (87 - 100)	83 (68 - 83)	100 (91 - 100)	0.59
100 (16 - 100)	67 (9 - 99)	100 (90 - 100)	100 (90 - 100)	100 (91 - 100)	97 (86 - 100)	0.78
25 (1 - 81)	50 (7 - 93)	97 (83 - 100)	100 (88 - 100)	88 (73 - 97)	94 (80 - 99)	0.15
0 (0 - 19)	NA	100 (82 - 100)	100 (82 - 100)	50 (33 - 67)	100 (82 - 100)	NA
88 (47 - 100)	88 (47 - 100)	91 (85 - 100)	97 (85 - 100)	95 (84 - 99)	95 (84 - 99)	1.0
67 (9 - 99)	91 (59 - 100)	77 (59 - 89)	100 (87 - 100)	76 (59 - 88)	97 (86 - 100)	0.18
75 (19 - 99)	83 (34 - 100)	90 (73 - 98)	100 (87 - 100)	88 (72 - 97)	97 (84 - 100)	0.37
0 (0 - 84)	NA	100 (79 - 100)	100 (82 - 100)	89 (65 - 99)	100 (82 - 100)	NA
100 (3 - 100)	100 (3 - 100)	100 (66 - 100)	100 (66 - 100)	100 (69 - 100)	100 (69 - 100)	1.0
78 (66 - 87)	87 (79 - 93)	91 (87 - 93)	99 (97 - 100)	89 (86 - 91)	96 (94 - 98)	0.58

Lesions with an average diameter stenosis of ≥50% in 2 orthogonal views were considered significant obstructions. The consensus reading of the MSCT-CA was used to calculate sensitivity, specificity, positive and negative predictive values, and diagnostic accuracy with 95% confidence intervals. The agreement between the 2 image analysis protocols (standard and interactive) was evaluated by the coefficient of variation k. Kappa values <0.4 indicate poor, and values ≥ 0.4, >0.6, and >0.8 indicate fair, moderate, and excellent agreement, respectively. The differences (and 95% confidence intervals for the difference) in sensitivity and specificity between the 2 analysis protocols were evaluated by a previously proposed method[4]. A p value <0.05 was considered significant.

Mean HR during the scan was 54 ± 8 beats/min. A total of 478 ≥2-mm segments were included in the analysis. Ninety-two segments (19%) had significant obstructions on CA. The proximal and middle right coronary artery and left anterior descending segments accounted for 63% of diseased segments ($n = 57$). In these segments, the sensitivity ranged from 43% to 83% for the standard protocol and from 86% to 100% for the interactive protocol. Overall, the standard protocol missed 37 significant lesions, whereas the interactive protocol missed 4 significant lesions. Interobserver agreement was excellent for interactive protocol ($k = 0.81$) and moderate for standard protocol ($\kappa = 0.64$).

The specificity did not differ significantly between the 2 protocols ($p > 0.05$); however, the interactive protocol had a significantly better sensitivity for the detection of coronary obstructions ($p < 0.05$) (Table 1).

The mean time required for the radiographer to prepare the 5 datasets for standard protocol was 6 ± 2 minutes. The mean time required for the observers to complete the analysis was 16 ± 9 minutes for the standard protocol and 23 ± 13 minutes for the interactive protocol ($p < 0.05$).

The present study assessed the diagnostic accuracy of 16-row MSCT-CA using 2 protocols for image visualization: the first protocol was based on a standard series of projections that the observer could assess using a workstation implemented in a digital archiving system. The second protocol required the interaction between the operator and the dataset using a 3-dimensional workstation equipped with all available postprocessing tools. The results show that an approach using standard projections prepared by a technician was faster. In addition, it was probably less expensive, in that image processing was performed by a radiographer and image assessment by a radiologist. However, the standard projections approach had a significantly lower diagnostic sensitivity compared with the interactive postprocessing. In particular, the proximal segments, where disease was more frequent and of greater clinical importance (the proximal left anterior descending artery alone represented of significant lesions), were the sites that showed a major and significant discrepancy between the techniques. This reflects the large number (37 of 92; 40%) of lesions that were missed using standard projections. Specificity, instead, did not differ significantly between techniques.

One limitation of our study is that patients were retrospectively enrolled and selected. Patients with severe residual motion artifacts were not enrolled. This can improve the overall diagnostic accuracy. The results cannot be extrapolated to other patient populations, such as those with stents or bypass grafts. Finally, our interactive postprocessing protocol is based on a single vendor platform.

References

1. Nieman K, Cademartiri F, Lemos PA, Raaijmakers R, Pattynama PM, de Feyter PJ. Reliable noninvasive coronary angiography with fast submillimeter multislice spiral computed tomography. Circulation 2002;106:2051–2054.
2. Ropers D, Baum U, Pohle K, Anders K, Ulzheimer S, Ohnesorge B, Schlundt C, Bautz W, Daniel WG, Achenbach S. Detection of coronary artery stenoses with thin-slice multi-detector row spiral computed tomography and multiplanar reconstruction. Circulation 2003;107:664–666.
3. Austen WG, Edwards JE, Frye RL, Gensini GG, Gott VL, Griffith LS, McGoon DC, Murphy ML, Roe BB. A reporting system on patients evaluated for coronary artery disease. Report of the Ad Hoc Committee for Grading of Coronary Artery Disease, Council on Cardiovascular Surgery, American Heart Association. Circulation 1975;51:5– 40.
4. Hawass NE. Comparing the sensitivities and specificities of two diagnostic procedures performed on the same group of patients. Br J Radiol 1997;70:360–366.

Chapter 12

Non-invasive assessment of Coronary plaque burden Using multislice computed tomography

Abstract

We performed coronary plaque imaging with 16-row multislice computed tomography in 85 patients who had stable angina pectoris and a high pre-test likelihood of having coronary plaque to evaluate plaque burden, i.e., extent (number of diseased coronary segments) and size (small vs large) of plaque. We also assessed type of plaque (calcified, noncalcified, or mixed) and its anatomic distribution. Of 85 patients included, 78 (92%) had fully evaluable multislice computed tomograms that allowed assessment of coronary plaque burden, including major and side branches (≥2 mm), yielding a total of 855 segments. These 78 patients (92% men; mean age ± SD 58 ± 11.5 years) were in sinus rhythm, with heart rates of <70 beats/min (spontaneous or induced by β-blocker). Plaque was detected in 57% of all segments (487 of 855). The mean number of segments with plaque per patient ± SD was 6.2 ± 3.9. Plaque was classified as large in 33% of segments and small in 67%. Overall, 65% of plaques were calcified, 24% were noncalcified, and 11% were mixed. Plaques were predominantly located in the proximal and middle segments of the main coronary vessels.

Nico R. Mollet [1,2]
Filippo Cademartiri [2]
Koen Nieman [1]
Francesco Saia [1]
Pedro A. Lemos [1]
Eugene P. McFadden [1]
Patrick W. Serruys [1]
Gabriel P. Krestin [2]
Pim J. de Feyter [1,2]

From the Departments of Cardiology [1] and Radiology [2] Erasmus MC, University Medical Center Rotterdam, The Netherlands

American Journal of Cardiology, 2005;95:1165-1169

Introduction

Several studies have shown that multislice computed tomographic (MSCT) coronary angiography can detect coronary plaques and may permit identification of different plaque tissue components[1–7]. In this study, we assessed the coronary plaque burden in patients who had stable angina pectoris using noninvasive 16-row MSCT coronary angiography.

Methods

Over a 4-month period, 85 patients who had stable angina pectoris underwent 16-row MSCT coronary angiography and conventional coronary angiography. Patients were eligible for inclusion if they were in sinus rhythm with a heart rate of <70 beats/min (spontaneously or after oral β blockade), and were able to hold their breath for 20 seconds. Patients who had known allergy to contrast media, impaired renal function (serum creatinine 120 mmol/L), acute coronary syndromes, and previous coronary artery bypass grafting or stent implantation were excluded. The institutional review board of Erasmus Medical Center (Rotterdam, The Netherlands) approved the study, and all patients gave written informed consent.

Forty-eight percent of patients (40 of 83) received an additional dose of 100 mg of metoprolol orally 1 hour before the examination because of a pre-scan heart rate of >65 beats/min. All examinations were performed in a 16-detector row MSCT scanner (Sensation 16, Siemens, Forchheim, Germany). A bolus of 120 ml of iodinated contrast material (Visipaque 320, Amersham Health, Little Chalfont, United Kingdom) was administered through an arm vein (4 ml/s). Scan parameters were a detector collimation of 16 x 0.75 mm, a table feed of 3.0 mm/rotation, a gantry rotation time of 0.42 second, and a tube voltage of 120 kV and 400 to 450 mAs. Prospective x-ray tube modulation was applied in 41 patients who had a regular and low (<60 beats/min) heart rate[8]. This feature has been estimated to decrease the radiation dose by 40% to 50% in low heart rates [9,10]. To obtain nearly motionfree image quality, axial slices were reconstructed within the mid- to end-diastolic phase. Three datasets were reconstructed, with a reconstruction window starting at 350, 400, and 450 ms before the next R wave. All datasets were screened by axial scrolling to determine the presence of motion artifacts, and datasets with the fewest artifacts of a single coronary vessel were selected and sent to a dedicated workstation (Leonardo, Siemens) for evaluation. Additional reconstruction windows were explored when this was deemed necessary.

Conventional x-ray coronary angiography

Conventional coronary angiography was performed ≤3 weeks after the MSCT scan according to standard techniques. Coronary arteries were divided into segments according to the classification of the American Heart Association[11]. Diameters of all coronary segments and branches were measured with a quantitative coronary angiographic algorithm (CAAS, Pie Medical Imaging, Maastricht, The Netherlands) by an observer who was unaware of the MSCT results. Only branches ≥2 mm were included for assessment of MSCT coronary plaque burden. Coronary lesions were quantified by quantitative coronary angiography and classified as significant if the mean luminal diameter decrease in 2 orthogonal views was ≥50%.

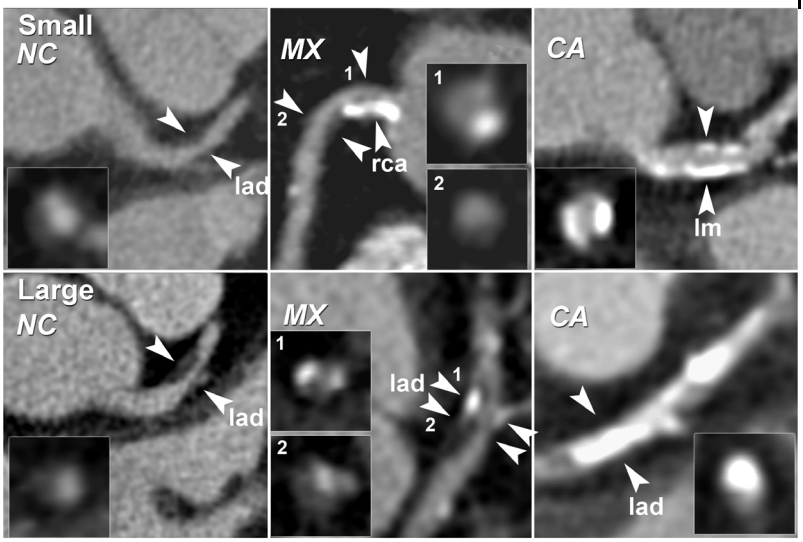

Figure 1. Plaque type and size with locations (arrowheads) of corresponding cross-sectional images (insets). CA calcified plaque; lad left anterior descending coronary artery; lm left main; MX mixed plaque; NC noncalcified plaque; rca right coronary artery.

MSCT image interpretation

Multislice computed tomograms were evaluated independently by 2 observers who were unaware of the coronary angiographic results. Disagreements were resolved by consensus after consultation with a third observer. Coronary segments were evaluated using multiplanar reconstructions and thin-slab maximum intensity projections to detect and classify plaques.

Plaque burden was assessed by determining the extent (number of diseased coronary segments) and size (small or large) of plaques. Plaques were also qualitatively classified into calcified, noncalcified, or mixed. The anatomic distribution of plaque in proximal, mid, and distal coronary segments of the left anterior descending artery, left circumflex coronary artery, right coronary artery, large side branches, and left main artery was also determined. Plaques were classified as small or large based on visual assessment with a threshold of 50% luminal decrease. Calcified plaques were defined as high-density lesions and noncalcified plaques as soft tissue density lesions that were clearly distinguishable from the adjacent epicardial fat and the coronary lumen.

Plaques were classified as mixed when calcified and noncalcified elements were detected within a single plaque (Figure 1).

Inter- and intraobserver variabilities of MSCT readers were calculated for plaque extent, distribution, and size using κ statistics. The diagnostic accuracy of MSCT coronary angiography to detect significant coronary obstructions was determined using quantitative coronary angiography as the reference standard. The precision of overall parameters with respect to stenosis detection was expressed with a 95% confidence interval.

RESULTS

Over a 4-month period, 85 eligible patients who had stable angina underwent multislice computed tomography. The mean interval between conventional coronary angiography and multislice computed tomography was 13 ± 5.2 days. Multislice computed tomograms were not of diagnostic quality in 7 patients. Motion artifacts were present in 6 patients due to premature beats (2) or residual motion despite a heart rate of <70 beats/min (4). Extravasation of contrast material during the injection resulted in low intravascular attenuation in 1 patient who thus was excluded from analysis. Thus, 78 patients had evaluable scans. Most patients (92%, 72 of 78) were men. Risk factors for atherosclerosis were hypercholesterolemia (62%, 48 of 78), hypertension (59%, 46 of 78), smoking (33%, 26 of 78), body mass index >27 kg/m^2 (32%, 25 of 78), and diabetes mellitus (22%, 17 of 78). Conventional coronary angiography showed nonsignificant stenoses in 9 patients, 1-vessel disease in 27 patients, and multivessel disease in 42 patients. Mean heart rate was 57 ± 6.6 beats/min during scanning. A total of 855 segments ≥2 mm was included for analysis.

Table 1. Extent, type, size, and anatomical distribution of plaque.

Coronary Artery	No of patients	Plaques (%)	Large (%)	Noncalcified (%)	Mixed (%)	Calcified (%)
LM	78	40 (51)	2 (3)	7 (18)	2 (5)	31 (78)
LAD overall	303	183 (60)	60 (20)	51 (28)	15 (8)	117 (64)
LAD proximal	78	62 (80)	22 (28)	17 (27)	9 (15)	36 (58)
LAD mid	72	56 (78)	27 (38)	19 (34)	3 (5)	34 (61)
LAD distal	63	22 (35)	3 (5)	2 (9)	3 (14)	7 (77)
First diagonal	59	32 (54)	7 (12)	9 (28)	0	23 (72)
Second diagonal	31	11 (36)	1 (3)	4 (36)	0	7 (64)
CX overall	245	114 (47)	37 (15)	28 (25)	12 (11)	74 (65)
CX proximal	68	45 (66)	15 (22)	7 (16)	6 (13)	32 (71)
CX mid	62	30 (46)	10 (16)	6 (20)	3 (10)	21 (70)
First marginal	65	30 (46)	8 (12)	8 (27)	3 (10)	19 (63)
Second marginal	39	8 (21)	3 (8)	6 (75)	0	2 (25)
Postero-lateral	11	1 (9)	1 (9)	1 (100)	0	0
RCA overall	229	150 (66)	62 (27)	32 (21)	22 (15)	96 (64)
RCA proximal	76	59 (78)	29 (38)	15 (25)	9 (15)	35 (59)
RCA mid	62	48 (77)	24 (39)	10 (21)	10 (21)	28 (58)
RCA distal	50	31 (62)	7 (14)	4 (13)	1 (3)	26 (84)
PDA	41	12 (29)	2 (5)	3 (25)	2 (17)	7 (58)
All vessels	**855**	**487 (57)**	**161 (33)**	**118 (24)**	**51 (11)**	**318 (65)**

CX, left circumflex coronary artery; LAD, left anterior descending coronary artery; LM, left main; PDA, posterior descending artery; RCA, right coronary artery.

MSCT coronary plaque burden

Plaque was observed in 487 of 855 coronary segments (57%; Table 1); 34% of plaques were classified as large and 66% as small. Large plaques were primarily located in the proximal and mid parts of the left anterior descending and right coronary arteries.

Overall, 65% of plaques were classified as calcified, 11% as mixed, and 24% as noncalcified (Figure 2).

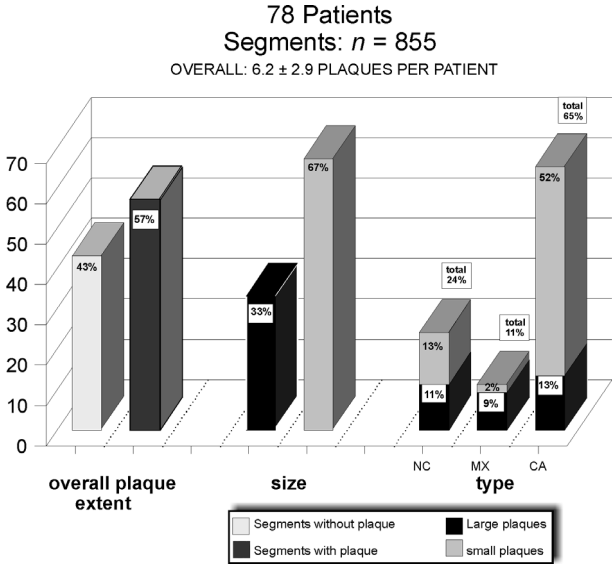

Figure 2. Plaque extent, type, and size in 78 patients and 855 segments without plaque (pale gray bars), with plaque (dark gray bars), with large plaque (black bars), and small plaque (light gray bars) (6.2 2.9 plaques per patient overall). Abbreviations as in Figure 1.

Although most (82%) mixed plaques were large, 49% of calcified plaques and 46% of noncalcified plaques were classified as large. Extent, size, type, and distribution of plaques are presented in Table 1. The segmental distribution of plaques shows that the proximal and mid segments of the left anterior descending, right coronary, and left circumflex coronary arteries were most frequently involved. In >50% of patients, plaque was detected in the left main artery. The relative frequency of each plaque type in each coronary vessel is shown in Figure 3.

The κ values for inter- and intraobserver agreements with regard to plaque extent and distribution were 83% and 87%, respectively, whereas κ values with regard to plaque size were 72% and 74%, respectively.

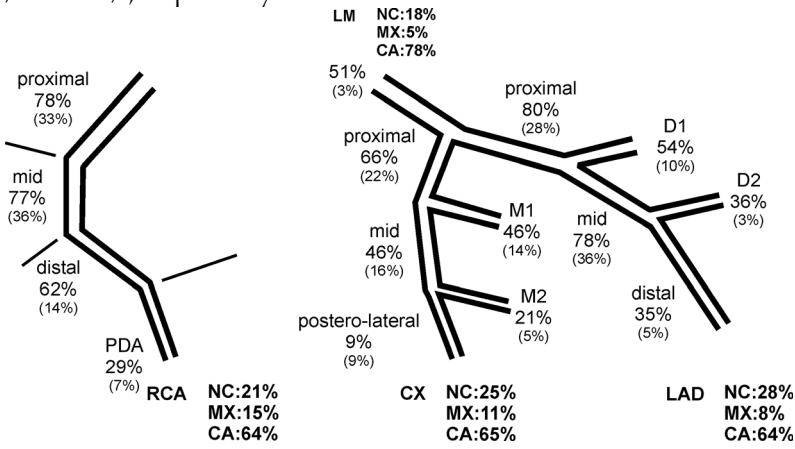

Figure 3. Anatomic distribution of plaque, plaque type, and plaque size and percentage of segments with plaque (percentage of large plaques, i.e., >50% luminal obstruction). CX circumflex coronary artery; D1 first diagonal branch; D2 second diagonal branch; LAD left anterior descending coronary artery; LM left main; M1 first marginal branch; M2 second marginal branch; PDA posterior descending artery; RCA right coronary artery. Other abbreviations as in Figure 1.

Diagnostic accuracy of MSCT coronary angiography for detection of significant stenoses

MSCT coronary angiographic results were compared with conventional coronary angiographic results. MSCT coronary angiography correctly detected 147 of 154 significant obstructive plaques. Seven plaques were detected with multislice computed tomography but incorrectly classified as nonsignificant (mean diameter decrease 61±6% on quantitative coronary angiography). Fourteen plaques, 13 of which were heavily calcified, were incorrectly classified by multislice computed tomography as significant obstructions (mean diameter decrease 31±12% on quantitative coronary angiography). Sensitivity, specificity, positive predictive value, and negative predictive value for all available segments ≥2 mm were calculated as 96% (95% confidence interval 90 to 98), 98% (95% confi- dence interval 96 to 98), 91% (95% confidence interval 85 to 95), and 99% (95% confidence interval 97 to 99), respectively.

Discussion

The major objectives of noninvasive imaging of coronary arteries are to identify significant luminal stenoses and to identify plaques that may become responsible for an acute coronary syndrome.

The diagnostic performance of current 16-row MSCT scanners in the detection of significant (>50% luminal decrease) coronary plaques has been reported [12–14]. The sensitivity has been reported to be 92% to 95% with a specificity of 86% to 93% compared with invasive conventional coronary angiography. Our study was not designed to evaluate the diagnostic accuracy of 16-detector row multislice computed tomography to detect significant coronary stenoses. However, the results extend previous observations that demonstrate the improved performance of 16-row MSCT scanners. In this study, the sensitivity (96%) and specificity (98%) of multislice computed tomography in the detection of significant coronary stenoses were extremely high. These results should be interpreted with caution, because only patients who had high-quality images were included in the analysis, although these patients represented 92% of the overall population. In addition, we included only coronary branches ≥2 mm in the comparative analysis, whereas a threshold of 1.5 mm was used in several previously reported studies. Previous studies have shown that noninvasive calcium quantification with electron-beam computed tomography correlates well with extent of atherosclerosis but seriously underestimates total coronary plaque burden[15–19]. Correlation with histology showed that the amount of calcium detected by electron-beam computed tomography reflected only ~20% of the measured atherosclerotic plaque burden[15]. Electronbeam and multislice computed tomography are used for calcium scoring, and a good correlation between these techniques has been reported [20].

The overall assessment of plaque burden using MSCT coronary angiography represents an advance on the established calcium quantification approach but still underestimates total measured atherosclerotic plaque burden as determined by histology, which is consistent with several histopathologic studies[15,21]. The reasons for underestimation are that the resolution of current MSCT scanners does not allow assessment of the earlier phases of atherosclerosis [6] and that the volume of plaques detected with 16-row MSCT coronary

angiography significantly underestimates the volume of plaques compared with intracoronary ultrasound [5]. Specifically, detection of small noncalcified plaques remains challenging. The high density of calcium permits detection of calcified small plaques, a fact that may partly account for our observation that most small plaques were calcified. Other problems concerning plaque assessment on multislice computed tomography are partial volume effects and blooming that limit evaluation of adjacent structures. These artifacts result in an overestimation of calcified tissue volumes and may underestimate the frequency of mixed plaques. Similarly, the presence of intravascular contrast material may render more difficult the detection of mild calcifications than on nonenhanced scans.

The most recent 64-row MSCT scanners have improved spatial and temporal resolutions. The effect of these technical advances on the assessment of coronary plaques needs to be established in future studies.

Study limitations

We studied a selected population that had a high pre-test likelihood of coronary plaques and that comprised patients who had stable angina pectoris and were scheduled for conventional coronary angiography. Moreover, we included only patients who were in stable sinus rhythm and had a relatively slow heart rate (spontaneous or induced by β blockade), which are variables predictive of high quality MSCT imaging. An important limitation of our study was a lack of comparison between intracoronary ultrasound and MSCT coronary angiography. However, the diagnostic performance of 16-row MSCT coronary angiography to detect coronary plaques has been previously reported [4–6]. In addition, the main objective of our study was to assess total MSCT coronary plaque burden, whereas intracoronary ultrasound generally is preserved for the evaluation of proximal or middle segments of a single coronary vessel. The high radiation exposure during MSCT coronary angiography ranges from 7.1 to 10.9 mSv and remains a matter of concern [9,10,22,23]. We attempted to decrease radiation exposure using prospective x-ray tube current modulation, an approach that is reliable only with regular slow heart rates (<60 beats/min). This was the case in >50% of our patients. This setting has been estimated to decrease the radiation dose by 40% to 50% in patients who have low heart rates [9,10]. However, using prospective x-ray tube current modulation limits the opportunity to reconstruct images during systolic and early diastolic phases, which can be of additional value, especially for evaluation of the rapidly moving right coronary artery.

References

1. Schroeder S, Kopp AF, Baumbach A, Meisner C, Kuettner A, Georg C, Ohnesorge B, Herdeg C, Claussen CD, Karsch KR. Noninvasive detection and evaluation of atherosclerotic coronary plaques with multislice computed tomography. J Am Coll Cardiol 2001;37:1430–1435.
2. Becker CR, Nikolaou K, Muders M, Babaryka G, Crispin A, Schoepf UJ, Loehrs U, Reiser MF. Ex vivo coronary atherosclerotic plaque characterization with multi-detector-row CT. Eur Radiol 2003;13:2094–2098.
3. Leber AW, Knez A, White CW, Becker A, von Ziegler F, Muehling O, Becker C, Reiser M, Steinbeck G, Boekstegers P. Composition of coronary atherosclerotic plaques in patients with acute myocardial infarction and stable angina pectoris determined by contrast-enhanced multislice computed tomography. Am J Cardiol 2003;91:714–718.

4. Schoenhagen P, Tuzcu EM, Stillman AE, Moliterno DJ, Halliburton SS, Kuzmiak SA, Kasper JM, Magyar WA, Lieber ML, Nissen SE, White RD. Non-invasive assessment of plaque morphology and remodeling in mildly stenotic coronary segments: comparison of 16-slice computed tomography and intravascular ultrasound. Coron Artery Dis 2003;14:459–462.
5. Achenbach S, Moselewski F, Ropers D, Ferencik M, Hoffmann U, MacNeill B, Pohle K, Baum U, Anders K, Jang IK, et al. Detection of calcified and noncalcified coronary atherosclerotic plaque by contrast-enhanced, submillimeter multidetector spiral computed tomography: a segment-based comparison with intravascular ultrasound. Circulation 2004;109:14 –17.
6. Leber AW, Knez A, Becker A, Becker C, von Ziegler F, Nikolaou K, Rist C, Reiser M, White C, Steinbeck G, Boekstegers P. Accuracy of multidetector spiral computed tomography in identifying and differentiating the composition of coronary atherosclerotic plaques: a comparative study with intracoronary ultrasound. J Am Coll Cardiol 2004;43:1241–1247.
7. Nikolaou K, Becker CR, Muders M, Babaryka G, Scheidler J, Flohr T, Loehrs U, Reiser MF, Fayad ZA. Multidetector-row computed tomography and magnetic resonance imaging of atherosclerotic lesions in human ex vivo coronary arteries. Atherosclerosis 2004;174:243–252.
8. Flohr TG, Schoepf UJ, Kuettner A, Halliburton S, Bruder H, Suess C, Schmidt B, Hofmann L, Yucel EK, Schaller S, Ohnesorge BM. Advances in cardiac imaging with 16-section CT systems. Acad Radiol 2003;10:386–401.
9. Jakobs TF, Becker CR, Ohnesorge B, Flohr T, Suess C, Schoepf UJ, Reiser MF. Multislice helical CT of the heart with retrospective ECG gating: reduction of radiation exposure by ECG-controlled tube current modulation. Eur Radiol 2002;12:1081–1086.
10. Trabold T, Buchgeister M, Kuttner A, Heuschmid M, Kopp AF, Schroder S, Claussen CD. Estimation of radiation exposure in 16-detector row computed tomography of the heart with retrospective ECG-gating. Rofo Fortschr Geb Rontgenstr Neuen Bildgeb Verfahr 2003;175:1051–1055.
11. Austen WG, Edwards JE, Frye RL, Gensini GG, Gott VL, Griffith LS, McGoon DC, Murphy ML, Roe BB. A reporting system on patients evaluated for coronary artery disease. Report of the Ad Hoc Committee for Grading of Coronary Artery Disease, Council on Cardiovascular Surgery, American Heart Association. Circulation 1975;51:5– 40.
12. Nieman K, Cademartiri F, Lemos PA, Raaijmakers R, Pattynama PM, de Feyter PJ. Reliable noninvasive coronary angiography with fast submillimeter multislice spiral computed tomography. Circulation 2002;106:2051–2054.
13. Ropers D, Baum U, Pohle K, Anders K, Ulzheimer S, Ohnesorge B, Schlundt C, Bautz W, Daniel WG, Achenbach S. Detection of coronary artery stenoses with thin-slice multi-detector row spiral computed tomography and multiplanar reconstruction. Circulation 2003;107:664–666.
14. Mollet NR, Cademartiri F, Nieman K, Saia F, Lemos PA, McFadden EP, Pattynama PMT, Serruys PW, Krestin GP, De Feyter PJ. Multislice spiral CT coronary angiography in patients with stable angina pectoris. J Am Coll Cardiol 2004;43:2265–2270.
15. Rumberger JA, Simons DB, Fitzpatrick LA, Sheedy PF, Schwartz RS. Coronary artery calcium area by electron-beam computed tomography and coronary atherosclerotic plaque area. A histopathologic correlative study. Circulation 1995;92:2157–2162.
16. Sangiorgi G, Rumberger JA, Severson A, Edwards WD, Gregoire J, Fitzpatrick LA, Schwartz RS. Arterial calcification and not lumen stenosis is highly correlated with atherosclerotic plaque burden in humans: a histologic study of 723 coronary artery segments using nondecalcifying methodology. J Am Coll Cardiol 1998;31:126 –133.

17. Schmermund A, Baumgart D, Adamzik M, Ge J, Gronemeyer D, Seibel R, Sehnert C, Gorge G, Haude M, Erbel R. Comparison of electron-beam computed tomography and intracoronary ultrasound in detecting calcified and noncalcified plaques in patients with acute coronary syndromes and no or minimal to moderate angiographic coronary artery disease. Am J Cardiol 1998;81:141–146.
18. Baumgart D, Schmermund A, Goerge G, Haude M, Ge J, Adamzik M, Sehnert C, Altmaier K, Groenemeyer D, Seibel R, Erbel R. Comparison of electron beam computed tomography with intracoronary ultrasound and coronary angiography for detection of coronary atherosclerosis. J Am Coll Cardiol 1997; 30:57– 64.
19. Simons DB, Schwartz RS, Edwards WD, Sheedy PF, Breen JF, Rumberger JA. Noninvasive definition of anatomic coronary artery disease by ultrafast computed tomographic scanning: a quantitative pathologic comparison study. J Am Coll Cardiol 1992;20:1118 –1126.
20. Becker CR, Knez A, Jakobs TF, Aydemir S, Becker A, Schoepf UJ, Bruening R, Haberl R, Reiser MF. Detection and quantification of coronary artery calcifi- cation with electron-beam and conventional CT. Eur Radiol 1999;9:620–624.
21. Schmermund A, Schwartz RS, Adamzik M, Sangiorgi G, Pfeifer EA, Rumberger JA, Burke AP, Farb A, Virmani R. Coronary atherosclerosis in unheralded sudden coronary death under age 50: histo-pathologic comparison with 'healthy' subjects dying out of hospital. Atherosclerosis 2001;155:499 –508.
22. Hunold P, Vogt FM, Schmermund A, Debatin JF, Kerkhoff G, Budde T, Erbel R, Ewen K, Barkhausen J. Radiation exposure during cardiac CT: effective doses at multi-detector row CT and electron-beam CT. Radiology 2003;226:145– 152.
23. Morin RL, Gerber TC, McCollough CH. Radiation dose in computed tomography of the heart. Circulation 2003;107:917–922.

Chapter 13

CORONARY PLAQUE BURDEN IN PATIENTS WITH STABLE AND UNSTABLE CORONARY ARTERY DISEASE USING MULTISLICE CT CORONARY ANGIOGRAPHY

Abstract

Nico R. Mollet [1,2]
Filippo Cademartiri [2]
Carlos van Mieghem [1,2]
Timo Baks [1,2]
Patrick W Serruys [1]
Gabriel P. Krestin [2]
Eugene P. McFadden [1]
Pim J. de Feyter [1,2]

From the Departments of Cardiology [1] and Radiology [2]
Erasmus MC,
University Medical Center,
Rotterdam,
The Netherlands

Submitted for publication

Purpose
To evaluate the Multislice Computed Tomography (MSCT) coronary plaque burden in patients with stable and unstable angina pectoris.

Materials and Methods
Twenty-one patients with stable and 20 patients with unstable angina pectoris scheduled for conventional coronary angiography (CCA) underwent MSCT coronary angiography using a 16-slice scanner offering a faster rotation time (375ms) and higher *X*-ray tube output (500-600 mAs) when compared to previous 16-slice scanners. To determine the MSCT coronary plaque burden, we assessed the extent (number of diseased segments), size (small or large), type (calcific, non-calcific, or mixed) of plaque, its anatomic distribution, and angiographic appearance in all available ≥2mm segments. In a subset of 15 (7 stable, 8 unstable) patients, the detection and classification of coronary plaques by MSCT was verified by intra-coronary ultrasound (ICUS).

Results
Sensitivity and specificity of MSCT as compared to ICUS to detect significant plaques (defined as ≥1mm plaque thickness on ICUS) was 83% and 87%. Overall, a total of 473 segments were included, resulting in 11.6±1.5 segments per patient. Plaques were present in 62% of segments, and classified as large in 47% of diseased segments. Thirty-two percent were non-calcific, 25% calcific, and 43% mixed. Plaques were most frequently located in the proximal and mid segments. Plaque was found in 33% of segments classified as normal on CCA. Unstable patients had significantly more non-calcific plaques when compared to stable patients (45% vs. 21%, $p<0.05$).

Conclusions
MSCT coronary angiography provides important information regarding the coronary plaque burden in patients with stable and unstable angina.

INTRODUCTION

Multislice Computed Tomography (MSCT) is a rapidly developing technique. The latest 16-row MSCT scanners have a higher *X*-ray tube rotation speed and allow scanning with a higher tube current, providing increased temporal resolution and contrast-to-noise ratio when compared to previous generation 16-row scanners. The sensitivity and specificity to detect significant obstructive coronary lesions using these scanners is high[1,2]. Preliminary in-vivo and ex-vivo studies using previous 16-row MSCT scanner generations showed that MSCT coronary imaging holds promise for the detection of non-obstructive coronary plaques and allows identification of different plaque tissue components [3-8]. These observations prompted us to evaluate the MSCT coronary plaque burden, defined as presence, severity, distribution, and type of coronary plaques using a second-generation 16-row MSCT scanner. We assessed the MSCT coronary plaque burden in all available ≥2 mm coronary segments in patients with stable and unstable angina pectoris. We compared these results with that of conventional angiography and, in a subgroup of patients, intra-coronary ultrasound (ICUS).

MATERIALS AND METHODS

Subjects

During a 3-month period, 21 patients (17 male, 4 female, mean age [±SD] 59.0±9.2 years) with stable angina pectoris and 20 patients (15 male, 5 female, mean age [±SD] 60.0±11.3 years) with unstable angina pectoris underwent 16-row MSCT coronary angiography prior to diagnostic coronary angiography followed in case of amenable lesions by percutaneous coronary intervention. Patients were eligible for inclusion if they were in sinus rhythm, with a heart rate of <70 beats/minute (spontaneously or β-blocker induced), and able to breath hold during 20 seconds. Exclusion criteria were known contrast allergy, significant renal dysfunction (serum creatinine >120 mmol/L), Braunwald class IA, IIA, IIIA (unstable angina caused by non–cardiac illness), and previous percutaneous or surgical revascularization. A subset of 15 patients (stable angina: 7, unstable angina: 8) underwent an ICUS examination of a vessel not targeted for percutaneous intervention. In order of preference, the left anterior descending artery (LAD, n=8), right coronary artery (RCA, n=4) or circumflex artery (CX, n=3) were selected.

The institutional review board of our institution approved the study and all patients gave written informed consent.

MSCT coronary angiography

All MSCT examinations were performed using a second generation 16-row MSCT scanner (Sensation 16 Straton®, Siemens, Forchheim, Germany) equipped with a faster *X*-ray tube rotation time (375 ms) and a higher tube output (up to 600 mAs) providing an improved temporal resolution and contrast-to-noise ratio when compared to previous 16-slice scanners. Other scan parameters: detector collimation 16 x 0.75 mm, table feed 3.0 mm/rotation, tube voltage 120 kV, no prospective *X*-ray tube modulation was applied. The radiation exposure using this scan protocol was estimated between 11.8-16.3 mSv (male/female) using dedicated software (WinDose®, Institute of Medical Physics, Erlangen, Germany). Patients with a pre-scan heart rate ≥65 beats/minute received a single oral dose of 100 mg metoprolol (Selokeen®, AstraZeneca Pharmaceutics, UK) one hour before the scan.

A bolus of 100 ml of iodinated contrast material (Iomeron® 400, Bracco, Milan, Italy) followed by a saline bolus chaser of 40 ml was administered through an arm vein (flow rate: 4 ml/s). Datasets were reconstructed during different time points of the cardiac phase using a retrospective ECG-gated reconstruction algorithm. This algorithm uses data of a single heart beat obtained in half gantry rotation time, resulting in a temporal resolution of up to 188 ms. Datasets reconstructed within the mid- to end-diastolic phase generally provided nearly motion-free image quality, but different reconstruction windows (e.g. within the early diastolic phase) were explored when deemed necessary. All MSCT datasets with least motion artifacts were analysed on an off-line workstation (Leonardo®, Siemens, Forchheim, Germany).

Conventional *X*-ray coronary angiography

Conventional coronary angiography was performed within 72 hours of the MSCT scan. The coronary arteries were divided into segments according to the AHA classification [9]. The diameters of all coronary segments and branches were measured using a quantitative coronary angiography (QCA) algorithm (CAAS®, Pie Medical Imaging, Maastricht, The Netherlands). The severity of coronary lesions was quantified in two orthogonal views and stenoses were classified as significant if the mean lumen narrowing was ≥50%. Only branches with a diameter of ≥2mm were included for comparison with MSCT. One observer, unaware of the MSCT results, classified these segments as normal (no luminal encroachment), wall irregularities (<20% lumen narrowing), moderately diseased (≥20%- <50% lumen narrowing), or significantly diseased: ≥50% lumen narrowing.

MSCT analysis (1): assessment of the coronary plaque burden in all available ≥2mm coronary segments

To evaluate the MSCT coronary plaque burden, we assessed the extent, type, size, and anatomic distribution of plaque along all ≥2mm segments, including the main coronary arteries and ≥2mm side branches. All coronary segments were evaluated regarding the presence of plaque using longitudinal and cross-sectional multiplanar reconstructed images. Plaque extent was defined as the number of diseased coronary segments. Plaque size and type was defined using the criteria mentioned above.

Two observers, unaware of the results of other imaging modalities, independently performed all MSCT analyses for the assessment of plaque burden. Disagreement between both observers was resolved by consensus. Inter- and intra-observer variability of MSCT readers for the assessment of the MSCT coronary plaque burden was calculated for plaque extent, type, and size, and differences in stable and unstable patients were compared using the Student's t-Test (p-values <0.05 were considered significant).

Intra-Coronary Ultrasound

All ICUS examinations were performed using an Ultracross 40 MH™ or CVIS Atlantis 30 MH™ SR Pro catheter (Boston Scientific, Santa Clara, USA). A region of interest (ROI) was selected on the angiogram after identification of an easily recognizable proximal and distal landmark (e.g. large side branches). The tip of the ICUS catheter was positioned at least 10 mm distal of the distal landmark and an automated pullback (speed: 0.5 mm/s) of the complete region of interest (ROI) was performed. The acquired data was stored, digitized and loaded into an off-line workstation. A validated software with retrospective image-based gating [10] was used (Curad®, Wijk bij Duurstede, The Netherlands) to perform all ICUS measurements.

MSCT analysis (2): assessment of coronary plaques in a selected ROI and comparison with ICUS

First, the selected ROI was identified on the MSCT coronary angiogram. A semi-automated vessel-tracking software (VesselView®, Siemens, Forchheim, Germany) was used to create a central lumen line throughout the ROI. Contiguous cross-sectional multiplanar reconstructions with a thickness of 1 mm were reconstructed orthogonal to this line and used for comparison with ICUS.

Plaque was defined as thickening of the coronary wall of at least 1 mm, clearly distinguishable of the coronary lumen. Plaques with a CT density below the coronary lumen and above the adjacent epicardial fat was classified as non-calcific, whereas plaques with a CT density ≥130 Hounsfield units (HU) were classified as calcific. Plaques with both non-calcific and calcific plaque tissue were classified as mixed. Plaque size was classified as small (≥1-<2 mm plaque thickness) or large (≥2 mm plaque thickness). The optimal window-level settings were chosen on an individual basis for the detection and classification of coronary plaques as previously described[7]. Two observers, unaware of the results of other imaging modalities, separately performed all MSCT analyses for comparison with ICUS. Disagreement between both observers was resolved by consensus in a joined session.

The selected ROI was divided in 5 mm sections to compare the results of MSCT and ICUS. Plaques with a minimum plaque thickness of 1 mm within a single section were classified as significant on ICUS. Sections with at least one cross-section with plaque were classified as significant on the MSCT-scan. All MSCT and ICUS evaluations were performed by observers unaware of the results of each technique. The diagnostic accuracy of MSCT to detect significant coronary plaque per section was determined using ICUS as the standard reference. The precision of the overall parameters with respect to plaque detection was expressed with a 95% confidence interval.

RESULTS

Fifty-six percent (23/41) of the patients was on long-term β-blockade. Fifty-one (21/41) received an (additional) β-blocker because of a pre-scan heart rate that was above 70 beats/minute. The mean heart rate (±SD) during the scan procedure in stable and unstable patients was 57.0±2.8 and 60.7±11.3 respectively. The total scan time was 17.6±1.3 seconds. Demographics of stable and unstable patients are listed in Table 1.

Evaluation of the MSCT coronary plaque burden and comparison with conventional angiography

A total of 473 ≥2mm coronary segments were included for the assessment of the MSCT coronary plaque burden. Per patient, 11.6±1.5 segments were included for analysis. Overall, 62% (292/473) of the segments contained plaque. Non-calcific plaques were found in 32% (93/292), calcific in 25% (73/292), and mixed in 43% (126/292) of diseased segments. Plaque size was classified as small in 53% (155/292), and large in 47% (137/292). The κ-value for inter- and intra-observer agreement regarding plaque extent was 78% and 82%, plaque type was 69% and 74%, and plaque size was 70% and 72% respectively. The extent, type, size, and relative frequency of different plaque type per coronary vessel in stable and unstable patients are tabulated in Table 2.

Table 1. Patient characteristics

	SAP (n=21)	UAP (n=20)	*p*-value
Age (years)	59.0±9.2	59.3±9.5	NS§
Gender (male/female)	19	15	NS†
Systemic hypertension *	13	9	NS†
Hypercholesterolemia **	14	15	NS†
Diabetes mellitus	2	0	NS†
Family history	9	9	NS†
Smoking	10	8	NS†
Obesity (BMI ≥30)	2	3	NS†
No significant stenosis	2	2	NS†
Single vessel disease	12	11	NS†
Multi-vessel disease	7	7	NS†

BMI: body mass index; NS: non significant; SAP: stable angina pectoris; UAP: unstable angina pectoris.
* Blood pressure ≥160/95 mmHg or treatment for hypertension,
** Total cholesterol >5.5 mmol/l (215 mg/dl) or treatment for hypercholesterolemia.
Differences between both patient populations were calculated using the Mann-Whitney U-test (†) or Student's t-Test (§). *P*-values <0.05 were considered significant.

Table 2. MSCT coronary plaque burden in stable (n=21) and unstable (n=20) patients

	SAP	UAP	p-value	Overall
Plaque extent	64% (161/250)	59% (131/223)	NS	62% (292/473)
Plaque type				
Non-Calcific	21% (34/161)	45% (59/131)	<0,05	32% (93/292)
RCA	28% (11/40)	36% (13/36)	NS	32% (24/76)
LM	46% (6/13)	38% (3/8)	NS	43% (9/21)
LAD	16% (11/68)	45% (24/53)	<0,05	29% (35/121)
CX	15% (6/40)	56% (19/34)	<0,05	34% (25/74)
Calcific	30% (48/161)	19% (25/131)	NS	25% (73/292)
RCA	15% (6/40)	28% (10/36)	NS	21% (16/76)
LM	15% (2/13)	0% (0/0)	NS	10% (2/21)
LAD	43% (29/68)	15% (8/53)	<0,05	31% (37/121)
CX	28% (11/40)	21% (7/34)	NS	24% (18/74)
Mixed	49% (79/161)	36% (47/131)	0,07	43% (126/292)
RCA	58% (23/40)	36% (13/36)	NS	47% (36/76)
LM	39% (5/13)	63% (5/8)	NS	48% (10/21)
LAD	41% (28/68)	40% (21/53)	NS	41% (49/121)
CX	58% (23/40)	24% (8/34)	<0,05	42% (31/74)
Plaque size				
Small	48% (77/161)	60% (78/131)	NS	53% (155/292)
Large	52% (84/161)	40% (53/131)	NS	47% (137/292)

CX: circumflex coronary artery; LAD: left anterior descending coronary artery;
LM: left main coronary artery; NS: non significant; RCA: right coronary artery;
SAP: stable angina pectoris; UAP: unstable angina pectoris.

Overall, plaque was found in 71% (115/161) of proximal segments, in 71% (79/111) of mid segments, and in 49% (98/201) of distal segments and side-branches of the main coronary arteries (LM, LAD, CX, and RCA). Plaque was detected in ≥90% of the proximal and mid segments of the LAD in both stable and unstable patients. The overall distribution of plaques in both patient groups is shown in Figure 1.

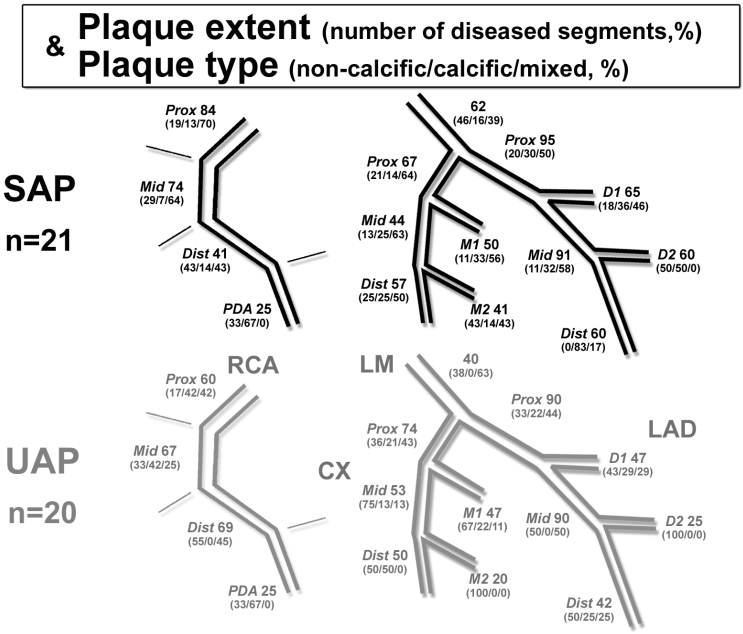

Figure 1. Extent, type, and distribution of coronary atherosclerosis in patients with stable (SAP) and unstable (UAP) angina pectoris.

The angiographically appearance of small and large plaques is shown in Table 3. In general, large plaques were more frequently found in segments with more luminal encroachment on the conventional angiogram.

Table 3. Detection of plaques with MSCT coronary angiography in normal and diseased segments on conventional angiography

			MSCT		
		Normal (%)	Small (%)	Large (%)	Any Plaque (%)
CCA	**Normal** n=207	139 (67)	49 (25)	19 (8)	68 (33)
	Wall irregularities n=138	40 (29)	55 (41)	43 (31)	98 (72)
	<50% stenosis n=59	2 (3)	26 (44)	31 (53)	57 (97)
	≥50% stenosis n=69	0 (0)	24 (35)	45 (65)	69 (100)

CCA: conventional coronary angiography; MSCT: Multislice computed tomography.

Plaque was detected in nearly all (99%, 126/128) coronary segments with non-significant or significant stenoses. In addition, plaque was detected in 33% of coronary segments classified as normal with conventional angiography, while angiographic wall irregularities were associated with 72% (98/138) of the segments with MSCT coronary plaque involvement. An example of the assessment of the coronary plaque burden in a patient with stable angina pectoris is shown in Figure 2.

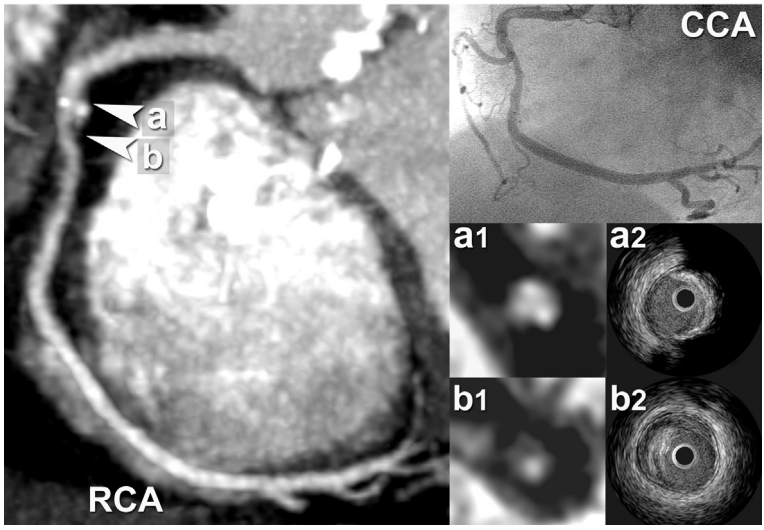

Figure 2. Curved planar reconstructions of the main coronary arteries showing the extent and distribution of atherosclerosis in a patient with stable angina and a high MSCT coronary plaque burden. Calcific plaques are indicated by blue, whereas non-calcific plaques are indicated by red in the annotated panels. A volume rendered CT image (coloured image) provides an overview of the coronary anatomy in this patient.
CX, circumflex coronary artery; D1, first diagonal branch; LAD, left anterior descending coronary artery; LM, left main coronary artery; PDA, posterior descending coronary artery; Prox, proximal; RCA, right coronary artery.

Diagnostic performance of MSCT vs. ICUS to detect significant plaques in a selected ROI

A total of 92 sections (each 5 mm) were included for comparison between MSCT and ICUS. On ICUS, significant plaque was found in 33% (30/92) of the included sections. Overall, the sensitivity and specificity of MSCT coronary angiography to detect significant coronary plaques was 83% (25/30, 95% CI: 65%-95%) and 87% (54/62, 95% CI: 76%-94%) respectively. The diagnostic performance of MSCT for the detection of non-calcific, calcific, and mixed plaques is detailed in Table 4.

Table 4. Diagnostic accuracy of MSCT coronary angiography for the detection of coronary plaques as compared to ICUS

	Non-Calcific	Calcific	Mixed	Overall
True positive	6	10	9	25
False positive	0	3	5	8
False negative	2	1	2	5
True negative	...	...	...	54
Sensitivity	(6/8)	(10/11)	(9/11)	(25/30)
(%)	75 (34%-93%)	91 (58%-97%)	82 (48%-95%)	83 (65%-95%)
Specificity	...	...	...	(54/62)
(%)				87 (76%-94%)

A higher sensitivity was found in segments containing calcific plaque tissue (calcific plaques: 91% [10/11, 95% CI: 58%-97%], mixed plaques: 82% [9/11, 95% CI: 48%-95%]) as compared to segments with exclusively non-calcific plaque tissue (non-calcific plaques: 75% [6/8, 95% CI: 34%-93%]). An example showing a comparison between the MSCT and ICUS findings is shown in Figure 3.

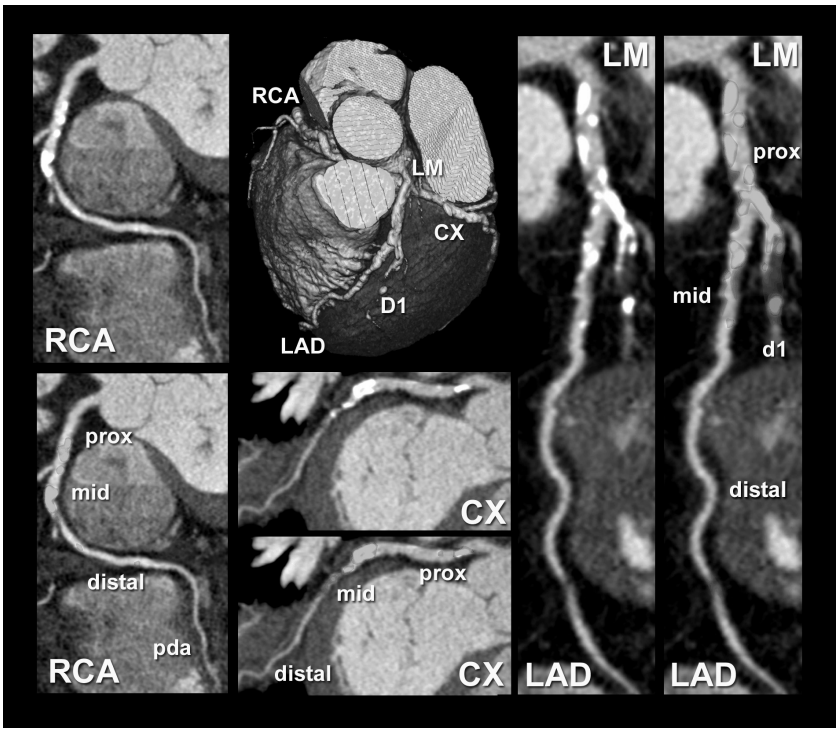

Figure 3. Maximum intensity projected CT image showing a non-significant obstructive coronary lesion located at the mid section of the right coronary artery (RCA), which was also found on the conventional coronary angiogram (CCA). Cross-sectional CT images at the site of the lesion demonstrate the presence of a large, mixed plaque with both calcific (panel A1) and non-calcific (panel B1) plaque tissue, which was confirmed with intra-coronary ultrasound (panels A2 and B2). (A full color version of this illustration can be found in the color section (Chapter 21)).

Discussion

Coronary atherosclerosis begins early in life and it takes several decades for plaques to advance into vulnerable plaques that underlie the progression to acute coronary syndromes (unstable angina pectoris or myocardial infarction) or progression of coronary stenosis. However, this process of progression of asymptomatic atherosclerosis into vulnerable plaques is to a large extent unknown. ICUS is currently the gold standard for in-vivo evaluation of coronary plaques and provides important anatomical information regarding the presence and type of coronary atherosclerosis. However, ICUS is an invasive, time-consuming, and expensive procedure. Consequently, ICUS examinations are usually restricted to the proximal and mid parts of a single coronary artery, thereby precluding evaluation of the overall coronary plaque burden. This has spurred the need for

non-invasive imaging modalities able to evaluate coronary plaques, e.g. MRI and MSCT. Sixteen-row MSCT coronary angiography has a nearly isotropic sub-millimetre spatial resolution that allows evaluation of the coronary vessel wall in all ≥2 mm coronary segments thereby providing a more comprehensive evaluation of coronary atherosclerosis throughout the coronary tree as compared to ICUS.

In our study we demonstrated that MSCT coronary angiography is able to assess the presence, extent, severity, distribution and type of coronary plaques. We found a high sensitivity and specificity (83% and 87%, respectively) of MSCT to detect significant coronary plaques when compared to ICUS, which is in line with previously published studies [6,7]. However, we found a higher sensitivity of MSCT to detect exclusively non-calcified plaques when compared to a previous study of Achenbach *et al*[6]. This observation may be the result of an improved image quality offered by second generation 16-row MSCT scanners due to the application of a higher *X*-ray tube current, which provides a more favourable contrast-to-noise ratio. Especially small, non-calcified plaques remain undetected when image noise becomes more apparent.

We evaluated the presence of coronary plaques in all available ≥2mm coronary segments (according to the AHA classification) and classified plaques into calcific, non-calcific and mixed [4-8]. It was of interest to note that one-third of the plaques were non-calcific and that around 40% of plaques consisted of non-calcific tissue while 25% of the plaques were predominantly calcific. Non-calcific plaques may consist of lipid core or fibrous tissue. Preliminary in-vivo studies suggested that plaques with predominantly lipid or fibrous tissue could be distinguished on the basis of tissue density differences (in Hounsfield units) with MSCT when comparing these tissue density values (low, moderate) with the degree of tissue echogenicity (hypo- or hyper-echogenicity) with ICUS [3,5,7,8]. However, classification of non-calcified plaques is limited by high intra-plaque variability in density values within a single plaque, which makes it difficult to reliably distinguish between lipid and fibrous plaque tissue. Furthermore, the distinction between different plaque tissues on the basis of density values is hampered due to partial voluming and interpolation, which may improve when scanners with higher spatial resolution become available [11].

The plaque extent and distribution was almost similar in stable and unstable patients, but we found significantly more non-calcified plaques in patients with unstable vs. stable angina pectoris. This observation is in line with the results presented by Leber *et al.* who found significantly more non-calcified plaques in patients with acute myocardial infarction when compared to patients with stable angina pectoris[12]. However, these findings should not be interpreted that patients with more calcific plaques are less vulnerable, or that a calcific plaque is stable.

We also demonstrated that coronary plaques were most frequently located in the proximal and mid-segments of the large coronary arteries (LAD, LCX, and RCA) as also has been demonstrated in earlier pathologic and ICUS studies.

In addition to previous studies, we evaluated the angiographically appearance of coronary plaques detected by MSCT. We found that coronary atherosclerosis was present in one third of angiographically normal coronary arteries indicating that MSCT is able to detect earlier stages of coronary artery disease when compared to conventional coronary

angiography. More specifically, plaques without encroachment of the coronary lumen due to compensatory outward remodeling of the vessel wall thereby alleviating the reduction of lumenal size (known as "positive remodeling") remain undetected by conventional angiography, but have been associated with acute coronary syndromes.

Our study indicates that the assessment of the MSCT coronary plaque burden provides important information regarding the presence and extent of coronary atherosclerosis in patients with stable and unstable angina pectoris. Further prospective studies are needed to determine whether the assessment of the MSCT coronary plaque burden has prognostic value in search of patients at risk of future cardiac events.

LIMITATIONS

We studied a relatively small patient population and included patients with a low and regular heart rhythm, which are variables of high-quality MSCT imaging. It should be noted that in our study the diagnostic performance of MSCT was compared to the presence of a coronary plaque that had a minimum plaque thickness of 1 mm as determined with ICUS, excluding smaller plaques from the analysis. Although these plaques were not associated with significant coronary lumen obstructions, these plaques should be classified as advanced plaques according to the pathological classification described by Stary[13]. To evaluate the coronary plaque burden we demonstrated that MSCT did not detect plaques in 28% of the segments that showed small angiographic wall abnormalities. In addition we noted a lower sensitivity for the detection of predominantly non-calcific plaques. These findings suggest that MSCT cannot detect the earlier stages of coronary atherosclerosis, which are associated with smaller sized, non-calcific plaques. Ideally a new technique should be able to quantify the plaque size using computed assisted contour detection algorithms. Current spatial resolution of MSCT does not allow accurate plaque volume assessment [6] and seriously hinders the reliability of contour detection software. The presence of partial volume and blooming artefacts result in overestimation of the size of calcific plaques and may mask adjacent non-calcific plaque tissue. A serious concern is the high radiation exposure during MSCT coronary angiography, which is estimated between 11.8-16.3 mSv (male/female) using this scan protocol. Radiation exposure can be reduced by technical adjustments such as prospective *X*-ray tube current modulation, which limits the radiation exposure by nearly 50% in patients with low heart rates. However, we did not apply this feature because it limits reconstruction of images during the early-diastolic phase, which can be of importance for evaluation of the RCA [1]. The high radiation exposure poses serious limitations in the application of MSCT coronary angiography for the assessment of progression or regression of coronary atherosclerosis, especially in asymptomatic patients.

REFERENCES

1. Mollet NR, Cademartiri F, Krestin GP, et al. Improved Diagnostic Accuracy With 16-row Multislice CT Coronary Angiography. J Am Coll Cardiol 2005; 45:128-132.
2. Kuettner A, Beck T, Drosch T, et al. Diagnostic accuracy of noninvasive coronary imaging using 16-detector spiral computed tomography with 188 ms temporal resolution. J Am Coll Cardiol 2005; 45:123-127.

3. Schroeder S, Kopp AF, Baumbach A, et al. Noninvasive detection and evaluation of atherosclerotic coronary plaques with multislice computed tomography. J Am Coll Cardiol 2001; 37:1430-1435.
4. Schoenhagen P, Tuzcu EM, Stillman AE, et al. Non-invasive assessment of plaque morphology and remodeling in mildly stenotic coronary segments: comparison of 16-slice computed tomography and intravascular ultrasound. Coron Artery Dis 2003; 14:459-462.
5. Becker CR, Nikolaou K, Muders M, et al. Ex vivo coronary atherosclerotic plaque characterization with multi-detector-row CT. Eur Radiol 2003; 13:2094-2098.
6. Achenbach S, Moselewski F, Ropers D, et al. Detection of calcified and noncalcified coronary atherosclerotic plaque by contrast-enhanced, submillimeter multidetector spiral computed tomography: a segment-based comparison with intravascular ultrasound. Circulation 2004; 109:14-17.
7. Leber AW, Knez A, Becker A, et al. Accuracy of multidetector spiral computed tomography in identifying and differentiating the composition of coronary atherosclerotic plaques: a comparative study with intracoronary ultrasound. J Am Coll Cardiol 2004; 43:1241-1247.
8. Nikolaou K, Becker CR, Muders M, et al. Multidetector-row computed tomography and magnetic resonance imaging of atherosclerotic lesions in human ex vivo coronary arteries. Atherosclerosis 2004; 174:243-252.
9. Austen WG, Edwards JE, Frye RL, et al. A reporting system on patients evaluated for coronary artery disease. Report of the Ad Hoc Committee for Grading of Coronary Artery Disease, Council on Cardiovascular Surgery, American Heart Association. Circulation 1975; 51:5-40.
10. De Winter SA, Hamers R, Degertekin M, et al. Retrospective image-based gating of intracoronary ultrasound images for improved quantitative analysis: the intelligate method. Catheter Cardiovasc Interv 2004; 61:84-94.
11. Schroeder S, Flohr T, Kopp AF, et al. Accuracy of density measurements within plaques located in artificial coronary arteries by X-ray multislice CT: results of a phantom study. J Comput Assist Tomogr 2001; 25:900-906.
12. Leber AW, Knez A, White CW, et al. Composition of coronary atherosclerotic plaques in patients with acute myocardial infarction and stable angina pectoris determined by contrast-enhanced multislice computed tomography. Am J Cardiol 2003; 91:714-718.
13. Stary HC. The Histological Classification of Atherosclerotic Lesions in Human Coronary Arteries. In: Fuster V, Ross R, and Topol J, editors. Atherosclerosis and coronary artery disease. Philadelphia: Lippincott-Raven Publishers, 1996:463–474.

Chapter 14

Influence of Intracoronary Attenuation on Coronary Plaque Measurements Using Multislice Computed Tomography: Observations in an Ex Vivo Model of Coronary Computed Tomography Angiography

Abstract

Assessment of attenuation (measured in Hounsfield units, HU) of human coronary plaques was performed using multislice computed tomography (MSCT) in an ex vivo model. In three ex vivo specimens of left coronary arteries in oil, MSCT was performed after intracoronary injection of four solutions of contrast material (400 mgI/ml iomeprol). The four solutions were diluted as follows: 1/∞, 1/200, 1/80, and 1/20. All scans were performed with the following parameters: slices/collimation 16/0.75 mm, rotation time 375 ms. Each specimen was scored for the presence of atherosclerotic plaques. In each plaque the attenuation was measured in four regions of interest for lumen, plaque (non-calcified thickening of the vessel wall), calcium, and surrounding (oil surrounding the vessel). The results were compared with a one-way analysis of variance test and were correlated with Pearson's test. There were no significant differences in the attenuation of calcium and oil in the four solutions. The mean attenuation in the four solutions for lumen (35±10, 91±7, 246±18, 511±89 HU) and plaque (22±22, 50±26, 107±36, 152±67 HU) was significantly different between each decreasing dilution (p<0.001). The mean attenuation of lumen and plaque of coronary plaques showed high correlation, while the values were significantly different (r=0.73; p<0.001). Intracoronary attenuation modifies significantly the attenuation of plaques assessed with MSCT.

Filippo Cademartiri[1]
Nico R. Mollet[1,2]
Giuseppe Runza[3]
Nico Bruining[2]
Ronald Hamers[2]
Pamela Somers[4]
Michiel Knaapen[4]
Stefan Verheye[5]
Massimo Midiri[3]
Gabriel P. Krestin[1]
Pim J. de Feyter[1,2]

Departments of Radiology[1] and Cardiology[2],
Erasmus MC,
University Medical Center Rotterdam,
The Netherlands
Departments of Radiology[3],
University of Palermo,
Palermo, Italy
Departments of Pathology[4] and Cardiology[5],
Middelheim Hospital,
Antwerp, Belgium

European Radiology
(in press)

INTRODUCTION

Several studies reported that atherosclerotic plaque composition and morphology are important predictors of plaque stability and clinical behaviour when compared with the degree of vessel stenosis[1–3].

Quantitative and qualitative information (e.g. lumen diameter, wall thickness, and morphology) can be obtained using intracoronary ultrasound (ICUS), which has been approved by Food and Drug Administration as the standard for the in vivo evaluation of coronary plaques [4–6]. This technique cannot be used for routine evaluation of plaque characteristics because of its invasiveness and cost.

Several non-invasive techniques have been tested for the visualisation and characterisation of coronary plaques. Preliminary reports using magnetic resonance imaging have reported the ability to detect and characterise the lipid pool in atherosclerotic plaques at the level of the carotid arteries[7], and in the coronary arteries [8–10].

Multislice computed tomography (MSCT) coronary angiography has showed good potential in the detection, quantification, and characterisation of coronary artery plaques[11–16]. Nevertheless, several aspects concerning the methodology for the assessment of coronary plaques with MSCT coronary angiography remain unexplored. With this study we address the issue of the variability of coronary plaque attenuation as measured with MSCT in an ex vivo model with varying intracoronary attenuation.

MATERIALS AND METHODS

Specimens

Three left coronary arteries were dissected during autopsy. The dissected arteries were sampled 1 cm proximal to the bifurcation of the LCx and covered a length of 4 cm. For orientation the anterior side of the arteries was inked in black and the left side of the artery in green. Two patients (both males, with ages of 78 and 63 years) died of non-cardiovascular diseases. One patient (female, with an age of 73 years) died of ischemic heart disease. The study was approved by the Medical Committee of the Middelheim Hospital.

The specimens were prepared and scanned separately. Each specimen was prepared with two sheaths. The sheaths were introduced and fixed at the proximal end (in the left main coronary artery) and at the distal end (in the anterior descending artery) of the specimens. The left circumflex was, previously, closed at its end with a wire.

Contrast material

Four saline solutions with decreasing dilution of contrast material (400 mgI/ml iomeprol, Bracco, Italy) were used: 1/∞, 1/200, 1/80, and 1/20. The attenuation values (Hounsfield units, HU) of the four solutions obtained in a 10-ml syringe after dilution were 3.2 ± 4.5 HU (1/8; defined as saline; no contrast material was diluted), 144.7 ± 8.6 HU (1/200; defined as low), 298.4 ± 3.4 HU (1/80; defined as medium), and 588.0 ± 6.0 HU (1/20; defined as high).

Experimental settings

The experimental settings included a box that was filled with vegetable oil. Prior to positioning the specimen in the oil, saline was instilled through the sheaths to wash out as much as possible.

The specimens were put into oil as a means of simulating the epicardial fat. Once the specimen had sunk into the oil, the solution was injected through the sheath using a 10-ml syringe from the sheath positioned at the proximal end of the specimen. The injection was finished when the solution was observed leaking out of the specimen. The leaking solution was removed from the specimen using an empty syringe. The specimen was not mobilised between the scans.

Scan parameters

A MSCT scan (Sensation 16, Siemens, Germany) was performed after intracoronary injection with increasing concentration of contrast material. After each scan the coronary arteries were washed out with saline before the injection of the following solution and the leaking solution was removed from the specimen using an empty syringe.

All scans were performed with the following parameters: slices/collimation 16/0.75 mm, rotation time 375 ms, feed/rotation 3.0 mm (pitch 0.25), 120 kV, 400 mAs, effective slice thickness 1 mm, reconstruction increment 0.5 mm, field of view (FOV) 100 mm, convolution filter medium smooth (B30f). The scan geometry was based on a retrospective ECG gated protocol (the same used for in vivo MSCT coronary angiography). This protocol is based on a low pitch that allows a retrospective reconstruction of multiple phases within the cardiac cycle. In this case, a demo ECG was switched on and the scan was performed as if the heart rate was 71 beats per minute. The reconstruction algorithm uses 180° of rotation, bringing the effective temporal resolution down to 187 ms.

Data preparation

In order to analyse the specimen with the same settings an experienced operator loaded the datasets into a dedicated workstation (Leonardo, Siemens, Germany) and performed a stack of orthogonal views in each solution for all the specimens with the following parameters: slice thickness 1 mm, increment 0.5 mm, FOV 50 mm.

Data collection

One observer performed all the measurements. Each specimen was evaluated for the presence of coronary atherosclerotic plaques. A coronary atherosclerotic plaque was defined as a thickening of the coronary wall clearly distinguished from the surrounding hypo-attenuating oil and from the lumen after injection of the solution with the lowest dilution of contrast material (e.g. high). Plaques where targeted regardless of their size.

The operator loaded the four datasets for each dilution of the same specimen onto a workstation screen divided 2×2, scrolling the datasets in parallel with standard window settings (window width 700 HU; window centre 140 HU). Once a plaque had been detected in the four solutions, the operator drew four regions of interest (ROIs) for contrast material in the lumen of the vessel (defined as lumen), the soft tissue of the coronary plaque (defined as plaque), the calcification within the coronary artery wall (defined as calcium), and the oil immediately surrounding the plaque (defined as surrounding). These four ROIs were defined as structures. The first drawing of the ROI was performed in the dataset with the lowest dilution of contrast material because the lumen was easier to identify. The ROIs were drawn as large as possible but avoiding the borders of each structure in order to limit the effect of interpolation and partial volume on the measurement.

Once the four ROIs of the structures had been drawn the operator could copy and paste the ROIs into the other stacks of images corresponding to different solutions. Therefore, the position of the ROIs was mirrored in each orthogonal slice with a plaque for each solution. The mean attenuation in each ROI was collected.

Statistical analysis

The values of attenuation are presented as means and standard deviations. Statistical evaluation was performed with dedicated software (SPSS 10.1, SPSS, Chicago, IL, USA). The attenuation measurements in each solution within the structure and clustered per structure were compared with a one-way analysis of variance test and were correlated with Pearson's test. For each structure (e.g. lumen, plaque, calcium, and surrounding), the attenuation values obtained in the four solutions were plotted in order to obtain a slope. The mean slope of each structure was tested for significant differences. For all comparisons tested, $p<0.05$ was considered significant.

RESULTS

Overall 109 levels (1-mm apart from each other) containing plaque were measured in the three coronary specimens. At each level four solutions were available (436 slices) and in each slice four ROIs were sampled (1,744 samples). The results are summarised in Table 1.

Table 1. Summary of the attenuation values measured in the different solutions in each slice

	Overall (HU)	Slope	Solutions (HU)			
			Saline	Low	Medium	High
Lumen	223.0 ± 186.5*	153.4 ± 30.7*	35.2 ± 9.7**	90.6 ± 6.7**	246.2 ± 17.8**	511.0 ± 88.7**
Plaque	86.1 ± 71.5*	45.7 ± 25.7*	21.9 ± 22.4**	49.9 ± 26.3**	106.7 ± 35.6**	152.0 ± 67.2**
Calcium	640.7 ± 533.7*	8.0 ± 31.5*	354.1 ± 152.2	343.6 ± 167.7	356.6 ± 150.0	351.3 ± 164.3
Surrounding	-123.9 ± 11.1*	0.9 ± 6.2*	-129.6 ± 6.9	-127 ± 12.2	-122 ± 6.6	-115 ± 7.1
HU Hounsfield units		*p<0.05 **p<0.01				

The mean attenuation obtained for all samples was 223±187 HU for the lumen, 86±71 HU for the plaque, 641±534 HU for the calcium, and -124±11 HU for the surrounding. The values were all significantly different ($p<0.05$).

The mean slopes obtained for all the four structures were: 153±31 for the lumen, 46±26 for the plaque, 8±31 for the calcium, and 1±6 for the surrounding. Values were all significantly different between the structures ($p<0.05$).

The mean attenuations in the four solutions for the four structures are displayed in Table 1 and Fig. 1. The attenuation values of the lumen and of the plaques were significantly different in each 5 structure ($p<0.01$). The attenuation values of the calcium and of the surrounding were not significantly different in each structure ($p>0.05$). After clustering the paired attenuation values obtained for the four structures in all the four solutions the correlation between the structures was good ($r=0.733$) only between the attenuation values of the lumen and the plaque (Table 2, Fig. 2).

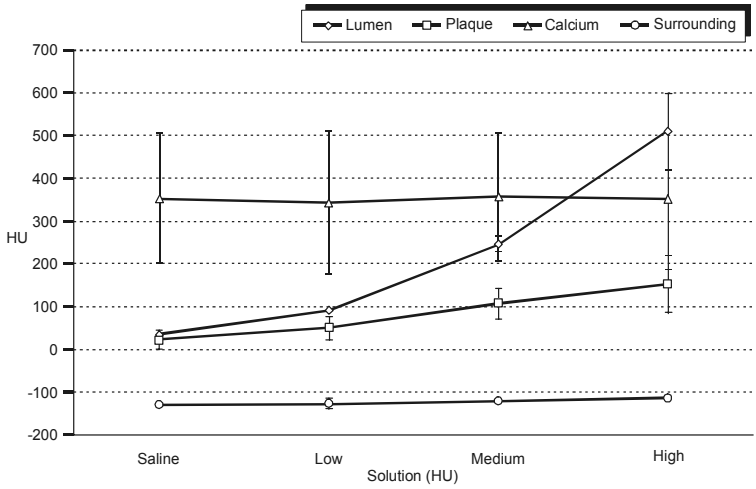

Figure 1. Mean attenuation of the four structures in the four solutions. The increasing attenuation in the lumen affects mainly the attenuation of the plaque. The calcium and the surrounding are, in contrast, almost not affected.

Table 2. Correlation between the clustered attenuation values in each structure

	Lumen vs plaque	Lumen vs calcium	Lumen vs surrounding	Plaque vs calcium	Plaque vs surrounding	Calcium vs surrounding
r	0.733**	0.063	0.106*	0.178**	0.166**	0.060

*p<0.05 **p<0.01

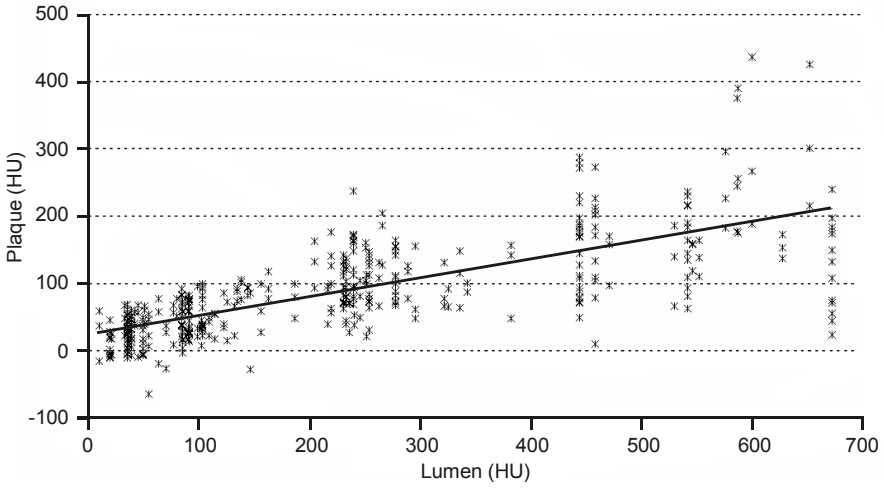

Figure 2. Lumen attenuation versus plaque attenuation. All the attenuation values measured within the lumen and the plaque are plotted. The distribution is clearly linear, demonstrating correlation between the two variables (*r*=0.73).

Discussion

Several studies reported the ability of MSCT to visualise coronary atherosclerotic plaque.[12,14,15,17–20]

An in vivo study by Kopp *et al.*[11] compared MSCT and ICUS in the characterisation of coronary plaques. The plaques were divided for the attenuation values into soft (6±28 and -5±25 HU; two plaques), intermediate (83±17 and 51±19 HU; two plaques) and calcified (489±372 and 423±111 HU; two plaques). The MSCT criteria based on attenuation values showed excellent correspondence with the ICUS criteria.

In an in vivo study, Schroeder *et al.* [12] analysed the composition of 34 plaques by comparing MSCT and ICUS. They found that plaque echogenicity as determined by ICUS corresponds well to plaque attenuation as measured by MSCT.

Leber *et al.*[16] in an in vivo study showed that lesion echogenicity correlates well with MSCT attenuation measurements in coronary plaques. The attenuation values for hypoechoic, hyperechoic, and calcified plaques were 49, 91, and 391 HU, respectively. The MSCT attenuation values reflect the predominant plaque composition (e.g. a plaque with a large lipid core with a low echogenicity on ICUS might be identified on the basis of a low attenuation value).

Becker *et al.* [13] investigated 11 human cadaver heart specimens and compared the atherosclerotic lesions detected by MSCT (n=40) with the histopathological macroscopic characterisation according to American Heart Association criteria. They concluded that MSCT is a promising tool for the characterisation of atherosclerotic coronary lesions. From the literature cited previously, it appears that MSCT can provide data and characterise coronary artery plaques, on the basis of the attenuation values.

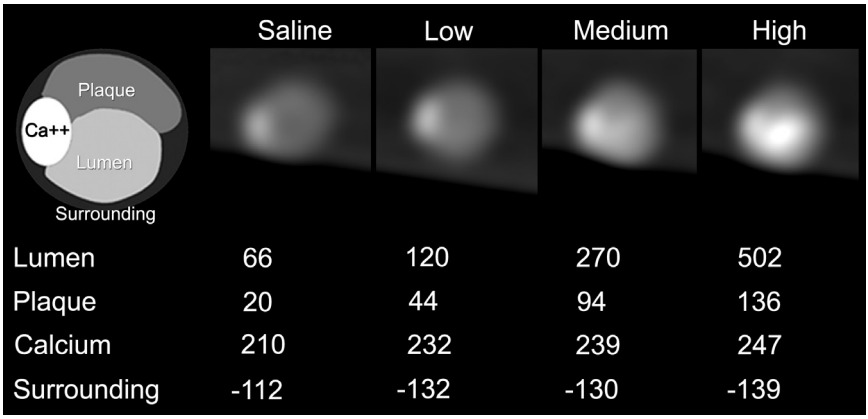

Figure 3. Example of plaque in the four solutions. The scheme in the upper left corner shows the configuration of the plaque in an orthogonal cut performed with multislice computed tomography. The four solutions producing a progressive increase in lumen attenuation are displayed from left to right in the upper part of the figure. Below The relevant attenuations are displayed for every structure.

In a phantom study, Schroeder *et al.* [17] measured the attenuation of two plaques made of rubber material after injection within a tube (simulating a coronary artery) of contrast material of three decreasing concentrations: 1:30 (336 HU), 1:40 (280 HU), and 1:50 (258 HU).

The increased attenuation of the contrast material determined an increase in the measured attenuation of the plaque. Because of this observation we studied the influence of intravascular attenuation on the assessment of coronary plaques with MSCT.

In our experimental study we showed that lumen attenuation measured by MSCT significantly affects the measured plaque attenuation (Fig. 3). The higher the lumen attenuation, the higher the plaque attenuation. Calcium attenuation and surrounding fat attenuation are, in contrast, not significantly affected. On the basis of this finding, it is difficult to identify absolute ranges of attenuation that relate to the specific plaque characteristics.

Several factors and parameters affect the accuracy of the attenuation measurement. Partial volume and interpolation modify the profiles of attenuation in the range of the soft tissues. This is particularly important when there are calcifications in the plaque and contrast material in the lumen in contiguity with the ROI; therefore, absolute plaque attenuation values determined in the various studies are not comparable.

Our observation has a potential impact on the approach to plaque measurements with MSCT. In fact, since the attenuation within the lumen affects the attenuation within the plaque, further studies should probably focus on the relationship between these two variables. On the basis of our results the relationship appears to be close to linear. Thus, a coefficient could be introduced when plaque measurements are performed in order to compare the different studies. One of the most important features of the vulnerable plaque is the lipid core. The usual location of the lipid core within the atherosclerotic plaque is just below the thin cap. This means that it is also very close to the attenuation of the lumen as displayed in MSCT. In this area the attenuation measurements will be affected the most by intravascular attenuation.

There are several limitations in our study. The first one is due to the lack of motion in the specimens. The artefacts derived from the heartbeat were not present and/or reproduced. The second limitation is related to the low number of specimens. Nevertheless, the high sampling rate using cross-sectional views of the vessels balanced this. The third limitation is that an excised coronary specimen does not necessarily represent the reality of a coronary vessel. The third limitation is inherent to the lack of a histopathological correlation. Yet, the aim of our study was not to correlate histopathology with MSCT, but to assess the influence of intracoronary attenuation on overall plaque attenuation measurements. The fourth limitation is that we cannot assume that what was described in our study could be directly transferred to different multislice techniques. The fifth limitation is that we did not investigate the influence of convolution kernels on plaque attenuation. Finally, a moving coronary phantom would provide more realistic information regarding plaque attenuation.

In addition it should be taken into account that the introduction of 64-slice CT systems will probably require an additional optimisation of this methodology. In conclusion, intravascular attenuation modifies significantly the attenuation of the coronary atherosclerotic plaques assessed with MSCT. Therefore, the characterisation of the plaque on the basis of absolute attenuation values should be reported with caution. When plaque attenuation is measured, intraluminal attenuation should also be reported. Probably, a calibration factor will be introduced in the future to address this issue.

References

1. Fuster V, Badimon L, Badimon JJ, Chesebro JH (1992) The pathogenesis of coronary artery disease and the acute coronary syndromes (1). N Engl J Med 326:242–250
2. Fuster V, Badimon L, Badimon JJ, Chesebro JH (1992) The pathogenesis of coronary artery disease and the acute coronary syndromes (2). N Engl J Med 326:310–318
3. Virmani R, Kolodgie FD, Burke AP, Farb A, Schwartz SM (2000) Lessons from sudden coronary death: a comprehensive morphological classification scheme for atherosclerotic lesions. Arterioscler Thromb Vasc Biol 20:1262–1275
4. Stone GW, Hodgson JM, St Goar FG, Frey A, Mudra H, Sheehan H, Linnemeier TJ (1997) Improved procedural results of coronary angioplasty with intravascular ultrasound-guided balloon sizing: the CLOUT pilot trial. Clinical Outcomes with Ultrasound Trial (CLOUT) investigators. Circulation 95:2044–2052
5. Schroeder S, Baumbach A, Haase KK, Oberhoff M, Marholdt H, Herdeg C, Athanasiadis A, Karsch KR (1999) Reduction of restenosis by vessel size adapted percutaneous transluminal coronary angioplasty using intravascular ultrasound. Am J Cardiol 83:875–879
6. Bruining N, Sabate M, de Feyter PJ, Kay IP, Ligthart J, Disco C, Kutryk MJ, Roelandt JR, Serruys PW (1999) Quantitative measurements of in-stent restenosis: a comparison between quantitative coronary ultrasound and quantitative coronary angiography. Catheter Cardiovasc Interv 48:133–142
7. Shinnar M, Fallon JT, Wehrli S, Levin M, Dalmacy D, Fayad ZA, Badimon JJ, Harrington M, Harrington E, Fuster V (1999) The diagnostic accuracy of ex vivo MRI for human atherosclerotic plaque characterization. Arterioscler Thromb Vasc Biol 19:2756–2761
8. Stuber M, Botnar RM, Danias PG, Sodickson DK, Kissinger KV, Van Cauteren M, De Becker J, Manning WJ (1999) Double-oblique free-breathing high resolution three-dimensional coronary magnetic resonance angiography. J Am Coll Cardiol 34:524–531
9. Bunce NH, Pennell DJ (1999) Coronary MRA—a clinical experience in Europe. J Magn Reson Imaging 10:721–727 9
10. Worthley SG, Helft G, Fuster V, Zaman AG, Fayad ZA, Fallon JT, Badimon JJ (2000) Serial in vivo MRI documents arterial remodeling in experimental atherosclerosis. Circulation 101:586–589
11. Kopp AF, Schroeder S, Baumbach A, Kuettner A, Georg C, Ohnesorge B, Heuschmid M, Kuzo R, Claussen CD (2001) Non-invasive characterisation of coronary lesion morphology and composition by multislice CT: first results in comparison with intracoronary ultrasound. Eur Radiol 11:1607–1611
12. Schroeder S, Kopp AF, Baumbach A, Meisner C, Kuettner A, Georg C, Ohnesorge B, Herdeg C, Claussen CD, Karsch KR (2001) Noninvasive detection and evaluation of atherosclerotic coronary plaques with multislice computed tomography. J Am Coll Cardiol 37:1430–1435
13. Becker CR, Nikolaou K, Muders M, Babaryka G, Crispin A, Schoepf UJ, Loehrs U, Reiser MF (2003) Ex vivo coronary atherosclerotic plaque characterization with multi-detector-row CT. Eur Radiol 13:2094–2098
14. Nikolaou K, Sagmeister S, Knez A, Klotz E, Wintersperger BJ, Becker CR, Reiser MF (2003) Multidetector-row computed tomography of the coronary arteries: predictive value and quantitative assessment of non-calcified vessel-wall changes. Eur Radiol 13:2505–2512
15. Achenbach S, Moselewski F, Ropers D, Ferencik M, Hoffmann U, MacNeill B, Pohle K, Baum U, Anders K, Jang IK, Daniel WG, Brady TJ (2004) Detection of calcified and noncalcified coronary atherosclerotic plaque by contrast-enhanced, submillimeter multidetector spiral computed tomography: a segment-based comparison with intravascular ultrasound. Circulation 109:14–17
16. Leber AW, Knez A, Becker A, Becker C, von Ziegler F, Nikolaou K, Rist C, Reiser M, White C,

Steinbeck G, Boekstegers P (2004) Accuracy of multidetector spiral computed tomography in identifying and differentiating the composition of coronary atherosclerotic plaques: a comparative study with intracoronary ultrasound. J Am Coll Cardiol 43:1241–1247

17. Schroeder S, Flohr T, Kopp AF, Meisner C, Kuettner A, Herdeg C, Baumbach A, Ohnesorge B (2001) Accuracy of density measurements within plaques located in artificial coronary arteries by X-ray multislice CT: results of a phantom study. J Comput Assist Tomogr 25:900–906
18. Leber AW, Knez A, White CW, Becker A, von Ziegler F, Muehling O, Becker C, Reiser M, Steinbeck G, Boekstegers P (2003) Composition of coronary atherosclerotic plaques in patients with acute myocardial infarction and stable angina pectoris determined by contrast-enhanced multislice computed tomography. Am J Cardiol 91:714–718
19. Schoenhagen P, Tuzcu EM, Stillman AE, Moliterno DJ, Halliburton SS, Kuzmiak SA, Kasper JM, Magyar WA, Lieber ML, Nissen SE, White RD (2003) Non-invasive assessment of plaque morphology and remodeling in mildly stenotic coronary segments: comparison of 16-slice computed tomography and intravascular ultrasound. Coron Artery Dis 14:459–462
20. Nikolaou K, Becker CR, Muders M, Babaryka G, Scheidler J, Flohr T, Loehrs U, Reiser MF, Fayad ZA (2004) Multidetector-row computed tomography and magnetic resonance imaging of atherosclerotic lesions in human ex vivo coronary arteries. Atherosclerosis 174:243–252

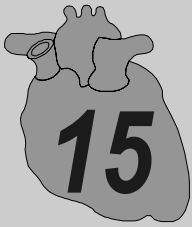

LUMENAL ENHANCEMENT STRONGLY INFLUENCES ABSOLUTE PLAQUE DENSITY ON MULTISLICE COMPUTED TOMOGRAPHY CORONARY ANGIOGRAPHY: IMPLICATIONS FOR PLAQUE CHARACTERISATION

Abstract

OBJECTIVES
To define the effects of intracoronary enhancement on the absolute density values of coronary plaques in vitro and in vivo during Multislice Computed Tomography (MSCT).

BACKGROUND
Preliminary reports indicated that absolute density measurements of non-calcified plaques could be used to identify predominantly lipid or fibrotic plaques.

METHODS
We studied 7 ex-vivo left coronary artery specimens surrounded by olive oil and filled with saline and 4 solutions with decreasing dilutions of contrast material: control (saline), 1/200, 1/80, 1/50 and 1/20. Scan parameters: 16/0.75mm slice/collimation, rotation time 375ms. The attenuation (HU) value of atherosclerotic plaques was measured for each dilution in: lumen, plaque (non-calcified coronary wall thickening), calcium and surrounding oil. In-vivo assessment was performed in 12 patients (males 9; mean age 58.7±9.9) who underwent two scans (arterial and delayed) after intravenous administration of a single bolus of contrast material. The attenuation values of lumen and plaques during the arterial and delayed phase were compared using a one-way ANOVA test and correlated with Pearson's test.

RESULTS
Mean lumen (45±38HU up to 669±151HU) and plaque (11±35HU up to 101±72HU) attenuation differed significantly (p<0.001) among the different dilutions. The attenuation of lumen and plaque of coronary plaques showed moderate correlation (r=0.54; p<0.001). The mean attenuation value in-vivo for the arterial and delayed phase differed significantly (p<0.001) for lumen (325±70HU; 174±46 HU) and plaque (138±71HU; 100±52HU).

CONCLUSIONS
Coronary plaque attenuation values are significantly modified by differences in lumen contrast densities, which should be taken into account when considering the distinction between lipid and fibrous plaques.

Filippo Cademartiri [1,2]
Nico R. Mollet [1,2]
Giuseppe Runza [1,3]
Nico Bruining [2]
Ronald Hamers [2]
Eugene P. McFadden [2]
Timo Baks [1,2]
Pamela Somers [4]
Michiel Knaapen [4]
Stefan Verheye [5]
Massimo Midiri [3]
Gabriel P. Krestin [1]
Pim J. de Feyter [1,2]

Departments of Radiology [1] and Cardiology [2], Erasmus MC, University Medical Center, Rotterdam, The Netherlands.
Department of Radiology [3], University of Palermo, Palermo, Italy.
Departments of Pathology [4] and Cardiology [5], Middelheim Hospital Antwerp, Belgium.

Submitted for publication

INTRODUCTION

Multislice Computed Tomography (MSCT) coronary angiography is a non-invasive imaging technique that has the potential to detect, quantify, and characterize coronary artery plaques [1-5]. Technological advances have led to rapid improvements in spatial and temporal resolution and MSCT is currently a highly sensitive and specific technique that has widespread applicability for the detection of significant coronary lesions. Heavy calcification and irregular heart rhythms are among the last remaining limitations.

Recent advances in interventional cardiology have resulted in improved procedural and long-term results after treatment of atherosclerotic coronary lesions. In parallel, multiple avenues of research have attempted to identify subclinical coronary lesions that may provoke future clinical events with a view to prophylactic intervention. MSCT has the potential to characterize plaque composition (lipid rich, fibrotic, and calcium) based on the different *X*-ray attenuation properties of these tissue components. Indeed, several studies have suggested that absolute density of plaque components, measured in Hounsfield Units, can reliably predict plaque composition.

However, intracoronary contrast attenuation has been shown to affect significantly measured plaque attenuation [6,7]. If this is indeed the case, it has major implications for the use of absolute density to reliably differentiate lipid and fibrous plaques, whose absolute density is within one order of magnitude. We therefore investigated the effect of increasing intracoronary attenuation on the absolute density values of various plaque tissue components lipid, fibrous and calcific in a) an ex-vivo coronary specimen and b) on plaques in a selected group of patients.

MATERIAL AND METHODS

Ex-Vivo Study

Specimens and Intravascular Solutions

Seven human left anterior descending (LAD) coronary arteries were obtained at autopsy. Four subjects were male and three were female. Mean age was 78±10 years. The study protocol was approved by the ethical committee of the Middelheim Hospital (Antwerp, Belgium).

A 3 cm long segment of the LAD was excised from the ostium to the mid-LAD. For orientation, the anterior side of the coronary arteries was marked with black ink and the right side with green ink. The arteries were flushed with phosphate-buffered saline. Then sheaths were introduced and fixed at the proximal and distal end of the specimens and all branches were ligated to produce a watertight circuit.

Five saline solutions with decreasing dilutions of contrast material (iomeprol 400mg/mL) were used: Saline (defined as Control; no contrast material was diluted), 1/200 (defined as low), 1/80 (defined as medium), 1/50 (defined as medium-high), and 1/20 (defined as High).

Experimental Setting

The experimental set-up has been extensively described previously [7]. In short, the arteries were suspended in a box filled with olive oil, after thorough flushing with saline, through the sheaths, to wash out any residual material in the lumen. Immersion in oil was chosen to simulate the presence of epicardial fat.

The various solutions were injected using a 10ml syringe through the sheath at the proximal end of the vessel. The injection was continued until the solution was leaking out of the specimen. Each arterial segment was scanned separately. The arteries were not mobilized between the scans; however, after each scan, the arteries were thoroughly flushed with saline before the injection of the subsequent dilution.

Scan Parameters

MSCT scans were performed with a 16-slice MSCT scanner (Sensation 16, Siemens, Germany). Scan parameters were: slices/collimation 16/0.75mm, rotation time 375ms, feed/rotation 3.0mm (pitch 0.25), kV 120, mAs 400, effective slice thickness 1mm, reconstruction increment 0.5mm, field of view (FOV) 100mm, medium smooth convolution filter (B30f). The scan geometry was based on a retrospective ECG gated protocol (as used for in-vivo MSCT coronary angiography), using a low pitch that allows retrospective reconstruction of multiple phases within the cardiac cycle. A demo ECG was switched on and the scan was performed as if the heart rate was 71bpm. The reconstruction algorithm uses 180° gantry rotation giving an resulting effective temporal resolution of 188ms.

Data Preparation

An experienced operator loaded the datasets into a dedicated workstation (Leonardo, Siemens, Germany) and prepared a stack of images for each imaging procedure on each specimen with the following parameters: slice thickness 1mm, increment 0.5mm, and FOV 50mm. The image plane was always orthogonal to the main longitudinal axis of the vessel.

In-Vivo Study

Study Population

We studied 12 patients (9 male, mean age 58.7±9.9) with stable angina scheduled for diagnostic coronary angiography. Only stable patients in sinus rhythm with a heart rate below 65 bpm, who had never undergone angioplasty or bypass surgery and were able to breath-hold for 20 seconds, were included. Our institutional review board approved the study protocol and all patients gave written informed consent.

Scan Protocol and Image Reconstruction

All scans were performed with the same 16-row MSCT scanner (Sensation16, Siemens, Forchheim, Germany) used for the in vitro experiments. Scan parameters were: 16x0.75 mm detector collimation, rotation time 375 ms, table feed 3.0 mm/rotation, effective temporal resolution 188ms, tube voltage 120 kV, effective mAs 500, effective slice thickness 0.75mm, increment 0.4mm, FOV 100mm, prospective *X*-ray tube modulation. A 100 ml bolus of contrast material (iomeprol 400mg/mL) was injected through an antecubital vein (rate: 4 ml/s). A bolus-tracking technique was used to synchronize the arrival of contrast in the coronary arteries with the initiation of the scan. A first scan (arterial phase) was performed using the bolus tracking synchronisation, while an additional partial scan (delayed phase) was performed immediately after repositioning of the table and re-start of the scan, which required 12 seconds. For both scans the dose was reduced down to 50% using prospective tube current modulation[8]. The estimated radiation exposure for the first scan was 5.9- 8.2mSv (Male-Female). The second scan was performed using the same protocol but with a craniocaudal coverage of only 40mm (1/3 of the average coverage required for a complete coronary angiography) focused on the

proximal segments of the coronary tree. The *X*-ray dose for the second scan was estimated at 1.0-1.9mSv for male and female subjects respectively.

ECG-gated images were reconstructed during mid-to-end diastole to obtain optimal image quality. Additional reconstruction windows were explored when deemed necessary. Generally, the best image quality was obtained when the reconstruction windows were positioned -350 ms before the next R-wave, or at 60% of the R-R interval.

DATA ANALYSIS

Data Collection

All the measurements were performed by the same observer. Each specimen was evaluated for the presence of coronary atherosclerotic plaques. A coronary atherosclerotic plaque was defined as a thickening of the coronary wall clearly distinguishable from the surrounding hypo-attenuating oil as well as from the lumen after injection of the solution with the lowest dilution (i.e. highest enhancement) of contrast material.

The operator loaded the 5 datasets of each dilution of the same specimen onto a workstation screen scrolling the datasets in parallel with standard window settings (window width= 700HU; window center = 140HU). When a plaque was detected, the operator manually defined 4 regions of interest (ROIs):

1) the contrast material in the lumen of the vessel (defined as lumen),
2) the soft tissue of the coronary plaque (defined as plaque),
3) the calcification within the coronary artery wall (defined as calcium), and
4) the oil immediately surrounding the plaque (defined as surrounding).

These 4 ROIs were classified as structures (Figure 1).

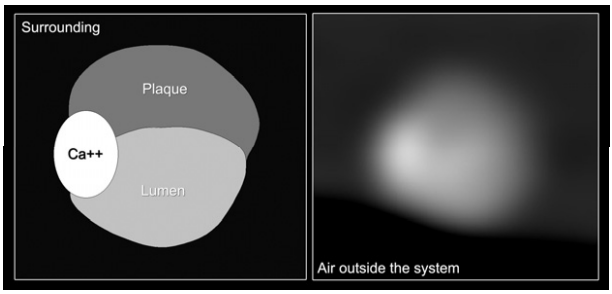

Figure 1. Scheme of the measurements. The figure shows a scheme (left panel) of a cross-sectional view of an ex-vivo coronary plaque that is displayed on the right panel with mutislice CT. The 4 different structures that have been measured (i.e. lumen, the plaque, the calcium, and the surrounding) are displayed.

The first determination of a ROI was performed in the dataset with lowest dilution of contrast material as the lumen was easier to identify. The largest possible ROI was defined but care was taken to ensure that the ROI chosen did not cross the borders of each structure in order to limit the effect of interpolation and partial volume on the measurement. Once the 4 ROIs of the structures were determined the operator copied and pasted the ROIs into the other stacks of images obtained after injection of different concentrations of contrast. The mean attenuation in each ROI was determined.

Statistical Analysis

The values of attenuation are presented as means and standard deviations. Statistical evaluation was performed with SPSS 10.1 (SPSS Inc., Chicago, Illinois, USA). The attenuation measurements in each solution within the structure and clustered per structure were compared with one-way ANOVA–test and correlated with Pearson's test. For each structure (lumen, plaque, calcium, and surrounding), the attenuation values obtained in the 5 solutions were plotted to obtain a slope. The mean slope of each structure was tested for significant differences with a one-way ANOVA–test. For all tested comparisons a $p<0.05$ was considered significant.

RESULTS

EX-VIVO Study

Five hundred plaques were available for analysis. In each plaque measurements at 5 dilutions were available (2.500 slices) and within each slice 4 ROIs were sampled (10.000 samples). The results are summarized in Table I.

Table 1.

				Solutions (HU)				
		Overall (HU)	Slope	Control	Low	Medium	Medium-high	High
Structures	Lumen	248.5±246.8**	148.5±36.1**	45.0±38.0**	85.3±38.2**	121.0±37.5**	322.1±103.5**	669.1±151.0**
	Plaque	45.2±62.0**	22.1±15.3**	10.5±35.2**	20.3±38.0**	33.6±42.8**	61.3±65.2**	100.5±72.3**
	Calcium	826.0±421.4**	10.4±47.4**	804.7±435.4	818.8±429.4	820.7±438.3	839.7±398.5	846.2±404.2
	Surrounding	−127.5±4.2**	-0.1±1.3**	−127.4±2.5	−127.4±3.0	−127.6±5.1	−127.6±3.3	−127.7±5.9

Summary of the attenuation values measured in the different solutions in each slice (*for p<0.05 and **for p<0.01).
Abbreviations: HU= Hounsfield Units; SD= Standard Deviation.

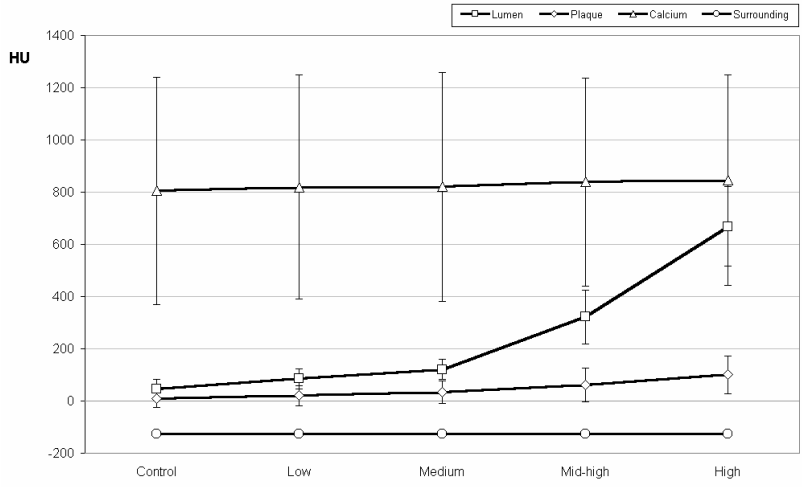

Figure 2. Plot of the mean attenuation of the 4 categories ex-vivo. The plot shows how the increasing attenuation in the lumen affects mainly the attenuation of the plaque. The calcium and the surrounding are, instead, not affected.

The mean attenuation obtained for all samples was: 249±247HU for the lumen, 45±62HU for plaque, 826±421HU for calcium, and -128±4HU for the surrounding oil. These values differed significantly ($p<0.001$). The mean slopes obtained for all 4 structures also differed significantly ($p<0.001$) and were: 149±36 for the lumen, 22±15 for plaque, 10±47 for calcium, and 0±1 for the surrounding oil.

The mean attenuation of the 4 structures for the 5 contrast dilutions studied are presented in Table I and Figure 2. The attenuation values of the lumen and of the plaques differed significantly among dilutions ($p<0.001$). In contrast, the attenuation values for calcium and for the surrounding oil did not differ significantly among dilutions ($p>0.05$). After clustering the paired attenuation values obtained for the 4 structures at all 5 dilutions the correlation between the structures was moderate ($r=0.54$; $p<0.001$) only for the attenuation values of the lumen and the plaque (Table II and Figure 3).

Table 2.

	Lumen vs. Plaque	Lumen vs. Calcium	Lumen vs. Surrounding	Plaque vs. Calcium	Plaque vs. Surrounding	Calcium vs. Surrounding
r	0.541**	0.032	0.013*	-0.015	0.038	0.230**

Correlation between the clustered attenuation values in each structure (*p<0.05; **p<0.01).

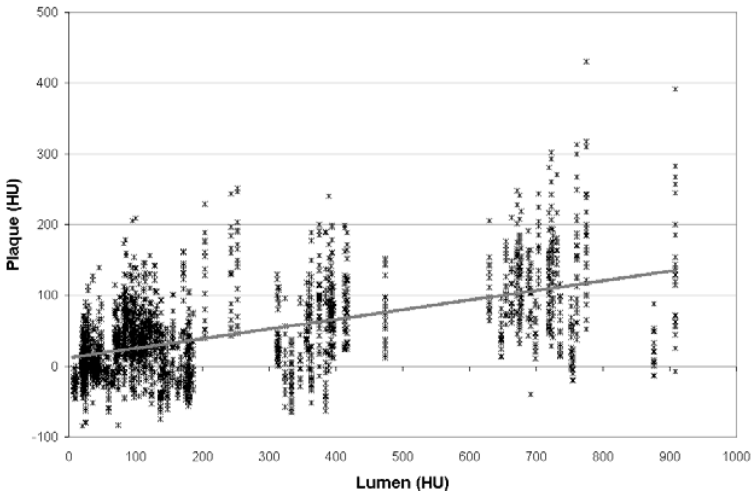

Figure 3. Lumen attenuation vs. plaque attenuation ex-vivo. All the attenuation values measured within the lumen and the plaque are plotted. The distribution is clearly linear demonstrating a moderate but significant correlation between the two variables (r= 0.54; p<0.01).

In Vivo Study

All double scans were completed successfully. No adverse reactions to the iodinated contrast material were recorded. The mean delay of the arterial scan was 19.2±2.5s and of the delayed scan was 50.1±4.5s. The mean heart rate during the arterial scan was 54.6±5.3s and during the delayed scan was 57.4±7.3s ($p<0.01$). The mean scan time was 17.2±1.0s.

Fifty plaques were available for analysis. For each plaque 2 scans were available (100 slices) and in each slice 4 ROIs were sampled (400 samples). The results are summarized in Table III. The mean attenuation obtained for all samples was: 294±96HU for the lumen, 119±65HU for plaque, 572±203HU for calcium, and -97±28HU for the surrounding (p<0.001). The mean slopes obtained for all the 4 structures were: 152±71 for the lumen, 39±42 for plaque, 12±44 for calcium, and 5±31 for the surrounding (p<0.001).

Table III

				Scan (HU)	
		Overall (HU)	Slope	Arterial	Delayed
Structure	Lumen	294.4±96.2**	151.7±70.9**	325.3±69.5**	173.6±46.0**
	Plaque	119.0±65.0**	38.6±41.8**	138.3±71.2**	99.7±52.1**
	Calcium	571.9±203.0**	11.9±43.9**º	577.9±206.7	566.0±201.6
	Surrounding	−96.6±28.3**	5.2±30.8**º	−94.0±23.9	−99.2±32.1

Summary of the attenuation values measured in the different solutions in each slice
(*for p<0.05 and **for p<0.01;**ºfor p<0.01 except the other highlighted with the same mark).
Abbreviations: HU= Hounsfield Units; SD= Standard Deviation.

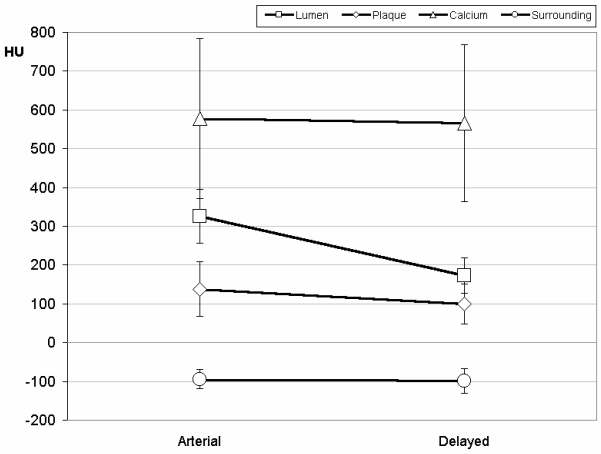

Figure 4. Plot of the mean attenuation of the 4 structures in-vivo. The plot reproduces the observation ex-vivo (Figure 2). In the arterial scan, when intracoronary attenuation is significantly higher, the attenuation of the plaque results also significantly higher when compared to the delayed scan. The calcium and the surrounding are, instead, not affected as already observed ex-vivo (Figure 2).

The mean attenuation in the 2 scans for the 4 structures is displayed in Table III and Figure 4. The attenuation values for lumen and plaque were significantly different (p<0.001). In contrast, the attenuation values for calcium and for the surrounding did significantly (p>0.05).

After clustering the paired attenuation values obtained from the 4 structures during both scans the correlation between the structures was moderate (r=0.40; p<0.001) only for the attenuation values of lumen and plaque (Table IV and Figure 5).

Table IV

	Lumen vs. Plaque	Lumen vs. Calcium	Lumen vs. Surrounding	Plaque vs. Calcium	Plaque vs. Surrounding	Calcium vs. Surrounding
r	0.395**	0.004	0.136	0.101	0.230	-0.031

Correlation between clustered attenuation values in each structure (*p<0.05; **p<0.01).

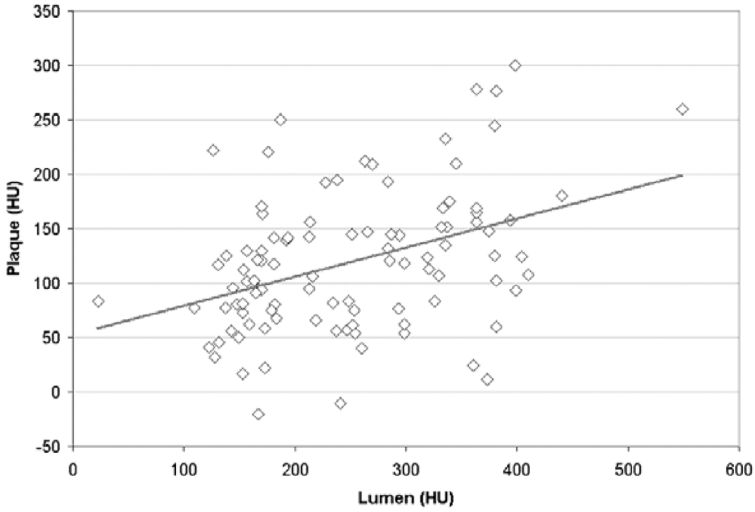

Figure 5. Lumen attenuation vs. plaque attenuation in-vivo. As observed ex-vivo (Figure 3), there is a moderate but significant correlation between the attenuation values measured within the lumen and the plaque (r= 0.395; p<0.01).

Discussion

Several studies have examined the potential of MSCT to visualize non-critical coronary atherosclerotic plaque[1,3-6,9-11]. The reported sensitivity of MSCT for the detection of non-calcific components of coronary artery plaques was lower (53-78%) than that for mixed (78%) or calcified (94-95%) plaques, as compared to ICUS[4,5]. The use of MSCT for noninvasive characterization of coronary plaques has also been reported. Schroeder *et al* analyzed the composition of 34 coronary plaques on MSCT using ICUS as a reference [1]. The mean attenuation values for hypoechoic, hyperechoic, and calcific plaques on ICUS were 14HU, 91HU, and 419HU, respectively on MSCT. In another study, Leber *et al* studied 68 coronary vessels with MSCT and ICUS and found that the mean attenuation values for hypoechoic, hyperechoic, and calcific plaques on ICUS were 49HU, 91HU, and 391HU, respectively on MSCT[5].

Plaque echogenicity as determined by ICUS corresponded well to plaque attenuation as measured by MSCT[1,5]. The MSCT attenuation values, thus, are presumed to reflect the dominant plaque composition (e.g. plaques with a large lipid core with a low echogenicity on ICUS might be identified on the basis of low attenuation value).

While the data suggest that MSCT may distinguish between lipid, fibrous and calcific tissue, there appears to be overlap between the density values for the different tissues.

In a coronary artery phantom study, Schroeder *et al* measured the attenuation of two plaques of rubber material with three decreasing concentrations of intra-luminal contrast material. The density of the contrast medium in the lumen significantly affected density measurements within the plaque. The higher the concentration of contrast medium in the lumen, the higher were the density measurements within the plaque [6]. The same observation was made in a preliminary ex-vivo study using a similar experimental set-up as present study [7].

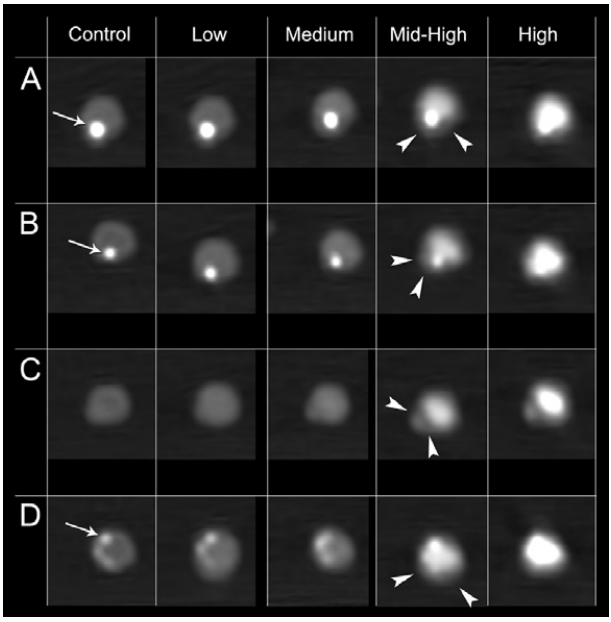

Figure 6 (left). Example of ex-vivo coronary arteries. Five (A-D) cross-sections of ex-vivo coronary plaques with progressively increasing intracoronary attenuation (left to right). The presence of calcium is clearly visible when intracoronary attenuation is Low for all samples (A-D; arrows). The lumen instead, becomes clearly visible only when intracoronary attenuation is Medium or Mid-High (average attenuation: 121±38HU and 322±104HU, respectively). When the intracoronary attenuation is High (average attenuation: 669±151HU), calcium is not anymore sharply distinguishable from the lumen itself. Under these conditions, the plaque is more easily depicted at Mid-High (average attenuation: 669±151HU) intracoronary attenuation for all samples (A-D; arrowheads). The increasing intracoronary attenuation affects the attenuation measurements for plaque and the visualisation.

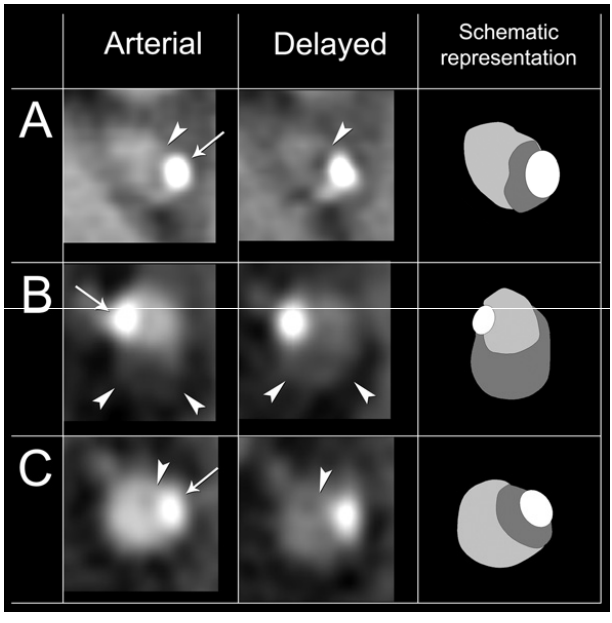

Figure 7 (right). Example of in-vivo coronary arteries. Three (A-C) cross-sections of in-vivo coronary plaques in arterial and delayed phase of contrast enhancement (left to right). A scheme shows the configuration of the several structures displayed (i.e. lumen, the plaque, the calcium, and the surrounding). Even though image quality is deteriorated in-vivo when compared to the experimental settings ex-vivo (Figure 6), the same patterns can be recognized. The presence of calcium (thin arrows – coloured white in the scheme) is usually easier to spot. The lumen (coloured light grey in the scheme) instead is more easily visualised with a higher intracoronary attenuation as it is obtained in the arterial phase. The plaque (arrowheads - coloured dark grey in the scheme) is more easily depicted at higher intracoronary attenuation.

The major finding of our study was the demonstration, both ex-vivo and in-vivo, that lumen attenuation measured by MSCT significantly affects measured plaque attenuation and that this phenomenon is particularly marked in the range of densities encountered for lipid and fibrous plaques (Figure 6 and 7). A higher attenuation in the lumen of the vessel is associated with a progressively higher plaque attenuation for non-calcified plaque components (Figure 8). On the other hand, neither attenuation values for calcium nor for the perivascular surroundings are significantly affected. These findings suggest that the use of absolute attenuation values to identify specific non-calcific plaque characteristics (e.g. lipid core, fibrotic, etc) should be regarded with caution.

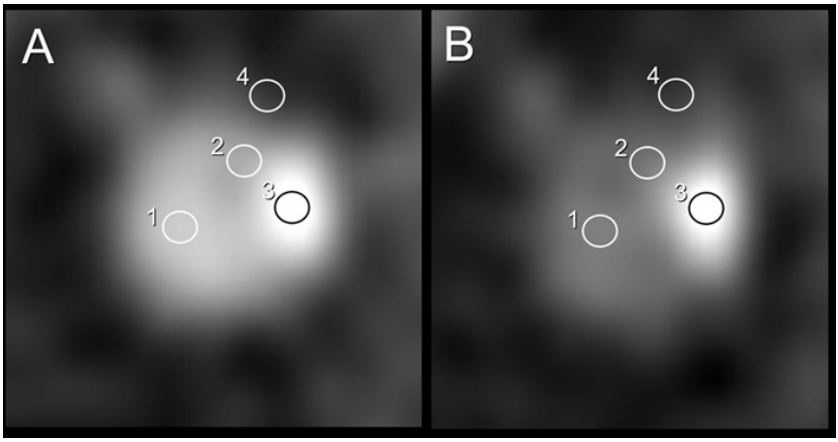

Figure 8. Influence of intra-coronary attenuation on plaque density measurements. The cross-section of a coronary artery is obtained in-vivo in the arterial (A) and delayed (B) phase of contrast enhancement. The regions of interest in A and B indicate the contrast material in the lumen of the vessel (1), the soft tissue of the coronary plaque (2), the calcification within the coronary artery wall (3), and the epicardial fat immediately surrounding the vessel (4). The average density values measured for the calcium (583HU vs. 564HU, respectively) and the epicardial fat (- 84HU vs. -81HU, respectively) are not significantly modified by the modification of density in the lumen (288HU vs. 159HU, respectively). The density of the soft tissue of the plaque, instead, changes from a density value of 98HU (compatible with a fibrous plaque) to a density value of 27HU (compatible with a lipid-rich plaque).

Our findings can readily be explained by reference to the artifacts that characterize CT image acquisition and reconstruction. In particular, partial volume and interpolation modify the profiles of attenuation in areas with sudden changes in attenuation (e.g. at the interface between calcium and plaque or between the contrast filled lumen and plaque). These two artefacts tend to average the attenuation values between two neighbouring voxels. Therefore, a low attenuation structure such as lipid-rich plaque located close to the highly attenuating contrast-enhanced vessel lumen or to a calcific plaque will affect the measured attenuation within each structure. The low-density tissue will appear more dense and the high density structure will appear less dense. The magnitude of this effect depends on both the spatial resolution (e.g. the size of the voxel), and on the convolution kernel (e.g. the algorithm of interpolation).

The observations made by Schroeder *et al* and our own observations may potentially affect the reliability to distinguish between lipid rich plaques and fibrous plaques [6,7]. The attenuation within the lumen affects the attenuation within the lower density plaques,

which requires further studies to more clearly establish the relationship between these two variables. Since partial volume and interpolation affect mainly neighbouring voxels, it might well be that only structures very close to each other are affected and that this effect is less marked or non-existent at a further distance. This would have particular consequences for studies on small plaques, which will be highly affected whereas large plaques would be less affected.

In conclusion, the extent of intracoronary contrast attenuation has a significant effect on the measured attenuation of coronary atherosclerotic plaques with densities, in the lower range, as assessed with MSCT. Therefore, attempts to distinguish such plaques into lipid-rich or fibrous plaque on the basis of absolute attenuation values should be regarded with caution. Further studies are needed to assess, for instance, whether it is possible to apply a correction factor to account for the confounding effects of intra-coronary attenuation on measured plaque density.

References

1. Schroeder S, Kopp AF, Baumbach A, et al. Noninvasive detection and evaluation of atherosclerotic coronary plaques with multislice computed tomography. J Am Coll Cardiol 2001;37:1430-5.
2. Becker CR, Nikolaou K, Muders M, et al. Ex vivo coronary atherosclerotic plaque characterization with multi-detector-row CT. Eur Radiol 2003;13:2094- 8.
3. Nikolaou K, Sagmeister S, Knez A, et al. Multidetector-row computed tomography of the coronary arteries: predictive value and quantitative assessment of non-calcified vessel-wall changes. Eur Radiol 2003;13:2505- 12.
4. Achenbach S, Moselewski F, Ropers D, et al. Detection of calcified and noncalcified coronary atherosclerotic plaque by contrast-enhanced, submillimeter multidetector spiral computed tomography: a segment-based comparison with intravascular ultrasound. Circulation 2004;109:14-7.
5. Leber AW, Knez A, Becker A, et al. Accuracy of multidetector spiral computed tomography in identifying and differentiating the composition of coronary atherosclerotic plaques: a comparative study with intracoronary ultrasound. J Am Coll Cardiol 2004;43:1241-7.
6. Schroeder S, Flohr T, Kopp AF, et al. Accuracy of density measurements within plaques located in artificial coronary arteries by X-ray multislice CT: results of a phantom study. J Comput Assist Tomogr 2001;25:900-6.
7. Cademartiri F, Mollet NR, Runza G, et al. Influence of intracoronary attenuation on coronary plaque measurements using multislice CT: observations in an ex-vivo model of coronary CT angiography. Eur Radiol 2005 (epub ahead of print).
8. Trabold T, Buchgeister M, Kuttner A, et al. Estimation of radiation exposure in 16-detector row computed tomography of the heart with retrospective ECGgating. Rofo 2003;175:1051-5.
9. Leber AW, Knez A, White CW, et al. Composition of coronary atherosclerotic plaques in patients with acute myocardial infarction and stable angina pectoris determined by contrast-enhanced multislice computed tomography. Am J Cardiol 2003;91:714-8.
10. Schoenhagen P, Tuzcu EM, Stillman AE, et al. Non-invasive assessment of plaque morphology and remodeling in mildly stenotic coronary segments: comparison of 16-slice computed tomography and intravascular ultrasound. Coron Artery Dis 2003;14:459-62.
11. Nikolaou K, Becker CR, Muders M, et al. Multidetector-row computed tomography and magnetic resonance imaging of atherosclerotic lesions in human ex vivo coronary arteries. Atherosclerosis 2004;174:243-52.

NEW CORONARY IMAGING IN ACUTE CORONARY SYNDROME

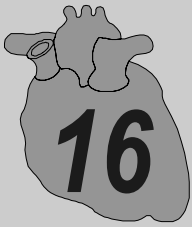

Chapter 16

Introduction

Pim J. de Feyter [1,2]
Evelyn Regar [2]
Nico R. Mollet [1,2]

Departments of Radiology [1] and Cardiology [2], Erasmus MC, University Medical Center, Rotterdam, The Netherlands.

Chapter in: **Acute Coronary Syndromes: a Handbook for Clinical Practice**, Blackwell Publishing (in press).

Atherosclerosis begins early in life. Before the age of twenty half of asymptomatic individuals already have detectable coronary intimal lesions.[1,2] Coronary atherosclerosis progresses relentlessly over years and accounts for more death and disability than any other disease entity in industrialized societies. [3] The progression from asymptomatic atherosclerosis to a high-risk (vulnerable) plaque to a thrombosed plaque causing an acute coronary syndrome (ACS) is to a large extent unravelled. The transition from a high-risk plaque to a thrombosed plaque is often caused by a rupture or erosion of the fibrous cap complicated by thrombosis extending into the coronary lumen.[4-7] The identification of a high-risk (vulnerable) plaque is of great clinical interest, but currently no widely accepted method to prospectively identify the vulnerable plaque is available. Many invasive and non-invasive imaging modalities have emerged that now are capable of identification of some, but not all, specific features of the vulnerable plaque.[8] In this chapter we describe as highly promising non-invasive diagnostic tools Multislice computed tomography (MSCT), Magnetic Resonance Imaging (MRI) and a few invasive intracoronary diagnostic tools that can be used in clinical practice: Optical coherence tomography (OCT), thermography, palpography and intravascular MRI.[9,10]

Definition of vulnerable plaque

Post mortem evaluation has shown that high-risk (vulnerable) plaques have several characteristics: a thin fibrous cap (< 65 μm) a large, lipid-rich pool (> 3 mm^3), often a non or modestly stenotic plaque, and increased macrophage activity (inflammation) and often associated with positive coronary wall remodeling.[4-7] It should be emphasized here that these histologic characteristics of the vulnerable plaque are "indirectly" and in retrospection obtained from plaques that show cap rupture or erosion with thrombus formation. The actual diagnosis of a vulnerable plaque, however, is a prospective diagnosis and implies the occurrence of a future adverse coronary event.

Non-invasive Imaging: Magnetic Resonance Imaging

MRI has emerged as a potential useful tool to image coronary plaques. In the thoracic aorta or carotid arteries the composition of the atherosclerotic plaque (lipid, fibrous, or calcium) can be assessed by using a multiple contrast MRI imaging technique. Accurate measurements of the carotid plaque size and fibrous cap thickness and visualization of the ruptured cap are possible with MRI.[11-15] MRI coronary angiography can detect coronary stenoses in the proximal and mid coronary artery segments but is limited by its inability to image distal epicardial coronary vessels and approximately 15% of the proximal epicardial vessels cannot be assessed due to motion-artefacts[16-18] (Figure 1). Preliminary studies have shown that MRI imaging of coronary plaques is possible, but so far has remained limited to measurements of the coronary wall (including the plaque) thickness[19,20] (Figure 2).

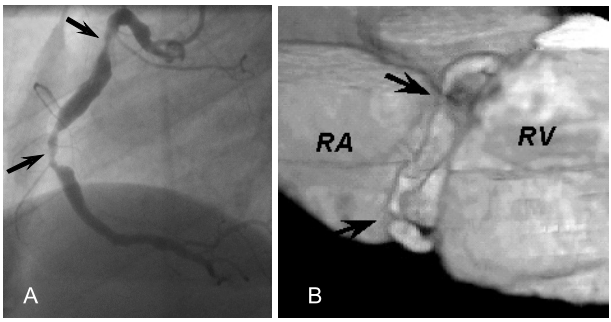

Figure 1. Non-invasive MR-coronary angiography of the right coronary artery (RCA). A: diagnostic invasive coronary angiography of RCA demonstrating 2 significant coronary stenoses (arrows). B: corresponding MR-coronary angiography. RA: right atrium. RV: right ventricular.

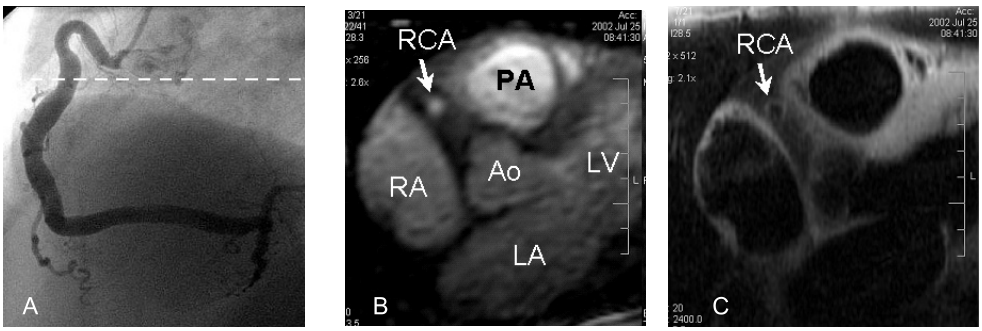

Figure 2. Non-invasive MR-coronary plaque imaging of diseased right coronary artery (RCA).
A: Diagnostic invasive coronary angiography. Dashec line indicated MR-cross-sectional images B,C.
B: MR-coronary angiography using bright blood imaging technique delineating the coronary lumen.
C: MR-coronary angiography using black blood imaging technique showing a thickened coronary wall.

Non-invasive Imaging: CT- Coronary calcium

Electron-beam computed tomography (EBCT) can accurately detect coronary calcium (Figure 3). The coronary artery calcium score (CACS) is related to the overall burden of coronary atherosclerosis [21,22] and can predict adverse coronary events as has been shown in several large-scale long-term studies (Table 1).[23-29]

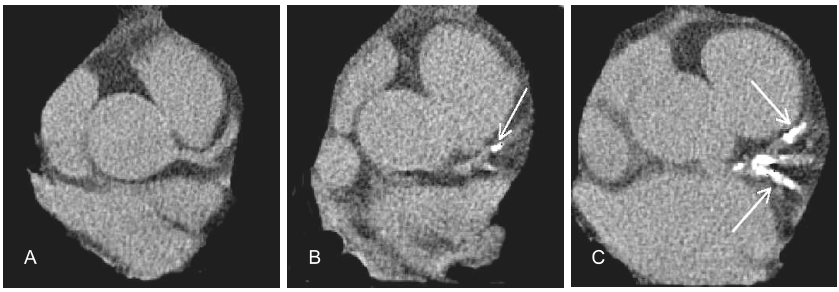

Figure 3. Electron-beam Computed Tomography demonstrating
A: normal left coronary artery
B: mild degree of calcium in left coronary artery
C: high degree of calcium in left coronary artery

Table 1. Coronary calcium to predict adverse cardiac events

Study	N	Mean age (yrs)	Gender (%male)	FUP yrs	Events (death/MI)	Calcium Score cut-off	Risk ratio
Wong	926	54	79	3.3	28	>81-270	4.5*
Arad	1172	53	71	3.7	18	>271	8.8*
Detrano	1196	66	89	3.4	44	>44	2.3*
Raggi	676	52	51	2.7	30	>100	>4.1%**
Kondos	5635	51	74	3.1	222	≥0	Men 10.5 Women 2.6
Shaw	10.377	53	60	5.0	249 (death)	>400-1000 >1000	6.15* 12.3*
Greenland	1029	65.7	90	7.0	84(death,MI)	>300	3.9

* compared to patients with 0 score. ** annualized event rate.

Table 2. Coronary Calcium Score and Risk adjusted mortality rate

Coronary calcium score	Relative risk
11 - 100	1.64 (1.12 , 2.41)
101 - 400	1.74 (1.16 , 2.61)
401 - 1000	2.54 (1.62 , 3.99)
> 1000	4.03 (2.52 , 6.40)

From Shaw *et al.* Radiology 2003;228:826

These studies provide ample evidence that coronary calcium is a predictor of adverse coronary events. The greater the overall calcium burden, which correlates with a greater overall coronary plaque burden, the greater is the likelihood of an adverse event (Table 2).[28]

But calcification of an individual plaque is neither a marker for plaque vulnerability nor for plaque stability. The absence of calcium does not exclude the presence of coronary atherosclerosis but is associated with a low likelihood of advanced coronary atherosclerosis and a very low likelihood of an adverse coronary event.

It would be important to establish that CACS assessment provides predictive information in addition to the predictive value of traditional risk factors or the Framingham risk score. Detrano *et al* showed that CACS offered no additional predictive value[25] but other studies showed that CACS results increased the risk prediction conveyed by traditional risk factors alone.[27,29] Furthermore, Kondos *et al* demonstrated in 5635 asymptomatic self-referred adults who responded to a questionnaire (only 65% of the initial group responded) that CAC provided incremental prognostic information in addition to age and risk factors.[27] And Greenland *et al* demonstrated that the Framingham score in combination with the CACS conveyed an increased risk compared to the Framingham score alone and a CACS score > 300 was more predictive amongst various Framingham risk score categories.[29]

Finally, Shaw *et al* showed in a large study of 10377 asymptomatic individuals that coronary calcium provided independent incremental information in addition to traditional risk factors in the prediction of all cause mortality (Table 2).[28]

Thus CACS can modify the predicted risk obtained from traditional risk factors, especially among patients in the intermediate risk category in whom clinical decision making is most uncertain.[28] Greenland *et al* have suggested to apply calcium quantification in patients with an intermediate risk, based on traditional risk factors.[30] In these patients the calcium score could determine whether they should be regarded as high-risk and receive more intensive therapy, or regarded as low risk (no calcium present) where life-style advice might be sufficient.[30]

Non-invasive Imaging: CT-Coronary plaque imaging

MSCT is able to detect obstructive and non-obstructive coronary plaques and may be useful to identify of the composition the atherosclerotic plaque (Figure 4 and 5).

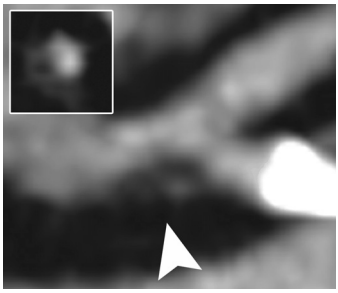

Figure 4 (left). CT-coronary plaque imaging
Maximum intensity projected CT image of the left main coronary artery. The arrowhead indicates the presence of a non-obstructive, predominantly non-calcified plaque located at the distal part of the left main and protruding in the circumflex coronary artery. A cross-sectional multiplanar reconstructed CT image (inlay) provides detailed information regarding the presence of non-calcified (low-density) plaque tissue adjacent to the contrast-enhanced coronary lumen.

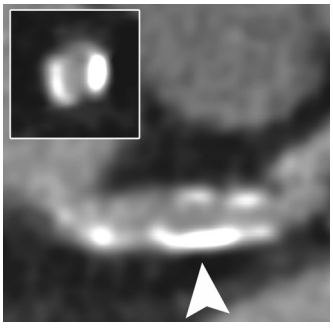

Figure 5 (right). CT-coronary plaque imaging
Maximum intensity projected CT image of the left main coronary artery. The arrowhead indicates the presence of a calcified plaque extending along the entire left main coronary artery. A cross-sectional multiplanar reconstructed CT image (inlay) confirms the presence of calcified (high-density) plaque tissue adjacent to the contrast-enhanced coronary lumen.

Based on the differences in density measurements of the various tissue it appears possible to differentiate between fibrous tissue, lipid and calcium.[31-36] Lipid is a low-density structure, fibrous tissue is an intermediate density structure and calcium is a high-density structure. A very low-density obstruction in the setting of an acute coronary syndrome may represent a thrombotic occlusion.

Schroeder *et al* demonstrated that MSCT density measurements differed significantly between coronary plaques classified as lipid (low echogenicity), fibrous (intermediate echogenicity) or calcified by IVUS, thereby suggesting that MSCT was able to distinguish between lipid, fibrous tissue and calcium.[37] These results were confirmed by the study of Leber *et al* who also compared IVUS determined echogenicity values of plaques with CT-densities and showing that lipid and fibrous tissue could be distinguished by MSCT (Table 3), although there is some overlap between density values of lipid and fibrous tissue.[38] Achenbach *et al* demonstrated that MSCT allowed the identification of positive and negative coronary wall remodelling.[39] The diagnostic accuracy of MSCT to detect coronary plaques compared to IVUS is reasonable good with a sensitivity of 82% to 86% and a specificity of 88% to 92%.[38,39] However, it appears that MSCT seriously underestimates the size of plaque with about 40%.[40] Mollet *et al* assessed the coronary plaque burden with MSCT, which was defined as the number of diseased coronary segments, location of disease, obstructive or non-obstructive plaque and type of plaque (calcific or non-calcific). The results obtained in 41 patients are shown in Figure 6.

Table 3. Plaque composition with contrast-enhanced CT coronary plaque imaging

IVUS	MS CT Schroeder HU ± SD (n=17)	 Leber HU ± SD (n=37)
Hypoechoïc	14 ± 26	49 ± 22
Hyperechoïc	91 ± 21	91 ± 22
Calcified	419 ± 194	391 ± 156

Schroeder JACC 2001;37:1430
Leber JACC 2004;43:1241

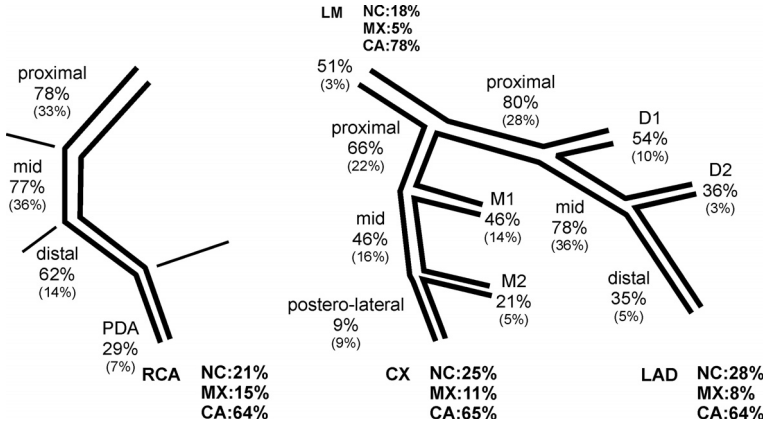

Figure 6. MSCT coronary plaque imaging
Extent, distribution and composition of coronary plaques in the coronary tree. RCA: right coronary artery. Cx: circumflex artery. LAD: left anterior descending artery. LM: Left main. NC: non-calcific plaque. MX: mixed plaque (calcific and non-calcific plaque). CA: calcific plaque.

The role of MSCT to non-invasively detect a vulnerable plaque or to identify a vulnerable patient is currently being evaluated in many studies.

Non-invasive Imaging: CT- Coronary Stenosis

Over the past decade, great strides have been to detect coronary stenoses using computed tomography. The most recent reports about the diagnostic performance concern the 16-multislice CT scanner. The sensitivity and specificity to detect a significant coronary stenosis is high (Table 4) but one should bear in mind that only the larger coronary artery segments (>2mm diameter) were analysed and that in a few reports 6% to 16% of the available segments were excluded from analysis in the majority due to motion artefacts or severe calcification obscuring the lumen.[42-48]

Table 4.

	CT	β	Pop. (n)	D (%)	Excl. (%)	Sens. (%)	Spec. (%)	PPV (%)	NPV (%)
Nieman	12	+	58	50	-	95	86	80	97
Ropers	12	+	77	50	12	92	93	79	97
Kuettner	16	+	60	50	6	72	97	72	97
Mollet	16	+	128	50	-	92	95	79	98
Martuscelli	16	+	64	>50	16	89	98	90	98
Kuettner	16	+	72	>50	6.6	82	98	87	97
Mollet	16	+	51	>50	0	95	98	87	99

Use of betablockers (β);diameter reduction considered significant (D);
Number of stenosed vessels or segments per patient (Prev.);
percentage of excluded segments or branches (Excl.); sensitivity (Sens.), specificity (Spec.),
positive (PPV) and negative predictive value (NPV) regarding the assessable segments or branches.

In a recent report of Mollet *et al*, we also evaluated patients with unstable angina and it appeared that the diagnostic performance was equally high in patients with unstable and stable angina.[47] Current limitations of MSCT are that patients with irregular heart rhythm cannot be evaluated, whereas the rather high radiation exposure with an effective dose ranging of 10 – 12 mSv, is of great concern.

Invasive Diagnostic Tools: Thermography

Coronary atherosclerosis is considered a chronic inflammatory disease and one of the characteristics of a high-risk plaque is the presence of intense inflammatory reaction manifested by the local invasion of macrophages and lymphocytes. Based on these findings the hypothesis was generated that these "activated" macrophages produce thermal energy, which might be detected on the surface of these atherosclerotic lesions. It appeared that the temperature heterogenecity is directly proportional to the degree of histologically detected inflammation.[49,50] Patients with an acute coronary syndrome had higher levels of coronary artery temperature heterogenecity and in a follow-up study these thermographic findings were predictive of an acute adverse coronary event.[51,52] An example of clinical thermography in a coronary artery is given in Figure 7.

Further studies are needed to establish the capability of thermography to identify an individual vulnerable plaque in the coronary arteries and the impact of coronary blood flow on the temperature, with a "cooling" effect of high blood flow, needs to be addressed.[53]

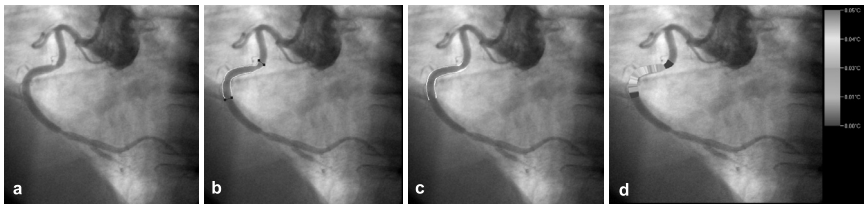

Figure 7(A). Clinical example of intracoronary thermography
a) Coronary angiogram of a mildly diseased right coronary artery with multiple lumen irregularities. **b**) Automated delineation of the vessel wall **c**) and plaque imaging **d**) Collected temperature data on vessel anatomy

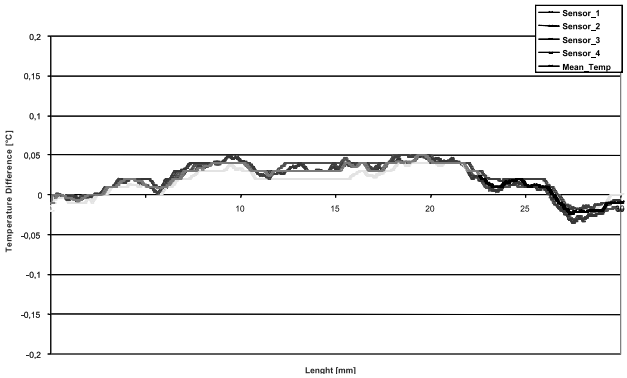

Figure 7(B). Example for the display of intracoronary temperature measurements. The lines indicate the temperature differences between the reference temperature and the temperature measured at the coronary wall by each individual thermistor sensor over the length of the arterial segment. (A full color version of these illustrations can be found in the color section (Chapter 21)).

Invasive Diagnostic Tools: Palpography

Features of the vulnerable plaque are the presence of large a lipid core covered by a rather thin fibrous cap which appeared to have different local mechanical properties as is manifested by a more readily deformation of these plaques compared to adjacent coronary structures. Upon a defined mechanical excitation soft tissue components will deform more (high-strain) than hard components (low-strain).[54] The deformations of structures can be measured by ultrasound. It has been demonstrated in an animal study that the strain pattern is different for fibrous, fibro-fatty and fatty plaques and that a high-strain value (a highly deformable structure) was associated with a fatty plaque and presence of macrophages.[55] The sensitivity and specificity of a high-strain spot to detect a vulnerable plaque as assessed in post-mortem human coronary arteries was 88% and 89% respectively.[56] In-vivo intracoronary palpography is feasible and the finding of high-strain spots is highly reproducible [57,58] (Figure 8). In a recent study it was shown that the number of high-strain spots in the coronary arteries was directly related to the magnitude of instability of patients with the highest number of high-strain spots in patients with an acute myocardial infarction, intermediate in unstable patients and lowest in stable patients.[59] The acquisition of a palpogram can be obtained from a motorized catheter pullback using special IVUS catheters which are commercial available.

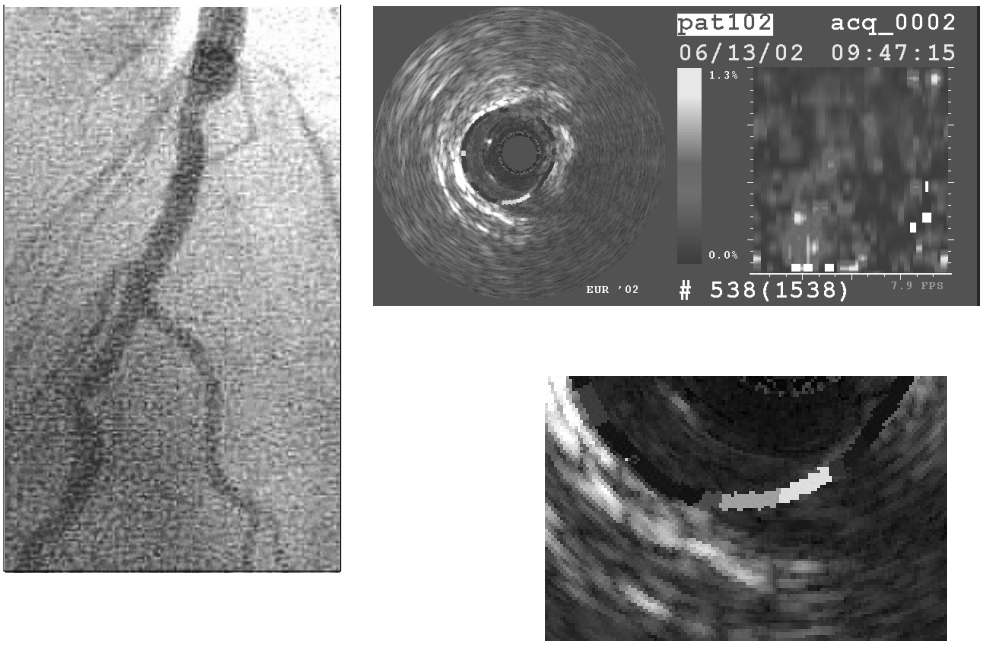

Figure 8. Clinical example of intracoronary palpography. Intravascular ultrasound palpography is assessing the local mechanical tissue properties of the luminal surface of the vessel wall. One strain value per angle lumen circumference is calculated and plotted as color-coded contour at the lumen vessel boundary.(A full color version of this illustration can be found in the color section (Chapter 21)).

Invasive Diagnostic Tools: Virtual Histology

More sophisticated tissue characterization by IVUS can be obtained by use of radio-frequency signal analysis (Figure 9).

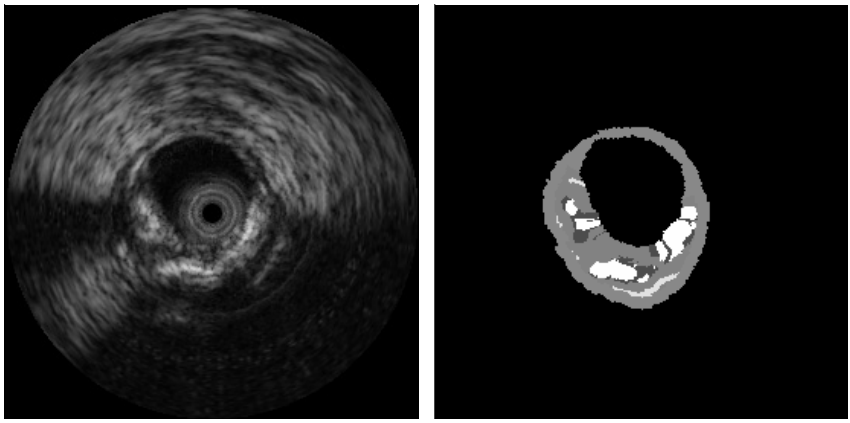

Figure 9. Virtual histology is based on backscatter analysis and mathematical modelling of the radio-frequency signals produced by the intravascular ultrasound unit. Data were used to develop classification schemes, which allow the differentiation between tissue types in regions of interest. Tissue types are assigned color values and overlaid on the tissue maps from IVUS (green= fibrous, yellow=lipid rich, red=lipid core, white= calcium tissue). (A full color version of this illustration can be found in the color section (Chapter 21)).

Virtual histology is based on IVUS backscatter analysis and mathematically modelling of the radio-frequency signal. This allows to differentiate between tissue types: lipid, lipid-fibrous, calcified and calcified necrotic, which has been validated by using ex-vivo histology of human coronary arteries.[60] The data necessary for virtual histology are acquired during an IVUS catheter motorized pullback. Special IVUS catheters are commercially available. The data are displayed as a colour map where the various tissue are represented by various colours. The clinical impact of the radio-frequency analysis of the ultrasound signal needs to be established and several prospective clinical trials are being initiated.

Invasive Diagnostic Tools: Optical Coherence Tomography (OCT)

Optical coherence tomography is an imaging technique that allows for high-resolution (Figure 10) (axial resolution of 15μm) imaging in biological systems.

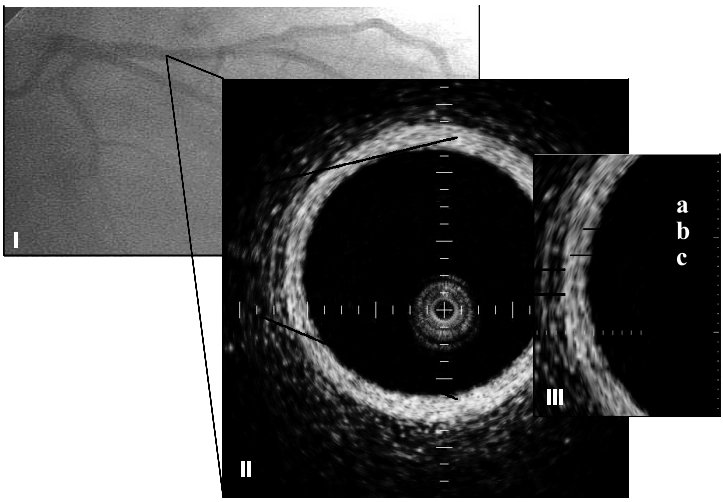

Figure 10. Clinical example of intravascular OCT imaging. I) coronary angiogram of a left descending coronary artery. II) cross-sectional, optical coherence tomography of the coronary artery showing a normal coronary artery with clear demarcation between a highly reflective intimal layer (a), a low-reflective media (b), and a highly reflective adventitial layer(c). (A full color version of this illustration can be found in the color section (Chapter 21)).

The high resolution capacity of OCT might allow for in-vivo real time visualization of a thin fibrous cap, that is present in high risk (vulnerable) plaques. Post-mortem studies demonstrated the accuracy of OCT in comparison to histology.[61-63] Intravascular application of OCT has proven feasible in the animal model. These studies showed, that OCT can detect both, normal and pathological artery structures. Recent experimental data suggest the possibility of detection of macrophages in atherosclerotic plaque in vitro.[64] The first clinical study proved the concept of in-vivo intravascular OCT using a modified IVUS catheter. Ten patients scheduled for coronary stent implantation, with mild moderate coronary lesions, that were remote from the target stenosis, were investigated. Most coronary structures that were detected by IVUS could also been visualized with OCT. Intimal hyperplasia and echolucent regions, which may correspond to lipid pools, were identified more frequently by OCT than by IVUS.[65,66]

We performed a pilot study using a dedicated OCT imaging catheters in patients scheduled for percutaneous coronary intervention. OCT analysis of coronary artery wall was possible in all patients and the entire vessel circumference was visualized at all times (Figure 10,11). A wide spectrum of different plaque morphologies was seen. OCT allowed for differentiation of the normal artery wall of as well as for inhomogeneous, mixed plaques and thin cap fibroatheromas with inhomogeneous, low reflecting necrotic cores, covered by highly reflecting fibrous caps with a thickness of approximately 50μm. Prospective in vivo validation is pending.

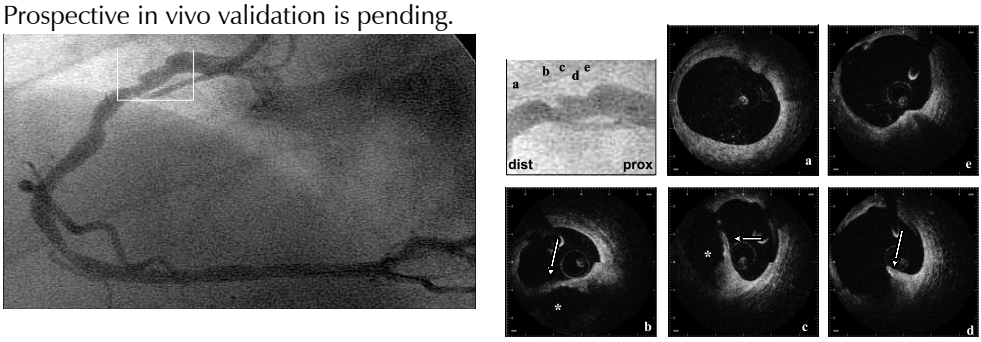

Figure 11. Clinical example of intravascular OCT imaging. I) Angiogram of the right coronary artery showing an exulcerated plaque in the proximal segment. II) Corresponding intravascular OCT imaging showing remnant of the ruptured fibrous cap. a) distal reference segment with circular lumen and eccentric, predominantly fibrous plaque b) distal portion of the lesion showing a fibrous cap that partially separates the true lumen from the neolumen (aterix) c) mid-portion of the lesion: communication between the true lumen and the neolumen (asterix) d) proximal portion of the lesion e) proximal reference showing circular lumen and eccentric fibro-fatty plaque. (A full color version of this illustration can be found in the color section (Chapter 21)).

Invasive Diagnostic Tools: Intravascular MRI

Intravascular magnetic resonance imaging (MRI) is another potential approach to determine plaque composition and locate potential "vulnerable plaques" within human coronary arteries. Hitherto, cardiac and respiratory motion has inhibited intravascular approaches but recent developments have allowed for the development of a self-contained intravascular MRI catheter unencumbered by cardiac motion.

Intravascular MRI can determine the presence of lipid within the arterial wall or, in combination with local delivery of contrast agents, determine the presence of specific cell types associated with plaque instability or thrombus.

The intravascular MRI system has been evaluated in non-atherosclerotic porcine coronary and femoral arteries to test proof of concept and device safety. Ex-vivo human carotid tissue, aortic tissue and coronary arteries were used to correlate MRI findings with histology. In ex-vivo aortic studies the MRI correctly predicting the histologic results in 15 of 16 aortic cases (95% sensitivity, 100% specificity) and in ex-vivo coronary arteries 16 of 18 lesions (89%) were correctly predicted, including the diagnosis of 3 thin cap fibroatheromas. Human safety studies have been initiated in Europe (Figure 12).

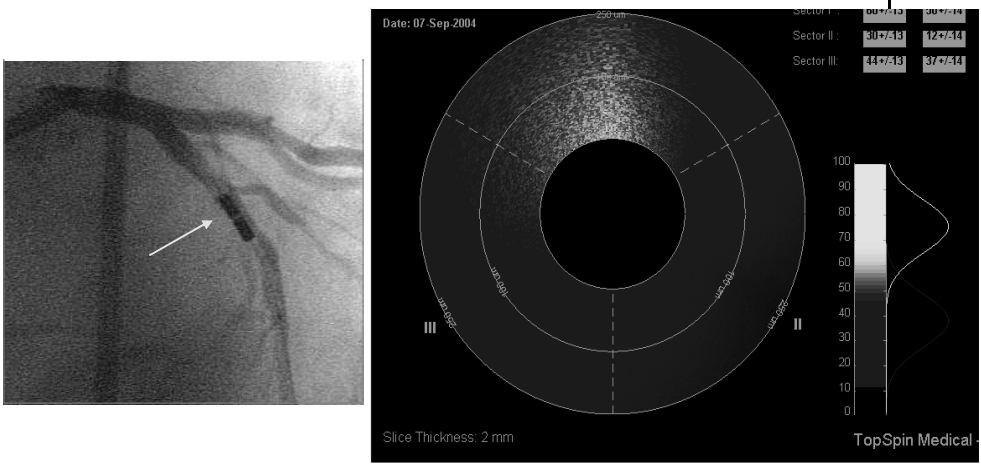

Figure 12. Clinical example of intracoronary MRI. Left: Coronary angiogram showing the intravascular MRI catheter in the proximal left descending coronary artery. Right: Corresponding intracoronary MRI. The vessel circumference is represented in 3-colour coded sectors of 120 degree. Blue colour indicates the predominance of non-lipid tissue, yellow colour indicates the predominance of lipid-rich tissue. In our patient, some lipid rich tissue signal (yellow) is visible in sector I, whereas the other sectors show non-lipid tissue (blue). (A full color version of this illustration can be found in the color section (Chapter 21)).

Conclusion

Non-invasive coronary plaque imaging with MRI and CT is feasible and have the potential to identify a vulnerable plaque but both techniques need substantial improvements before they can be accepted as clinically reliable tools. CT coronary calcium scoring is slowly emerging as a imaging technique that is able to identify high-risk individuals independent of the traditional risk factors. However, further studies are needed in particular in non-self referred individuals, to establish the true predictive value of coronary calcium scoring.
To date, none of the described invasive techniques is validated on a broad basis in-vivo and there is no gold standard available. However, these new modalities have the potential to provide new levels of anatomical detail and new dimensions of information for the diagnosis of coronary artery disease. In the future these technologies have to be validated. Their scientific, clinical and prognostic value needs to be determined and the indications for clinical applications established.

References

1. Strong JP, Malcom GT, McMahan CA, et al. Prevalence and extent of atherosclerosis in adolescents and young adults: implications for prevention from the Pathobiological Determinants of Atherosclerosis in Youth Study. JAMA. 1999 Feb 24;281(8):727-35.
2. Tuzcu EM, Kapadia SR, Tutar E, et al. High prevalence of coronary atherosclerosis in asymptomatic teenagers and young adults: evidence from intravascular ultrasound. Circulation. 2001 Jun 5;103(22):2705-10.
3. Murray CJ, Lopez AD. Alternative projections of mortality and disability by cause 1990-2020: Global Burden of Disease Study. Lancet. 1997 May 24;349(9064):1498-504.
4. Davies MJ, Thomas AC. Plaque fissuring--the cause of acute myocardial infarction, sudden ischaemic death, and crescendo angina. Br Heart J. 1985 Apr;53(4):363-73.

5. Falk E, Shah PK, Fuster V. Coronary plaque disruption. Circulation. 1995 Aug 1;92(3):657-71.
6. Virmani R, Kolodgie FD, Burke AP, Farb A, Schwartz SM. Lessons from sudden coronary death: a comprehensive morphological classification scheme for atherosclerotic lesions. Arterioscler Thromb Vasc Biol. 2000 May;20(5):1262-75.
7. Libby P. Inflammation in atherosclerosis. Nature. 2002 Dec 19-26;420(6917):868-74.
8. Fayad ZA, Fuster V. Clinical imaging of the high-risk or vulnerable atherosclerotic plaque. Circ Res. 2001 Aug 17;89(4):305-16.
9. de Feyter PJ, Nieman K. New coronary imaging techniques: what to expect? Heart. 2002 Mar;87(3):195-7.
10. MacNeill BD, Lowe HC, Takano M, Fuster V, Jang IK. Intravascular modalities for detection of vulnerable plaque: current status. Arterioscler Thromb Vasc Biol. 2003 Aug 1;23(8):1333-42. Epub 2003 Jun 12.
11. Fayad ZA, Nahar T, Fallon JT, et al. In vivo magnetic resonance evaluation of atherosclerotic plaques in the human thoracic aorta: a comparison with transesophageal echocardiography. Circulation. 2000 May 30;101(21):2503-9.
12. Yuan C, Mitsumori LM, Beach KW, Maravilla KR. Carotid atherosclerotic plaque: noninvasive MR characterization and identification of vulnerable lesions. Radiology. 2001 Nov;221(2):285-99.
13. Toussaint JF, LaMuraglia GM, Southern JF, Fuster V, Kantor HL. Magnetic resonance images lipid, fibrous, calcified, hemorrhagic, and thrombotic components of human atherosclerosis in vivo. Circulation. 1996 Sep 1;94(5):932-8.
14. Yuan C, Beach KW, Smith LH Jr, Hatsukami TS. Measurement of atherosclerotic carotid plaque size in vivo using high resolution magnetic resonance imaging. Circulation. 1998 Dec 15;98(24):2666-71.
15. Hatsukami TS, Ross R, Polissar NL, Yuan C. Visualization of fibrous cap thickness and rupture in human atherosclerotic carotid plaque in vivo with high-resolution magnetic resonance imaging. Circulation. 2000 Aug 29;102(9):959-64.
16. Kim WY, Danias PG, Stuber M, et al. Coronary magnetic resonance angiography for the detection of coronary stenoses. N Engl J Med. 2001 Dec 27;345(26):1863-9.
17. Budoff MJ, Achenbach S, Duerinckx A. Clinical utility of computed tomography and magnetic resonance techniques for noninvasive coronary angiography. J Am Coll Cardiol. 2003 Dec 3;42(11):1867-78.
18. van Geuns RJ, Wielopolski PA, de Bruin HG, et al. MR coronary angiography with breath-hold targeted volumes: preliminary clinical results. Radiology 2000;217:270-7.
19. Fayad ZA, Fuster V, Fallon JT, et al. Noninvasive in vivo human coronary artery lumen and wall imaging using black-blood magnetic resonance imaging. Circulation. 2000 Aug 1;102(5):506-10.
20. Botnar RM, Stuber M, Kissinger KV, Kim WY, Spuentrup E, Manning WJ. Noninvasive coronary vessel wall and plaque imaging with magnetic resonance imaging. Circulation. 2000 Nov 21;102(21):2582-7.
21. Rumberger JA, Simons DB, Fitzpatrick LA, Sheedy PF, Schwartz RS. Coronary artery calcium area by electron-beam computed tomography and coronary atherosclerotic plaque area. A histopathologic correlative study. Circulation. 1995 Oct 15;92(8):2157-62.
22. O'Rourke RA, Brundage BH, Froelicher VF, et al. American College of Cardiology/American Heart Association Expert Consensus Document on electron-beam computed tomography for the diagnosis and prognosis of coronary artery disease. J Am Coll Cardiol. 2000 Jul;36(1):326-40.

23. Wong ND, Hsu JC, et al. Coronary artery calcium evaluation by electron beam computed tomography and its relation to new cardiovascular events. Am J Cardiol 2000;86:498-508.
24. Arad Y, Spadaro LA, Goodman K, Newstein D, Guerci AD. Prediction of coronary events with electron beam computed tomography. J Am Coll Cardiol. 2000 Oct;36(4):1253-60.
25. Detrano RC, Wong ND, Doherty TM, et al. Coronary calcium does not accurately predict near-term future coronary events in high-risk adults. Circulation. 1999 May 25;99(20):2633-8.
26. Raggi P, Cooil B, Callister TQ. Use of electron beam tomography data to develop models for prediction of hard coronary events. Am Heart J. 2001 Mar;141(3):375-82.
27. Kondos GT, Hoff JA, Sevrukov A, et al. Electron-beam tomography coronary artery calcium and cardiac events: a 37-month follow-up of 5635 initially asymptomatic low- to intermediate-risk adults. Circulation. 2003 May 27;107(20):2571-6. Epub 2003 May 12.
28. Shaw LJ, Raggi P, Schisterman E, Berman DS, Callister TQ. Prognostic Value of Cardiac Risk Factors and Coronary Artery Calcium Screening for All-Cause Mortality. Radiology 2003 228: 826-833.
29. Greenland Ph, LaBree L, Azen SP, Doherty TM, Detrano RC. Coronary Artery Calcium score combined with Framingham Score for Risk prediction in Asymptomatic Individuals. JAMA 2004;291:210-215.
30. Greenland P, Abrams J, Aurigemma GP, et al. Prevention Conference V: Beyond secondary prevention: identifying the high-risk patient for primary prevention: noninvasive tests of atherosclerotic burden: Writing Group III. Circulation. 2000 Jan 4;101(1):E16-22.
31. Becker CR, Knez A, Ohnesorge B, Schoepf UJ, Reiser MF. Imaging of noncalcified coronary plaques using helical CT with retrospective ECG gating. AJR Am J Roentgenol. 2000 Aug;175(2):423-4.
32. Becker CR, Nikolaou K, Muders M, et al. Ex vivo coronary atherosclerotic plaque characterization with multi-detector-row CT. Eur Radiol. 2003 Sep;13(9):2094-8. Epub 2003 Apr 12.
33. Estes JM, Quist WC, Lo Gerfo FW, Costello P. Noninvasive characterization of plaque morphology using helical computed tomography. J Cardiovasc Surg (Torino). 1998 Oct;39(5):527-34.
34. Nikolaou K, Sagmeister S, Knez A, et al. Multidetector-row computed tomography of the coronary arteries: predictive value and quantitative assessment of non-calcified vessel-wall changes. Eur Radiol. 2003 Nov;13(11):2505-12.
35. Leber AW, Knez A, White CW, et al. Composition of coronary atherosclerotic plaques in patients with acute myocardial infarction and stable angina pectoris determined by contrast-enhanced multislice computed tomography. Am J Cardiol. 2003 Mar 15;91(6):714-8.
36. Caussin C, Ohanessian A, Lancelin B, et al. Coronary plaque burden detected by multislice computed tomography after acute myocardial infarction with near-normal coronary arteries by angiography. Am J Cardiol. 2003 Oct 1;92(7):849-52.
37. Schroeder S, Kopp AF, Baumbach A, et al. Noninvasive detection and evaluation of atherosclerotic coronary plaques with multislice computed tomography. J Am Coll Cardiol. 2001 Apr;37(5):1430-5.
38. Leber AW, Knez A, Becker A, et al. Accuracy of multidetector spiral computed tomography in identifying and differentiating the composition of coronary atherosclerotic plaques; A comparative study with intracoronary ultrasound. J Am Coll Cardiol. 2004 Apr 7;43(7):1241-7.

39. Achenbach S, Ropers D, Hoffmann U, et al. Assessment of coronary remodeling in stenotic and nonstenotic coronary atherosclerotic lesions by multidetector spiral computed tomography. J Am Coll Cardiol. 2004 Mar 3;43(5):842-7.
40. Achenbach S, Moselewski F, Ropers D, et al. Detection of calcified and noncalcified coronary atherosclerotic plaque by contrast-enhanced, submillimeter multidetector spiral computed tomography: a segment-based comparison with intravascular ultrasound. Circulation. 2004 Jan 6;109(1):14-7.
41. Mollet NR, Cademartiri F, Nieman K et al. Non-invasive assessment of coronary plaque burden using multislice computed tomography. AJC 2005; in press.
42. Nieman K, Cademartiri F, Lemos PA, et al. Reliable noninvasive coronary angiography with fast submillimeter multi-slice spiral computed tomography. Circulation 2002;106:2051-2054.
43. Ropers D, Baum U, Pohle K, et al. Detection of coronary artery stenoses with thin-slice multi-detector row spiral computed tomography and multi-planar reconstruction. Circulation 2003; 107: 664-666.
44. Kuettner A, Trabold T, Schroeder S, Feyer A, Beck T, Brueckner A, Heuschmid M, Burgstahler C, Kopp AF, Claussen CD. Non-invasive detection of coronary lesions using 16-slice MDCT technology: initial clinical results. J Am Coll Cardiol 2004 Sep 15;44(6):1230-7.
45. Mollet, NR, Cademartiri F, Nieman K, Saia F, Lemos PA, McFadden EP, Pattynama PMT, Serruys PW, Krestin GP, de Feyter PJ. Multi-slice spiral CT coronary angiography in patients with stable angina pectoris. J Am Coll Cardiol. 2004 Jun 16;43(12):2265-70.
46. Martuscelli E, Romagnoli A, D'Eliseo, Razzini C, et al. Accuracy of thin-slice computed tomography in the detection of coronary stenoses. European Heart Journal 2004;25:1043-1048.
47. Mollet NR, Cademartiri F, Krestin GP, et al. Improved diagnostic accuracy with 16-row multi-slice computed tomography coronary angiography. J Am Coll Cardiol. 2005 Jan 4;45(1):128-32.
48. Kuettner A, Beck T, Drosch T, et al. Diagnostic Accuracy of Noninvasive Coronary Imaging Using 16-slice spiral Computed Tomography with 188 ms temporal resolution. JACC 2005;45:123-127.
49. Casscells W, Hathorn B, David M, et al. Thermal detection of cellular infiltrates in living atherosclerotic plaques: possible implications for plaque rupture and thrombosis. Lancet. 1996 May 25;347(9013):1447-51.
50. Verheye S, De Meyer GR, Van Langenhove G, Knaapen MW, Kockx MM. In vivo temperature heterogeneity of atherosclerotic plaques is determined by plaque composition. Circulation. 2002 Apr 2;105(13):1596-601.
51. Stefanadis C, Diamantopoulos L, Vlachopoulos C, et al. Thermal heterogeneity within human atherosclerotic coronary arteries detected in vivo: A new method of detection by application of a special thermography catheter. Circulation. 1999 Apr 20;99(15):1965-71.
52. Stefanadis C, Toutouzas K, Tsiamis E, et al. Increased local temperature in human coronary atherosclerotic plaques: an independent predictor of clinical outcome in patients undergoing a percutaneous coronary intervention. J Am Coll Cardiol. 2001 Apr;37(5):1277-83.
53. Diamantopoulos L, Liu X, De Scheerder I, et al. The effect of reduced blood-flow on the coronary wall temperature. Are significant lesions suitable for intravascular thermography? Eur Heart J. 2003 Oct;24(19):1788-95.

54. Cespedes EI, de Korte CL, van der Steen AF, von Birgelen C, Lancee CT. Intravascular elastography: principles and potentials. Semin Interv Cardiol. 1997 Mar;2(1):55-62.
55. de Korte CL, Pasterkamp G, van der Steen AF, Woutman HA, Bom N. Characterization of plaque components with intravascular ultrasound elastography in human femoral and coronary arteries in vitro. Circulation. 2000 Aug 8;102(6):617-23.
56. de Korte CL, Carlier SG, Mastik F, et al. Morphological and mechanical information of coronary arteries obtained with intravascular elastography; feasibility study in vivo. Eur Heart J. 2002 Mar;23(5):405-13.
57. Schaar JA, de Korte CL, Mastik F, et al. Intravascular palpography for high-risk vulnerable plaque assessment. Herz. 2003 Sep;28(6):488-95.
58. Schaar JA, de Korte CL, Mastik F, et al. Characterizing vulnerable plaque features with intravascular elastography. Circulation 2003;108:2636-2641.
59. Schaar JA, Regar E, Mastik F, et al. Incidence of high-strain patterns in human coronary arteries: assessment with three-dimensional intravascular palpography and correlation with clinical presentation. Circulation. 2004 Jun 8;109(22):2716-9. Epub 2004 May 24.
60. Nair A, Kuban BD, Tuzcu EM, Schoenhagen P, Nissen SE, Vince DG. Coronary plaque classification with intravascular ultrasound radiofrequency data analysis. Circulation. 2002 Oct 22;106(17):2200-6.
61. Jang Ik, Bouma BE, Kang DH, et al. Visualization of coronary atherosclerotic plaques in patients using optical coherence tomography: comparison with intravascular ultrasound. J Am Coll Cardiol 2002;39:604-609.
62. Brezinski ME, Tearney GJ, Weismann NJ, et al. Assessing atherosclerotic plaque morphology: comparison of optical coherence tomography and high frequency intra-vascular ultrasound. Heart 1997;77:397-403.
63. Yabushita H, Bouma BE, Houser SL, Aretz HT, Jang I-K, Schlendorf KH, Kauffman CR, Shishkov M, Kang D-H, Halpern EF, Tearney GJ. Characterization of Human Atherosclerosis by Optical Coherence Tomography. Circulation 2002;106:1640-1645.
64. Tearney GJ, Yabushita H, Houser SL, et al. Quantification of Macrophage Content in Atherosclerotic Plaques by Optical Coherence Tomography. Circulation 2003; 107:113-119.
65. Patwari P, Weissman NJ, Boppart SA, Jesser C, Stamper D, Fujimoto JG, Brezinski ME. Assessment of coronary plaque with optical coherence tomography and high-frequency ultrasound. Am J Cardiol 2000;85:641-644.
66. Jang IK, Bouma BE, Kang DH, et al. Visualization of coronary atherosclerotic plaques in patients using optical coherence tomography: comparison with intravascular ultrasound. J Am Coll Cardiol 2002; 39:604-9.

Chapter 17

MULTISLICE COMPUTED TOMOGRAPHY CORONARY ANGIOGRAPHY TO ASSESS IN-STENT RE-STENOSIS

Summary

51 patients (42 males, aged 59.8±11.6 years) with previous stent-implantation underwent, multislice computed tomography coronary angiography (MSCT-CA). All coronary branches ≥2.0-mm were independently evaluated by two observers and screened for in-stent restenosis (≥50%) and occlusion. The consensus reading was compared with quantitative coronary angiography.

Six (3 restenosis; 3 occlusions) of the 74 (8.1%) evaluated stents were significantly diseased. The sensitivity, specificity and positive and negative predictive value to identify was 83.3% (CI: 35.9-99.6), 98.5% (CI: 92.1-100), 83.3% (CI: 35.9-99.6), and 97.3% (CI: 92.1-100), respectively. One in-stent restenosis remained undetected.

Filippo Cademartiri [1,2]
Nico R. Mollet [1,2]
Carlos Van Mieghem [2]
Timo Baks [1,2]
Eugene P. McFadden [2]
Gabriel P. Krestin [1]
Patrick W. Serruys [2]
Pim J. de Feyter [1,2]

Departments of Radiology [1] and Cardiology [2], Erasmus MC, University Medical Center, Rotterdam, The Netherlands.

Submitted for publication

INTRODUCTION

Stent-implantation has significantly reduced the occurrence of restenosis compared to balloon angioplasty (1,2). Drug-eluting stents have further reduced the frequency of in-stent restenosis compared to bare stent implantation (3-5).

Traditionally, in-stent restenosis had been assessed by invasive coronary angiography. Multislice Computed Tomography coronary angiography (MSCT-CA) is a promising non-invasive alternative to evaluate in-stent restenosis (6).

We report the diagnostic performance of MSCT to identify in-stent restenosis compared to invasive coronary angiography.

METHODS

Study population

Fifty-one patients (42 males, aged 59.8±11.6 years) who were referred for evaluation of in-stent restenosis were retrospectively enrolled in the study. The average time interval between previous stent implantation and MSCT-CA was 5.8±1.5 months. The average interval between MSCT and conventional angiography was 4±16 days. A total of 76 stents (mean 1.5±0.7 stent per patient) were implanted.

Table 1. Demographic and angiographic characteristics of assessable segments (n=51 pts; 76 stented segments).

Patient		***Ste nt localization****	
age	59.8 ± 11.6	prox rca	11%
males	83%	mid rca	9%
previous MI	22%	distal rca	8%
previous CABG	4%	LMC	5%
previous PCI	16%	prox LAD	25%
hypertension	26%	mid LAD	13%
current smoking	36%	distal LAD	3%
diabetes	13%	diagonal	9%
Characteristics		prox LCx	5%
single vessel disease	56%	marginals and intermediate	9%
double vessel disease	27%	SVG	1%
triple vessel disease	18%		
hypercholesterolemia	53%		

*count may not sum 100% due to rounding

The site of stent implantation was (Table 1): saphenous vein graft in 1 (1%), right coronary artery in 22 (29%), left main coronary in 4 (5%), left anterior descending in 38 (50%), and left circumflex in 11 (15%). The ethics committee of the university medical center approved the study, and all participating patients gave informed consent.

Scan protocol and image reconstruction

MSCT-CA was performed using a 16-row MSCT scanner with a 0.37s rotation time (Sensation 16®, Siemens, Forchheim, Germany). Thirty-four patients (58%) had a pre-scan heart rate (HR) ≥65bpm, and were given a single oral dose of 100 mg metoprolol one hour

before the examination in the absence of contraindications. A bolus of 100ml iomeprol (400 mgI/ml; Iomeron®, Bracco, Milan, Italy) was intravenously injected (4ml/s). To trigger the start of the scan a real-time bolus tracking technique was used. During the scan performed in inspiratory breath hold (18.3±1.4 s) the MSCT data and ECG trace were acquired. Scan parameters: detector collimation 16x0.75mm, table feed 8.0mm/s, tube voltage 120kV, 600mAs, and estimated radiation exposure between 11.8-16.3mSv (male-female). Reconstruction parameters: effective slice width 0.75mm, increment 0.4mm, standard and sharp heart view convolution filters.

Axial slices synchronized to the recorded ECG, were reconstructed from the acquired MSCT data with the use of an algorithm that uses only the data from a half gantry rotation per slice, resulting in a temporal resolution of ≥188ms.

The continuous data acquisition allows slice reconstruction at any time position within the cardiac cycle. An image data set was reconstructed during the mid-to-end diastolic phase, during which coronary artery displacement is relatively little, with reconstruction window positions starting at 400ms before the next R wave. If indicated, additional window positions were explored (usually, 350 and 450ms before the next R wave).

MSCT image interpretation

Two observers independently evaluated the MSCT scans by assessment of the axial slices, multiplanar and curved reconstructions. Both reviewers were blinded to the angiographic findings. Sites with multiple stents in the same vessel were evaluated as a single stent, while stents in bifurcations were evaluated separately as main vessel stent and branch stent.

A stent was considered occluded when the lumen inside the stent was darker than the contrast-enhanced vessel before the stent. This may be associated with absence of vessel lumen opacification distal to the stent. Non-occlusive in-stent re-stenosis was defined if the lumen inside the stent showed a darker rim (eccentric or concentric non-contrast enhanced neo-intimal hyperplasia) between the stent and the contrast-enhanced vessel lumen with a lumen diameter reduction ≥50% (Figure 1, 2, 3). Disagreement was settled by a joined consensus reading.

X-ray coronary angiography

Conventional selective coronary angiography was performed with standard techniques and evaluated by an independent reviewer using quantitative coronary angiography (CAAS II, Pie Medical, Maastricht, The Netherlands). The percentage in-stent diameter stenosis, was determined in two orthogonal projections and the percentage stenosis was taken as average of the 2 values.

Statistical analysis

The diagnostic accuracy of MSCT to detect in-stent re-stenosis (≥50%) and occlusion inside the stents was evaluated regarding quantitative coronary angiography as the standard of reference. Standard descriptive statistics were calculated for each observer and the precision of the overall parameters was expressed with a 95% confidence interval. Concordance between observers was calculated and expressed by the κ value.

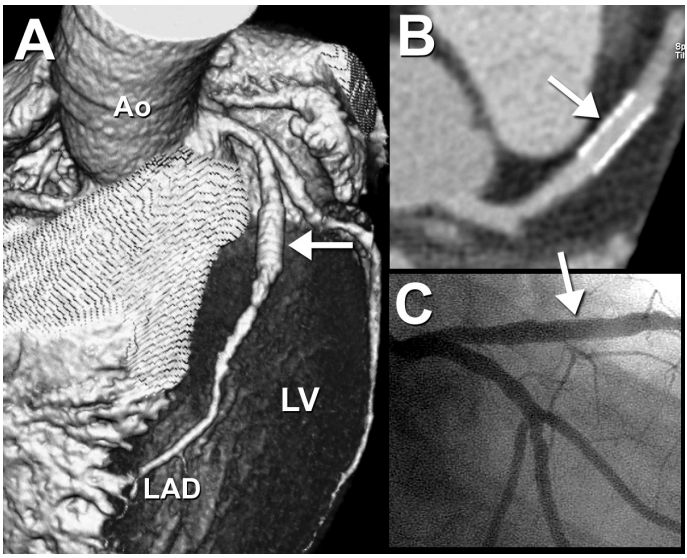

Figure 1. Patent stent in LAD.
A: Three-dimensional volume rendering of the heart showing the left coronary artery and a stent in of the proximal LAD (arrow).
B:Multiplanar reconstructions showing the left main and the LAD with the patent stent (arrow). The contrast enhancement in the lumen of the stent is comparable with the one before and after the stent.
C: The corresponding diagnostic coronary angiogram confirming the absence of in-stent restenosis

Abbreviations: Ao= ascending aorta; LAD= left anterior descending; LV= left ventricle. (A full color version of this illustration can be found in the color section (Chapter 21)).

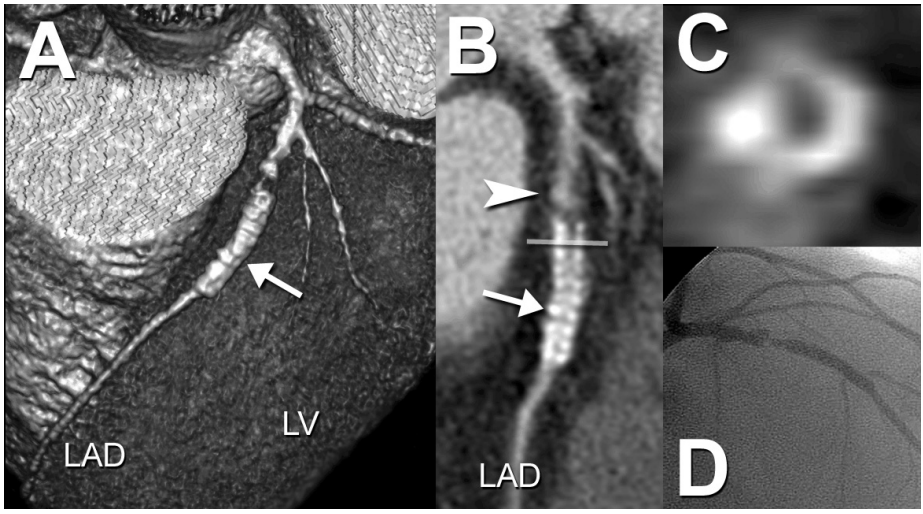

Figure 2. In-stent restenosis in a LAD stent.
A: three-dimensional volume rendering of the heart showing the left coronary artery and a stent in the proximal LAD (arrow).
B: a curved reconstructions shows the left main and the LAD with the stent (arrow). An obstructive plaque beginning at the proximal edge of the stent (arrowhead) and continuing within the proximal segment of the stent is visualized. A cross section performed at the level of the proximal segment of the stent (**C**) shows the in-stent restenosis appearing as hypo-attenuating tissue within the stent. The bright zone represents the remaining lumen and on the right side a stent strut.
D: the corresponding diagnostic angiogram
Abbreviations: LAD= left anterior descending; LV= left ventricle.
(A full color version of this illustration can be found in the color section (Chapter 21)).

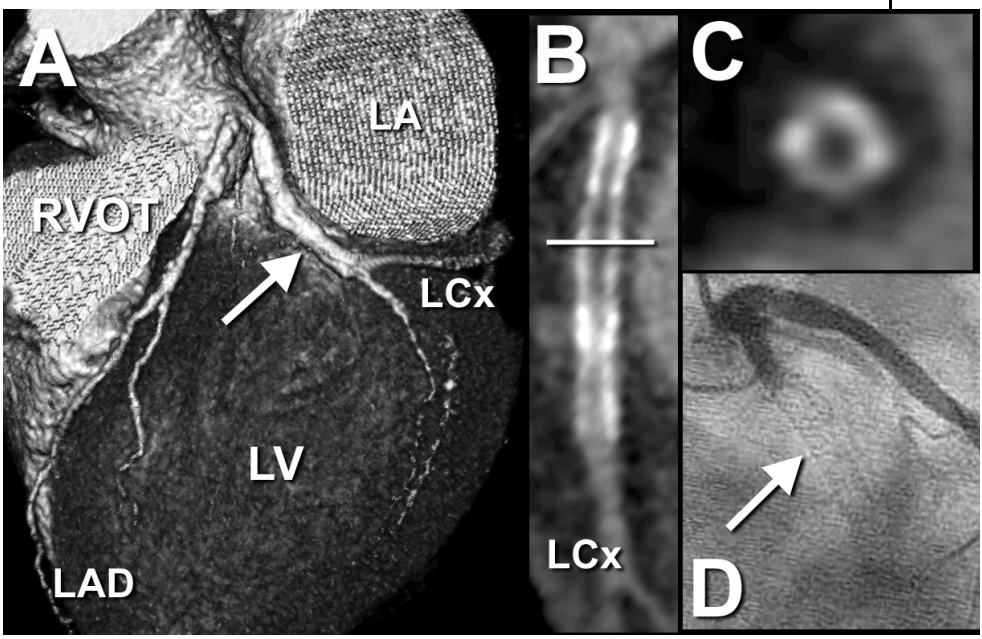

Figure 3. Occluded stent in LCx.
A: a three-dimensional volume rendering of the left coronary artery, showing a stent in the proximal segment of the the LCx (arrow).
B: a curved multiplanar reconstruction along the lumen of the LCx, shows the in-stent occlusion appearing as a hypo-attenuating region, occupying the whole in-stent lumen. An orthogonal view performed at this level (**C**) shows the lack of contrast enhancement (dark zone) within the lumen of the occluded stent.
D: the corresponding diagnostic angiogram. It should be noticed that with CT coronary imaging the distal segment of LCx appears patent (due to collateral retrograde flow), while at conventional coronary angiography there is only faint distal filling of the occluded vessel.
Abbreviations: LAD= left anterior descending; LCx= left circumflex; LV= left ventricle; RVOT= right ventricle outflow tract. (A full color version of this illustration can be found in the color section (Chapter 21)).

Results

The average HR was 57.1±2.7bpm. In total, 74 stents were available for evaluation. Two stented segments (1.3%) were considered uninterpretable due to residual motion.

Table 2. Crosstable MSCT vs. angio for the classification of restenosis (n=51 pts; 76 stented segments).

		Angio		
		without restenosis	with restenosis	Total
MSCT	without restenosis	67	1	68
	with restenosis	3	5	6
	with occlusion	3		
	Total	68	6	74

The incidence of significant intra-stent luminal obstructions (non-occlusive in-stent restenosis (3) and total stent occlusions (3) was 8.1% (6/74), as assessed by conventional angiography.
The overall sensitivity, specificity, positive and negative predictive value to detect significant intra-stent obstructions was 83.3% (CI: 35.9-99.6), 98.5% (CI: 92.1-100), 83.3% (CI: 35.9-99.6), and 98.5% (CI: 92.1-100), respectively (Table 2).
One undetected in-stent re-stenosis was located in the first diagonal (segment 9) and one false positive was located in distal circumflex. In both cases the diameter of the vessel was 2mm. Concordance between both MSCT observers was good (κ value 0.75).

Discussion

Stents are difficult to visualize with CT because the metallic struts cause a severe artifact due to the "blooming effect". This results in an enlarged appearance of the stent struts that affects the capability to visualize the lumen. The artefact depends on the material and design of the stent: (the higher the density the larger the "blooming"). This effect is less important in large vessels, such as the aorta and its abdominal branches, but it impairs the visualization of the lumen in smaller vessels such as coronary arteries.
An earlier study with electron beam CT reported a sensitivity of 78% and specificity of 98% to identify coronary stent patency (7). In vitro studies have shown that MSCT scanners offer a good delineation of the stent struts and of the presence of in-stent restenosis (8). However, in-vivo in-stent lumen evaluation with CT remained difficult and by using a 4-row MSCT scanner it was not possible to visualize stent lumen (9). In a recent report with 16-row MSCT scanner a sensitivity and specificity of 78% and 100% was reported for the assessment of stent-patency (6). However, only fifty (77%) of the 65 included stents were assessable due to insufficient image quality (6).

In that study patency of the stent was defined if the vessel distal to the stent was contrast opacified. However, we have noted in a few instances that that criterion is not full-proof and that collaterals can retrogradely opacify the entire vessel distal to the stent occlusion (Figure 3). We therefore defined in-stent restenosis as the presence of a darker, non-contrast enhanced rim of tissue within the stent-lumen and occlusion as a dark non-opacified occluded region within the stent. In addition an occlusion may be associated with a non-contrast-enhanced vessel distal to the stent.

The size of the study population is reasonable but due to the use of drug eluting stents the number of patients with an in-stent restenosis or occlusion is rather low. Only patients with stable rhythm and heart rates below 75 bpm were included. The high radiation exposure remains a matter of concern.

Conclusion

Our first experience with coronary in-stent restenosis evaluation is promising. We were able to visualize both in-stent restenosis and re-occlusion in the majority of the cases. For clinical implementation higher spatial and temporal resolution will be required.

REFERENCES

1. Serruys PW, de Jaegere P, Kiemeneij F, et al. A comparison of balloon-expandable-stent implantation with balloon angioplasty in patients with coronary artery disease. Benestent Study Group. N Engl J Med 1994;331:489-95.
2. Fischman DL, Leon MB, Baim DS, et al. A randomized comparison of coronary-stent placement and balloon angioplasty in the treatment of coronary artery disease. Stent Restenosis Study Investigators. N Engl J Med 1994;331:496-501.
3. Moses JW, Leon MB, Popma JJ, et al. Sirolimus-eluting stents versus standard stents in patients with stenosis in a native coronary artery. N Engl J Med 2003;349:1315-23.
4. Morice MC, Serruys PW, Sousa JE, et al. A randomized comparison of a sirolimus-eluting stent with a standard stent for coronary revascularization. N Engl J Med 2002;346:1773-80.
5. Stone GW, Ellis SG, Cox DA, et al. A polymer-based, paclitaxel-eluting stent in patients with coronary artery disease. N Engl J Med 2004;350:221-31.
6. Schuijf JD, Bax JJ, Jukema JW, et al. Feasibility of assessment of coronary stent patency using 16-slice computed tomography. Am J Cardiol 2004;94:427-30.
7. Pump H, Mohlenkamp S, Sehnert CA, et al. Coronary arterial stent patency: assessment with electron-beam CT. Radiology 2000;214:447-52.
8. Maintz D, Seifarth H, Flohr T, et al. Improved coronary artery stent visualization and in-stent stenosis detection using 16-slice computed-tomography and dedicated image reconstruction technique. Invest Radiol 2003;38:790-5.
9. Kruger S, Mahnken AH, Sinha AM, et al. Multislice spiral computed tomography for the detection of coronary stent restenosis and patency. Int J Cardiol 2003;89:167-72.

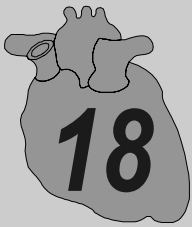

MULTISLICE SPIRAL COMPUTED TOMOGRAPHY FOR THE EVALUATION OF STENT PATENCY AFTER LEFT MAIN CORONARY ARTERY STENTING: A COMPARISON WITH CONVENTIONAL ANGIOGRAPHY AND INTRAVASCULAR ULTRASOUND

Carlos A.G. Van Mieghem [1,2]
Filippo Cademartiri [2]
Nico R. Mollet [1,2]
Patrizia Malagutti [2]
Marco Valgimigli [1]
Eugene P. McFadden [1]
Jurgen M.R. Ligthart [1]
Giuseppe Runza [2]
Nico Bruining [1]
Pieter C. Smits [3]
Evelyn Regar [1]
Willem J.van der Giessen [1]
Georgios Sianos [1]
Ron T. van Domburg [11]
Gabriel P. Krestin [2]
Patrick W. Serruys [1]
Pim de Feyter [1,2]

Departments of Cardiology [1] and Radiology [2], Erasmus MC, University Medical Center, Rotterdam, The Netherlands. Medical Center Rijnmond Zuid [3], Rotterdam, The Netherlands

Submitted for publication

Abstract

BACKGROUND
Surveillance conventional coronary angiography is generally recommended 3 to 6 months after stent-supported left main coronary artery (LMCA) percutaneous coronary intervention due to the unpredictable occurrence of in-stent restenosis, with its attendant risks. Multislice computed tomography (MSCT) is a promising technique for non-invasive coronary evaluation. We evaluated the diagnostic performance of high-resolution MSCT to detect in-stent restenosis after stenting of the LMCA.

METHODS AND RESULTS
Fifty-six patients were prospectively identified from a consecutive patient population scheduled for follow-up coronary angiography after LMCA stenting and participated in a protocol to compare MSCT with conventional angiography. Until August 2004 a 16-slice MSCT (n= 28), and since then a 64-slice MSCT (n=28), was used. Sixty-four percent of patients received additional β-blockers resulting in a mean peri-scan heart rate of 57±8 beats/min. Among patients with technically adequate scans (n=53) MSCT correctly identified all patients with in-stent restenosis (7/53), but misclassified 4 patients without in-stent restenosis (false positives). Overall the accuracy of MSCT for detection of angiographic restenosis was 92%. The sensitivity and specificity was 100% and 91%, respectively. Accuracy was 97% when restricting the analysis to patients with stenting of the LMCA stem alone or where the stent extended into a single major side branch. Where both branches of the LMCA bifurcation were stented, accuracy was reduced to 84%.

CONCLUSIONS
Current MSCT technology, in combination with optimal heart rate control, allows reliable evaluation of selected patients after LMCA stenting. Non-invasive evaluation with MSCT as a first-line strategy to detect in-stent restenosis is a feasible alternative to conventional angiography.

MSCT in the evaluation of left main stents

INTRODUCTION

Multislice computed tomography coronary angiography (MSCTA) is a promising non-invasive coronary imaging modality[1,2]. Although several reports have shown that MSCT may be used to evaluate stent patency, more precise evaluation of the lumen within the stent is markedly hindered by artificial enlargement of the metallic stent struts causing blooming artefact[3]. The impact of blooming artefact on the evaluation of structures inside stents is inversely related to stent diameter[4]. In large diameter coronary stents, such as those implanted in the left main or proximal left anterior descending coronary artery, neointimal hyperplasia within the stent can be visualized on MSCT demonstrating its potential for the detection of in-stent restenosis, in addition to stent patency, in specific lesion subsets.

Although coronary artery bypass graft surgery (CABG) is still the recommended treatment for significant left main disease, the introduction of drug-eluting stents (DES) with much lower restenosis rates has resulted in an increasing use of percutaneous intervention as an alternative[5-8]. However, left main stem in-stent restenosis still occurs with DES and may result in fatal myocardial infarction or sudden death [9-11]. Careful surveillance, including routine coronary angiography at 3 to 6 months after PCI, is therefore strongly recommended by several experts[9,12]. A non-invasive method to detect in-stent restenosis and potentially pre-empt their clinical consequences would be of evident clinical value. In this study we evaluated the potential of MSCT to detect left main in-stent restenosis.

METHODS

Patient Selection

Between March 2004 and January 2005, we screened 67 consecutive patients scheduled for follow-up coronary angiography after LMCA stenting for inclusion in a protocol to compare MSCT with conventional angiography. In addition, most patients also underwent intravascular ultrasound (IVUS) evaluation of the LMCA. All patients in sinus rhythm who were able to breath-hold for 20-seconds were eligible for inclusion. Patients with a previous allergic reaction to contrast, impaired renal function (serum creatinine >1.6 mg/dl), contra-indication to β-blockers (high-degree heart block, poor left ventricular function, asthma or severe chronic obstructive pulmonary disease), obesity (body mass index >30 kg/m^2 for patients scanned with the 16-row MSCT scanner), or who had an acute coronary syndrome at the time of scheduled angiography, were excluded. The institutional review board of the Erasmus MC Rotterdam approved the study and all subjects gave informed consent.

MSCT Protocol and Image Acquisition

Multislice computed tomography was performed in the fortnight before conventional angiography. Patients with a heart rate above 65 bpm received 100 mg metoprolol orally 1 hour before the scan. Up to July 2004, MSCT data were acquired using a 16-row MSCT scanner (Sensation 16, Siemens, Germany). From August on, all scans were performed with a 64-row MSCT scanner (Sensation 64, Siemens, Germany). A bolus of 100 ml of contrast (iodixanol, 320 mgI/ml; Visipaque™, Amersham Health, Germany) was injected intravenously at 4 to 5 ml/s. MSCT data were acquired during a single breath-hold once the contrast material in the ascending aorta reached a predefined threshold of 100 Hounsfield units.

For the 16-detector row MSCT scanner, scan parameters were: detector collimation 16 x 0.75 mm, table feed 3.0 mm per rotation, gantry rotation time 420ms, tube voltage 120 kV, and tube current 400-450 mAs. For the 64-detector row MSCT scanner, scan parameters were: detector collimation 64 x 0.6 mm, table feed 3.8 mm per rotation, gantry rotation time 330ms, tube voltage120 kV, and tube current of 900 mAs. Using dedicated software (WinDose, Institute of Medical Physics, Erlangen, Germany), the average radiation exposure was calculated as 11.8 to 16.3 mSv for the 16-row MSCT scanner and 15.2 to 21.4 mSv for the 64-row MSCT scanner. All data were reconstructed using a field of view of 50x50 mm, image matrix of 512x512 pixels, and a sharp heart view (B46f) convolution kernel. Image reconstruction was retrospectively gated to the ECG. The position of the reconstructed window within the cardiac cycle was individually optimized to minimize motion artifacts. Datasets containing no or minimal motion artifacts were transferred to a remote workstation (Leonardo, Siemens Medical Solutions) for further evaluation.

MSCT Data Analysis

Two experienced observers, unaware of the results of convential angiography, evaluated the MSCT data sets on both the original axial images and on multiplanar reformatted reconstructions rendered orthogonal and perpendicular to the vessel course. In case of left main bifurcation stenting, each of the 3 segments (left main, LAD and CX) was individually evaluated. For the assessment of significant restenosis (≥50% decrease of lumen diameter as defined by angiography) the stent in the LMCA and, where applicable, related branches were evaluated, including the 5mm borders proximal and distal to the stent. The stent lumen was visually evaluated as (1) patent with no visible neointimal hyperplasia (NIH) (2) patent with non-obstructive (<50% lumen diameter) NIH (3) patent with obstructive (≥50% lumen diameter) NIH, i.e. restenosis and (4) occluded. Disagreements were resolved by consensus. Where a single stent was placed across the left main bifurcation into the left anterior descending or circumflex artery, with no intervention, or balloon dilatation only in the other branch, we also evaluated the proximal 5 mm of the untreated side branch unless a functional bypass graft was attached to the non-stented branch.

Angiographic analysis

Conventional *x*-ray coronary angiography was performed with standard techniques after intracoronary injection of 2 mg isosorbide dinitrate. Care was taken to ensure that the same views of the left main were obtained as at the time of intervention. An experienced cardiologist, unaware of the results of MSCT, analyzed all angiographic data quantitatively, using validated, automated, edge-detection software (CAAS II, Pie Medical, Maastricht, the Netherlands). With the outer diameter of the catheter tip, not filled with contrast, as the calibration standard, we measured from multiple projections in diastole the minimal lumen diameter (MLD), reference diameter (RD) and percent diameter stenosis of the left main coronary artery and, where indicated, the left anterior descending artery (LAD) and circumflex artery (CX); the averaged results were recorded. Binary angiographic restenosis was defined as percent diameter stenosis ≥50% anywhere within the stent or within the 5-mm segments proximal or distal to the stent margins. This definition also applied to the proximal 5mm vessel segment of the untreated LAD or CX where a stent was placed over the distal left main bifurcation.

IVUS Imaging

IVUS was performed with a 2.9F, 40-MHz or a 3.2F, 30-MHz single-element mechanical transducer (Boston Scientific). After intracoronary injection of 2 mg isosorbide dinitrate, the IVUS catheter was positioned at least 1 cm distal to the stent in the LMCA; for patients with bifurcation stenting a sufficiently distal starting point in LAD or CX was chosen. IVUS images were recorded after initiation of automated pullback at 0.5 mm/s. In case of bifurcation stenting, only one of the 2 major branches, preferentially the LAD, was investigated. IVUS images of the entire pullback were recorded on both S-VHS videotape and CD-ROM for off-line analysis.

IVUS Analysis

In our institution all IVUS pullbacks are retrospectively gated using a program that selects images recorded in the end-diastolic phase[13]. Two experienced observers, blinded to the angiography and MSCT results, analyzed and reviewed the IVUS image data sets using an off-line semi-automated software package (Curad, version 3.1, Wijk bij Duurstede, The Netherlands)[14]. The stented portion of the LMCA, including the stented parts of the side branches, were evaluated for the presence of neointima hyperplasia (NIH). For each of the 3 coronary segments (i.e. stented part of left main, LAD and CX) the following IVUS parameters were measured: (1) minimal lumen and mean stent cross-sectional area (CSA, mm^2); (2) minimal lumen and mean stent diameter (mm); (3) maximal NIH diameter (mm).

Statistical Analysis

Continuous variables are presented as mean ± standard deviation or median with 25% and 75% interquartile ranges (IQR). Categorical variables are presented as counts and percentages. Continuous variables were compared by Student's t test for normally distributed values; otherwise the Mann-Whitney U test was used. All tests were two-tailed, and a p-value of <0.05 was considered as significant. Accuracy (percentage of patients correctly classified), sensitivity, specificity, positive and negative predictive value of MSCT for the detection of ≥50% in-stent restenosis, as determined by quantitative coronary angiography (QCA), was calculated on a per-patient basis. Diagnostic test results are reported with associated 95% confidence intervals based on binomial probabilities. The intraobserver and interobserver variability for the detection of in-stent restenosis was determined using the kappa statistic. The degree of agreement between IVUS and MSCT was also measured by the kappa statistic as a function of NIH thickness as determined by IVUS. Statistical analysis was performed with SPSS, version 12.1 (SPSS Inc., Chicago, USA).

RESULTS

Eleven out of the 67 potentially eligible patients (i.e. those scheduled for conventional angiography during the inclusion period) had exclusion criteria as outlined in Table 1; 3 of the 56 patients included had a technically inadequate scan. One of those 3 patients had restenosis on conventional angiography. The remaining 53 patients comprise the study population. The baseline clinical characteristics of these patients are summarized in Table 2. The average interval between MSCT and conventional coronary angiography was 14±16 days. Mean basal heart rate was 67±10 beats/min: 34 (64%) patients received additional β-blockers resulting in a mean peri-scan heart rate of 57±8 beats/min.

Table 1. Reasons for exclusion to perform MSCT

	Number
Total number	**14**
Patients with exclusion criteria	**11**
Severe renal insufficiency (serum creatinin was 3.1 mg/dl)	1
Respiratory insufficiency	1
Contra-indication to β-blocker (poor left ventricular function)	1
Obesity (BMI> 30 kg/m^2) *	3
Atrial fibrillation	3
Acute coronary syndrome	1
Patient refusal	1
Technically inadequate MSCT scan	**3**
Arrhythmia during the scan	1
Heart rate > 70 bpm	1
Scan failure	1

* This exclusion criterion only applied to patients analyzed with the 16-row MSCT scanner

Mean scan time with the 64-row detector MSCT (n=26, 11.1±1.4 s) was significantly ($p < 0.001$) shorter compared to the 16-row detector MSCT (n=27, 15.9±1.5 s).

Table 2. Clinical characteristics

	Number
Total number of patients	53
Age, years ± SD	62±11
Male, %	79
Cardiac risk factors	
Hypertension, %*	51
Hypercholesterolemia, %†	91
Diabetes mellitus, %	21
Current smoking, %	23
Family history of coronary artery disease, %	55
Body mass index (kg/m^2), median (IQR)	26.2 (24.1-28.4)
Previous PCI, %	32
"Protected" left main, %	17
Serum creatinine, mg/dl ± SD	85.8±18.8
Previous heart rate lowering medication, %	89

*Blood pressure > 160/95 mmHg or treatment for hypertension, † total cholesterol >200 mg/dl or treatment for hypercholesterolemia
CABG indicates coronary artery bypass graft surgery; PCI, percutaneous coronary intervention; Protected left main = left main disease with at least one patent arterial or venous conduit to the left anterior descending or circumflex artery
Values are mean±SD, number of patients (%), or median (IQR)

Anatomic Characteristics and Procedural Details of Index Interventions

The anatomic characteristics of the lesions treated and the procedural details of the index interventions are presented in Table 3.

Table 3. Procedural Characteristics (53 patients)

	Number
Number and type of stents	**n=122**
Stents per patient, median (IQR)	3 (2-5)
Paclitaxel-eluting stent, n (%)	84 (69%)
Sirolimus-eluting stent, n (%)	32 (26%)
Bare metal stent, n (%)	6 (5%)
Stent and Balloon size	
Nominal stent diameter, mm, median (IQR)	3 (3-3.5)
Postdilatation with bigger balloon, %	64
Balloon size for postdilatation, mm, median (IQR)	4 (3.5-4)
Stenting Technique	
Simple Stenting, n	**34 (64%)**
Stent only in left main, n	13
Stent from left main to LAD/ LCX*, n	15/6
Complex Bifurcation Stenting, n	**19 (36%)**
Culotte stenting, n	12
Crush stenting§, n	2
T-stenting or V-stenting	5

CX indicates circumflex coronary artery; IQR; interquartile range; LAD, left anterior descending coronary artery; MLD, minimal lumen diameter; RD, reference diameter.
* additional balloon dilatation of the other branch vessel in 3 patients.
§ kissing balloon postdilatation in one of the two patients.

The vast majority of patients (83%, 44/53) had intervention at unprotected left main stem lesions and drug-eluting stents were used in all but 3 (94%) patients.

Two groups of patients were defined, based upon the characteristics of the PCI procedure. The first group (n=34) was defined as a "simple stenting group" and comprised patients in whom single or overlapping stents were implanted in the left main stem alone (n=13) or extended from the left main stem into only the left anterior descending or the left circumflex artery (n=21). The second group was defined as a "complex bifurcation stenting group" and comprised patients in whom the left main stem and both the LAD and LCX were stented (n=19). Further details are presented in Table 3.

Overall MSCT Results

The diagnostic accuracy of MSCT is summarized in Table 4. Restenosis on conventional angiography occurred in 13% (7/53) of the study population. In the overall population, MSCT identified all patients with restenosis and correctly classified 42 patients as having no in-stent restenosis (Figures 1 and 2). In the group of patients (n=34) in whom simple stenting was performed, all restenoses, on conventional angiography, were identified on MSCT. However, one patient who did not have in-stent restenosis on conventional angiography was incorrectly scored (false positive) on MSCT. In the 19 patients who underwent complex bifurcation stenting, all restenoses on conventional angiography were correctly identified on MSCT.

Table 4. Diagnostic accuracy of MSCT to detect in-stent restenosis as defined by conventional coronary angiography

	All patients	Simple stenting	Complex bifurcation stenting
Total number	53	34	19
No. of true negatives	42	30	12
No. of true positives	7	3	4
No. of false negatives	0	0	0
No. of false positives	4	1	3
Sensitivity, %	100 (65-100)	100 (44-100)	100 (51-100)
Specificity, %	91 (80-97)	97 (84-99)	80 (55-93)
Accuracy, %	92 (82-97)	97 (85-99)	84 (62-94)
Positive predictive value, %	63 (35-85)	75 (30-95)	57 (25-84)
Negative predictive value, %	100 (92-100)	100 (89-100)	100 (76-100)

"Simple stenting group" includes patients who underwent stenting of the left main stem only or stenting of the distal left main extending into a single major side branch. The "complex bifurcation stenting group" comprises patients in whom the left main stem and both the LAD and LCX were stented. Values in parentheses are 95 percent confidence intervals.

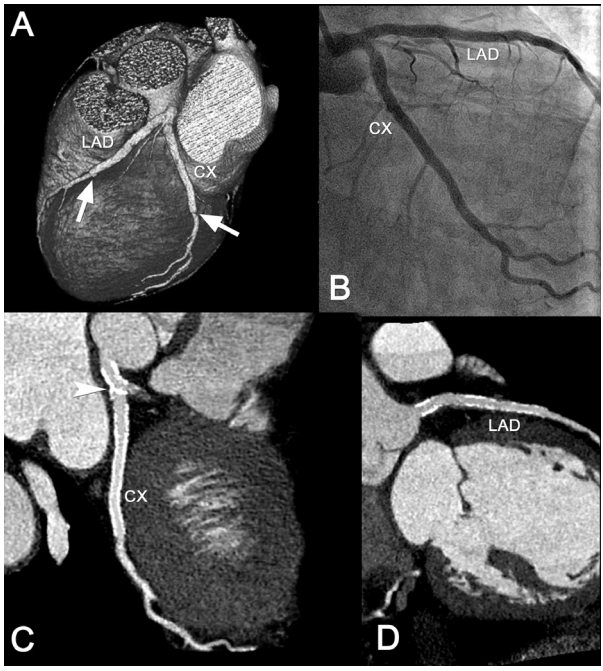

Figure 1. Example of stent patency 5 months after culotte stenting (all DES) of the distal left main coronary artery: 3 overlapping stents had been placed towards the LAD (total stent length 60 mm, each stent with a diameter of 3.5mm) and 2 overlapping stents towards the CX (3.5x20 mm proximal and 3x32 mm distal). Final kissing balloon inflation was performed at the end of the procedure (4mm balloon towards LAD, 3 mm balloon towards CX). Panels A and B show the MSCT coronary angiogram (volume-rendered 3D image, panel A) and the corresponding conventional coronary angiogram (panel B). The stents in LAD and CX are well delineated (panel A, arrows). Panels C and D: the curved multiplanar reconstructions show stent patency of LM, LAD and CX and confirm the findings on conventional angiography (panel B). The arrow in panel C shows the metal overlapping the ostium of the CX, as a result of culotte bifurcation stenting. (A full color version of this illustration can be found in the color section (Chapter 21)).

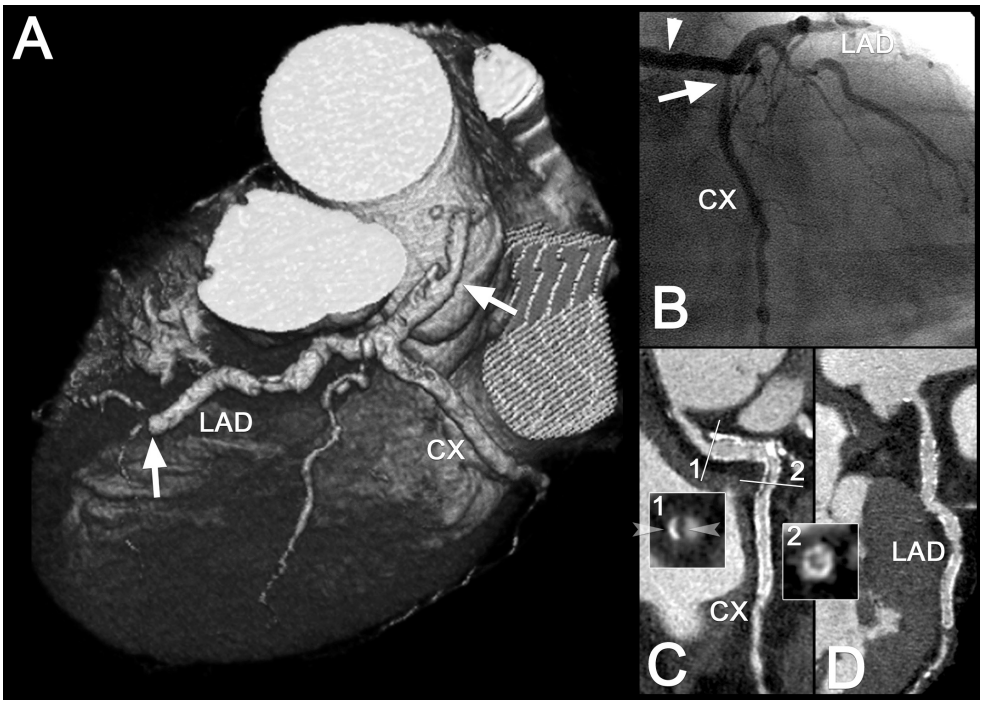

Figure 2. 59-year-old woman presenting with restenosis of the ostium of the CX 6 months after stenting of the distal left main coronary artery (crush technique): 3 overlapping stents had been placed from the LM to mid LAD (3.5x24, 3.5x8 and 2.75x28 mm) and 2 overlapping stents towards the CX (each with a dimension of 3x20mm). The procedure was finalized using kissing balloons (3.5mm balloon towards LAD, 3 mm balloon towards CX). Because of severe angina she underwent coronary artery bypass graft surgery.
Panels A and B show the MSCT coronary angiogram (volume-rendered 3D image, panel A) and the corresponding conventional coronary angiogram (panel B). The extent of the stenting procedure can be well appreciated (panel A, arrows delineate the proximal and distal end of the stents in respectively LM and LAD). Panels C and D: curved multiplanar reconstructions of CX and LAD. Restenosis of the proximal CX is well visualized (cross section 2 with inset) and correlates with the angiographic findings (panel B, arrow). Inset 2 illustrates the in-stent restenosis which appears as hypo-attenuating tissue within the stent reducing the stent lumen diameter by >50%. The proximal stent edge in the LM shows a non-obstructive plaque with <50% reduction of the normal contrast-enhanced lumen (panel A, arrow and panel C, cross section 1 with inset), as confirmed by conventional angiography (panel B, arrowhead). Cross section 1 discloses a large plaque (in between the arrowheads) with a calcified (outer rim) and non-calcified (inner rim) component. The bright zone represents the lumen. (A full color version of this illustration can be found in the color section (Chapter 21)).

However 3 patients who did not have restenosis (although all had visible NIH) on conventional angiography were incorrectly scored (false positives) on MSCT.

In 8 patients, non-significant (<50% stenosis) in-stent NIH in the left main (n=2), LAD (n=4), CX (n=2) on diagnostic coronary angiography (Figure 3) was also detected on MSCT and correctly classified as non-obstructive.

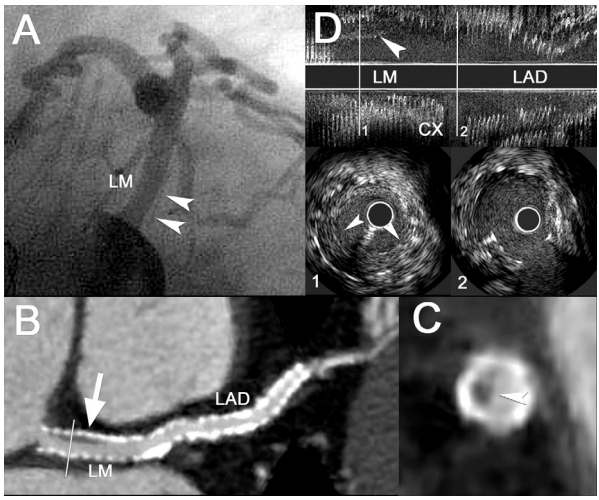

Figure 3. 63-year-old asymptomatic man underwent invasive and non-invasive coronary imaging 19 months after placement of 4 overlapping stents from LM towards LAD. Panels A and B show the conventional coronary angiogram (panel A) and the corresponding MSCT coronary angiogram (curved multiplanar reconstruction of LM and LAD, panel B). Neo-intimal hyperplasia (NIH) presenting as a dark eccentric rim (panel B, arrow) was documented within the left main portion of the stent. The cross sectional image confirms its non-obstructive nature (panel C, arrowhead). Although not clearly visible with conventional angiography (panel A, arrowheads), NIH was clearly present on IVUS at the level of the proximal left main (arrowheads in panel D, longitudinal view, and in cross-section 1). Cross-section 2 is a cross-section at the level of the origin of the CX.

Quantitative Coronary Angiography (QCA) and IVUS

QCA and IVUS data are shown in Table 5. The median reference diameter (RD) and minimal lumen diameter (MLD) of the segments that were wrongly classified did not differ from those that were correctly analyzed by MSCT {RD LAD: 2.51mm (IQR 2.06 –2.79mm) vs. 2.59mm (IQR 2-3.15mm), p= 0.8; MLD LAD: 2,26 (IQR: 1,74-2,76) vs. 1,95 (IQR: 1,65-2,37), p=0,41: RD CX: 1.98mm (IQR 1.64-2.42mm) vs. 2.32mm (IQR 1.39-3.12mm), p=0.5; MLD CX: 1,66 (IQR 1,33-2,56) vs. 1,82 (IQR 1,42-2,12), p=0,89}.

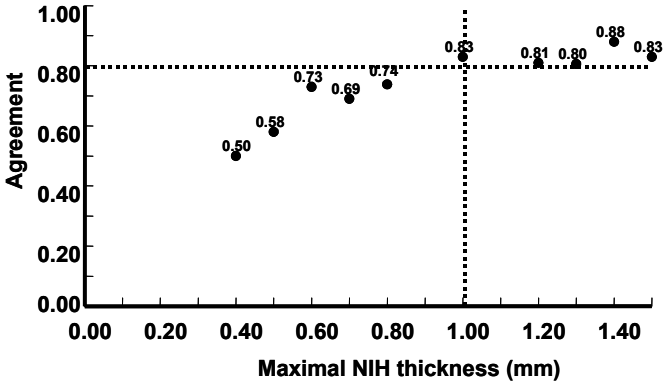

Figure 4. Maximal value (in mm) of neo-intima hyperplasia (NIH) thickness as measured by IVUS as a function of degree of agreement (expressed by the kappa value) between IVUS and MSCT. This analysis includes all patients with technically adequate IVUS examinations (n= 38 patiens, i.e. 54 segments). Values of NIH thickness below 0.4 mm are not related to a kappa value, since values below this threshold are beyond the spatial resolution of currently available MSCT scanners.

Thirty-eight patients (54 segments) had technically adequate IVUS examinations. NIH was present in 23 patients (32 segments). Based on a kappa value above 0.80 which indicates a very good agreement between the 2 imaging techniques, i.e. MSCT and IVUS, a cut-off value of 1 mm was identified in which NIH could be identified with good confidence by MSCT (Figure 4).

Table 5. Quantitative angiographic and IVUS characteristics at follow-up

	Number
Quantitative coronary angiography, n	**53**
Reference diameter LM, mm	3.19±0.55
Minimal lumen diameter LM, mm	2.84±0.55
Reference diameter LAD, mm	2.54±0.51
Minimal lumen diameter LAD, mm	2.03±0.47
Reference diameter CX, mm	2.07±0.69
Minimal lumen diameter CX, mm	1.74 ±0.54
Quantitative IVUS	
Technically adequate IVUS pullback, n (%)	38 (72%)
LAD, n	26
Minimal lumen CSA, mm^2	6.41 ± 2.8
Stent CSA, mm^2	9 ± 2.74
Minimal lumen diameter, mm	2.79 ± 0.58
Stent diameter, mm	3.34 ± 0.5
CX, n	14
Minimal lumen CSA, mm^2	5.45 ± 2.44
Stent CSA, mm^2	8.07 ± 2.7
Lumen diameter, mm	2.59 ± 0.48
Stent diameter, mm	3.15 ± 0.5
LM without sidebranch, n	35
Minimal lumen CSA, mm^2	9.40 ± 2.94
Stent CSA, mm^2	12 ± 2.7
Minimal lumen diameter, mm	3.42 ± 0.53
Stent diameter, mm	3.89 ± 0.45

Values are mean±SD.
CSA indicates cross-sectional area; CX, circumflex coronary artery; LAD, left anterior descending coronary artery; LM, left main.

Observer Variability

Thirty MSCT datasets were analyzed twice to assess internal validity. Interobserver (κ value 0.74) and intraobserver (κ value 0.82) agreement was good to very good.

Discussion

Stent implantation in the left main and proximal LAD/LCX provides the "best case scenario" for the use of MSCT in the detection of in-stent restenosis for several reasons.

First, stents implanted in the left main stem and proximal LAD/LCX are relatively large; second, the left main and proximal LAD are usually situated in a single axial plane; finally, this part of the coronary tree is relatively protected from motion artefact.

Recent technical improvements, including improved z-resolution, faster tube rotation, and the development of dedicated filters for image reconstruction in the presence of stents, have also significantly improved the potential of MSCT to assess coronary stent patency. Furthermore, preliminary experience with the current-generation 16-detector row CT scanners showed promise for the evaluation of stents in the LMCA [4,15].

Our study demonstrates that the evaluation of stent patency in the LMCA is feasible with current 16-slice and the latest 64-slice MSCT scanners. The technique is reliable (accuracy of 97%) for the evaluation of patients with stenting of the LM stem and for those patients with distal left main bifurcation lesions, in whom only one of the major branch vessels (i.e. the LAD or the LCX) is stented. However, in patients who required complex bifurcation stenting, i.e. treatment of the left main and both major side branches, reliability was significantly less (accuracy of 84%). The most obvious explanation is the large quantity of metal, involving up to three layers of struts for crush bifurcation stenting, at and around the ostium of the branch vessels, which is a major source of artefact on MCST.

LMCA stent implantation traditionally represented a relatively small proportion of percutaneous coronary interventions (PCI). Until recently, more widespread applicability of this revascularization modality had been hampered by the high occurrence of in-stent restenosis [10-12,16]. The advent of DES has both significantly reduced restenosis rates and improved long-term clinical outcome; this has already resulted in an increasing proportion of patients with left main disease being treated percutaneously [7,8,17]. However, restenosis still occurs in approximately 10% of the patients treated with DES, and this rate is even higher after stenting of bifurcation lesions [18,19]. For this reason, the use of DES to treat distal LM bifurcation lesions, remains a controversial issue. Given the potentially fatal consequences of LM restenosis, a non-invasive method for its detection, before clinical events occur, would be of major clinical value. Within a well defined patient population, current MSCT scanners may provide an alternative to conventional coronary angiography in the evaluation of patients with previous stenting of the LMCA. The low number of false-positive MSCT evaluations, as shown in our study, leading to "unnecessary" diagnostic coronary angiograms should in the light of potential serious consequences of in-stent restenosis of the LMCA be acceptable.

Limitations of the study

The use of two different MSCT scanners in our study might be criticized. However, the spatial resolution of the 16- and 64-slice scanner in the x- and y-axes has remained identical (0.4 mm) and only the resolution in the z-axis has improved with the 64-slice scanner. Because the left main and proximal LAD generally course in an axial plane, only the resolution in the x- and y-axes play a major role in the high-resolution visualization of these segments.

The rather high radiation exposure of MSCTA as compared to conventional coronary angiography is of concern [20]. The radiation dose can be reduced by 50% with use of prospective *X*-ray tube current modulation [21]. However, the technique needs improvement because it is sensitive to arrhythmia and furthermore limits the possibility to reconstruct datasets during the tele-systolic phase.

Conclusions

Current MSCT technology, in combination with optimal heart rate control, allows reliable evaluation of selected patients after LMCA stenting. The use of non-invasive evaluation with MSCT as a first-line strategy to detect in-stent restenosis is a feasible alternative to conventional angiography.

References

1. Nieman K, Cademartiri F, Lemos PA, Raaijmakers R, Pattynama PM, de Feyter PJ. Reliable noninvasive coronary angiography with fast submillimeter multislice spiral computed tomography. Circulation. 2002;106:2051-4.
2. Ropers D, Baum U, Pohle K, Anders K, Ulzheimer S, Ohnesorge B, Schlundt C, Bautz W, Daniel WG, Achenbach S. Detection of coronary artery stenoses with thin-slice multi-detector row spiral computed tomography and multiplanar reconstruction. Circulation. 2003;107:664-6.
3. Mahnken AH, Buecker A, Wildberger JE, Ruebben A, Stanzel S, Vogt F, Gunther RW, Blindt R. Coronary artery stents in multislice computed tomography: in vitro artifact evaluation. Invest Radiol. 2004;39:27-33.
4. Schuijf JD, Bax JJ, Jukema JW, Lamb HJ, Warda HM, Vliegen HW, de Roos A, van der Wall EE. Feasibility of assessment of coronary stent patency using 16-slice computed tomography. Am J Cardiol. 2004;94:427-30.
5. Eagle KA, Guyton RA, Davidoff R, Edwards FH, Ewy GA, Gardner TJ, Hart JC, Herrmann HC, Hillis LD, Hutter AM, Jr., Lytle BW, Marlow RA, Nugent WC, Orszulak TA. ACC/AHA 2004 guideline update for coronary artery bypass graft surgery: a report of the American College of Cardiology/American Heart Association Task Force on Practice Guidelines (Committee to Update the 1999 Guidelines for Coronary Artery Bypass Graft Surgery). Circulation. 2004;110:e340-437.
6. Gibbons RJ, Abrams J, Chatterjee K, Daley J, Deedwania PC, Douglas JS, Ferguson TB, Jr., Fihn SD, Fraker TD, Jr., Gardin JM, O'Rourke RA, Pasternak RC, Williams SV, Alpert JS, Antman EM, Hiratzka LF, Fuster V, Faxon DP, Gregoratos G, Jacobs AK, Smith SC, Jr. ACC/AHA 2002 guideline update for the management of patients with chronic stable angina--summary article: a report of the American College of Cardiology/American Heart Association Task Force on Practice Guidelines (Committee on the Management of Patients With Chronic Stable Angina). Circulation. 2003;107:149-58.
7. Chieffo A, Stankovic G, Bonizzoni E, Tsagalou E, Iakovou I, Montorfano M, Airoldi F, Michev I, Sangiorgi MG, Carlino M, Vitrella G, Colombo A. Early and mid-term results of drug-eluting stent implantation in unprotected left main. Circulation. 2005;111:791-5.
8. Park SJ, Kim YH, Lee BK, Lee SW, Lee CW, Hong MK, Kim JJ, Mintz GS, Park SW. Sirolimus-eluting stent implantation for unprotected left main coronary artery stenosis: comparison with bare metal stent implantation. J Am Coll Cardiol. 2005;45:351-6.
9. Baim DS. Is it time to offer elective percutaneous treatment of the unprotected left main coronary artery? J Am Coll Cardiol. 2000;35:1551-3.

10. Takagi T, Stankovic G, Finci L, Toutouzas K, Chieffo A, Spanos V, Liistro F, Briguori C, Corvaja N, Albero R, Sivieri G, Paloschi R, Di Mario C, Colombo A. Results and long-term predictors of adverse clinical events after elective percutaneous interventions on unprotected left main coronary artery. Circulation. 2002;106:698-702.
11. Kelley MP, Klugherz BD, Hashemi SM, Meneveau NF, Johnston JM, Matthai WH, Jr., Banka VS, Herrmann HC, Hirshfeld JW, Jr., Kimmel SE, Kolansky DM, Horwitz PA, Schiele F, Bassand JP, Wilensky RL. One-year clinical outcomes of protected and unprotected left main coronary artery stenting. Eur Heart J. 2003;24:1554-9.
12. Tan WA, Tamai H, Park SJ, Plokker HW, Nobuyoshi M, Suzuki T, Colombo A, Macaya C, Holmes DR, Jr., Cohen DJ, Whitlow PL, Ellis SG. Long-term clinical outcomes after unprotected left main trunk percutaneous revascularization in 279 patients. Circulation. 2001;104:1609-14.
13. De Winter SA, Hamers R, Degertekin M, Tanabe K, Lemos PA, Serruys PW, Roelandt JR, Bruining N. Retrospective image-based gating of intracoronary ultrasound images for improved quantitative analysis: the intelligate method. Catheter Cardiovasc Interv. 2004;61:84-94.
14. Hamers R BN, Knook M, Sabate M, Roelandt JRTC. A novel approach to quantitative analysis of Intravascular Ultrasound Images. Computers Cardiol. 2001;28:589-592.
15. Gilard M, Cornily JC, Rioufol G, Finet G, Pennec PY, Mansourati J, Blanc JJ, Boschat J. Noninvasive assessment of left main coronary stent patency with 16-slice computed tomography. Am J Cardiol. 2005;95:110-2.
16. Silvestri M, Barragan P, Sainsous J, Bayet G, Simeoni JB, Roquebert PO, Macaluso G, Bouvier JL, Comet B. Unprotected left main coronary artery stenting: immediate and medium-term outcomes of 140 elective procedures. J Am Coll Cardiol. 2000;35:1543-50.
17. Valgimigli M, van Mieghem CA, Ong AT, Aoki J, Granillo GA, McFadden EP, Kappetein AP, de Feyter PJ, Smits PC, Regar E, Van der Giessen WJ, Sianos G, de Jaegere P, Van Domburg RT, Serruys PW. Short- and long-term clinical outcome after drug-eluting stent implantation for the percutaneous treatment of left main coronary artery disease: insights from the Rapamycin-Eluting and Taxus Stent Evaluated At Rotterdam Cardiology Hospital registries (RESEARCH and T-SEARCH). Circulation. 2005;111:1383-9.
18. Babapulle MN, Joseph L, Belisle P, Brophy JM, Eisenberg MJ. A hierarchical Bayesian meta-analysis of randomised clinical trials of drug-eluting stents. Lancet. 2004;364:583-91.
19. Colombo A, Moses JW, Morice MC, Ludwig J, Holmes DR, Jr., Spanos V, Louvard Y, Desmedt B, Di Mario C, Leon MB. Randomized study to evaluate sirolimus-eluting stents implanted at coronary bifurcation lesions. Circulation. 2004;109:1244-9.
20. Morin RL, Gerber TC, McCollough CH. Radiation dose in computed tomography of the heart. Circulation. 2003;107:917-22.
21. Jakobs TF, Becker CR, Ohnesorge B, Flohr T, Suess C, Schoepf UJ, Reiser MF. Multislice helical CT of the heart with retrospective ECG gating: reduction of radiation exposure by ECG-controlled tube current modulation. Eur Radiol. 2002;12:1081-6.

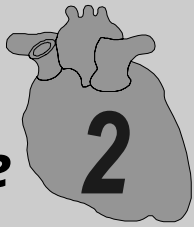

Interlude 2

Case Description

In-Stent Neo-Intimal Hyperplasia With 16-row Multislice CT Coronary Angiography

Nico R. Mollet [1,2]
Filippo Cademartiri [2]

From the Departments of
Cardiology [1]
and Radiology [2],
Erasmus MC,
University Medical Center
Rotterdam, The Netherlands

Circulation
2004;110(21):514

A 55-year-old woman was admitted with unstable angina pectoris. She had no risk factors for coronary artery disease. The admission ECG showed ST-depression in leads I, II, aVL, aVF, V2-V6. Serial Troponin T and cardiac enzyme measurements were normal. Multislice CT (MS-CT) coronary angiography, using a 16-row MS-CT scanner, showed a high-grade stenosis of the left main coronary artery with no other significant lesions (Figure 1a-c). Conventional angiography was performed the same day and confirmed the diagnosis. Immediate percutaneous intervention was undertaken and a bare-metal stent (diameter 5.0 mm, length 18 mm) was successfully implanted from the left main into the left anterior descending coronary artery with excellent final angiographic result.

Follow-up MSCT coronary angiography four months later showed moderate neo-intimal hyperplasia within the stent (Figure 2 a-b), which was confirmed by conventional angiography (Figure 2 c-d).

MSCT coronary angiography is a useful clinical tool for diagnosis and in-stent neo-intimal hyperplasia assessment of left main coronary artery disease.

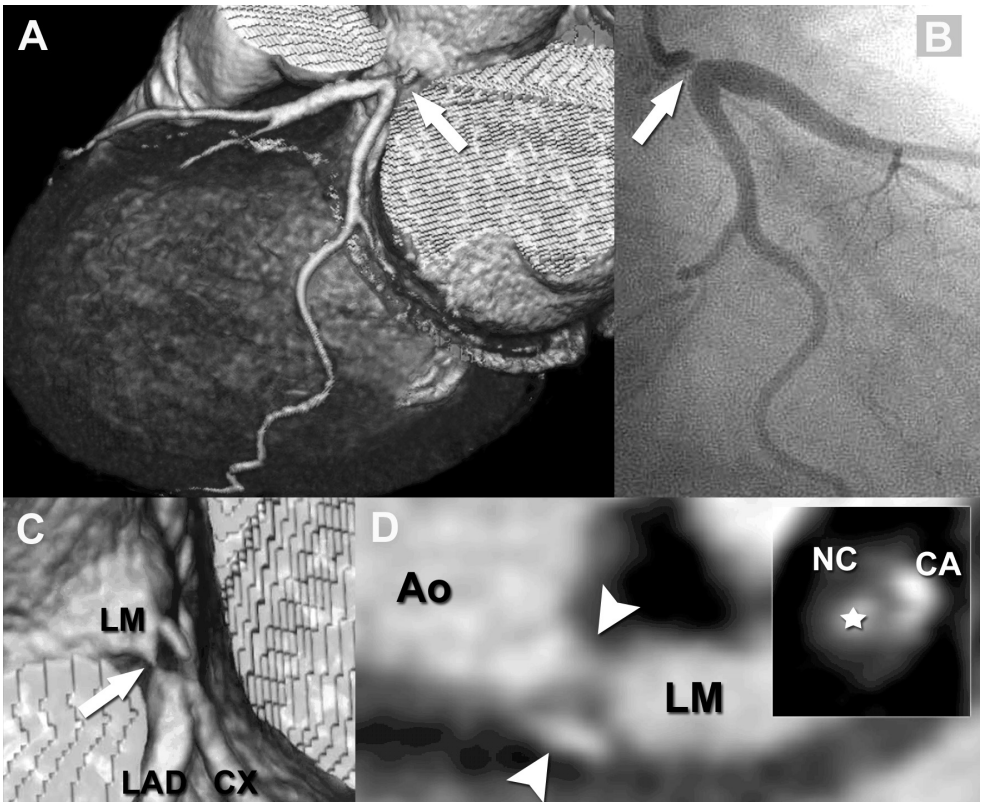

Figure 1. Volume Rendered (**A, B**) and Multiplanar Reconstruction (**C**) images show a high-grade stenosis of the left main coronary artery (arrows), afterwards confirmed on conventional angiography (arrow, **D**). A cross-sectional image of the lesion (inlay) shows calcified (CA) and non-calcified (NC) plaque tissue components surrounding the lumen (asterisk). (A full color version of this illustration can be found in the color section (chapter 21)).

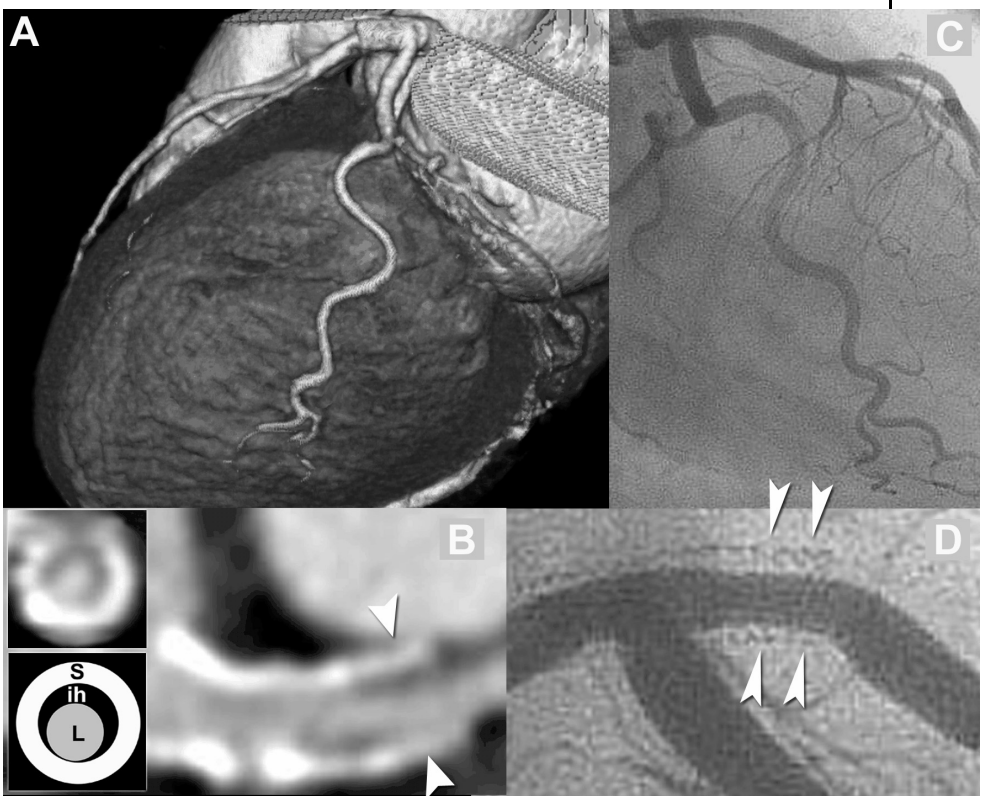

Figure 2. Volume Rendered image (**A**) and corresponding conventional angiography image (**D**) after 4 months follow-up. Figure **B** (including inlays) show moderate neo-intimal hyperplasia (ih) presenting as a dark rim surrounding the lumen (L), located at the distal part of the stent (S), afterwards confirmed on conventional angiography (arrowheads, **D**). (A full color version of this illustration can be found in the color section (chapter 21)).

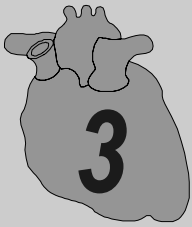

Interlude 3

LATE-LATE OCCLUSION AFTER INTRACORONARY BRACHYTHERAPY

Case Description

A57-year-old man with a history of anterior myocardial infarction in April 1997, initially treated with successful thrombolysis, underwent cardiac catheterization due to persistent postinfarction angina. Single-vessel disease, with a significant lesion in the left anterior descending coronary artery (LAD), was found. The patient was treated with balloon angioplasty followed by intracoronary beta radiation therapy according to the Beta Energy Restenosis Trial (BERT). He received 16 Gy at 2 mm from the centerline of the 90Sr/90Y source. He remained asymptomatic for 41/2 years. During this period, he underwent control angiography with the use of Intravascular Ultrasound (IVUS) at 6 months and 3 years, as mandated by protocol. After this period, he again developed angina, and an exercise test was positive for ischemia. Diagnostic coronary angiogram at almost 5 years revealed single-vessel disease, with totally occluded LAD with collateral filling from the right coronary artery. The angiographic sequence is presented in Figure 1. The IVUS images are presented in Figure 2. Before the reintervention, a 16-row, electrocardiographic-gated, cardiac, multislice spiral CT scan was also performed (Figure 3). An attempt at percutaneous recanalization was not successful, and the patient underwent coronary artery bypass surgery with implantation of the left internal mammary artery in the LAD.

Georgios Sianos [1]
Nico Mollet [1,2]
Sjoerd Hofma [1]
Pim J. de Feyter [1,2]
Patrick W. Serruys [1]

From the Departments of Cardiology [1] and Radiology [2] ErasmusMC, University Medical Center, Rotterdam, the Netherlands

Circulation
2003;108:69-70

Late-late occlusion after Intracoronary brachytherapy

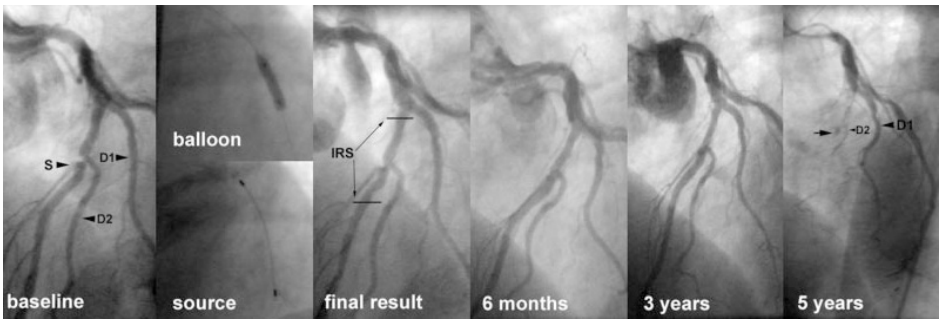

Figure 1. The LAD, filmed at the left anterior oblique and cranial projection. At baseline a severe focal lesion just before the bifurcation of the second diagonal branch (D2) with a septal perforator branch (S) was observed. A big first diagonal branch (D1) can also be seen. The patient was treated with balloon angioplasty (single dilatation with a 312-mm balloon at 12 atm) followed by catheter-based irradiation with the use of the 30-mm-long, 90Sr/90Y Beta-Cath source, with a good final result. The balloon and the radiation source were filmed in the right anterior oblique and cranial projection. The irradiated segment (IRS) is indicated by the 2 black horizontal lines in the "final result" frame. Control angiogram at 6 months and 3 years revealed well-preserved result without restenosis. At 5 years, there is severe lumen compromise throughout the length of the irradiated segment, with minimal contrast penetration up to the D2 and complete occlusion after its takeoff (arrow).

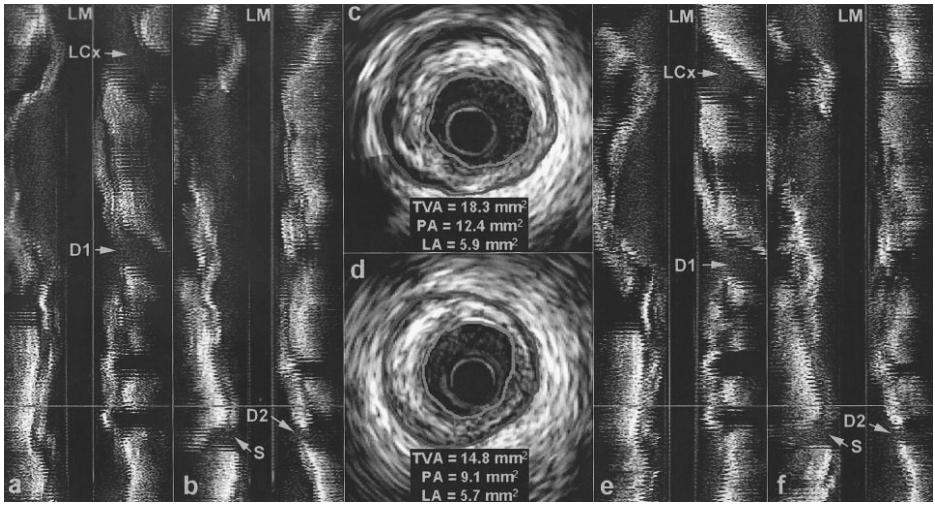

Figure 2. Left panels, Longitudinal intravascular ultrasound reconstruction of the LAD at 6 months follow-up, corresponding to the angiographic projection in Figure 1. The left main coronary artery (LM) is on top of the image and the distal LAD at the bottom. a, Slice showing the bifurcations with the left circumflex coronary artery (LCx) and the first diagonal branch (D1). b, Slice showing the bifurcations with the second diagonal (D2) and the septal (S) branches. There is a 60-degree difference between the planes of slices shown in panels a and b. Right panels, Longitudinal intravascular ultrasound reconstruction of the LAD at 3 years follow-up. Slice shown in panel e corresponds to that in panel a. Slice shown in panel f corresponds to that in panel b. Middle panel, Cross-sectional images corresponding to the site of the initial stenosis at baseline, just before the bifurcations of the LAD with the D2 and the septal branches, as indicated by the yellow and red horizontal lines at the longitudinal reconstructions shown in the lower half of the other panels, at 6 months (c) and 3 years (d). The red line delineates the external elastic membrane and the green line the lumen surface. Between 6 months and 3 years, a reduction in the total vessel area (TVA) can be observed (negative remodeling) with accompanying reduction in the plaque area (PA) (plaque regression). This results in an unchanged lumen area (LA) between 6 months and 3 years. (A full color version of this illustration can be found in the color section (Chapter 21)).

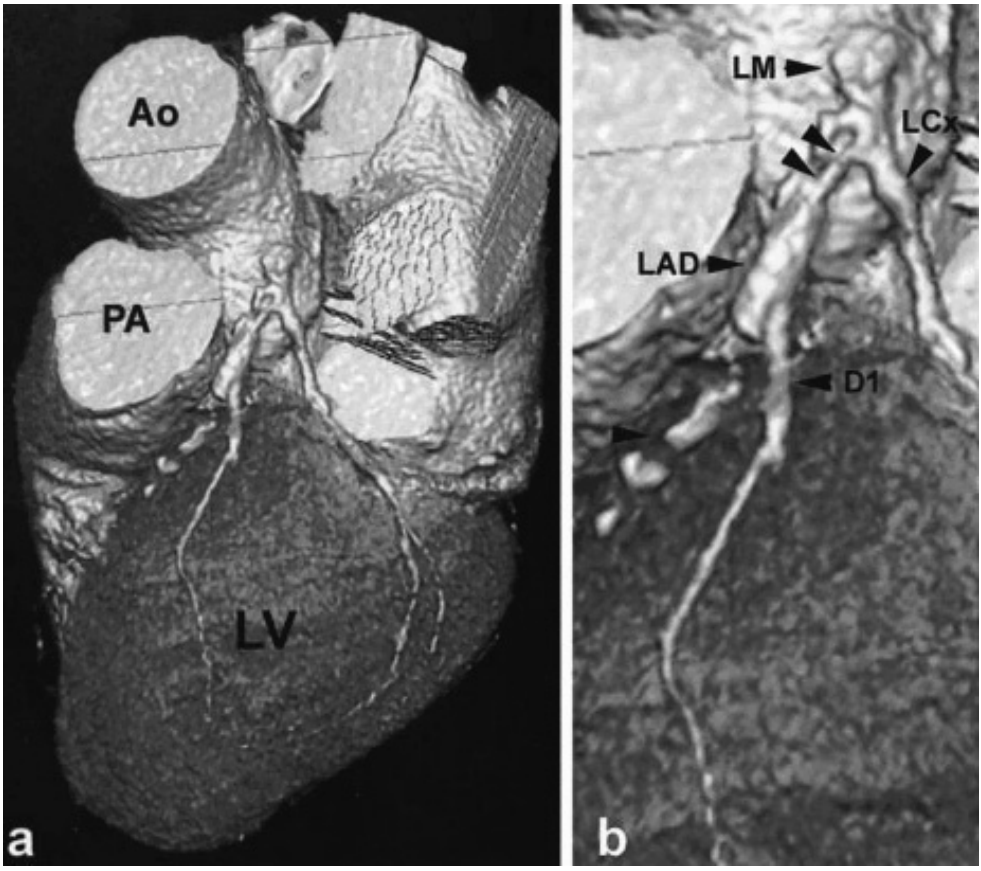

Figure 3. a, Electrocardiographic-gated multislice CT 3D volume-rendered image of the heart and the great vessels. The aortic root (Ao), the pulmonary artery (PA), and the left ventricle (LV) are clearly visible. b, Detailed picture of the left coronary artery corresponding to the angiographic frames in Figure 1. The left main coronary artery (LM) is divided into the left anterior descending (LAD) and the left circumflex (LCx) coronary arteries. A severe stenosis at the ostium of the LAD (double arrowhead) can be seen. This lesion was not obvious in the angiographic images presented, because of overlap of the ostium of the LAD with LCx. More distally, the LAD is occluded (arrowhead) after the takeoff of the first diagonal branch (D1), at the site of previous treatment with balloon dilatation and beta irradiation. (A full color version of this illustration can be found in the color section (Chapter 21)).

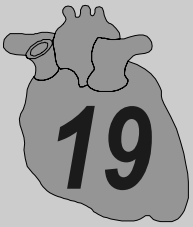

Chapter 19

ADJUNCTIVE VALUE OF CT CORONARY ANGIOGRAPHY IN THE DIAGNOSTIC WORK-UP OF PATIENTS WITH STABLE ANGINA PECTORIS

Nico R. Mollet [1,2]
Filippo Cademartiri [1,2]
Carlos Van Mieghem [1,2]
Giuseppe Runza [2]
Bob Meijboom [1,2]
Timo Baks [1,2]
Jolmer Dikkeboer [2]
Eugène P. Mc Fadden [1]
Eric Boersma [1]
Gabriel P. Krestin [2]
Pim.J. de Feyter [1,2]

From the Departments of Cardiology [1] and Radiology [2], Erasmus MC, University Medical Center, Rotterdam, The Netherlands

Submitted for publication

Abstract

AIMS

To determine the adjunctive value of CT coronary angiography (CTCA) in the diagnostic work-up of patients with stable angina.

METHODS AND RESULTS

CTCA was performed in 62 consecutive patients (45 male, mean age 58.8±7.7 years) with stable angina undergoing diagnostic work-up including exercise-ECG and conventional coronary angiography. Only patients with sinus heart rhythm and ability to breath hold for 20 seconds were included. Patients with initial heart rates ≥70 beats/minute received β-blockers. We determined the post-test likelihood ratios, to detect or exclude patients with significant (≥50% lumen diameter reduction) stenoses, of exercise-ECG and CTCA separately, and of CT performed after exercise-ECG testing.

The prevalence of patients with significant coronary artery disease (CAD) was 74%. Positive and negative likelihood-ratios for exercise-ECG were 2.3 (95%CI: 1.0-5.3) and 0.3 (95%CI: 0.2-0.7) and for CTCA 12.0 (95%CI: 1.8-78.4) and 0.0 (95%CI: 0.0-∞), respectively. CTCA increased the post-test probability of significant CAD after a negative exercise-ECG from 53% to 90%, and after a positive exercise-ECG from 89% to 100%, while CT correctly identified patients without CAD (probability 0%).

CONCLUSIONS

Non-invasive CTCA is a potentially useful tool, in the diagnostic work-up of patients with stable angina pectoris, both to detect and to exclude significant CAD.

INTRODUCTION

Stress-testing in patients with stable angina has demonstrated prognostic value; it is useful in selecting patients for coronary angiography and can help guide subsequent revascularization strategies. Current guidelines recommend stress-testing in the work-up of patients with stable angina and a treadmill exercise-ECG is the first-choice stress-test in the majority of patients [1-4]. Computed Tomography coronary angiography (CTCA) is a non-invasive technique that can reliably detect significant coronary stenoses in selected patient populations [5-14]. However, the value of CTCA in addition to exercise-ECG in the diagnostic work-up of patients with stable angina pectoris in the clinical setting is yet unknown.

We sought to establish the diagnostic value, to detect or exclude significant coronary artery disease (CAD), of exercise-ECG and CTCA, alone and in combination, in a consecutive cohort of patients with stable angina pectoris.

METHODS

Study Population

We studied 62 (45 male, mean age 58.8±7.7 years) consecutive patients who fulfilled all of the following criteria: stable angina pectoris, and 2 specific CT criteria: sinus heart rhythm, and ability to breath hold for ≥20 s. Of 103 patients eligible for inclusion, 41 patients were excluded with contra-indications (known allergy, serum creatinine >120 μmol/L, or thyroid disorders) to iodinated contrast (n=4), baseline ECG abnormalities precluding reliable exercise-ECG interpretation (≥1 mm rest ST-depression, complete left bundle-branch block, n=6), and inability to perform CTCA before conventional angiography for logistic reasons (n=23); Eight patient refused to participate in the study. Patients were recruited in a community hospital where the diagnostic work-up including exercise-ECG and conventional coronary angiography (CCA) was performed. CTCA was performed in a university hospital on an outpatient basis. The study complies with the Declaration of Helsinki. The institutional review boards of both hospitals approved the study protocol and all patients gave informed consent.

Patient Preparation

Patients with a heart rate above 70 beats/minute received a single oral dose of 100mg metoprolol ≥45min before the scan, unless contraindicated (e.g. overt heart failure or chronic obstructive pulmonary disease).

Scan Protocol, Image Reconstruction and Evaluation

All patients were scanned using a second generation 16-slice CT-scanner (Sensation16 Straton®, Siemens, Forchheim, Germany). Scan parameters were: 16x0.75mm collimation, rotation time 375ms, temporal resolution 188ms, table feed 3.0 mm/rotation, tube voltage 120kV, 600mAs, tube modulation was not applied. Radiation exposure was estimated as 11.8-16.3 mSv (WinDose®, Institute of Medical Physics, Erlangen, Germany). A bolus of 100ml contrast material (Iomeron®400, Bracco, Milan, Italy) was injected through an arm vein (4 ml/s) using a bolus-tracking technique to initiate the CT-scan (mean scan time: 18.2±1.0s). Datasets were reconstructed using ECG-gating and high image quality was generally obtained when datasets were reconstructed during the mid-to-end diastolic phase.

All available ≥2mm coronary branches were independently analysed by 2 observers, unaware of the results of CCA, using conventional post-processing techniques.

Quantitative Coronary Angiography

All CT-scans were performed within 4 weeks of CCA. A single observer, unaware of the results of CTCA, determined the diameter of all coronary branches using a quantitative algorithm (CAAS, Pie Medical, Maastricht, The Netherlands). All ≥2mm branches were included for comparison with CT. Stenoses were evaluated in two orthogonal views, and classified as significant if the mean lumen diameter reduction was ≥50%. Patients were labelled as having significant CAD if they had at least 1 significant coronary stenosis.

Exercise-ECG

Exercise-ECG was performed using a cycle ergometer and a protocol starting with an initial workload of 25W, followed by increments of 25W every 2 minutes. Heart rate and blood pressure were recorded at rest and at the end of each stage of exercise. A 12-channel electrocardiogram was obtained each minute and 3-channel monitoring of cardiac rhythm was performed continuously. Exercise-ECG examinations were classified as positive where there was horizontal or downsloping ST-segment depression of ≥1mm at 80 ms after the J-point [3]. Negative exercise-ECG tests in patients who did not reach the reference exercise capacity normalized for age, gender, and weight were classified as inconclusive.

Statistical Analysis

Descriptive statistics were used to evaluate the diagnostic performance of exercise-ECG and CTCA to detect patients with significant CAD, including sensitivity, specificity, positive and negative predictive value, and positive (Sensitivity /[1-Specificity]) and negative ([1-Sensitivity] / Specificity]) likelihood ratio's.

RESULTS

Patient characteristics of those included and excluded from the study are shown in Table 1. There were no significant differences between the 2 groups. Fifty percent (31/62) of the patients received a pre-scan β-blocker; mean heart rate during scanning was 59.3±8.3 beats/minute. One CT-examination was classified as inconclusive due to the presence of extensive motion artifacts (mean heart rate: 84 beats/minute). CCA revealed absence of significant stenoses in 26% (16/62), single vessel disease in 32% (20/62), and multi-vessel disease in 42% (26/62) of patients. Thus, the pre-test probability of significant CAD was 74%.

Diagnostic Performance of Exercise-ECG and CTCA

Nine exercise-ECG tests were classified as inconclusive. Sensitivity of exercise-ECG to detect significant CAD in the remaining 53 patients was 78% (95%CI: 62-92), specificity was 67% (95%CI: 34-90), and positive and negative predictive value was 89% (95%CI: 73-93) and 47% (95%CI: 22-72), respectively. Sensitivity of CTCA to detect significant CAD in 61 patients was 100% (95%CI: 91-100), specificity was 92% (95%CI: 61-99), and positive and negative predictive value was 98% (95%CI: 87-99) and 100% (95%CI: 71-100), respectively. Agreement between CCA and CTCA on a per-patient level was high (0.91, 95%CI: 0.78-1.0).

Positive and negative likelihood ratios to detect or exclude significant CAD were; 2.3 (95%CI: 1.0-5.3) and 0.3 (95%CI: 0.2-0.7) for exercise-ECG; 12.0 (95%CI: 1.8-78.4) and 0.0 (95%CI: 0.0-∞) for CTCA respectively.

Table 1. Patient characteristics

	Included patients N=62	Excluded patients N=41	*p*-value
Risk factors N (%)			
Hypercholesterolemia	43 (69)	27 (66)	NS
Systemic hypertension	42 (68)	24 (59)	NS
Smoking	25 (40)	18 (44)	NS
Family history of premature CAD	23 (37)	17 (41)	NS
Obese (BMI ≥30)	16 (26)	11 (27)	NS
Diabetes Mellitus	8 (13)	4 (10)	NS
Medication N (%)			
Aspirin	59 (95)	37 (90)	NS
β-blocker	51 (82)	34 (84)	NS
ACE inhibitors / AT-II antagonist	20 (32)	10 (24)	NS
Calcium-antagonist	20 (32)	14 (34)	NS
Nitrates (systemic)	18 (29)	9 (22)	NS
Statins	43 (69)	28 (68)	NS

Differences between both patient populations were calculated using the Mann-Whitney U-test. *p*-values <0.05 were considered significant. NS: Non-significant.

Exercise-ECG did not correctly classify 14 patients with significant CAD (9 false-negative and 5 inconclusive exercise-tests [Figure 1]). All patients with significant CAD were correctly classified on CT, and patients without significant CAD were correctly classified by CTCA in 13 of 16 cases (2 false-positive and 1 inconclusive scans [Figure 2]).

Diagnostic Performance of CTCA in Addition to Exercise-ECG to Detect Significant Stenoses

The post-test probability of significant CAD after a positive exercise-ECG test of 89% was refined by CTCA to respectively 100% (positive CT-scan) and 0% (negative CT-scan [Figures 3]). The post-test probability of significant CAD after a negative exercise-ECG test of 53% was refined by CTCA to respectively 90% (positive CT-scan [Figure 4]) and 0% (negative CT-scan).

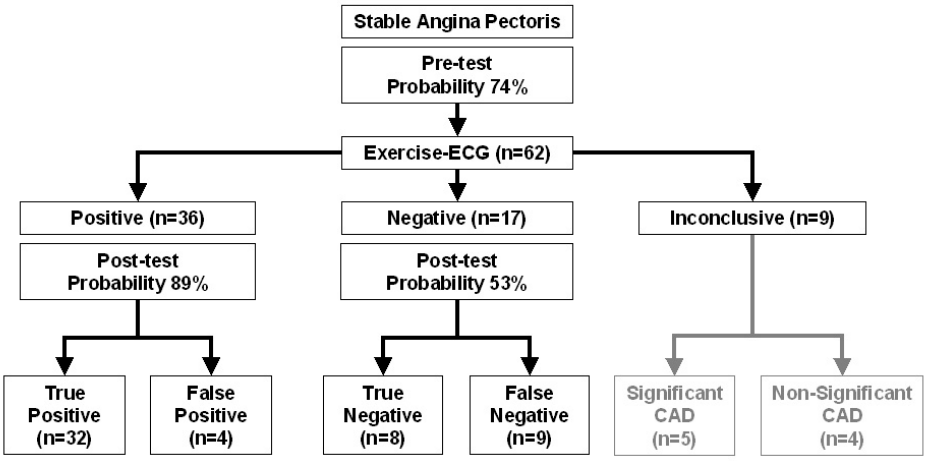

Figure 1. The diagnostic impact on the probability of significant coronary artery disease of exercise-ECG.

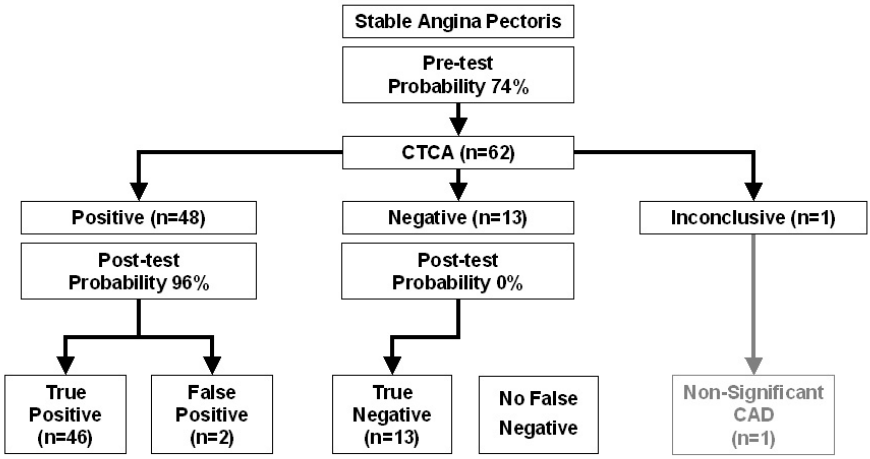

Figure 2. The diagnostic impact on the probability of significant coronary artery disease of CT coronary angiography. CTCA: CT Coronary Angiography.

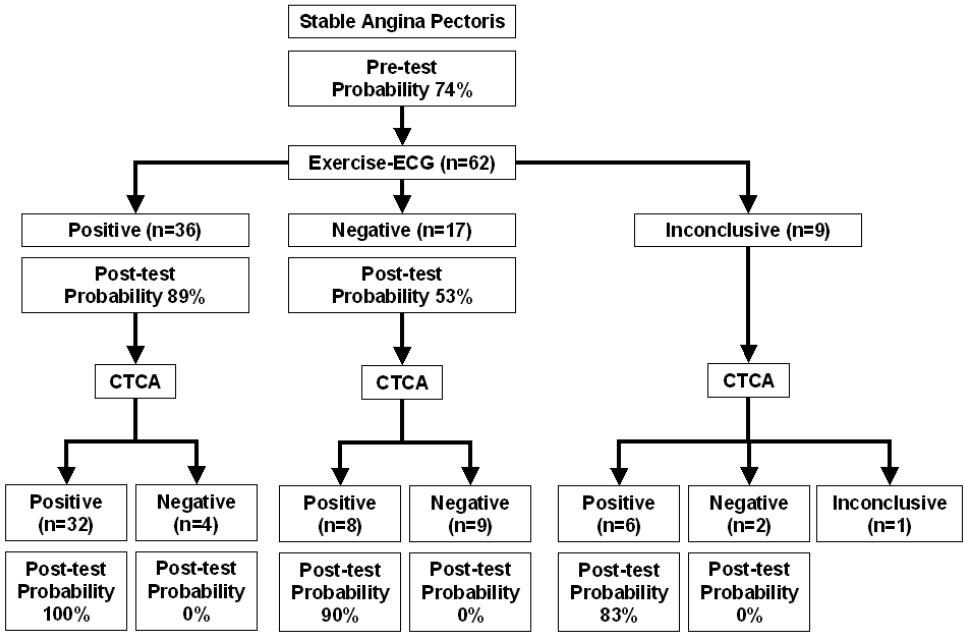

Figure 3. The diagnostic impact on the probability of significant coronary artery disease of CT coronary angiography as an adjunct to exercise-ECG. CTCA: CT Coronary Angiography.

The post-test probability of significant CAD after CTCA in patients with an inconclusive exercise-ECG test was respectively 83% (positive CT-scan [Figure 5]) and 0% (negative CT-scan).

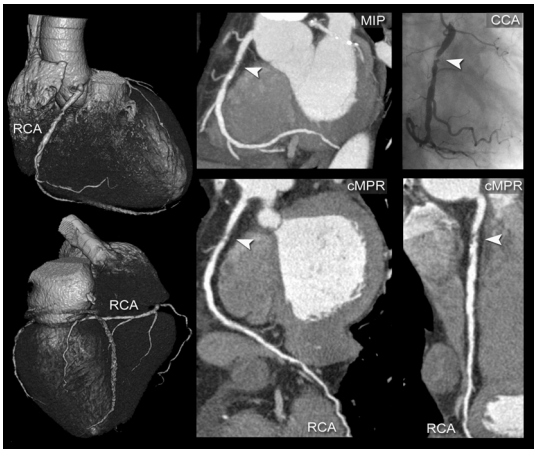

Figure 4. Example of CT vs. conventional coronary angiography in a patient with single vessel disease and a negative exercise-ECG test.
Volume rendered CT images (colored images) provide a nice anatomical overview of a dominant right coronary artery (RCA). Maximum intensity projected (MIP) and 2 orthogonal curved multiplanar reconstructed (cMPR) CT images indicate the presence of a significant stenosis at the proximal RCA (arrowhead), which was confirmed on the conventional coronary angiogram (CCA). (A full color version of this illustration can be found in the color section (Chapter 21)).

Figure 5. Example of CT vs. conventional coronary angiography in a patient with single vessel disease and an inconclusive exercise-ECG test.
A volume rendered CT image (colored image) suggests the presence of a significant stenosis of the proximal circumflex coronary artery. More detailed analyses using maximum intensity projected (MIP) curved multiplanar reconstructed (cMPR) post-processing techniques confirm these findings, which was also found on the conventional angiogram (CCA). (A full color version of this illustration can be found in the color section (Chapter 21)).

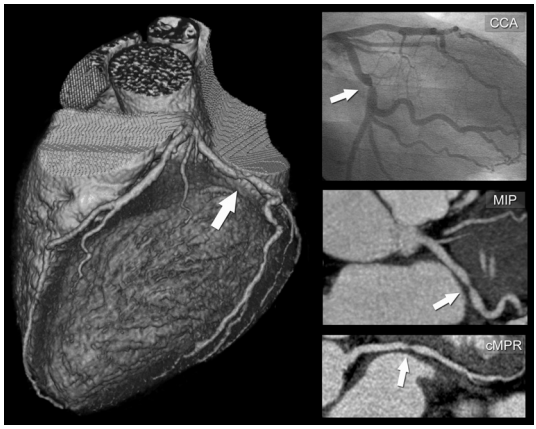

Discussion

We evaluated the role of CTCA in the diagnostic work-up of patients with stable angina pectoris and an intermediate-to-high pre-test probability of significant CAD. Direct referral for conventional diagnostic coronary angiography may be indicated when non-invasive testing is contra-indicated or when the pre-test probability of CAD is high. However, most of these patients will be candidates for a stress test prior to conventional coronary angiography.

Exercise-ECG testing is safe, inexpensive, and widely available. Current guidelines recommend documentation of exercise- or stress-induced ischemia in patients with stable angina who are evaluated for revascularization [1,2].

Patients with a positive exercise-ECG test will be further evaluated by diagnostic conventional coronary angiography to determine further management with percutaneous intervention, bypass surgery, or pharmacological treatment. Patients with a negative exercise-ECG require (depending on the level of clinical suspicion of the presence of CAD based upon history, physical examination, and rest-ECG), either further non-invasive diagnostic work-up, or referral for conventional coronary angiography, or a regular clinical follow-up on an outpatient basis.

In our study, we evaluated the diagnostic value of exercise-ECG alone, of CTCA alone, and in particular the additional value of CTCA after exercise-ECG in 62 consecutive patients with stable angina and an intermediate-to-high pre-test probability of significant CAD. The prevalence of significant CAD in our patient cohort was 74%. Our results show that exercise-ECG was able to correctly predict the presence or absence of significant CAD in 65% (40/62) of patients, whereas CTCA correctly classified all patients (46) with significant CAD, but misclassified 19% (3/16) of patients without significant CAD.

The post-test probability of significant CAD after a negative exercise-ECG test was 53%, which underlies such a high diagnostic uncertainty level that further diagnostic work-up is required. In this context, CTCA proved particularly useful; a positive CTCA increased the probability of significant CAD to 90% whereas a negative CTCA decreased it to 0%. Thus, the additional information provided by CTCA has potential to influence further management of patients with an intermediate pre-test likelihood (e.g. patients with stable angina but a negative stress test).

The post-test probability of significant CAD after a positive exercise-ECG test was 89%. The subsequent step in such patients, where indicated, is conventional diagnostic angiography, as the high probability of significant CAD in patients with stable angina pectoris and a positive stress test makes further non-invasive diagnostic work-up unhelpful. However, despite this high probability of disease, CTCA was able to even further perfect this to a post-test probability of 100% in case of a positive CT-scan and to 0% in case of a negative CT-scan.

The question remains what would be the role of CTCA in the diagnostic work-up of patients with a (very) high pre-test likelihood of significant CAD. According to the guidelines, the majority of patients with a high pre-test likelihood should undergo non-invasive testing, followed by diagnostic conventional coronary angiography to refer these patients for appropriate therapy. The findings of our pilot study suggest that CTCA may be used as an "intermediate" step to guide referral for percutaneous intervention (patients with 1- or 2-vessel disease) or bypass surgery (left main or 3-vessel disease). However, other investigators suggest that these patients should immediately be referred for a diagnostic coronary angiogram, followed in the same session by percutaneous intervention, thereby obviating the need for further non-invasive diagnostic tests including CTCA. In keeping with current guidelines, such an ad-hoc approach has several disadvantages when compared to a staged approach, which allows time to inform the patient about risks, benefits, and alternatives of the selected therapy as well as optimal hydration and pre-treatment with oral anti-platelet agents before coronary intervention [4]. In fact, the majority of patients who undergo elective percutaneous revascularization procedures in the Netherlands -as in many other European countries- are being sent to

referral hospitals after a complete diagnostic work-up including conventional coronary angiography in a community hospital without percutaneous intervention facilitations. For these reasons, CT coronary angiography may still be of use in patients with a high pre-test likelihood of significant CAD.

Larger prospective studies are needed evaluating the diagnostic value of CTCA in addition to stress testing in specific subgroups including patients with a lower pre-test likelihood of significant CAD (e.g. patients with atypical angina or non-cardiac chest pain) who potentially may benefit more from non-invasive testing. If such studies would confirm our initial results, CTCA may become a routinely used technique in the diagnostic work-up of patients suspected of having CAD.

Conclusions

While exercise-ECG testing provides important information that aids in the management of patients with stable angina, it is of limited diagnostic value for the detection of significant coronary disease. A combined diagnostic work-up of exercise-ECG testing and CTCA markedly improved the post-test probability of the presence or absence of significant CAD. CTCA has, however, specific limitations; it is only reliable in selected patients with a slow (<70 beats/minute, spontaneous or β-blocker induced), regular heart rhythm, who are able to breath hold for at least 20 s. Furthermore, the high radiation exposure associated with CTCA (11.8-16.3 mSv) is a matter of concern.

Acknowledgements

We would like to thank Michel P. Freericks, MD, Jacques P. Kerker, MD, and Stieneke K. Zoet, MD for their contribution to the study.

References

1. Management of stable angina pectoris. Recommendations of the Task Force of the European Society of Cardiology. Eur Heart J. 1997;18:394-413.
2. Gibbons RJ, Abrams J, Chatterjee K, Daley J, Deedwania PC, Douglas JS, Ferguson TB, Jr., Fihn SD, Fraker TD, Jr., Gardin JM, O'Rourke RA, Pasternak RC, Williams SV. ACC/AHA 2002 guideline update for the management of patients with chronic stable angina--summary article: a report of the American College of Cardiology/American Heart Association Task Force on practice guidelines (Committee on the Management of Patients With Chronic Stable Angina). J Am Coll Cardiol. 2003;41:159-68.
3. Gibbons RJ, Balady GJ, Bricker JT, Chaitman BR, Fletcher GF, Froelicher VF, Mark DB, McCallister BD, Mooss AN, O'Reilly MG, Winters WL, Antman EM, Alpert JS, Faxon DP, Fuster V, Gregoratos G, Hiratzka LF, Jacobs AK, Russell RO, Smith SC. ACC/AHA 2002 guideline update for exercise testing: summary article. A report of the American College of Cardiology/American Heart Association Task Force on Practice Guidelines (Committee to Update the 1997 Exercise Testing Guidelines). J Am Coll Cardiol. 2002;40:1531-40.

4. Smith SC, Jr., Dove JT, Jacobs AK, Kennedy JW, Kereiakes D, Kern MJ, Kuntz RE, Popma JJ, Schaff HV, Williams DO, Gibbons RJ, Alpert JP, Eagle KA, Faxon DP, Fuster V, Gardner TJ, Gregoratos G, Russell RO. ACC/AHA guidelines for percutaneous coronary intervention (revision of the 1993 PTCA guidelines)-executive summary: a report of the American College of Cardiology/American Heart Association task force on practice guidelines (Committee to revise the 1993 guidelines for percutaneous transluminal coronary angioplasty) endorsed by the Society for Cardiac Angiography and Interventions. Circulation. 2001;103:3019-41.
5. Nieman K, Cademartiri F, Lemos PA, Raaijmakers R, Pattynama PM, de Feyter PJ. Reliable noninvasive coronary angiography with fast submillimeter multislice spiral computed tomography. Circulation. 2002;106:2051-4.
6. Ropers D, Baum U, Pohle K, Anders K, Ulzheimer S, Ohnesorge B, Schlundt C, Bautz W, Daniel WG, Achenbach S. Detection of coronary artery stenoses with thin-slice multi-detector row spiral computed tomography and multiplanar reconstruction. Circulation. 2003;107:664-6.
7. Mollet NR, Cademartiri F, Nieman K, Saia F, Lemos PA, McFadden EP, Pattynama PMT, Serruys PW, Krestin GP, De Feyter PJ. Multislice Spiral CT Coronary Angiography in Patients With Stable Angina Pectoris. J Am Coll Cardiol. 2004;43:2265-70.
8. Martuscelli E, Romagnoli A, D'Eliseo A, Razzini C, Tomassini M, Sperandio M, Simonetti G, Romeo F. Accuracy of thin-slice computed tomography in the detection of coronary stenoses. Eur Heart J. 2004;25:1043-8.
9. Kuettner A, Trabold T, Schroeder S, Feyer A, Beck T, Brueckner A, Heuschmid M, Burgstahler C, Kopp AF, Claussen CD. Noninvasive detection of coronary lesions using 16-detector multislice spiral computed tomography technology: initial clinical results. J Am Coll Cardiol. 2004;44:1230-7.
10. Hoffmann U, Moselewski F, Cury RC, Ferencik M, Jang IK, Diaz LJ, Abbara S, Brady TJ, Achenbach S. Predictive value of 16-slice multidetector spiral computed tomography to detect significant obstructive coronary artery disease in patients at high risk for coronary artery disease: patient-versus segment-based analysis. Circulation. 2004;110:2638-43.
11. Mollet NR, Cademartiri F, Krestin GP, McFadden EP, Arampatzis CA, Serruys PW, de Feyter PJ. Improved diagnostic accuracy with 16-row multi-slice computed tomography coronary angiography. J Am Coll Cardiol. 2005;45:128-32.
12. Kuettner A, Beck T, Drosch T, Kettering K, Heuschmid M, Burgstahler C, Claussen CD, Kopp AF, Schroeder S. Diagnostic accuracy of noninvasive coronary imaging using 16-detector slice spiral computed tomography with 188 ms temporal resolution. J Am Coll Cardiol. 2005;45:123-7.
13. Hoffmann MH, Shi H, Schmitz BL, Schmid FT, Lieberknecht M, Schulze R, Ludwig B, Kroschel U, Jahnke N, Haerer W, Brambs HJ, Aschoff AJ. Noninvasive coronary angiography with multislice computed tomography. Jama. 2005;293:2471-8.
14. Achenbach S, Ropers D, Pohle FK, Raaz D, von Erffa J, Yilmaz A, Muschiol G, Daniel WG. Detection of coronary artery stenoses using multi-detector CT with 16 x 0.75 collimation and 375 ms rotation. Eur Heart J. 2005 (in press).

VALUE OF PREPROCEDURE MULTISLICE COMPUTED TOMOGRAPHIC CORONARY ANGIOGRAPHY TO PREDICT THE OUTCOME OF PERCUTANEOUS RECANALIZATION OF CHRONIC TOTAL OCCLUSIONS

Abstract

We performed multislice computed tomographic coronary angiography in 45 patients who had chronic total occlusions and were scheduled for percutaneous recanalization. Multivariate analysis identified a blunt stump (by conventional angiography), occlusion length >15 mm, and severe calcification (by multislice computed tomographic coronary angiography) as independent predictors of procedural failure.

Nico R. Mollet [1,2]
Angela Hoye [1]
Pedro A. Lemos [1]
Filippo Cademartiri [2]
Georgios Sianos [1]
Eugene P. McFadden [1]
Gabriel P. Krestin [2]
Patrick W. Serruys [1]
Pim J. de Feyter [1,2]

From the Departments of Cardiology [1], and Radiology [2], Erasmus MC, University Medical Center, Rotterdam, The Netherlands.

American Journal of Cardiology
2005;95:240–243

INTRODUCTION

Sixteen-row multislice spiral computed tomographic (MSCT) coronary angiography has recently been shown to allow reliable noninvasive evaluation of coronary morphology[1-3]. In the present study, we analyzed the potential of preprocedural MSCT coronary angiography to provide additional information and thus predict the procedural outcome in patients who had chronic total occlusion (CTO) and were referred for percutaneous coronary recanalization.

MATERIAL AND METHODS

Forty-five patients referred for percutaneous recanalization of ≥1 CTO lesion underwent MSCT coronary angiography before the coronary procedure (median interval 29 days, interquartile range 9 to 53). The diagnosis of CTO was made on diagnostic angiograms that demonstrated complete occlusion of a major epicardial coronary artery, which was deemed to be of ≥3 months' duration from the date from the previous angiogram, a clinical history of myocardial infarction, or onset of or a severe episode of prolonged anginal chest pain. In addition, inclusion into the study required a serum creatinine level <120 mmol/L, presence of sinus rhythm, and the ability to hold a breath for 20 seconds. The protocol was approved by the institutional review board, and all patients gave written informed consent.

Conventional angiographic assessment was performed by observers who were unaware of the results of MSCT scans. Parameters previously reported to have prognostic importance for procedural failure were assessed: absence of anterograde flow through bridging collaterals, absence of a tapered stump, presence of severe calcification at the occluded segment, side branch at the occlusion site, and tortuosity of the vessel proximal to the occlusion (defined as an angle >45° in any projection). Where possible, occlusion length was measured from the view with the longest lesion on quantitative coronary angiography as the distance between a stump and a distal vessel as visualized by anterograde filling through bridging collaterals. In addition, in some other patients, length was determined from the baseline angioplastic procedure film using a bilateral coronary injection.

Twenty-two patients who had a heart rate >65 beats/ min before multislice spiral computed tomography received an oral dose of 100 mg of metoprolol 1 hour before scanning. All examinations were performed with a 16-row MSCT scanner (Sensation 16, Siemens, Forchheim, Germany; collimation 16 x 0.75 mm, rotation time 420 ms, table feed 3.0 mm/rotation, tube voltage 120 kV, tube current 400 to 450 mAs). After intravenous administration of 120 ml of nonionic contrast material (Visipaque 320, Amersham Health, Little Chalfont, United Kingdom), an automatic bolus-tracking technique triggered the start of MSCT scanning. Images were reconstructed with retrospective electrocardiographic gating during the mid- to end-diastolic phase to provide nearly motion-free image quality; additional reconstruction windows (e.g., early diastolic phase) were explored when necessary. All MSCT scans were analyzed off-line by operators who were blinded to angiographic and procedural data. Parameters similar to those of conventional angiography were evaluated: a blunt rather than tapered stump, severe calcification, side branch at the occlusion site, proximal tortuosity, and occlusion length.

Severe calcification was defined as the presence of high-density plaques (≥130 HU) involving >50% of the coronary wall on a cros-ssectional image and localized within the occlusion stump or occluded segment.

All procedures were performed by operators who were highly experienced in the treatment of CTOs, with the interventional strategy left to the discretion of the operator. Wires were used in a stepwise progression, starting with a wire that had a relatively less traumatic tip (Graphix Intermediate, Boston Scientific Corporation, Miami, Florida) or a hydrophilic wire (Choice PT Plus, Boston Scientific Corporation, or Crosswire NT, Terumo Corporation, Tokyo, Japan) and progressing to stiffer wires (Miracle, Asahi Intec, Nagoya, Japan) and specialized technologies (Safe- Cross, Intraluminal Therapeutics, Carlsbad, New Mexico) [4,5]. Procedural failure was defined as an inability to cross the occlusion with a guidewire.

Multivariate logistic regression analyses were performed to identify angiographic and MSCT parameters associated with procedural failure (all univariate predictors with a *p* value ≤0.1 were tested for their multivariate predictive value, and final models were built by backward stepwise selection). Angiographic parameters assessed were those identified in previous studies[6]: the occluded artery, duration of occlusion, multivessel disease, anterograde and retrograde collateral filling, type of stump, side branch at the site of occlusion, calcific deposits, vessel tortuosity, and occlusion length 15 mm. The predictive strengths of the models were evaluated by means of the −2 log-likelihood statistic, and models' lack of fit with the Hosmer-Lemeshow test, and their global predictive accuracy were assessed by the C index (area under the receiver-operating characteristic curve).

Patients' mean age ±SD was 57.0 ± 10.1 years, 40 (89%) were men, 10 (22%) were diabetic, and 14 (31%) had multivessel disease. Forty- seven CTO lesions were treated. Angiographic measurement of CTO length was possible in 39 lesions (83%), 31 (66%) from the diagnostic film and an additional 8 (17%) from bilateral injection and assessment of retrograde collateral filling. The mean length of occlusion was longer by MSCT coronary angiography than by angiography (21.8 ± 18.6 vs. 14.6 ± 10.9 mm, respectively). Procedural data, including type and number of guidewires used, are presented in Table 1.

Table 1. Procedural Duration and Use of Contrast Material and Guidewires for Percutaneous Intervention of a CTO With Respect to Successful Versus Unsuccessful Recanalization

	Success (n =26 lesions)	Failure (n =21 lesions)	*p* Value
Mean total procedural time (min)	148 ± 61	148 ± 44	1.0
Mean volume of contrast used (ml)	451 ± 258	453 ± 265	1.0
Mean no. of wires	2.0 ± 1.2	2.1 ± 0.8	0.9
Wire type*			
Graphix Intermediate	20 (76.9%)	12 (57.1%)	0.2
Choice PT Plus	5 (19.2%)	3 (14.3%)	0.8
Crosswire NT	8 (30.8%)	10 (47.6%)	0.3
Miracle	5 (19.2%)	12 (57.1%)	<0.01
Intraluminal	3 (11.5%)	4 (19.0%)	0.5
Over-the-wire balloon support	15 (57.7%)	17 (81.0%)	0.1

*Wire type not mutually exclusive.

The only difference between success and failure was in the increased use of the Miracle wire in the failure group. Overall mean procedural time was 148 ± 53 minutes, with a mean fluoroscopic time of 47 ± 24 minutes. Overall, 45% of interventional procedures failed (Table 2). Success versus failure was not dependent on the operator or choice of interventional strategy. At univariate analysis, the following were associated with procedural failure: clinical assessment (occlusion duration ≥9 months), angiographic assessment (lack of anterograde collateral filling, a blunt rather than a tapered stump, and side branch at the occlusion site), and MSCT coronary angiographic assessment (a blunt rather than a tapered stump, severe calcification, and occlusion length >15 mm; Table 2).

Table 2. Clinical, Angiographic, and MSCT Coronary Angiography Lesion Characteristics (n = 47)

	Angiography				MSCT Coronary Angiography			
	Frequency (%)	Failure Rate (%)	OR (95% CI)	*p* Value	Frequency (%)	Failure Rate (%)	OR (95% CI)	*p* Value
Right coronary artery	43	50	1.45 (0.45–4.66)	0.5	—	—	—	—
Left anterior descending artery	43	40	0.72 (0.22–2.32)	0.6	—	—	—	—
Left circumflex artery	15	43	0.92 (0.18–4.64)	0.9	—	—	—	—
Occlusion duration ≥9 months	51	63	4.72 (1.36–16.39)	0.02	—	—	—	—
Multivessel disease	34	38	0.64 (0.19–2.20)	0.5	—	—	—	—
Anterograde filling	60	32	0.27 (0.08–0.94)	0.04	—	—	—	—
Retrograde collateral filling	72	44	0.92 (0.26–3.32)	0.9	—	—	—	—
Bridging collaterals	38	39	0.68 (0.21–2.25)	0.5	—	—	—	—
Tapered stump	60	25	0.12 (0.03–0.45)	<0.01	60	32	0.16 (0.03–0.73)	0.02
Stump morphology not determinable	0				15	43	0.25 (0.34–1.82)	0.2
Side branch at occlusion site	57	59	4.37 (1.23–15.54)	0.02	45	52	1.76 (0.55–5.64)	0.3
Severe calcification	34	50	1.39 (0.41–4.65)		38	67	4.44 (1.27–15.61)	0.02
Vessel tortuosity	23	64	2.75 (0.68–11.14)	0.2	21	50	1.31 (0.32–5.32)	0.7
Occlusion length >15 mm	26	67	3.39 (0.85–13.48)	0.08	51	63	4.72 (1.36–16.39)	0.02
Occlusion length not determinable	17	50	1.29 (0.28–5.94)	0.7	0	—	—	—
Overall	100	45	—		—	—	—	—

CI = confidence interval; MSCT = multislice computed tomography; OR = odds ratio.

When analyzed separately, the following "traditional" clinical and angiographic characteristics were identified as multivariate predictors of procedural failure: occlusion duration >9 months and stump morphology (Table 3). Separate multivariate analysis that assessed only MSCT coronary angiographic parameters identified the following predictors: occlusion length >15 mm, severe calcification, and stump morphology. Final best model testing for pooled clinical, angiographic, and MSCT parameters identified a blunt rather than a tapered stump (by angiography), occlusion length 15 mm (by MSCT coronary angiography), and severe calcification (by MSCT coronary angiography) as multivariate independent predictors of procedural failure (Figure 1).

Table 3. Angiographic and MSCT Coronary Angiographic Multivariate Predictors of Procedural Failure for Chronic Total Occlusion

Variable	Coefficient	Wald's Chi-square	DF	*p* Value	OR (95% CI)	-2 Log Likelihood	Hosmer-Lemeshow Test DF	Hosmer-Lemeshow Test *p* Value	C Index
Clinical/angiographic predictors						50.0	2	0.66	0.80
Occlusion duration >9 mo	1.27	3.30	1	0.07	3.56 (0.90–14.02)				
Tapered stump	-1.93	7.46	1	<0.01	0.15 (0.04–0.58)				
Constant	0.24	0.13	1	0.7					
MSCT coronary angiography predictors						44.2	6	0.99	0.84
Occlusion length >15 mm	1.86	5.21	1	0.02	6.39 (1.30–31.41)				
Severe calcification	2.49	6.51	1	0.01	12.01 (1.78–81.1)				
Stump morphology	—	5.63	2	0.06	—				
Blunt	1 (reference)	—	—	—	—				
Tapered	-2.19	5.23	1	0.02	0.11 (0.02–0.73)				
Not determinable	-2.65	3.46	1	0.06	0.07 (0.00–1.15)				
Constant	-0.45	0.26	1	0.6	—				
Clinical/angiographic + MSCT coronary angiographic predictors						41.0	5	0.60	0.85
Tapered stump*	-2.43	7.98	1	<0.01	0.09 (0.02–0.48)				
Occlusion length >15 mm	2.17	6.16	1	0.01	8.77 (1.58–48.76)				
Severe calcification	2.03	5.18	1	0.02	7.62 (1.33–43.74)				
Constant	-0.67	0.74	1	0.4	—				

*A -2 log-likelihood change in the global model if 1 variable is removed: tapered stump -10.7 (p <0.01 for change), occlusion length -8.2 (p <0.01), and calcification -6.6 (p = 0.01 for change).
DF = degrees of freedom; other abbreviations as in Table 2.

RESULTS

The current selection process of technically appropriate candidates for percutaneous recanalization of CTO is based on the evaluation of a relatively restricted number of clinical and angiographic characteristics. In this study, we show that noninvasive evaluation of patients who have CTO by preprocedural MSCT coronary angiography improves the ability to predict the outcome of a percutaneous recanalization attempt. Our findings indicate that MSCT coronary angiography may aid in the therapeutic decision making for patients who have CTO. In addition, accurate preprocedural characterization of CTO features may assist in outlining the therapeutic interventional strategy.

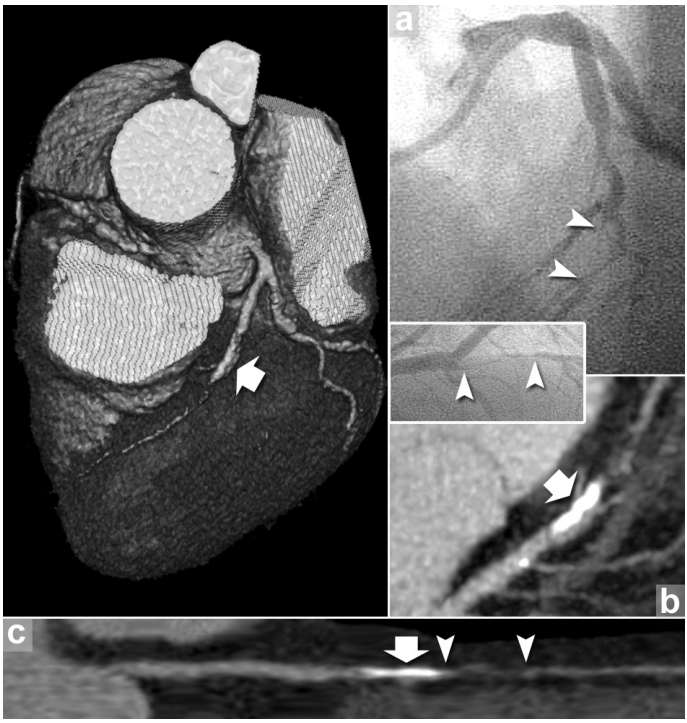

Figure 1. (**A**, inset) CTO of the left anterior descending coronary artery with favorable invasive angiographic CTO characteristics, tapered stump, absence of calcifications, and occlusion length <15 mm (*arrowheads*) in a patient who had been referred for percutaneous recanalization. Volume-rendered MSCT image that provides a 3-dimensional overview of the coronary arteries, and (**B**) maximum intensity projection of the same MSCT image show a severely calcified occlusion stump (*arrows*). (**C**) Curved multiplanar reconstructed MSCT image of the left anterior descending coronary artery shows a severely calcified stump (arrow) and an occluded segment (*arrowheads*). Collateral filling is clearly visible distal to the occlusion. This percutaneous attempt at recanalization of the CTO was unsuccessful. (A full color version of this illustration can be found in the color section (Chapter 21)).

MSCT coronary angiography of CTOs adds important information compared with "conventional" coronary angiography. The length of the occluded segment has long been identified as an important predictor of failed recanalization. However, accurate measurement of lesion length using conventional angiography may be difficult, mainly due to foreshortening, calibration limitations, and lack of visualization of the distal vessel in the absence of collateral filling. In the present study, lesion length could be measured in only 66% of diagnostic films. Conversely, MSCT coronary angiography allowed reliable 3-dimensional length measurement of coronary segments [7]. In the present series, when angiographic and MSCT coronary angiographic occlusion lengths were measured, results of the MSCT coronary angiography were "longer," perhaps reflecting the inaccuracy of quantitative coronary angiography as previously described. Moreover, MSCT coronary angiography allows evaluation of the morphology of the occlusion trajectory, including detailed delineation of coronary calcification. Long occlusions and severe calcifications on MSCT coronary angiograms were found to be important predictors of procedural failure,

whereas neither feature was identified as an independent predictor on conventional angiograms.

The need to use contrast material may pose a limitation to preprocedural MSCT coronary angiography for interventions scheduled to be performed shortly after scanning. However, the elective nature of CTO recanalization angioplasty allows a safe time lag between these procedures. In our study, multislice computed tomography was performed approximately 1 month before coronary intervention. The relatively high radiation exposure during MSCT coronary angiography, reportedly between 6.7 and 13.0 mSv[8-10], remains a matter of concern. However, MSCT coronary angiography may optimize therapeutic strategy (e.g., calcifications may require intraluminal techniques), resulting in shorter procedures. MSCT coronary angiography is currently feasible for selected patients, and further studies are needed to evaluate its value in a more general patient population.

REFERENCES

1. Nieman K, Cademartiri F, Lemos PA, Raaijmakers R, Pattynama PM, de Feyter PJ. Reliable noninvasive coronary angiography with fast submillimeter multislice spiral computed tomography. Circulation 2002;106:2051–2054.
2. Ropers D, Baum U, Pohle K, Anders K, Ulzheimer S, Ohnesorge B, Schlundt C, Bautz W, Daniel WG, Achenbach S. Detection of coronary artery stenoses with thin-slice multi-detector row spiral computed tomography and multiplanar reconstruction. Circulation 2003;107:664–666.
3. Mollet NR, Cademartiri F, Nieman K, Saia F, Lemos PA, McFadden EP, Pattynama PMT, Serruys PW, Krestin GP, De Feyter PJ. Multislice spiral CT coronary angiography in patients with stable angina pectoris. J Am Coll Cardiol 2004;43:2265–2270.
4. Ng W, Chen WH, Lee PY, Lau CP. Initial experience and safety in the treatment of chronic total coronary occlusions with a new optical coherent reflectometryguided radiofrequency ablation guidewire. Am J Cardiol 2003;92:732–734.
5. Hoye A, Onderwater E, Cummins P, Sianos G, Serruys P. Improved recanalization of chronic total coronary occlusions using an optical coherence reflectometry-guided guidewire. Catheter Cardiovasc Interv 2004;63:158 –163.
6. Puma JA, Sketch MH Jr, Tcheng JE, Harrington RA, Phillips HR, Stack RS, Califf RM. Percutaneous revascularization of chronic coronary occlusions: an overview. J Am Coll Cardiol 1995;26:1–11.
7. Ferencik M, Moselewski F, Ropers D, Hoffmann U, Baum U, Anders K, Pomerantsev EV, Abbara S, Brady TJ, Achenbach S. Quantitative parameters of image quality in multidetector spiral computed tomographic coronary imaging with submillimeter collimation. Am J Cardiol 2003;92:1257–1262.
8. Morin RL, Gerber TC, McCollough CH. Radiation dose in computed tomography of the heart. Circulation 2003;107:917–922.
9. Trabold T, Buchgeister M, Kuttner A, Heuschmid M, Kopp AF, Schroder S, Claussen CD. Estimation of radiation exposure in 16-detector row computed tomography of the heart with retrospective ECG-gating. Rofo Fortschr Geb Rontgenstr Neuen Bildgeb Verfahr 2003;175:1051–1055.
10. Hunold P, Vogt FM, Schmermund A, Debatin JF, Kerkhoff G, Budde T, Erbel R, Ewen K, Barkhausen J. Radiation exposure during cardiac CT: effective doses at multi-detector row CT and electron-beam CT. Radiology 2003;226:145–152.

Chapter 21

SUMMARY AND CONCLUSIONS

Nico R. Mollet

Technical Optimisation of Multislice Computed Tomography Coronary Angiography

Multislice Computed Tomography (MSCT) coronary angiography is a rapidly developing technique. Several technical features depending on CT scanner hardware characteristics are prerequisites to obtain good image quality, e.g. high spatial and temporal resolution, and fast data acquisition. These features have been progressively improved with the introduction of 16-slice, and more recently, 64-slice CT scanners (**Chapters 1-3**). Less recognized, but probably as important, is the fact that data acquisition and image reconstruction protocols must be optimised to achieve high quality scans. One of these issues is the correct use of contrast material. We observed that a better performance of CT coronary angiography to detect significant stenoses was achieved in patients with a higher intra-coronary contrast enhancement. This observation prompted us to evaluate the effect of various types of contrast material with a different Iodine content. We found that the use of contrast material with a high Iodine content (400 mg/ml) resulted in a significantly improved intra-coronary enhancement when compared to contrast materials with a lower Iodine content (**Chapter 4**). Another important parameter in the administration of intravenous contrast material is the injection flow rate. A higher flow rate generally results in higher intra-coronary enhancement, but requires administration of a larger amount of contrast material to maintain sufficient enhancement throughout the entire scan. We evaluated the use of a saline bolus chaser, which was injected immediately after the contrast bolus, to explore whether this contrast protocol resulted in a more effective utilization of contrast material.

The use of a bolus chaser allowed reduction with 35% of the total amount of contrast material administered during MSCT coronary angiography (**Chapter 5**). On the basis of these studies, we recommend the use of contrast material with a high Iodine content, injected with a high flow rate, and followed by a saline bolus chaser for the purpose of the detection of coronary stenoses with CT. Whether this contrast protocol should be used for the purpose of the detection and classification of different coronary plaque types remains controversial (see: Coronary Plaque Imaging With Multislice Computed Tomography Coronary Angiography).

Retrospective ECG-gating is always used in MSCT coronary angiography to reconstruct images during a certain phase of the cardiac cycle to diminish artifacts arising from rapid coronary motion throughout the cardiac cycle (**Chapter 2**). This technique allows flexibility in the positions of the reconstruction windows to define the optimal reconstruction interval to obtain maximum image quality on a per-vessel, and even per-segment, level. Other imaging modalities such as Magnetic Resonance Imaging or Electron-Beam CT use prospective ECG-triggering, a technique in which the positions of the reconstruction windows are pre-defined. We evaluated the potential benefit of image reconstruction using retrospective ECG-gating in patients with mild heart rhythm irregularities by manually repositioning the reconstruction windows (so called ECG-editing). We found an important increase in the number of assessable coronary segments after ECG-editing when compared to standard image reconstruction resulting in a higher diagnostic accuracy of MSCT coronary angiography to detect significant stenoses (**Chapter 6**). However, it should be noted that patients with severe heart rhythm irregularities (e.g. atrial fibrillation with rapid ventricular response) should be excluded from MSCT coronary angiography due to the presence of extensive motion artifacts on the CT scan, which cannot be corrected by ECG-editing.

Multislice Computed Tomography Coronary Angiography for the Detection of Obstructive Coronary Artery Disease

MSCT coronary angiography is a promising technique to non-invasively detect coronary stenoses. We explored the diagnostic performance of several generations CT scanners in various patient populations and compared these results with quantitative coronary angiography (QCA). We used a first-generation 16-slice CT scanner to study a selected group of patients with stable angina pectoris (**Chapter 7**). We included all available ≥2 mm coronary segments and found a high sensitivity and specificity (both above 90%) to detect significant (defined as ≥50% lumen diameter reduction) coronary stenoses. These results were an important improvement when compared to the results of previously published studies using 4-slice CT scanners. These studies reported already considerably high diagnostic accuracy values, however, up to 30% of the included vessels were excluded from the comparative analysis due to impaired image quality related to coronary calcifications or motion artifacts. We also studied a population comprising patients with atypical chest pain and stable angina pectoris after the introduction of a second-generation 16-slice CT scanner. These scanners are equipped with a faster *X*-ray tube rotation speed and have the ability to scan with a higher tube current during MSCT coronary angiography, resulting in a higher temporal resolution and improved contrast-to-noise ratio.

Again we included all available ≥2 mm segments, and found a remarkably high diagnostic accuracy to detect significant coronary stenoses (**Chapter 8**). Most recently, the latest generation CT scanner was introduced. These scanners render 64-slices per rotation, have a thinner individual detector width, and are able to scan the entire heart within a single breath hold of approximately 12 seconds. Moreover, these scanners have an increased spatial resolution (resulting in an isotropic voxel of 0.4 mm^3) due to the development of sophisticated z-axis flying focus technology. These improved technical features prompted us to evaluate the diagnostic accuracy of 64-slice CT coronary angiography in a consecutive group of patients with atypical chest pain, stable or unstable angina pectoris, or non-ST segment elevated myocardial infarction. We included the entire coronary tree using a 17-segment AHA classification model and found a sensitivity of 99% and a specificity of 95% to detect significant stenoses on a per-segment based analysis (**Chapter 9**). These values indicate that MSCT coronary angiography using state-of-the-art 64-slice scanners is a reliable technique to detect significant coronary artery disease and might be used as an alternative to diagnostic conventional coronary angiography in a selected patient population.

Pitfalls of Multislice Computed Tomography Coronary Angiography in the Detection of Obstructive Coronary Artery Disease

Coronary calcification is a marker of coronary artery disease. The presence and extent of coronary calcification is depending on age and gender and does not reliably correlate with the presence of significant coronary stenoses. Large deposits of calcification in the coronary vessel wall cause beam-hardening, partial voluming, and blooming artifacts on CT. These artifacts result in overestimation of the degree of the lumenal encroachment of calcified lesions, which may cause false positive findings on the CT scan. The amount of coronary calcification can be quantified using dedicated software after performing a low-dose, non-enhanced CT scan. It has been suggested that coronary calcium scoring can be used as a yardstick for the quality of MSCT coronary angiography. We explored the impact of coronary calcification on the diagnostic accuracy of MSCT coronary angiography to detect significant stenoses in 2 groups of patients with a low and with a high calcium score (**Chapter 10**). We demonstrated that, although the diagnostic performance of this technique is less in patients with a high calcium score, this still allowed accurate assessment of the coronary integrity in the majority of cases. We therefore concluded that patients with a high calcium load may also benefit from this non-invasive technique, in contrast to the results of previously published studies.

The limited resolution of MSCT coronary angiography combined with the presence of calcification related artifacts preclude application of software able to detect and quantify the degree of coronary stenoses. For these reasons, only a qualitative scoring to detect significant coronary stenoses can be applied with MSCT coronary angiography. However, qualitative scoring is highly operator-dependent. We explored the use of an interactive image evaluation protocol allowing the use of all available post-processing techniques on a dedicated cardiac workstation, and compared the diagnostic performance to detect significant stenoses with that of an image evaluation protocol only including standard projections that can be used on any digital archiving workstation (**Chapter 11**).

We found that the use of standard projections resulted in a significantly lower sensitivity as compared to the interactive approach, while specificity was maintained using both image evaluation protocols. This study demonstrates that MSCT coronary angiograms should be analysed by highly experienced observers able to use all available post-processing techniques.

Coronary Plaque Imaging With Multislice Computed Tomography Coronary Angiography

MSCT coronary angiography permits non-invasive evaluation of both the coronary lumen as well as the coronary vessel wall. Coronary plaques can be detected and classified into calcified, non-calcified, and mixed plaques, and their impact on the coronary lumen can be evaluated. We evaluated the coronary plaque burden (defined as the extent, size, type, and anatomical distribution of coronary plaques) in a selected population of patients with stable angina pectoris and a low pre-scan heart rhythm using a first-generation 16-slice scanner (**Chapter 12**). We detected plaque in 57% of all available ≥2 mm coronary segments and found that plaques were predominantly located in proximal and mid parts of the main coronary arteries, which is consistent with previously reported pathology studies. We also evaluated the coronary plaque burden in a population comprising patients with stable and unstable angina pectoris using a second-generation 16-slice CT scanner. We compared these results with the appearance of coronary plaques on conventional coronary angiography, and, in a subset of patients, with intra-vascular ultrasound (**Chapter 13**). We found a good diagnostic accuracy to detect significant plaques (defined as ≥1 mm plaque thickness on intra-vascular ultrasound), with a high sensitivity for the detection of calcified or mixed plaques and a somewhat lower sensitivity for the detection of non-calcified plaques. We found plaques with CT in 62% of all available ≥2 mm segments, and in one third of segments classified as normal on the conventional coronary angiogram. In addition, patients with unstable angina pectoris had significantly more non-calcified plaques when compared to patients with stable angina. These studies demonstrate the potential of MSCT coronary angiography in the assessment of the coronary plaque burden, but additional follow-up studies are needed to determine its clinical value.

Preliminary reports suggested that MSCT coronary angiography is able to classify non-calcified plaques into fibrous and soft plaques on the basis of density measurements expressed as Hounsfield units. However, we experienced high intra-plaque variability in Hounsfield units of coronary plaques and noted increased attenuation values in parts of plaques nearby the adjacent contrast-enhanced coronary lumen. This observation prompted us to evaluate the impact of intra-vascular attenuation of the coronary lumen on intra-plaque density measurements. In a first, preliminary study, we performed CT angiography in explanted left coronary artery specimens with increasing concentrations of contrast material and found that coronary plaque attenuation is significantly modified by lumen attenuation (**Chapter 14**). This observation was confirmed in a second study, in which we performed both an ex-vivo and in-vivo evaluation to explore the impact of different contrast attenuation values on plaque attenuation measurements.

We found that increased intra-coronary attenuation is associated with progressively higher plaque attenuation of non-calcified plaque tissue, whereas calcified plaque tissue and surrounding epicardial fat are not significantly affected (**Chapter 15**). This observation demonstrates that a high intra-coronary enhancement, which is beneficial for the detection of significant stenoses, may preclude reliable distinction between lipid-rich and fibrous plaques on the basis of absolute attenuation values. Further studies should focus on the development of calibration factors able to correct coronary plaque attenuation on the basis of intra-coronary attenuation values.

In conclusion, MSCT coronary angiography provides important information regarding the presence and extent of coronary atherosclerosis. This technique could be used for the assessment of several vulnerable plaque characteristics or as a roadmap for the application of other non-invasive or invasive imaging modalities able to assess specific vulnerable plaque features, such as Magnetic Resonance Imaging, Thermography, Palpography, Virtual Histology, or Optical Coherence Tomography (**Chapter 16**).

Multislice Computed Tomography Coronary Stent Imaging

MSCT coronary angiography could be of value in the non-invasive follow-up of stent implantation. Initial studies evaluating the diagnostic performance of MSCT coronary angiography to detect stent patency used the distal run-off of contrast material as a main criterion, because image quality of the in-stent lumen was insufficient to detect in-stent re-stenosis. However, occluded stents sometimes have extensive collateral retrograde filling, mimicking distal run-off of contrast material and, if unnoticed, these stents would be incorrectly classified as patent. Thus, direct visualization of the in-stent lumen is a prerequisite to reliably detect in-stent re-stenosis with CT. We performed the first study in which a comprehensive analysis including evaluation of the in-stent lumen was used. We compared the results of 16-slice MSCT coronary angiography with that of conventional angiography and found promising diagnostic accuracy values to detect significant in-stent re-stenosis (**Chapter 17**). Patients after percutaneous intervention of the left main coronary artery are a group of patients of particular interest to non-invasively detect in-stent re-stenosis. These patients need to be monitored intensively because in-stent re-stenosis of the left main coronary artery may result in sudden cardiac death. Left main stents are more reliably visualized with MSCT when compared to stents located in other parts of the coronary tree due to their larger size and lesser mobility. We performed a study comparing the results of MSCT coronary angiography with that of conventional angiography and intra-vascular ultrasound to detect in-stent re-stenosis in drug-eluting left main coronary stents (**Chapter 18**). We found a high diagnostic accuracy of MSCT coronary angiography to detect significant in-stent re-stenosis, but these results should be interpreted with caution, because the numbers of diseased stents (as expected due to the application of drug-eluting stents) were small.

Clinical Applications of Multislice Computed Tomography Coronary Angiography

Several studies reported a high diagnostic accuracy of MSCT coronary angiography to detect significant coronary stenoses using 16-, and 64-slice CT scanners (see: Multislice Computed Tomography Coronary Angiography in the Detection of Obstructive Coronary Artery Disease).

However, clinical application of MSCT coronary angiography is still limited, because studies evaluating the role of MSCT in the work-up of patients with suspected or known coronary artery disease are not available yet. We investigated the diagnostic value of MSCT coronary angiography in addition to exercise-ECG in a consecutive group of patients with stable angina pectoris and a relatively high (74%) pre-test likelihood of significant coronary artery disease (**Chapter 19**). We found that all patients with significant stenoses were correctly identified on the CT scan, whereas 28% of these patients remained undetected with exercise-ECG. MSCT coronary angiography was especially useful in patients with a negative exercise-ECG test and an intermediate (53%) likelihood of disease by increasing the likelihood to 90% and 0% in case of a positive or negative CT scan, respectively. This preliminary study demonstrated the potential of MSCT coronary angiography in the diagnostic work-up of patients with stable angina pectoris. This technique may particularly be useful in the setting of a local community hospital that is not equipped with a catheterization laboratory. Further studies are needed to determine the role of MSCT coronary angiography in other patient populations.

MSCT coronary angiography provides reliable non-invasive information regarding coronary morphology, which may be of help in patients requiring complex percutaneous coronary intervention procedures. Of particular interest are patients scheduled for percutaneous recanalization of a chronic total occlusion of a coronary artery. Selection of these patients is based on several angiographic occlusion features, which are known to have prognostic value in the outcome of a percutaneous recanalization procedure. However, even in selected patients, failure rates of more than 40% have been reported in most recent series. We explored the additional value of MSCT coronary angiography to predict the outcome of percutaneous recanalization of a chronic total occlusion as compared to diagnostic conventional coronary angiography (**Chapter 20**). We found that MSCT coronary angiography added important information to the conventional angiogram, whereas both occlusion length and presence of severe calcifications, as determined by CT, significantly improved the ability to predict the outcome of a percutaneous recanalization attempt. This observation may result in an improved patient selection for percutaneous recanalization of a chronic total occlusion, which should be the focus of further studies.

Conclusions

MSCT coronary angiography is able to visualize both the coronary lumen and the coronary vessel wall. Excellent results have been published for the detection of significant coronary stenoses in selected patients. Based on currently available literature, clinical application of this technique appear to be feasible in the evaluation of patients with an intermediate pre-test likelihood of the presence of a significant coronary stenosis, the follow-up of patients who previously underwent bypass surgery, the follow-up of coronary stents located in proximal branches, the evaluation of chronic total coronary occlusion prior to percutaneous recanalization, and coronary artery anomalies. However, the results of ongoing multi-center studies with a large number of included patients with different prevalences of coronary artery disease are needed to determine its real clinical potential.

Coronary plaque imaging with MSCT coronary angiography is of particular interest, whereas this technique provides information regarding the presence, extent, type, size, and anatomical distribution of coronary plaques. Such a comprehensive, non-invasive assessment of coronary plaques may have prognostic value and may enhance our understanding in the development of coronary atherosclerosis. Development of software able to quantify the coronary plaque load (including both non-calcified and calcified plaque tissue) may create the possibility to monitor the development of coronary atherosclerosis or the response to treatment after administration of lipid-lowering drugs. However, many problems related to clinical implementation of MSCT coronary angiography still need to be resolved. Training of future operators is essential before this technique may become part of the routine diagnostic armamentarium. Operators need to be extensively trained in CT technology and cardiac pathophysiology, requiring the input of both Radiology and Cardiology knowledge. Cooperation between the Radiology and Cardiology departments in the field of cardiac CT was the starting point of success in the Erasmus Medical Center, and hopefully many more institutes will follow our approach in order to improve the quality of patient-care.

Chapter 21

SAMENVATTING EN CONCLUSIES

Nico R. Mollet

Technische Optimalisatie van Multislice CT Coronair Angiografie

Multislice Computed Tomography (MSCT) is een techniek in volle ontwikkeling. Bepaalde factoren die te maken hebben met de hardware van een CT scanner bepalen een goede beeldkwaliteit, bv. een goede spatiële en temporele resolutie en een snelle data acquisitie. Deze factoren zijn recent aanzienlijk verbeterd met de introductie van de 16- en 64-slice CT scanners (**Hoofdstukken 1-3**). Minder bekend, maar waarschijnlijk net zo belangrijk, is het feit dat de data acquisitie en beeldreconstructie protocollen ook geoptimalizeerd moeten worden om CT scans met een goede beeldkwaliteit te verkrijgen. Een goed contrast middel protocol is hier een voorbeeld van. Uit ervaring hadden we reeds ondervonden dat significante vernauwingen t.h.v. de kransslagaders bij patiënten met een goede aankleuring van contrastmiddel beter gedetecteerd werden dan bij patiënten met een minder goede aankleuring. Om deze reden hebben we het effect van verschillende contrast materialen met verschillende concentraties Iodium op de contrast aankleuring in de kransslagvaten onderzocht. Wij ontdekten dat een significant betere aankleuring werd verkregen als een contrast middel werd toegediend met een hoog concentratie Iodium (400 mg/ml) dan wanneer andere contrast middelen met een lager Iodium concentratie werden gebruikt (**Hoofdstuk 4**).

Een andere belangrijke parameter bij het toedienen van een contrast middel is de snelheid waarmee het contrast wordt ingespoten. Als een contrast middel sneller wordt ingespoten wordt in het algemeen een betere aankleuring van de kransslagvaten verkregen, maar vereist een grotere hoeveelheid contrast middel om de kransslagvaten gedurende een bepaalde tijd aan te laten kleuren.

Wij hebben onderzocht of een zoutoplossing, die direct na toediening van het contrast middel werd ingespoten, resulteerde in een efficiënter gebruik van dit contrast middel. Wij ontdekten dat, door het gebruik van deze zoutoplossing, er 35% minder contrast middel nodig was om een goede aankleuring t.h.v. de kransslagaders te verkrijgen (**Hoofdstuk 5**). Op basis van deze waarnemingen adviseren we om vernauwingen van de kransslagaders zo betrouwbaar mogelijk vast te kunnen stellen, een contrast middel met een hoog Iodium gehalte te gebruiken, dit middel met een hoge snelheid toe te dienen en direct na de contrast-injectie een zoutoplossing in te spuiten. Of dit contrast protocol geschikt is om plaques t.h.v. de kransslagvaten op te sporen en onder te verdelen in vershillende plaque types blijft voorlopig nog controversieel (zie: Evaluatie van Kransslagader verkalking Met Multislice Computed Tomografie Coronair Angiografie).

Om artefacten als gevolg van het bewegen van de kransslagvaten tijdens de hartcyclus te voorkomen, worden bij Multislice CT coronair angiografie de beelden altijd retrospectief aan het ECG gekoppeld (zgn. "ECG-gating"), waardoor het mogelijk is om beelden te reconstrueren gedurende een specifieke fase van de hartcyclus (**Hoofdstuk 2**). Deze techniek laat het toe om, nadat de scan uitgevoerd is, achteraf de meest optimale fase van de hartcyclus te kiezen waardoor optimale beeldkwaliteit wordt verkregen van een kransslagvat. Andere beeldvormende technieken zoals Magnetische Resonantie of Electron-Beam CT gebruiken een andere, prospectieve manier om beelden te koppelen aan de hartcyclus (zgn. "ECG-triggering"). Deze techniek laat niet toe om het juiste moment te zoeken na afloop van de scan, gezien alleen gedurende een voorafbepaalde fase van de hartcyclus data verkregen wordt. Wij hebben onderzocht of de "ECG-gating" techniek gebruikt kan worden om bewegingsartefacten als gevolg van een onregelmatige hartslag te verminderen. Hiervoor werden er op basis van het ECG verschillende tijdstippen van de hartcyclus gekozen om één dataset (een verzameling van beelden) te reconstrueren (zgn. "ECG-editing"). Wij ontdekten dat er significant meer segmenten van de kransslagaders beoordeeld konden worden m.b.v. "ECG-editing" dan wanneer datasets werden gereconstrueerd zonder deze techniek. Dit vertaalde zich in een betere detectie van significante vernauwingen t.h.v. de kransslagaders (**Hoofdstuk 6**). Patiënten met een erg onregelmatige hartslag (bv. voorkamer fibrilleren met een snelle respons van de kamers) komen echter niet in aanmerking voor MSCT coronair angiografie door de aanwezigheid van belangrijke bewegingsartefacten die niet gecorrigeerd kunnen worden m.b.v. "ECG-editing".

Multislice Computed Tomografie Coronair Angiografie om Vernauwingen van de Kransslagvaten op te Sporen

MSCT coronair angiografie is een veelbelovende techniek om op een patiëntvriendelijke manier vernauwingen t.h.v. de kransslagvaten op te sporen. Wij hebben verschillende patiëntengroepen m.b.v. verschillende generaties CT scanners onderzocht en hebben de resultaten van de CT scans vergeleken met de resultaten van een hartkatheterisatie. Bij de beoordeling van de hartkatherisatie gebruikten we speciale software om de vernauwingen exact te kunnen meten (zgn. 'quantitative coronary angiography'). Allereerst hebben we een 1ste generatie 16-slice CT scanner gebruikt om een patiëntengroep met stabiele angina pectoris te onderzoeken (**Hoofdstuk 7**).

We hebben alle anatomisch aanwezige segmenten met een minimum diameter van ≥2 mm beoordeeld en vonden een hoge sensitiviteit en specificiteit (beiden meer dan 90%) om significante vernauwingen (≥50% lumen diameter reductie) van de kransslagvaten op te sporen. Deze resultaten waren duidelijk beter dan eerder gepubliceerde studies waarin de oudere 4-slice CT scanners werden gebruikt; Hoewel met 4-slice CT scanners goede resultaten werden gepubliceerd waren tot 30% van de geïncludeerde kransslagvaten niet beoordeelbaar door de aanwezigheid van bewegingsartefacten en artefacten gerelateerd aan de neerslag van kalk t.h.v. de vaatwand. Deze vaten werden dan ook niet geïncludeerd in de sensitiviteits-analyse, waardoor kunstmatig hoge waarden werden gepubliceerd. Na de introductie van een 2de generatie 16-slice CT scanners, hebben we deze scanner gebruikt om een patiëntengroep met stabiele angina pectoris en atypische pijn op de borst te onderzoeken. Deze scanners zijn uitgerust met een snellere rotatiesnelheid van de röntgenbuis en bieden een betere röntgenpenetratie, wat zich vertaalt in een betere temporele resolutie en contrast-ruis verhouding. Opnieuw includeerden we alle anatomisch aanwezige segmenten met een minimum diameter van ≥2 mm en we vonden uitzonderlijk hoge sensitiviteit- en specificiteit-waarden om significante vernauwingen t.h.v. de kransslagvaten op te sporen (**Hoofdstuk 8**).

Zeer recent werd er een nieuwe generatie 64-slice CT scanners geïntroduceerd. Deze scanners hebben een dunnere individuele detector breedte en kunnen in ongeveer 12 seconden het hele hart scannen. Bovendien bieden deze scanners een verbeterde spatiële resolutie (0.4 mm^3 in alle dimensies) door de ontwikkeling van de zogenaamde "z-axis flying focus" technologie. Met behulp van deze 64-slice scanner hebben we een patiëntengroep met stabiele en instabiele angina pectoris, atypische pijn op de borst en myocardinfarct zonder ST-segment stijging onderzocht. We hebben alle segmenten van de kransslagvaten, geclassificeerd volgens het model van de American Heart Association, beoordeeld en vonden een sensitiviteit van 99% en een specificiteit van 95% om significante vernauwingen op te sporen (**Hoofdstuk 9**). Deze waarden suggereren dat MSCT coronair angiografie, gebruik makend van de laatste 64-slice technologie, een betrouwbare techniek is om significante vernauwingen t.h.v. de kransslagvaten op te sporen, waardoor deze techniek kan dienen als een alternatief voor een diagnostische hartkatheterisatie in een geselecteerde patiëntengroep.

Valkuilen bij het Opsporen van Vernauwingen van de Kransslagvaten met Behulp van Multislice Computed Tomografie Coronair Angiografie

Kransslagaderverkalking (ook wel 'coronair atherosclerose' genoemd) is een teken van ziekte van de kransslagvaten. De aanwezigheid en uitgebreidheid van kransslagaderverkalking is afhankelijk van leeftijd en geslacht, maar komt niet goed overeen met de aanwezigheid van significante vernauwingen t.h.v. de kransslagaderen. Uitgebreid verkalkte plaques als gevolg van kransslagaderverkalking veroorzaken verschillende artefacten op de CT beelden. Hierdoor worden vernauwingen t.h.v. de kransslagaders frequent ten onrechte geclassificeerd worden als significant op de CT-scan. De hoeveelheid kransslagaderverkalking kan worden gekwantificeerd d.m.v. een speciale CT-scan met een zeer lage stralingsbelasting, zonder dat er contrast middel gebruikt hoeft te worden.

Sommige onderzoekers zijn van mening dat zo een speciale CT scan gebruikt kan worden om te voorspellen of het nuttig is om een MSCT coronair angiografie scan uit te voeren bij een patiënt met veel kransslagaderverkalking. Wij hebben de invloed van kransslagaderverkalking onderzocht op de capaciteit van MSCT coronair angiografie om significante vernauwingen op te sporen door een groep met weinig kransslagaderverkalking te vergelijken met een groep met uitgesproken kransslagaderverkalking (**Hoofdstuk 10**). Wij vonden dat, hoewel het moeilijker is om vernauwingen op te sporen bij patiënten met uitgesproken kransslagaderverkalking m.b.v. deze techniek, de juiste diagnose alsnog gesteld kon worden in de meerderheid van de onderzochte patiënten. Op basis hiervan hebben we geconcludeerd dat ook patiënten met uitgesproken kransslagaderverkalking onderzocht kunnen worden m.b.v. MSCT coronair angiografie, hoewel eerdere publicaties het tegendeel lieten zien.
De beperkte resolutie van MSCT coronair angiografie en de artefacten gerelateerd aan kransslagaderverkalking zorgen ervoor dat er tot op heden geen software is ontwikkeld die op een betrouwbare manier vernauwingen van de kransslagaders kan opsporen en kwantificeren. Om deze reden kunnen de kransslagaders alleen visueel geanalyseerd worden op de CT-scan, waardoor de resultaten van deze techniek om vernauwingen op te sporen erg afhankelijk zijn van de ervaring van diegene die de scan beoordeelt. Wij hebben 2 verschillende protocollen om de kransslagaders te analyseren met elkaar vergeleken. Het eerste protocol liet toe om alle beschikbare post-processing technieken te gebruiken, terwijl bij het tweede protocol alleen standaard beelden, die geanalyseerd kunnen worden op elk willekeurig PACS station, gebruikt mochten worden (**Hoofdstuk 11**). Wij ontdekten dat het gebruik van standaard beelden resulteerde in een significant lagere sensitiviteit om vernauwingen t.h.v. de kransslagvaten op te sporen. Deze studie laat zien dat MSCT coronair angiografie scans geanalyseerd zouden moeten worden door artsen met voldoende ervaring met alle beschikbare post-processing technieken.

Evaluatie van Kransslagaderverkalking Met Multislice Computed Tomografie Coronair Angiografie

MSCT coronair angiografie verstrekt zowel informatie over het lumen als over de vaatwand van de kransslagvaten. Plaques t.h.v. de kransslagvaten kunnen niet alleen gedetecteerd worden, maar ook onderverdeeld worden in niet-verkalkte, verkalkte en gemengde plaques, waarbij ook hun invloed op het lumen van het kransslagvat beoordeeld kan worden. We hebben het totaal aantal zieke segmenten (gedefinieerd als segmenten met plaque) alsmede de grootte, het type en de distributie van plaques beoordeeld in een geselecteerde patiëntengroep met stabiele angina pectoris waarbij we gebruik maakten van een 1ste generatie 16-slice CT scanner (**Hoofdstuk 12**). We ontdekten dat er plaque aanwezig was in 57% van alle anatomisch aanwezige segmenten van de kransslagaders met een minimum diameter van ≥2 mm. Bovendien vonden we dat plaques vooral aanwezig waren t.h.v. van de proximale en middelste segmenten van de kransslagaders, wat in overeenstemming is met eerder gepubliceerde resultaten van anatomo-pathologische en angiografische studies. We hebben een zelfde soort analyse gedaan in een patiëntengroep met stabiele en instabiele angina pectoris, waarbij we gebruik maakten van een 2de generatie 16-slice CT scanner.

We hebben deze resultaten vergeleken met de resultaten van de hartkatherisatie van deze patiënten en -in een deel van de patiëntenpopulatie- met intra-coronaire echografie (**Hoofdstuk 13**). Wij stelden vast dat significante plaques (plaques met een minimum grootte van ≥1 mm op intra-coronaire echografie) betrouwbaar gedetecteerd konden worden m.b.v. MSCT coronair angiografie. Verder ontdekten we dat verkalkte en gemengde plaques beter geïdentificeerd werden dan niet-verkalkte plaques. Ook vonden we plaques in 62% van alle aanwezige segmenten en in 1/3 van alle segmenten die geclassificeerd waren als ziektevrij op basis van de hartkatheterisatie. Patiënten met instabiele angina hadden significant meer niet-verkalkte plaques dan patiënten met stabiele angina pectoris. Deze studies laten veelbelovende resultaten zien bij het beoordelen van kransslagaderverkalking, maar de uiteindelijke klinische waarde van deze resultaten zal moeten blijken uit toekomstige follow-up studies.
Resultaten van initiële studies suggereerden dat niet-verkalkte plaques verder konden worden onderverdeeld in fibreuze en lipide-rijke plaques op basis van CT densiteitsmetingen (uitgedrukt in Hounsfield units). We ondervonden echter een hoge intra-plaque variabiliteit in Hounsfield untis in deze niet-verkalkte plaques en bovendien verkregen we erg hoge waarden t.h.v. het deel van de plaque dat grenst aan het lumen (gevuld met contrast middel) van de kransslagader. In een eerste, ex-vivo studie hebben we kransslagaders gevuld met verschillende oplossingen van contrastmiddel, waarna een MSCT coronair angiografie scan werd verricht. Wij ontdekten dat de densiteitswaarden gemeten t.h.v. de plaques afhankelijk waren van de densiteitswaarden die gemeten werden t.h.v. het lumen (**Hoofdstuk 14**). Deze waarneming werd bevestigd in een 2de studie, waarin we de invloed van verschillende densiteitswaarden t.h.v. het lumen -door het gebruik van verschillende oplossingen van contrastmiddelen- op in-vivo en ex-vivo plaque densiteitsmetingen onderzocht. Wij ontdekten dat progressief hogere densiteitswaarden gemeten t.h.v. het lumen geassocieerd waren met progressief hogere densiteitswaarden gemeten t.h.v. niet-verkalkte plaques, terwijl de waarden gemeten t.h.v. verkalkte plaques en aanliggend vetweefsel onveranderd bleven (**Hoofdstuk 15**). Dit laat zien dat hoge densiteitswaarden t.h.v. het lumen -wat belangrijk is om vernauwingen t.h.v. de kransslagvaten betrouwbaar op te kunnen sporen- mogelijks inhoudt dat niet-verkalkte plaques niet verder onderverdeeld kunnen worden in fibreuze en lipide-rijke plaques op basis van absolute densiteitswaarden. Verdere studies moeten worden uitgevoerd om calibratie-factoren te identificeren die de densiteitswaarden gemeten t.h.v. plaques kunnen corrigeren op basis van de waarden gemeten t.h.v. het lumen.
Gezien MSCT coronair angiografie belangrijke informatie over de vaatwand van de kransslagaders verstrekt, kan deze techniek gebruikt worden om vulnerabele plaque eigenschappen op te sporen of om plaques in kaart te brengen, waarna andere beeldvormende technieken gebruikt kunnen worden die in staat zijn specifieke vulnerabele plaque eigenschappen kunnen identificeren, zoals Magnetische Resonantie, Thermografie, Palpografie, Virtuele Histologie, of Optische Coherence Tomografie (**Hoofdstuk 16**).

Evaluatie van Stents m.b.v. Multislice Computed Tomografie Coronair Angiografie
MSCT coronair angiografie kan gebruikt worden om op een niet-invasieve manier stents ('veertjes' die worden geïmplanteerd tijdens een dotterbehandeling) op te volgen. Aanvankelijk werden er studies gepubliceerd die, als belangrijkste argument om de doorgankelijkheid van stents te bepalen, de aanwezigheid van contrast middel distaal van de stent gebruikten. Dit argument werd gebruikt omdat de beeldkwaliteit van stents niet voldoende was om contrast middel binnenin stents aan te kunnen tonen. Als een stent echter dichtgegroeid is kunnen er echter nieuwe bloedvaten gevormd worden die het kransslagvat distaal van de geoccludeerde stent alsnog van bloed (en dus contrast middel) kunnen voorzien. Hierdoor kan uit de aanwezigheid van contrastmiddel distaal van de stent niet zonder meer geconcludeerd worden dat de stent doorgankelijk is. Het is dus een absolute voorwaarde om contrast middel binnenin de stent aan te kunnen tonen om te kunnen concluderen dat een stent echt doorgankelijk is. Wij hebben de eerste CT studie uitgevoerd waarin zowel de doorgankelijkheid als wel de aanwezigheid van vernauwingen binnenin stents t.h.v. de kransslagaders werd geëvalueerd. We hebben in deze studie de resultaten van 16-slice CT corornair angiografie vergeleken met de resultaten van een hartkatherisatie en vonden veelbelovende CT resultaten (**Hoofdstuk 17**). Een specifieke groep die van deze niet-invasieve techniek zou kunnen profiteren zijn patiënten waarbij een stent t.h.v. de hoofdstam van de linker kransslagader geïmplanteerd is. Bij deze patiënten kan een nieuwe vernauwing, ontstaan binnenin een stent, leiden tot een plotse dood. Bovendien zijn deze stents beter beoordeelbaar met CT dan andere stents doordat ze een grotere diameter hebben en minder snel bewegen tijdens de hartcyclus. Wij hebben een studie verricht waarbij we de CT resultaten om vernauwingen binnenin stents, die waren gecoat met een materiaal dat vernauwingen moet tegengaan, hebben vergeleken met de resultaten van een hartkatherisatie en intra-coronaire echografie (**Hoofdstuk 18**). We ontdekten dat MSCT coronair angiografie inderdaad vernauwingen t.h.v. deze stents betrouwbaar kan aantonen, hoewel deze resultaten met de nodige reserve bekeken moeten worden gezien slechts een beperkt aantal patiënten een nieuwe vernauwing t.h.v. de hoofdstam hadden.

Klinische Toepassingen van Multislice Computed Tomografie Coronair Angiografie
Verschillende studies hebben aangetoond dat vernauwingen op de kransslagaders betrouwbaar kunnen worden opgespoord m.b.v MSCT coronair angiografie (zie: Multislice Computed Tomografie Coronair Angiografie om Vernauwingen van de Kransslagvaten op te Sporen). De klinische toepassing van deze techniek wordt echter op dit moment nog erg beperkt door het feit dat er nog geen studies beschikbaar zijn die aantonen dat MSCT coronair angiografie in vergelijking met andere niet-invasieve technieken toegevoegde diagnostische waarde heeft. Wij hebben de diagnostische waarde van MSCT coronair angiografie bestudeerd in een groep van patiënten met een relatief hoge prevalentie (74%) van significante vernauwingen t.h.v. de kransslagaders (**Hoofdstuk 19**). Wij vonden dat alle patiënten met significante vernauwingen correct werden geïdentificeerd op de CT scan, terwijl 28% van deze patiënten niet werden gedetecteerd met behulp van een fietsproef. MSCT coronair angiografie bleek vooral erg nuttig te zijn bij patiënten met een negatieve fietsproef, waardoor deze patiënten een intermediair risico op significante vernauwingen hadden (53%).

We stelden vast dat de waarschijnlijkheid dat er significante vernauwingen aanwezig waren na een positieve CT scan 90% was en na een negatieve scan 0% was. Deze eerste studie toont aan dat MSCT coronair angiografie wellicht een toegevoegde diagnostische waarde heeft bij het beoordelen van patiënten met stabiele angina pectoris. Deze techniek kan vooral van pas komen voor ziekenhuizen die geen angiografie kamer beschikken, wat noodzakelijk is om een diagnostische hartkatheterisatie uit te kunnen voeren. Er moeten echter nog veel meer studies uitgevoerd worden die de waarde van MSCT coronair angiografie in andere patiëntengroepen onderzoeken.

MSCT coronair angiografie levert belangrijke morfologische informatie op dat goed van pas kan komen tijdens complexe dotterbehandelingen. Vooral voor patiënten die sinds lange tijd een volledig afgesloten kransslagader hebben en geselecteerd zijn voor een dotterbehandeling om dit vat opnieuw te openen, kan deze techniek nuttig zijn. Deze patiënten worden geselecteerd voor een dotterbehandeling op basis van een diagnostische hartkatherisatie, waarbij morfologische eigenschappen van het afgesloten vat in kaart worden gebracht waarvan men weet dat ze geassocieerd zijn met een goede kans dat de dotterbehandeling zal slagen. In de meest recente studies is zo een complexe dotterbehandeling van een totaal afgesloten vat slechts succesvol in 40% van de geselecteerde patiënten. Wij hebben onderzocht of de bijkomende morfologische informatie verkregen met MSCT coronair angiografie gebruikt kan worden om beter te kunnen voorspellen of een dotterbehandeling zal slagen in deze patiëntengroep (**Hoofdstuk 20**). We stelden vast dat MSCT coronair angiografie inderdaad toegevoegde informatie verstrekte in vergelijking met de hartkatheterisatie. Vooral de lengte van het afgesloten segment en de hoeveelheid kransslagaderverkalking, gemeten op de CT scan, leidden tot een significant betere voorspelling m.b.t. het slagen van de dotterbehandeling. Deze bevindingen zouden in de toekomst kunnen leiden tot een betere selectie van patiënten die in aanmerking komen voor een dotterbehandeling van een sinds lange tijd volledig afgesloten kransslagader.

Conclusies

MSCT coronair angiografie verstrekt zowel informatie over het lumen als over de vaatwand van de kransslagvaten. Er zijn veelbelovende resultaten gepubliceerd waarbij de resultaten van MSCT coronair angiografie voor het opsporen van significante vernauwingen op de kransslagaders werden vergeleken met de resultaten van de conventionele hartkatheterisatie. Deze techniek, gebaseerd op de huidig beschikbare gegevens, zou gebruikt kunnen worden om patiënten met een intermediair risico op significante vernauwingen van de kransslagaders te beoordelen, patiënten die een bypass operatie van de kransslagaders hebben ondergaan op te volgen, patiënten na dotterbehandeling van een vernauwing gelokaliseerd in de proximale delen van de kransslagaders op te volgen, het selecteren van patiënten die eventueel in aanmerking komen voor een dotterbehandeling van een chronisch volledig afgesloten kransslagader en voor het beoordelen van congenitale afwijkingen van de kransslagaders. Op relatief korte termijn worden de resultaten van grote, multi-center studies verwacht, waardoor de mogelijkheden van deze techniek beter in kaart zullen worden gebracht.

Samenvatting en Conclusies

Een veelbelovende toepassing van MSCT coronair angiografie is het beoordelen van plaques t.h.v. de kransslagaders, gezien deze techniek het toelaat om het totaal aantal zieke segmenten te bepalen en bovendien de grootte, het type en de distributie van deze plaques te beoordelen. Deze uitgebreide analyse zou niet alleen prognostische waarde kunnen hebben, maar ook bijkomende informatie kunnen verstrekken m.b.t. het ontstaan en ontwikkelen van kransslagaderverkalking. Als er software beschikbaar zou komen die toelaat de totale hoeveelheid kransslagaderverkalking (inclusief verkalkte en niet-verkalkte plaques) te kwantificeren, zou het in de toekomst bijvoorbeeld mogelijk kunnen worden om de verdere ontwikkeling van kransslagaderverkalking op te volgen na toediening van lipide-verlagende medicatie.

Er moeten echter nog belangrijke problemen overwonnen worden voordat deze techniek op ruime schaal toegepast kan worden. Een goede training van artsen die deze techniek willen uitvoeren is essentieel. Zij moeten kennis hebben van zowel de CT technologie als de pathofysiologie van het hart, waardoor Radiologische en Cardiologische kennis onontbeerlijk is. Het is dan ook niet verwonderlijk dat het Erasmus Medisch Centrum, door de vruchtbare samenwerking tussen de afdelingen Radiologie en Cardiologie, op dit onderzoeksgebied aansprekende resultaten heeft geboekt. Hopelijk zullen andere centra ons voorbeeld volgen wat uiteindelijk zal leiden tot een betere patiëntenzorg.

Chapter 21

DANKWOORD

Als eerste wil ik mijn beide promotors, professor De Feyter en professor Krestin, bedanken voor hun bijdrage aan dit proefschrift.

Beste Pim, zonder jou was dit proefschrift niet in zijn huidige vorm tot stand gekomen. Je kwaliteiten om complexe materies te reduceren tot een paar overzichtelijke probleemstellingen waren onmisbaar. Als het even tegen zat omdat een artikel was afgewezen of een concurrerende onderzoeksgroep ons net voor was, wist je altijd met een paar nuchtere -en bovenal geestige- opmerkingen de moed erin te houden. Ontzettend bedankt voor de leerzame, maar bovenal leuke jaren en ik hoop dat we nog vele jaren samen zullen werken aan dit project.

Beste Gabriel, de kansen die je me hebt gegeven, zowel tijdens als na mijn promotieonderzoek, zal ik nooit vergeten. Mede dankzij jouw visie kwam de vruchtbare samenwerking tussen de afdelingen Radiologie en Cardiologie tot stand, waarvan dit proefschrift een mooi voorbeeld is. Bedankt voor je steun en inzet voor dit project.

Uiteraard verdient mijn co-promotor Filippo Cademartiri de nodige aandacht in dit dankwoord.
Dear Filippo, I want to thank you for sharing with me your great knowledge of Multislice Computed Tomography and people who know you are all aware of your remarkable capacities. Your future is extremely bright and it will not take long before you will reach your academic goals. I know that you will always remain a good friend, despite the fact that you will never understand “the art of wearing green trousers”.

Graag wil ik de overige leden van mijn promotiecommissie van harte bedanken voor de beoordeling van mijn proefschrift, professor Poldermans, professor Bogaert, professor Serruys, professor Pattynama, professor Prokop en professor Van der Wall.

Acknowledgements

Veel dank ben ik verschuldigd aan Jan Bogaert. Je hebt me als eerste de kans gegeven om me te verdiepen in de cardiale beeldvorming en je goede begeleiding is bijzonder waardevol gebleken. Patrick Serruys en Peter Pattynama wil ik bedanken voor hun enthousiasme voor de cardiale CT. Iedere jonge techniek heeft 'believers' nodig en jullie enthousiasme is een hart onder de riem voor alle onderzoekers die werkzaam zijn op dit onderzoeksgebied.

Uiteraard zijn er vele collega's die direct hebben bijgedragen aan dit proefschrift. Als eerste wil ik Andries Zwamborn bedanken. Je hebt me altijd fantastisch geholpen, maar je hulp de afgelopen maanden was ronduit onmisbaar. Het meest tastbare bewijs van je kwaliteiten heeft de lezer nu in zijn handen, want voor het bundelen van mijn stapeltje artikelen tot dit buitengewoon mooi vormgegeven proefschrift ben jij volledig verantwoordelijk.

Graag wil ik Koen Nieman bedanken, omdat hij me de eerste kneepjes van het vak heeft geleerd. Beste Koen, ontzettend bedankt voor je hulp en geduldige uitleg. Ik hoop dat we nog lang samen zullen werken om de mogelijkheden van deze techniek verder uit te diepen.

De CT laborantengroep, Rolf Raaijmakers, Marcel Dijkshoorn, Berend Koudstaal, Marieke Kreiter-De Jonge en Ronald Booij, kan ik niet genoeg bedanken. Beste Rolf, je enthousiasme en charme zijn ongekend en garanderen je een mooie carrière bij je huidige werkgever. Beste Marcel, je hebt een geweldige kennis van Multislice CT en je bent ook nog in staat deze kennis over te brengen aan je collega's, een eigenschap waar ik erg veel waardering voor heb. Bedankt voor je inzet en goede technische adviezen. Beste Berend, Marieke en Ronald, bedankt voor jullie flexibiliteit als er weer eens een cardiale patiënt tussen het reguliere programma door gescand moest worden. Het was erg gezellig om met jullie allemaal te werken.

Door de jaren heen is onze cardiale CT groep steeds groter geworden, vandaar de vele personen die ik wil bedanken. Allereerst wil ik diegene bedanken die helaas niet meer in Rotterdam werkzaam zijn: Pedro Lemos, Fransesco Saia, Giuseppe Runza en Manuel Belgrano. Dear Pedro, I truly admire your ambition and scientific capacities. Above all, you're a great guy. You have a great future ahead. Dear Fransesco, thank you for helping me with all the QCA analyses. I do not know somebody else who completed his PhD as soon as you did, but this achievement did not prevent you from having lots of fun in Rotterdam. Respect. Dear Giuseppe -Don Peppe- thank you for the great time and wonderful cooking. I hope I will be able to visit you soon so you can show me the truly Southern way of living. Ps Yvette asks you to give me a refresher course in Italian cooking. Dear Manuel, thank you for your support and the Italian language lessons (however, I still don't know whether these words can be used on every occasion). Later kwamen Carlos van Mieghem en Bob Meijboom ons team versterken. Beste Carlos, dank je wel voor je fantastische hulp. Je betrokkenheid bij de patiëntenzorg siert je enorm en als patiënt zou ik me geen betere arts kunnen voorstellen. Ik hoop dat we zullen slagen in onze pogingen om de karige catering van het Erasmus MC te laten vervangen door Leuvense broodjes, maar ja, tot die tijd moeten we het toch maar doen met de Italiaanse variant.

Beste Nase, ik had me geen betere opvolger kunnen bedenken. Ik weet dat je behoorlijk wat werk kan verzetten (ik heb je onder meer m.b.v. een schamele schep een "zwembad" zien graven van 2,5 meter diep midden in de examenperiode) en dat zal je geen windeieren leggen. Ik weet dat je mooie jaren tegemoet gaat. De huidige onderzoeksgroepgroep bestaat verder uit Patrizia Malagutti, Fransesca Pugliese, Ludovico La Grutta, Allessandro Palumbo, Eleni Vourvouri en Anieck Weustink. Soms zeggen beelden meer dan woorden, vandaar de foto op de volgende pagina. Grazie.

Verder wil ik mijn kamergenoten, Timo Baks en Cecile de Monyé, bedanken voor de leuke tijd die we gehad hebben in ons onderzoekshok. Beste Timo, je was immer relaxed en opgewekt en we hebben heel wat afgelachen. Beste Cecile, dank je wel voor de gezelligheid en je goede adviezen m.b.t. de nieuwste computersnufjes (beter dan de nieuwste Correct-gids).

Uiteraard wil ik de medewerkers van de angiografie kamers van harte bedanken voor hun hulp. In de eerste plaats wil ik de (voormalige) fellows bedanken: Angela Hoye, Akiz Arampatzis, George Sianos, Andrew Ong, Marco Valgimigli, Robert-Jan van Geuns en Erik Duckers. Dear Angela, thank you for your great help. I'm happy that we were finally able to complete the CTO paper, probably one of the most time consuming manuscripts ever if you would divide the number of hours by the number of included patients. George, I also want to thank you for your contribution in this manuscript as well as your support in general. Special thanks to Eugene McFadden. Dear Eugene, thank you for your time and effort in reviewing the manuscripts. I hope you will achieve your goals in Ireland (I understand your move: beautiful country and fantastic people). I think you are relieved that you do not have to speak Dutch anymore, however we truly miss your English-French-Dutch pronunciation and great company. Verder wil ik Laetitia Bautz, Paul Cummins, Arno Ruiter en Jan Tuin bedanken. Beste Titia, dank je wel voor je hulp bij het verzamelen van alle patiëntgegevens. Beste Paul en Arno, jullie hulp bij het rekruteren van patiënten voor dit onderzoek was echt onmisbaar. Beste Jan, dank je wel voor al die uren die je hebt gestopt in het maken van video's voor een presentatie of de organisatie voor een live-case. Het was altijd bijzonder aangenaam om op je kamer te zitten werken met een relaxed jazzmuziekje op de achtergrond. Het enige wat ik miste was de fles wijn, maar die heb je nog tegoed (ik ben het dus toch niet vergeten). Ook wil ik Nico Bruining en Ronald Hamers bedanken. De samenwerking tussen jullie groep en de cardiale CT groep is veelbelovend en ik ben ervan overtuigd dat jullie een mooi softwarepakket zullen ontwikkelen. Eric Boersma, dank je wel voor je zeer kundige statistische advies, waardoor ik heel wat valkuilen van de reviewers heb kunnen omzeilen. Karin ten Wolde en Teun Rijsdijk, dank jullie wel voor jullie hulp bij het maken van de posters en figuren.

Graag wil ik Denise Vrouenraets, Marijke Heijer, Pat Quintelier en Marja Thijse bedanken. Beste Denise, dank je wel voor je geweldige hulp door de jaren heen en de rugdekking als ik weer een deadline gemist had. Beste Marijke, dank je wel voor het goede nieuws als er een acceptatie-fax binnenkwam en je opbeurende woorden als dat niet het geval was. Beste Pat, dank je wel voor je fantastische begeleiding bij de organisatie van mijn promotie. Je hebt echt orde in de chaos gebracht en ik vrees dat ik zonder jou waarschijnlijk nog steeds geen promotiedatum zou hebben.

Acknowledgements

Beste Marja, dank je wel voor je hulp bij alle mogelijke organisatorische problemen, die je altijd weer in goede banen wist te brengen. Bedankt voor de gezellige tijd.
Een speciaal dankwoord ben ik verschuldigd aan mijn paranimfen, Thijs Vogten en Bernard Linthorst, die me gedurende mijn promotieonderzoek niet alleen geweldig gesteund hebben, maar ook hebben gezorgd voor de broodnodige ontspanning. Er zijn van die momenten die je niet kan beschrijven, maar je nooit zal vergeten, zoals een duidelijk zenuwachtige rector magnificus ("waar blijven ze nou?") die staat te wachten op Dickie, de promovendus die wat verlaat is door een wat uit de hand gelopen diner de avond ervoor. Ook de doorgeknipte Diners' creditcard van Ciske ("laat mij maar even betalen") na een grand diner in Parkheuvel was zo'n hoogtepunt. Mannen, bedankt voor jullie fantastische vriendschap. Natuurlijk wil ik ook de andere leden van het dispuut "De Bokkerijders" bedanken voor de mooie tijd, niet alleen in Leuven, maar zeker ook erna. Een speciaal woordje wil ik wijden aan mijn huisgenoten waar ik het langste mee in Leuven heb gewoond, Joost Colaris, Willem Willaert en Martijn Raaijmaakers. Het klinkt cliché, maar volgens mij kan ik volstaan met vier woorden: vrienden voor het leven.

Uiteraard wil ik mijn familie bedanken voor hun fantastische steun. Beste Guy, van jou heb ik geleerd dat je niet alleen moet kunnen reproduceren maar vooral begrijpen, alhoewel ik vroeger altijd hoopte dat je mijn wiskunde vraagstukken even voor me zou oplossen i.p.v. uitleggen. Je hebt me als snotneus van alles geleerd (van werkwoorden vervoegen tot bier drinken) waar ik nu nog steeds profijt van heb. Dank je wel voor je vriendschap. Lieve ma en pa, jullie staan altijd voor me klaar en hebben me altijd geholpen wanneer het kon. Dank jullie wel voor alle kansen die jullie me hebben geboden en de onvoorwaardelijke steun en liefde.

Lieve Yvette, je hebt me altijd geweldig gesteund, ondanks de vele avonduren en weekenden die ik met dit proefschrift bezig was. Je hebt me ontelbare keren uit de brand geholpen als ik -zoals gewoonlijk- weer eens in tijdnood was en zonder jou was dit proefschrift waarschijnlijk een stuk dunner. Dank je wel voor de fantastische tijd die we samen hebben.

Cardiac imaging groep zomer 2005.
Boven, van links naar rechts: Patrizia Malagutti, Nico Mollet, Carlos van Mieghem, Timo Baks, Fransesca Pugliese. Onder, van links naar rechts: Filippo Cademartiri, Bob Meijboom, Ludovico La Grutta, Allessandro Palumbo.

Nico Mollet

Chapter 21

LIST OF PUBLICATIONS

Nico R. Mollet

1. **Mollet NR**, Dymarkowski S, Volders W, Wathiong J, Herbots L, Rademakers FE, Bogaert J.
   Visualization of ventricular thrombi with contrast-enhanced magnetic resonance imaging in patients with ischemic heart disease.
   Circulation. 2002;106(23):2873-6.
2. Cademartiri F, Nieman K, **Mollet NR**.
   An unusual case of chest murmur demonstrated with three dimensional volume rendering with 16 row multislice spiral computed tomography.
   Heart. 2003;89(6):586.
3. Giorgi B, **Mollet NR**, Dymarkowski S, Rademakers FE, Bogaert J.
   Clinically suspected constrictive pericarditis: MR imaging assessment of ventricular septal motion and configuration in patients and healthy subjects.
   Radiology. 2003;228(2):417-24.
4. Cademartiri F, Nieman K, **Mollet NR**.
   The dynamics of an ascending aorta dissection by 16 row multislice computed tomography.
   Heart. 2003;89(9):970.
5. Sianos G, **Mollet NR**, Hofma S, de Feyter PJ, Serruys PW.
   Images in cardiovascular medicine. Late-late occlusion after intracoronary brachytherapy.
   Circulation. 2003;108(10):e69-70.
6. Cademartiri F, Nieman K, **Mollet NR**, Flohr TG, Alfieri O, de Feyter PJ, Krestin GP.
   Non-invasive 16-row spiral multislice computed tomography coronary angiography after one year of experience.
   Ital Heart J. 2003;4(7):587-93.
7. Cademartiri F, Nieman K, **Mollet NR**, Alfieri O, de Feyter PJ, Krestin GP.
   Sixteen-row multislice computed tomography of tuberculous pericardial abscess.
   Ital Heart J. 2003;4(8):575-6.

8. de Feyter PJ, Serruys PW, Nieman K, **Mollet NR**, Cademartiri F, van Geuns RJ, Slager C, van der Steen AFW, Krams R, Schaar JA, Wielopolski P, Pattynama PMT, Arampatzis A, van der Lugt A, Regar E, Lightart J, Smits P.
Imaging of coronary atherosclerosis and identification of the vulnerable plaque.
Netherlands Heart Journal 2003;11(9):347-56.
9. Cademartiri F, Luccichenti G, Marano R, Nieman K, **Mollet NR**, de Feyter PJ, Krestin GP, Pavone P, Bonomo L.
Spiral CT-angiography with one, four, and sixteen slice scanners. Technical note.
Radiol Med 2003;106(4):269-83.
10. Cademartiri F, Luccichenti G, Marano R, Nieman K, **Mollet NR**, De Feyter P, Krestin GP, Pavone P, Bonomo L.
Non-invasive angiography of the coronary arteries with multislice computed tomography: state of the art and future prospects.
Radiol Med 2003;106(4):284-96.
11. De Feyter PJ, **Mollet NR**, Cadermartiri F, Nieman K, Pattynama P.
MS-CT coronary imaging.
J Interv Cardiol. 2003;16(6):465-8.
12. Cademartiri F, **Mollet NR**, Nieman K, Krestin GP, de Feyter PJ.
Neointimal hyperplasia in carotid stent detected with multislice computed tomography.
Circulation. 2003 Nov 25;108(21):147.
13. **Mollet NR**, Dymarkowski S, Bogaert J.
MRI and CT revealing carcinoid heart disease.
Eur Radiol. 2003;13(4) :14-8.
14. De Feyter PJ, **Mollet NR**, Nieman K, Cademartiri F, Marano R, Pattynama PMT.
Computed Tomography – coronary angiography.
The Reviews 2003;Mar-Apr:1-3.
15. **Mollet NR**, Nieman K, Cademartiri F, Raaijmakers R, Pattynama PMT, de Feyter PJ.
MSCT coronary angiography: present and future.
Applied Radiology 2003:Dec;22-25.
16. Cademartiri F, **Mollet NR**, van der Lugt A, Nieman K, Pattynama PM, de Feyter PJ, Krestin GP.
Non-invasive 16-row multislice CT coronary angiography: usefulness of saline chaser.
Eur Radiol. 2004;14(2):178-83.
17. Cademartiri F, Nieman K, **Mollet NR**, de Feyter PJ, Krestin GP.
Pseudoaneurysms of the ascending aorta demonstrated with "motion-free" multislice computed tomography.
Circulation. 2004;109(6):42-3.
18. Cademartiri F, Marano R, Luccichenti G, **Mollet NR**, Nieman K, De Feyter PJ, Krestin GP, Bonomo L.
Normal anatomy of the vessels of the heart with 16-row multislice computed tomography.
Radiol Med 2004;107(1-2):11-21.
19. Cademartiri F, **Mollet NR**, Nieman K, Alfieri O, Krestin GP.
Motion-free ECG-gated 16-row multislice computed tomography in the follow-up of aortic coarctation with three-dimensional volume rendering.
Ital Heart J. 2004;5(2):167-8.
20. Cademartiri F, **Mollet NR**, Nieman K, Szili-Torok T, de Feyter PJ.
Right coronary artery arising from the left circumflex demonstrated with multislice computed tomography.
Circulation. 2004;109(15):e185-6.

21. **Mollet NR**, Cademartiri F, Nieman K, Saia F, Lemos PA, McFadden EP, Pattynama PMT, Serruys PW, Krestin GP, De Feyter PJ.
Multislice spiral CT coronary angiography in patients with stable angina pectoris
J. Am. Coll. Cardiol. 2004;43:2265-70.
22. De Feyter P, **Mollet NR**, Nieman K, Arampatzis CA, Cademartiri F, Pattynama PMT, Serruys, PW.
Non-invasive visualization of coronary atherosclerosis with multislice computed tomography.
Cardiovasc. Radiat. Med. 2004;5(1):49-56.
23. **Mollet NR**, Cademartiri F.
Diagnosis and follow-up of left main coronary artery disease with 16-row Multislice CT coronary angiography.
Circulation 2004;110(21):e514.
24. Cademartiri F, Nieman K, Van der Lugt A, Raaijmakers RH, **Mollet NR**, Pattynama PMT, De Feyter PJ, Krestin GP.
Intravenous contrast material administration at 16-detector row helical CT coronary angiography: test bolus versus bolus-tracking technique.
Radiology 2004; 233(3):817-23.
25. Cademartiri F, **Mollet NR**, Lemos PA, McFadden EP, Marano R, Baks T, Stijnen T, De Feyter PJ, Krestin GP.
Standard versus user-interactive assessment of significant coronary stenoses with multislice computed tomography coronary angiography.
Am. J. Cardiol. 2004;94(12):1590-3.
26. **Mollet NR**, Cademartiri F, Krestin GP, McFadden EP, Arampatzis CA, Serruys PW, De Feyter PJ.
Improved diagnostic accuracy with 16-row multislice computed tomography coronary angiography.
J. Am. Coll. Cardiol. 2005;95(2):240-3.
27. **Mollet NR**, Hoye A, Lemos PA, Cademartiri F, Sianos G, McFadden EP, Krestin GP, Serruys PW, De Feyter PJ.
Value of pre-procedure multislice computed tomography coronary angiography to predict the outcome of percutaneous recanalization of chronic total occlusions.
Am. J. Cardiol. 2005;95(2):240-3.
28. **Mollet NR**, Cademartiri F, De Feyter PJ.
Non-invasive Multislice CT Coronary Imaging.
Heart 2005;91(3):401-7.
29. Baks T, Van Geuns RJ, Biagini E, Wielopolski P, **Mollet NR**, Cademartiri F, Boersma E, Van der Giessen, WJ, Krestin GP, Duncker DJ, Serruys PW, De Feyter, PJ.
Recovery of left ventricular function after primary angioplasty for acute myocardial infarction.
Eur. Heart J. 2005;91(3):401-7.
30. Cademartiri F, Marano R, Luccichenti G, **Mollet NR**, Runza G, Galia M, Gualerzi M, Brambilla L, Coruzzi P, Midiri M, Belgran M.
Image assessment with multislice CT coronary angiography.
Radiol. Med. 2005;109(3):198-207.
31. Cademartiri F, **Mollet NR**, Lemos PA, McFadden EP, Marano R, Baks T, Stijnen T, De Feyter PJ, Krestin GP.
Impact of Coronary Calcium Score on Diagnostic Accuracy for the Detection of Significant Stenosis With Multislice Computed Tomography Coronary Angiography.
Am. J. of Cardiol. 2005;95(10):1225-7.

32. **Mollet NR**, Cademartiri F, PJ de Feyter.
Imaging the coronary vasculature using Multislice Computed Tomography.
Heart and Metabolism 2004;24:13-16.
33. **Mollet NR**, Cademartiri F, Nieman K, Saia F, Lemos PA, McFadden EP, Serruys PW, Krestin GP, De Feyter PJ.
Non-Invasive Assessment of Coronary Plaque Burden Using Multislice Computed Tomography
Am. J. of Cardiol. 2005;95(10):1165-9.
34. **Mollet NR**, Cademartiri, F.
Computed Tomography Assessment of Coronary Bypass Grafts: Ready to Replace Conventional Angiography?
Int. J. Cardiovasc. Imaging 2005;21(4):453-4.
35. Cademartiri F, **Mollet NR**, Van der Lugt A, Stijnen T, De Feyter PJ, Krestin GP.
IV Contrast Administration for CT Coronary Angiography on Multidetector-Row Helical CT: Effect of Iodine Concentration on Vascular Attenuation,
Radiology 2005;236(2):661-5
36. Mieghem CA, Bruining N, Schaar JA, McFadden E, **Mollet NR**, Cademartiri F, Mastik F, Ligthart JM, Granillo GA, Valgimigli M, Sianos G, Giessen WJ, Backx B, Morel MA, Es GA, Sawyer JD, Kaplow J, Zalewski A, Steen AF, Feyter P, Serruys PW.
Rationale and methods of the integrated biomarker and imaging study (IBIS): combining invasive and non-invasive imaging with biomarkers to detect subclinical atherosclerosis and assess coronary lesion biology.
Int J Cardiovasc Imaging. 2005;21(4):425-41.
37. Cademartiri F, **Mollet NR**, Runza G, Bruining N, Hamers R, Somers P, Knaapen M, Verheye S, Midiri M, Krestin GP, De Feyter, PJ.
Influence of intracoronary attenuation on coronary plaque measurements using multislice computed tomography: observations in an ex vivo model of coronary computed tomography angiography.
Eur. Radiology 2005 (in press).
38. Cademartiri F, **Mollet NR**, Nieman K, van der Lugt A, de Feyter PJ, Pattynama PMT, Krestin GP.
Pre-operative evaluation of aortic isthmic coarctation with multislice computed tomography and three-dimensional volume rendering.
Serbian Archives of Radiology (in press).
39. De Feyter PJ, **Mollet NR**, Nieman K, Cademartiri F, Marano R, Pattynama P.
Computed Tomography: Coronary angiography: Current status and future directions.
Indian Heart Journal (in press).
40. **Mollet NR**, Cademartiri F, Runza G, Belgrano M, Baks T, Meijboom WB, De Feyter PJ.
Four-dimensional evaluation of a giant pseudo-aneurysm by multislice computed tomography.
Int. J. Cardiovasc. Imaging (in press).
41. Cademartiri F, **Mollet NR**, McFadden EP, Flohr TG, Ohnesorge B, De Feyter PJ, Krestin GP.
Reduction of Motion Artifacts from Mild Heart Rhythm Irregularities With ECG-editing Using Multidetector-row Computed Tomography Coronary Angiography.
Am. J. of Roentgenol. (in press).
42. Cademartiri F, **Mollet NR**, Runza G, Belgrano M, Midiri M, De Feyter PJ, Krestin GP.
Diagnostic accuracy of multislice computed tomography coronary angiography is improved at low heart rates.
Int. J. Cardiovasc. Imaging (in press).

43. Baks T, Van Geuns RJ, Biagini E, Wielopolski P, **Mollet NR**, Cademartiri F, Van Der Giessen WJ, Krestin GP, Serruys PW, Duncker DJ, De Feyter PJ.
Effects of Primary Angioplasty for Acute Myocardial Infarction on Early and Late Infarct Size and Left Ventricular Wall Characteristics.
J. Am. Coll. Cardiol. (in press).
44. **Mollet NR**, Cademartiri F, Van Mieghem CAG, Runza GP, McFadden EP, Baks T, Serruys PW, Krestin GP, De Feyter PJ.
High-resolution Spiral CT Coronary Angiography in Patients Referred for Diagnostic Conventional Coronary Angiography.
Circulation (in press).
45. Van Mieghem C, McFadden E, De Feyter PJ, Bruining N, Schaar J, **Mollet NR**, Cademartiri F, Goedhart D, De Winter S, Rodriguez Granillo G, Valgimigli M, Mastik F, Van der Steen A, Van der Giessen W, Sianos G, Backx B, Morel M-A, Van Es G-A, Kaplow J, Zalewski A.
Non-invasive Detection of Subclinical Coronary Atherosclerosis Coupled With Assessment, Using Novel Invasive Imaging Modalities, of Changes in Plaque Characteristics: The IBIS Study (Integrated Biomarker and Imaging Study).
J. Am. Coll. Cardiol. (accepted).
46. Cademartiri F, Schuijf JD, **Mollet NR**, Malagutti P, Runza G, Bax JJ, de Feyter PJ.
Multislice CT coronary angiography: how to do it and what is the current clinical performance?
Eur J Nucl Med Mol Imaging. 2005 (in press)

Books (co-editor)

1. De Feyter PJ, Krestin GP, Cademartiri F, **Mollet NR**, Nieman K.
Computed tomography of the coronary arteries.
Martin-Dunitz, Taylor & Francis Group. ISBN: 184184439X

Book chapters

1. De Feyter PJ, **Mollet NR**, Nieman K, Cademartiri F, Pattynama PMT, Serruys PW.
Non-invasive visualization of coronary atherosclerosis with multislice computed tomography.
In: Handbook of the vulnerable plaque. Eds: Waksman R and Serruys PW.
Chapter 13, pgs 237-54. Martin-Dunitz, Taylor & Francis Group.
ISBN: 1841843237
2. Nieman K, **Mollet NR**, Cademartiri F, De Feyter PJ.
Coronary spiral computed tomography. In: The Paris course on revascularization. Chapter 14, pgs 197-202. Groupe Composer. ISBN: 2913628168
3. **Mollet NR**, Cademartiri F, De Feyter PJ.
Non-invasive Multislice CT Coronary Imaging.
In: A Colour Handbook of Adult Interventional Cardiology, Manson Publishing (in press)
4. **Mollet NR**
MSCT Coronary Angiography
In: Advances in MDCT Volume 2, Pt. 1: Cardiac Imaging.
Clinical Publishing Ltd (in press).

Abstracts

(Co-)author of 60 abstracts presented at international congresses (AHA, ACC, ESC, EuroPCR, RSNA, ECR)

Chapter 21

CURRICULUM VITAE

Nico Mollet was born on the 4th of July 1975 in Delft (The Netherlands). After finishing high school in 1993 at the St. Stanislas College in Delft, he studied Biomedical Science at the University of Leiden (The Netherlands). After 1 year, he decided to go back to his Belgian roots and started studying Medicine at the Catholic University of Leuven (Belgium). During his study, he gained initial experience in cardiovascular research as a research-fellow in the group of Professor Jan Bogaert at the MRI Research Center (Leuven, Belgium). His first publications were in the field of clinical application of Cardiac Magnetic Resonance. After graduating in 2002, he was employed as a research fellow at the Erasmus Medical Center in Rotterdam (the Netherlands) under leadership of Professor Pim de Feyter (department of Cardiology) and Professor Gabriel Krestin (chairman of the department of Radiology). His achievements in the field of cardiac imaging with Multislice Computed Tomography has resulted in this PhD-thesis. To date, he is (co-)author of nearly 50 publications in peer-reviewed journals, 60 abstracts presented at international congresses, several book chapters, and co-editor of the textbook "Computed Tomography of the Coronary Arteries". He co-organizes the course "Clinical Workshop on Cardiac CT Somatom Sensation 16/64", which takes place at the Radiology department of the Erasmus Medical Center. Among his other educational activities are regular visits to other hospitals for on-site training in Cardiac Computed Tomography. He is currently completing his training in radiology at the Erasmus Medical Center.

STELLINGEN BEHORENDE BIJ HET PROEFSCHRIFT

Non-invasive Coronary Imaging with Multislice Computed Tomography Coronary Angiography

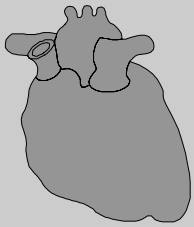

Nico R. Mollet

Rotterdam,

12 oktober 2005

STELLINGEN

1. Multislice CT coronair angiografie kan in een geselecteerde patiëntenpopulatie als vervanging van een diagnostische hartkatheterisatie dienen (dit proefschrift).

2. De diagnostische nauwkeurigheid van multislice CT coronair angiografie hangt af van het scan protocol, de hartfrequentie en hartritme van de patiënt, de mate van kransslagaderverkalking en de ervaring van de arts (dit proefschrift).

3. Multislice CT coronair angiografie kan onafhankelijk van conventionele risicofactoren bijdragen tot een betere identificatie van patiënten met een groot risico op coronaire hartziekten (dit proefschrift).

4. De diagnostische nauwkeurigheid van 64-slice CT coronair angiografie voor het opsporen van significante vernauwingen in proximale stents is veelbelovend (dit proefschrift).

5. Multislice CT coronair angiografie is bijzonder nuttig bij de beoordeling van patiënten met een intermediair risico op kransslagaderziekte (dit proefschrift).

6. Gegeven de hoge incidentie van plotse dood en myocardinfarct als eerste presentatie van kransslagaderziekte is een vaccin tegen atherosclerose dringend nodig.

7. Screening met multislice CT coronair angiografie zou gepaard moeten gaan met screening naar straling geïnduceerde pathologie.

8. "Evidence-based" wordt vaak onterecht geassocieerd met ingewikkelde statistiek.

9. Experience is simply the name we give our mistakes (Oscar Wilde).

10. De belangrijkste medische doorbraak in 2003 was niet de ontwikkeling van de 64-slice CT scanner, maar de 60ste verjaardag van Keith Richards.

11. Het cynische van het "kwartje van Kok" en de "Zalm snip" is dat de eerste de automobilist minstens een snip kost en van de tweede netto een kwartje overblijft.